

# **An Investigation into the Use of a Plant-Expressed Virus-Like Particle as an Oral Vaccine Candidate**

---



**Alberto Berardi**

University of East Anglia  
School of Pharmacy

Thesis Submitted for the Degree of Doctor of Philosophy  
August, 2013

## Acknowledgements

First and foremost I would like to thank Dr Susan Barker for her invaluable knowledge and continuous support throughout the whole period of my PhD. I thank her also for the constant care at a personal level. I would also like to thank Prof George Lomonosoff for his experience, unique personality and cheerful approach that made this journey funnier and more interesting. Big thanks also go to Prof Dave Evans who was punctually present and available to help me. I would also like to thank Prof Duncan Craig for being a great source of positivity and inspiration.

Thanks are also to Prof Claudio Nicoletti for his appreciated collaboration and addition to this work. Thanks also to Miss Nadezhda Gicheva for her assistance during my work at the Institute of Food Research. Special thanks go to my friends and colleagues at John Innes Centre Alaa, Paolo, Eva, Hadrien, Pooja, Yulia, Keith and Elaine. Moreover, I thank all my many colleagues at University of East Anglia.

Particular thanks are also to Francesca, Claudia, Simone, Yohan and Davide, that as real friends sweetened the path of this intense journey. A big thank you goes also to my dear 26 Ivory Road flatmates Dorothy, Sam, Fatima and Giulia.

I would also like to thank my endurable “CDP” friends back home, constantly present on Skype, ready to cheer me up with a laugh! I am also grateful to my grandmothers who always showed care, admiration and faith in me, despite their disagreement on living abroad!

At last I want to thank my parents, who have supported me throughout the PhD, in any possible manner, going way beyond what a son could expect.

I cannot forget to thank my fiancée Lorina. Her love, solid support and faith in me have been the constant positive note of this journey.

## Abstract

*Plant-expressed virus-like particles (VLPs) could offer an alternative method for the oral delivery of vaccines. VLPs' robustness, combined with their compartmentalisation within the plant cells, should favour their stability in the harsh gastro-intestinal (GI) environment. In the small intestine, intact VLPs should be available for absorption by the Follicle-associated epithelium (FAE), considered the main portal of entry for antigens in the gut. In this work, Hepatitis B core antigen (HBcAg) VLPs, expressed transiently in Nicotiana benthamiana leaves, were extracted, purified and characterised. The stability of purified HBcAg VLPs in simulated human gastric and intestinal media was investigated. The results suggested that the antigen was unstable when subjected to various simulated gastric fluids. Upon incubation in simulated human and ex vivo pig intestinal fluids, HBcAg maintained higher stability. Leaves expressing HBcAg VLPs could be dried, retaining good antigen stability, but the natural encapsulation in the leaves failed to protect the antigen from degradation in the simulated GI fluids. However, enteric-coated “green” tablets containing dried leaves expressing HBcAg could be produced and were shown to confer protection in simulated gastric fluids but allowed the release of intact antigen in simulated intestinal fluids. Purified HBcAg VLPs could be formulated into spray-dried and spray freeze-dried microparticles using a pH-responsive polymer. However, such formulations showed poor gastro-resistance, negating their use for targeted intestinal delivery. HBcAg VLPs could be also freeze-dried, suggesting the potential use of freeze-drying for further processing of the antigen into an oral formulation. A human cell culture model of the small intestinal epithelium indicated selective absorption of HBcAg VLPs by the FAE but limited overall absorption. In vivo ligated loop studies in mice suggested poor intestinal absorption, mainly relegated to the FAE. This research represents an original investigation into the possible applications of plant-expressed HBcAg VLPs for oral drug delivery.*

# Table of Contents

---

|                              |             |
|------------------------------|-------------|
| <b>Acknowledgements</b>      | <b>I</b>    |
| <b>Abstract</b>              | <b>II</b>   |
| <b>Table of Contents</b>     | <b>III</b>  |
| <b>List of Tables</b>        | <b>X</b>    |
| <b>List of Figures</b>       | <b>XI</b>   |
| <b>List of Abbreviations</b> | <b>XIII</b> |

|          |   |          |
|----------|---|----------|
| <b>1</b> | <b>Introduction .....</b>   | <b>1</b> |
| 1.1      | The Immune System - Basic Principles .....  | 1        |
| 1.1.1    | Introduction .....  | 1        |
| 1.1.2    | Exploitation of the Immune System for Prophylactic Vaccination.....                       | 4        |
| 1.1.3    | Mucosal Immunity .....  | 5        |
| 1.2      | Oral Vaccination .....  | 6        |
| 1.2.1    | Advantages of Oral Vaccination .....  | 6        |
| 1.2.2    | Immunophysiology of the Gastro-Intestinal (GI) Tract - A Barrier to Vaccine Delivery..... | 7        |
| 1.2.2.1  | Introduction .....  | 7        |
| 1.2.2.2  | Stability of Vaccines in the Fluids of Stomach and Intestine .....                        | 8        |
| 1.2.2.3  | Permeability of Vaccines in the Intestine.....  | 9        |
| 1.2.2.4  | Oral Tolerance vs. Immunogenic Response.....  | 17       |
| 1.3      | Technological Approaches for Oral Vaccine Delivery .....                                  | 20       |
| 1.3.1    | A Unique Class of Vaccines: Virus-like Particles (VLP) .....                              | 20       |
| 1.3.2    | Oral Vaccine Delivery - State of Art.....   | 22       |
| 1.3.3    | VLPs as Oral Vaccines.....  | 24       |
| 1.4      | Hepatitis B Core Antigen (HBcAg) .....  | 26       |
| 1.4.1    | Hepatitis B Virus (HBV).....  | 26       |
| 1.4.2    | Hepatitis B Core Antigen (HBcAg) Structure.....   | 28       |
| 1.4.3    | Hepatitis B Core Antigen (HBcAg) as a Vaccine .....                                       | 30       |
| 1.4.4    | Hepatitis B Core Antigen (HBcAg) Tandem Technology .....                                  | 32       |
| 1.5      | Plants as Bioreactors for Recombinant Proteins .....                                      | 33       |
| 1.5.1    | Introduction .....  | 33       |
| 1.5.2    | Stable Transformation <i>vs</i> Transient Expression.....                                 | 34       |
| 1.5.3    | CPMV- <i>HT</i> and pEAQ Expression Systems .....   | 35       |
| 1.5.4    | Transient Expression of Hepatitis B Core Antigen (HBcAg) in Plant.....                    | 38       |

|          |  |           |
|----------|--|-----------|
| 1.5.5    | Plant Oral Vaccines - the History of an Unmet Challenge .....  | 39        |
| 1.6      | Plant-expressed Oral Hepatitis B Vaccine - Where Are We?.....  | 43        |
| 1.7      | Objectives of the Research.....  | 46        |
| <b>2</b> | <b>Production, Purification and Characterisation of Plant-expressed HBcAg VLP .....</b>              | <b>48</b> |
| 2.1      | Introduction .....   | 48        |
| 2.2      | Materials.....   | 48        |
| 2.2.1    | Molecular Biology Media, Buffers and Solutions .....   | 48        |
| 2.2.2    | Antibodies and Antigens .....  | 49        |
| 2.2.3    | Plasmids .....   | 50        |
| 2.2.4    | Other Materials Used in the Molecular Biology Studies .....  | 51        |
| 2.3      | Methods.....   | 51        |
| 2.3.1    | Plant Expression of HBcAg and Protein Extraction .....   | 51        |
| 2.3.1.1  | Agroinfiltration .....   | 51        |
| 2.3.1.2  | Harvesting .....   | 52        |
| 2.3.1.3  | Protein Extraction.....  | 52        |
| 2.3.2    | HBcAg Purification.....  | 54        |
| 2.3.2.1  | Sucrose Density Gradient.....  | 54        |
| 2.3.2.2  | Dialysis.....  | 56        |
| 2.3.2.3  | Ultrafiltration.....   | 56        |
| 2.3.3    | Protein Qualitative Analysis .....   | 56        |
| 2.3.3.1  | Sodium Dodecyl Sulfate Polyacrylamide Gel Electrophoresis (SDS-PAGE) - Coomassie Blue Staining ..... | 56        |
| 2.3.3.2  | Dot Blot .....   | 57        |
| 2.3.3.3  | Western Blot.....  | 58        |
| 2.3.3.4  | Fluorescence Microscopy .....  | 58        |
| 2.3.4    | HBcAg Physical Characterisation .....  | 59        |
| 2.3.4.1  | Transmission Electron Microscopy (TEM) .....   | 59        |
| 2.3.4.2  | Native Agarose Gel Electrophoresis .....   | 59        |
| 2.3.4.3  | Sucrose Density Gradient.....  | 60        |
| 2.3.5    | Protein Quantitative Analysis.....   | 60        |
| 2.3.5.1  | Direct Enzyme-Linked Immunosorbent Assay (ELISA) .....   | 60        |
| 2.3.5.2  | Sandwich Enzyme-Linked Immunosorbent Assay (ELISA) .....   | 61        |
| 2.4      | Results and Discussion.....  | 62        |
| 2.4.1    | Expression of HBcAg and CoHe7e-eGFP in Plant.....  | 62        |
| 2.4.2    | Purification and Characterisation of Plant-expressed HBcAg VLPs .....                                | 64        |
| 2.4.2.1  | HBcAg Assembly in Plant Crude Extracts - A Qualitative Approach.....                                 | 65        |

|          |  |           |
|----------|--|-----------|
| 2.4.2.2  | HBcAg Assembly in Plant Crude Extracts - A Quantitative Approach.....  | 68        |
| 2.4.2.3  | Purified HBcAg VLP Characterisation .....  | 70        |
| 2.4.2.4  | Preparation of Purified VLP Batches .....  | 74        |
| 2.4.3    | Plant-expressed CoHe7e-eGFP Characterisation.....  | 77        |
| 2.4.4    | HBcAg Expression in Lettuce.....   | 81        |
| 2.4.5    | Conclusions .....  | 82        |
| <b>3</b> | <b>Stability of HBcAg VLP in Bio-relevant Gastro-Intestinal (GI) Media.....</b>  | <b>85</b> |
| 3.1      | Introduction .....   | 85        |
| 3.2      | Materials.....   | 88        |
| 3.2.1    | Molecular Biology Media, Buffers and Solutions .....   | 88        |
| 3.2.2    | Antibodies and Antigens .....  | 88        |
| 3.2.3    | Enzymes and Other Materials Used for Stability Studies .....   | 88        |
| 3.2.4    | Pig Small Intestinal Fluids .....  | 89        |
| 3.2.5    | Other Materials Used in the Molecular Biology Studies .....  | 89        |
| 3.3      | Methods.....   | 89        |
| 3.3.1    | HBcAg Stability in Simulated Gastric Conditions.....   | 89        |
| 3.3.1.1  | HBcAg Stability in Simulated Gastric Fluid (SGF) without Pepsin.....   | 90        |
| 3.3.1.2  | HBcAg Stability in Simulated Gastric Fluid (SGF) without Pepsin, Followed by pH Neutralisation .....                             | 91        |
| 3.3.1.3  | HBcAg Physical Stability in Acid Without Pepsin.....   | 92        |
| 3.3.1.4  | HBcAg Chemical Stability in Simulated Gastric Fluid (SGF) with Different Pepsin Concentrations .....                             | 93        |
| 3.3.1.5  | HBcAg Chemical Stability in Fasted State Simulated Gastric Fluid (FaSSGF) and in Fed State Simulated Gastric Fluid (FeSSGF)..... | 94        |
| 3.3.2    | HBcAg Stability in Simulated Intestinal Conditions and Pig Intestinal Fluids   | 95        |
| 3.3.2.1  | HBcAg Chemical Stability in Simulated Intestinal Fluid (SIF).....  | 96        |
| 3.3.2.2  | HBcAg Physical Stability in Simulated Intestinal Fluid (SIF) .....   | 96        |
| 3.3.2.3  | <i>Ex Vivo</i> HBcAg Stability in Natural Intestinal Fluid (natIF) .....   | 97        |
| 3.4      | Results and Discussion.....  | 98        |
| 3.4.1    | HBcAg Stability in Simulated Gastric Fluid (SGF).....  | 99        |
| 3.4.1.1  | HBcAg Stability in Simulated Gastric Fluid (SGF) without Pepsin.....   | 99        |
| 3.4.1.2  | HBcAg Chemical Stability in Simulated Gastric Fluid (SGF) with Pepsin....  | 107       |
| 3.4.1.3  | HBcAg Chemical Stability in Fasted State Simulated Gastric Fluid (FaSSGF) and in Fed State Simulated Gastric Fluid (FeSSGF)..... | 108       |
| 3.4.2    | HBcAg in Intestinal Fluids: An <i>In Vitro</i> and <i>Ex Vivo</i> Stability Approach .....                                       | 110       |
| 3.4.2.1  | HBcAg Stability in Simulated Intestinal Fluid (SIF) .....  | 111       |
| 3.4.2.2  | <i>Ex Vivo</i> HBcAg Stability in Natural Intestinal Fluids (natIFs) .....   | 115       |
| 3.4.3    | Contextualisation and Relevance of the Findings .....  | 118       |

|          |   |            |
|----------|---|------------|
| 3.5      | Conclusions .....   | 120        |
| <b>4</b> | <b>Exploitation of the Expression in Plant for Oral HBcAg Delivery .....</b>                          | <b>121</b> |
| 4.1      | Introduction .....  | 121        |
| 4.2      | Materials.....  | 123        |
| 4.2.1    | Molecular Biology Media, Buffers and Solutions .....  | 123        |
| 4.2.2    | Antibodies and Antigens .....   | 123        |
| 4.2.3    | Enzymes and Other Materials Used for Stability and Release Studies.....                               | 123        |
| 4.2.4    | Other Materials Used in Molecular Biology Studies .....   | 123        |
| 4.2.5    | Excipients Used for the Formulation of Tablets .....  | 123        |
| 4.2.6    | Excipients Used for the Coating of Tablets .....  | 124        |
| 4.3      | Methods.....  | 125        |
| 4.3.1    | Oven-drying .....   | 125        |
| 4.3.1.1  | In Process Dehydration of Oven-dried Leaves .....   | 125        |
| 4.3.2    | Freeze-drying .....   | 126        |
| 4.3.3    | Thermogravimetric Analysis (TGA).....   | 126        |
| 4.3.4    | HBcAg VLP Stability upon Oven- and Freeze-drying of Leaves.....                                       | 127        |
| 4.3.4.1  | HBcAg VLP Chemical and Physical Stability: A Qualitative Investigation ..                             | 127        |
| 4.3.4.2  | HBcAg VLP Stability: A Quantitative Measurement.....  | 128        |
| 4.3.5    | Delivery of Bio-encapsulated HBcAg in Simulated GI fluids .....                                       | 129        |
| 4.3.5.1  | Freeze-dried Bio-encapsulated HBcAg in Simulated Gastric and Intestinal Fluids.....                   | 129        |
| 4.3.5.2  | Delivery of Bio-encapsulated HBcAg in Intestinal Fluids, after Pre-incubation in Gastric Fluids ..... | 129        |
| 4.3.6    | Formulation of Tablets .....  | 131        |
| 4.3.7    | Physical Characterisation of Tablets .....  | 132        |
| 4.3.7.1  | Weight Uniformity and Hardness Tests .....  | 132        |
| 4.3.7.2  | Disintegration Time Test.....   | 132        |
| 4.3.8    | Coating of Tablets .....  | 133        |
| 4.3.8.1  | Preparation of Coating Dispersion .....   | 133        |
| 4.3.8.2  | Fluid-bed Coating.....  | 134        |
| 4.3.9    | Dissolution-Stability Test of the Enteric-coated Tablets .....  | 135        |
| 4.3.9.1  | Preparation of the Dissolution Media.....   | 136        |
| 4.3.9.2  | Dissolution Method .....  | 137        |
| 4.3.10   | Imaging of Uncoated and Coated Tablets .....  | 137        |
| 4.3.10.1 | Light Microscopy .....  | 137        |
| 4.3.10.2 | Scanning Electron Microscopy (SEM) .....  | 138        |
| 4.4      | Results and Discussion.....   | 138        |

|          |  |            |
|----------|--|------------|
| 4.4.1    | Drying of <i>Nicotiana benthamiana</i> Leaves Expressing HBcAg .....                             | 138        |
| 4.4.1.1  | Drying of <i>Nicotiana benthamiana</i> Leaves: Dehydration and Residual Moisture Content .....   | 139        |
| 4.4.1.2  | Stability of HBcAg VLP upon Oven- and Freeze-drying of Leaves .....                              | 141        |
| 4.4.2    | Delivery of Bio-encapsulated HBcAg in Simulated GI fluids .....                                  | 145        |
| 4.4.3    | Development of an HBcAg VLP Enteric-coated Tablet Formulation .....                              | 152        |
| 4.4.3.1  | Preparation of Tablets .....   | 153        |
| 4.4.3.2  | Enteric Coating of Tablets .....   | 154        |
| 4.4.4    | Contextualisation and Relevance of the Findings .....  | 159        |
| 4.5      | Conclusions .....  | 161        |
| <b>5</b> | <b>Formulation Development of Purified HBcAg VLPs Potentially Usable for Oral Delivery .....</b> | <b>163</b> |
| 5.1      | Introduction .....   | 163        |
| 5.1.1    | Granulation .....  | 164        |
| 5.1.2    | Spray Drying and Spray Freeze-Drying of pH Responsive Microparticles .....                       | 164        |
| 5.1.2.1  | Stability of Proteins within Microparticles - Encapsulation Efficiency .....                     | 166        |
| 5.1.3    | Freeze-drying of Biopharmaceutical Proteins .....  | 167        |
| 5.2      | Materials .....  | 168        |
| 5.2.1    | Excipients Used for Wet Granulation .....  | 168        |
| 5.2.2    | Excipients Used for the Microencapsulation Studies .....   | 169        |
| 5.2.3    | Excipients Used for the Freeze-drying Studies .....  | 170        |
| 5.3      | Methods .....  | 170        |
| 5.3.1    | Wet Granulation .....  | 170        |
| 5.3.2    | Formulation of HBcAg Containing Microparticles .....   | 172        |
| 5.3.2.1  | Stability Pre-formulation Assessment .....   | 172        |
| 5.3.2.2  | Spray Drying Process .....   | 173        |
| 5.3.2.3  | Spray Freeze-drying Process .....  | 174        |
| 5.3.2.4  | Characterisation of the Eudragit Particles .....   | 174        |
| 5.3.3    | Freeze-drying .....  | 176        |
| 5.3.3.1  | Stability of HBcAg upon Freeze-drying with Different Excipients .....                            | 176        |
| 5.3.3.2  | Thermal Analysis of Freeze-dried Excipients .....  | 177        |
| 5.4      | Results and Discussion .....   | 179        |
| 5.4.1    | HBcAg Stability upon Granulation – Preliminary Study .....                                       | 179        |
| 5.4.2    | Preparation of Eudragit Particles by Spray Drying and Spray Freeze-Drying .....                  | 182        |
| 5.4.2.1  | Spray Drying Process .....   | 182        |
| 5.4.2.2  | Spray Freeze-drying Process .....  | 186        |
| 5.4.2.3  | SEM Imaging of Eudragit Particles .....  | 186        |

|          |   |            |
|----------|---|------------|
| 5.4.2.4  | Encapsulation Efficiency and Gastro-Protective Properties .....                             | 188        |
| 5.4.3    | Freeze-Drying.....  | 191        |
| 5.4.3.1  | Stability of Purified HBcAg upon Freeze-drying with Different Excipients..                  | 191        |
| 5.4.3.2  | Thermal Analysis of Freeze-dried Excipients .....   | 195        |
| 5.4.4    | Contextualisation and Relevance of the Findings .....                                       | 204        |
| 5.5      | Conclusions .....   | 207        |
| <b>6</b> | <b>HBcAg Intestinal Permeability - an <i>in vitro</i> and <i>in vivo</i> Approach .....</b> | <b>208</b> |
| 6.1      | Introduction .....  | 208        |
| 6.1.1    | Human FAE Uptake Assay .....  | 209        |
| 6.1.2    | <i>In vivo</i> Ligated Intestinal Loop Model .....  | 210        |
| 6.2      | Materials.....  | 210        |
| 6.2.1    | Molecular Biology Media, Buffers and Solutions .....  | 210        |
| 6.2.2    | Antibodies and Antigens .....   | 210        |
| 6.2.3    | Human FAE Model Components.....   | 211        |
| 6.2.3.1  | Cell Lines .....  | 211        |
| 6.2.3.2  | Cell Culture Media, Chemicals and Plates.....   | 211        |
| 6.2.3.3  | Experimental Instruments .....  | 212        |
| 6.2.4    | <i>In vivo</i> Loop Study Materials .....   | 212        |
| 6.3      | Methods .....   | 212        |
| 6.3.1    | Transport of HBcAg VLPs through the Human FAE Model.....                                    | 212        |
| 6.3.1.1  | <i>In vitro</i> Human FAE Culture.....  | 212        |
| 6.3.1.2  | VLP Transport.....  | 213        |
| 6.3.1.3  | Quantification of Transport and $P_{app}$ .....   | 215        |
| 6.3.2    | <i>In vivo</i> VLP Uptake Assay .....   | 216        |
| 6.3.2.1  | VLPs Preparation and Quantification .....   | 216        |
| 6.3.2.2  | Small Intestinal Loop Assay .....   | 217        |
| 6.3.2.3  | HBcAg Quantification in Intestinal Tissue .....   | 219        |
| 6.3.2.4  | Fluorescent Microscopy and Immunohistochemistry .....                                       | 219        |
| 6.4      | Results and Discussion.....   | 220        |
| 6.4.1    | <i>In vitro</i> Human FAE Culture- Transport of HBcAg VLPs .....                            | 221        |
| 6.4.1.1  | Dose-dependent Transport .....  | 222        |
| 6.4.1.2  | FAE Selective Transport .....   | 223        |
| 6.4.2    | HBcAg VLPs Intestinal Permeability <i>In vivo</i> .....                                     | 225        |
| 6.4.2.1  | Fluorescent VLPs and HBcAg Preparation.....   | 225        |
| 6.4.2.2  | Localisation of Fluorescent VLPs in the Ileum.....  | 227        |
| 6.4.2.3  | Immunological Localisation of HBcAg in the Ileum.....                                       | 229        |

|          |  |            |
|----------|--|------------|
| 6.4.2.4  | Immunological Quantification of HBcAg in the Ileum ..... | 238        |
| 6.4.3    | Contextualisation and Relevance of the Findings .....    | 240        |
| 6.4.4    | Conclusions .....  | 241        |
| <b>7</b> | <b>Outlook and Future Work.....</b>                      | <b>243</b> |
| <b>8</b> | <b>References .....</b>                                  | <b>252</b> |

## List of Tables

|  |     |
|--|-----|
| Table 1.1. Characteristics of different classes of vaccines.....   | 22  |
| Table 2.1 Media, buffers and solutions used for molecular biology experiments. ....  | 49  |
| Table 2.2 Antibodies and antigens used for immunodetection assays.....   | 50  |
| Table 3.1. <i>In vitro</i> models of gastric fluids [adapted from(O'Neill et al., 2011)] .....   | 85  |
| Table 3.2. Components of incubation media. ....  | 88  |
| Table 4.1. HBcAg stability in bio-relevant GI fluids (summary of Chapter 3) .....  | 121 |
| Table 4.2. Formulation of the coating dispersion. ....   | 134 |
| Table 4.3. A summary of the residual moisture content (%) of oven- and freeze-dried leaf material (mean $\pm$ SD) as measured by TGA. .... | 140 |
| Table 4.4. Physical characterisation data for plant-based tablets (mean $\pm$ SD).....   | 154 |
| Table 5.1. Eudragit polymers characteristics .....   | 169 |
| Table 5.2. Granulation protocols.....  | 171 |
| Table 5.3. Eudragit re-dispersion. ....  | 172 |
| Table 5.4. HBcAg stability upon granulation. ....  | 181 |
| Table 5.5. HBcAg stability in Eudragit.....  | 182 |
| Table 5.6. Microparticles encapsulation efficiency and gastro-protection (%, mean $\pm$ SD; n = 3). ....                                   | 189 |
| Table 5.7. Summary of TGA/MTDSC thermograms of freeze-dried glycine (mean $\pm$ SD, n = 3) .....   | 196 |
| Table 5.8. Summary of TGA/MTDSC thermograms of freeze-dried lactose (mean $\pm$ SD, n = 3). ....   | 197 |
| Table 5.9. Summary of TGA/MTDSC thermograms of freeze-dried mannitol (mean $\pm$ SD, n = 3). ....  | 199 |
| Table 5.10. Summary of TGA/MTDSC thermograms of freeze-dried trehalose (mean $\pm$ SD, n = 3). ....  | 201 |
| Table 6.1 Antibodies used for immunohistochemistry (IHC) studies. ....   | 211 |

# List of Figures

|   |     |
|---|-----|
| Figure 1.1. Organs of the immune system (Moser and Leo, 2010). ....   | 2   |
| Figure 1.2. Peyer's patches compartments and cell distribution.....   | 10  |
| Figure 1.3. Overview of PP compartments with focus on the epithelium. ....  | 13  |
| Figure 1.4. Hepatitis B virus structure. ....   | 27  |
| Figure 1.5. HBcAg structure. ....   | 30  |
| Figure 1.6. Foreign protein expression using pEAQ-expression system.....  | 37  |
| Figure 1.7. Structure of the thesis. ....   | 47  |
| Figure 2.1. HBcAg virus-like particles (VLP) plant expression and protein extraction....                                    | 54  |
| Figure 2.2. A schematic representation of sucrose gradient purification.....  | 55  |
| Figure 2.3. HBcAg and CoHe7e-eGFP identification in <i>Nicotiana benthamiana</i> protein extracts. ....                     | 63  |
| Figure 2.4. Qualitative sucrose gradient analysis of plant crude extract. ....  | 66  |
| Figure 2.5. Quantitative analysis of sucrose gradient density fractions of plant crude extract.....                         | 69  |
| Figure 2.6. Purified HBcAg assembled into VLP.....  | 72  |
| Figure 2.7. Sucrose gradient analysis of purified VLPs.....   | 73  |
| Figure 2.8. VLP purification and concentration efficiency.....  | 75  |
| Figure 2.9 CoHe7e-eGFP purification and characterisation. ....  | 79  |
| Figure 2.10. HBcAg expression in lettuce. ....  | 82  |
| Figure 3.1. HBcAg stability in simulated gastric fluid (without pepsin). ....   | 101 |
| Figure 3.2. HBcAg stability upon incubation in simulated gastric fluid (without pepsin) and subsequent neutralisation. .... | 104 |
| Figure 3.3. HBcAg VLP stability in different acidic conditions. ....  | 106 |
| Figure 3.4. HBcAg digestion in SGF (with pepsin).....   | 108 |
| Figure 3.5. HBcAg digestion in FaSSGF and FeSSGF. ....  | 109 |
| Figure 3.6. HBcAg Chemical Stability in SIF. ....   | 111 |
| Figure 3.7 HBcAg Physical Stability in SIF. ....  | 113 |
| Figure 3.8. <i>Ex vivo</i> HBcAg Stability in pig intestinal fluids.....  | 116 |
| Figure 4.1. Preparation of leaf disks for different treatments. ....  | 128 |
| Figure 4.2. Fluid-bed coating. ....   | 135 |
| Figure 4.3. In process Gravimetric Analysis (GA) of oven-dried leaves.....  | 139 |

|   |     |
|---|-----|
| Figure 4.4. Stability of unpurified plant-expressed HBcAg upon drying of leaves.....                                | 142 |
| Figure 4.5. Quantitative evaluation of HBcAg stability upon drying of leaves.....                                   | 144 |
| Figure 4.6. Delivery of HBcAg from freeze-dried plant material into SGF and SIF. ....                               | 147 |
| Figure 4.7. Delivery of HBcAg from processed plant material upon incubation in GI simulating media.....             | 149 |
| Figure 4.8. Images of uncoated tablets.....   | 153 |
| Figure 4.9. Imaging of tablets coated using the short re-dispersion protocol. ....                                  | 155 |
| Figure 4.10. Imaging of tablets coated using the long re-dispersion protocol.....                                   | 156 |
| Figure 4.11. Gastro-resistance of the enteric coated formulation. ....  | 158 |
| Figure 5.1. Chemical structure of PVP. ....   | 168 |
| Figure 5.2. Chemical structure of HPMC. ....  | 169 |
| Figure 5.3. FTIR spectra of Eudragit microparticles. ....   | 185 |
| Figure 5.4. Schematic representation of the effect of heat and/or vacuum treatment on Eudragit microparticles. .... | 185 |
| Figure 5.5. SEM images of Eudragit spray dried microparticles containing HBcAg.....                                 | 187 |
| Figure 5.6. SEM images of Eudragit spray freeze-dried microparticles containing HBcAg. ....                         | 188 |
| Figure 5.7. Stability of HBcAg freeze-dried with different excipients.....  | 193 |
| Figure 5.8. MTDSC thermograms of freeze-dried glycine. ....   | 196 |
| Figure 5.9. MTDSC thermograms of freeze-dried lactose.....  | 198 |
| Figure 5.10. MTDSC thermograms of freeze-dried mannitol. ....   | 200 |
| Figure 5.11. MTDSC thermograms of freeze-dried trehalose. ....  | 202 |
| Figure 6.1. Representation of the human FAE model.....  | 215 |
| Figure 6.2. HBcAg dose-dependent transport.....   | 223 |
| Figure 6.3. HBcAg transport in co-culture and mono-culture. ....  | 224 |
| Figure 6.4. Coomassie stained SDS-PAGE gel of the formulations administered. ....                                   | 226 |
| Figure 6.5. Fluorescence microscopy. ....   | 228 |
| Figure 6.6. IHC of intestinal sections (control). ....  | 231 |
| Figure 6.7. IHC of intestinal sections after after 15 minutes incubation with HBcAg. ....                           | 233 |
| Figure 6.8. IHC of intestinal sections after 40 minutes incubation with HBcAg. ....                                 | 235 |
| Figure 6.9. IHC of the FAE after incubation with HBcAg. ....  | 237 |
| Figure 6.10. HBcAg quantification in the intestinal tissue. ....  | 239 |

## List of Abbreviations

---

|   |                  |
|---|------------------|
| 2-[ <i>N</i> -morpholino]ethanesulfonic acid                                  | MES              |
| 3-( <i>N</i> -morpholino)propanesulfonic acid                                 | MOPS             |
| 3,3',5,5'-Tetramethylbenzidine  | TMB              |
| Antigen-presenting cells  | APC              |
| Apparent permeability   | P <sub>app</sub> |
| B subunit of the heat labile toxin of enterotoxigenic <i>Escherichia coli</i> | LTB              |
| Bovine serum albumin  | BSA              |
| British Pharmacopoeia   | BP               |
| Cholera toxin   | CT               |
| Construct heterotandem core-GFP   | CoHe7e-eGFP      |
| Cowpea Mosaic Virus   | CPMV             |
| Days post-infiltration  | DPI              |
| Degree of substitution  | DS               |
| Dendritic cells   | DC               |
| Dithiothreitol  | DTT              |
| Dulbecco modified Eagle's minimal essential medium                            | DMEM             |
| Enzyme-linked immunosorbent assay   | ELISA            |
| Ethylenediaminetetraacetic acid   | EDTA             |
| Fasting state simulated intestinal fluid                                      | FaSSIF           |
| Fed state simulated intestinal fluid  | FeSSIF           |
| Fetal bovin serum   | FBS              |
| Follicle-associated epithelium  | FAE              |
| Follicles   | FO               |

|   |         |
|---|---------|
| Fresh weight  | FW      |
| Gastro-intestinal                                       | GI      |
| Germinal centers  | GC      |
| Gravimetric analysis                                    | GA      |
| Green fluorescent protein                               | GFP     |
| Gut-associated lymphoid tissue                          | GALT    |
| Hepatitis B core antigen                                | HBcAg   |
| Hepatitis B surface antigen                             | HBsAg   |
| Hepatitis B Virus                                       | HBV     |
| Horseradish peroxidase                                  | HRP     |
| Hypertranslatable                                       | -HT     |
| Immunohistochemistry                                    | IHC     |
| Immunostimulatory complexes                             | ISCOM   |
| Interfollicular region                                  | IFR     |
| kilo-ponds  | kp      |
| Luria-Bertani   | LB      |
| Mesenteric lymph node                                   | MLN     |
| Microcrystalline cellulose                              | MCC     |
| Microfold or membranous cells                           | M cells |
| Modulated temperature differential scanning calorimetry | MTDSC   |
| Mucosa-associated lymphoid tissue                       | MALT    |
| Natural intestinal fluid                                | natIF   |
| Optical density   | OD      |
| Pathogen- associated molecular pattern                  | PAMP    |
| Pattern-recognition receptors                           | PRR     |
| Peyer's patch   | PP      |

|   |                |
|---|----------------|
| Phosphate-buffered saline                                 | PBS            |
| Plasmid easy and quick                                    | pEAQ           |
| Polyethylene glycol                                       | PEG            |
| Polyvinylidene fluoride                                   | PVDF           |
| Polyvinylpyrrolidone                                      | PVP            |
| Relative humidity   | RH             |
| Scanning electron microscope                              | SEM            |
| Simulated gastric fluid                                   | SGF            |
| Simulated intestinal fluid                                | SIF            |
| Sodium dodecyl sulfate polyacrylamide gel electrophoresis | SDS-PAGE       |
| Standard deviation  | SD             |
| Subepithelial dome region                                 | SED            |
| T cell antigen receptor                                   | TCR            |
| T helper  | T <sub>h</sub> |
| Thermogravimetric analysis                                | TGA            |
| Thermolabile toxin  | LT             |
| Toll-like receptors                                       | TLR            |
| Total weight gain   | TWG            |
| Transepithelial electric resistance                       | TEER           |
| Transmission Electron Microscopy                          | TEM            |
| Triethyl citrate  | TEC            |
| Tris/Borate/EDTA  | TBE            |
| Tumor-inducing  | Ti             |
| VLP binding Green fluorescent protein                     | VLP-GFP        |
| Wild-type   | wt             |

## **1 Introduction**

The work described in this thesis was aimed to investigate the potential use of a recombinant protein expressed in plants for the formulation of an oral candidate vaccine. The model antigen used is the recombinant Hepatitis B core antigen (HBcAg).

This Chapter will cover the main background aspects of this research. General concepts of immunology, with particular emphasis on the immunophysiology of the gastro-intestinal (GI) tract will be initially described. Then after a brief discussion of the most common vaccine approaches, the particular features of a relatively new class of vaccine, i.e. virus-like particles (VLPs), will be described. Subsequently, a general background about Hepatitis B virus and about the current vaccination strategies against Hepatitis B will be given. Then the structure of HBcAg and its possible use as a model vaccine will be examined. Finally, the production of recombinant proteins, including that of HBcAg, in plant will be discussed. At the end, the specific objectives of the research will be defined.

### **1.1 The Immune System - Basic Principles**

#### **1.1.1 Introduction**

The immune system is an extremely complex apparatus whose function is to patrol and protect the organism from invasion by pathogens and subsequent infection. The organs of the immune system are often referred to as lymphoid and are divided into primary and secondary lymphoid organs. The primary lymphoid organs are responsible for the production of immune cells (i.e. lymphocytes) from immature progenitor cells and are located in the bone marrow and thymus. The secondary lymphoid tissues are constituted by organised aggregation of mature lymphocytes, together with other specialised cells of the immune system that are distributed all over the body: they include the lymph nodes, the spleen and the mucosal- and gut-associated lymphoid tissues (MALT and GALT respectively), i.e. tonsils and Peyer's patches (Hannigan et al., 2009a). Figure 1.1 shows the distribution of the main lymphoid sites in the body.

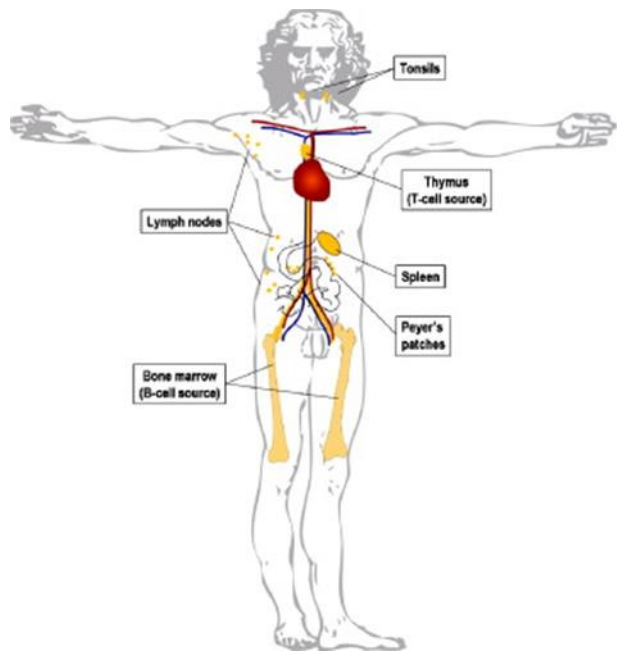


**Figure 1.1. Organs of the immune system (Moser and Leo, 2010).**

The immune system operates at different levels. The first line of defence is constituted by a series of non-specific physical and chemical barriers, which aim to prevent pathogen invasion. These include the skin's physical barrier, the mucosal membranes and the harsh and destructive GI environment. If pathogens do breach the physical and/or physio-chemical barriers, the innate immune system, considered the second line of defence, is usually capable of recognising and “inactivating” the invasive pathogen. As the word “innate” indicates, the activity of this apparatus is not based on specific memory patterns, but depends on the function of certain receptors to recognise generic molecular structures typical of most pathogens. These receptors of the innate immune system are called pattern recognition receptors (PRRs) and they recognise pathogen-associated molecular patterns (PAMPs), which are distinctive and recurrent molecular moieties present in numerous types of micro-organisms. Among other PRRs, toll-like receptors (TLR) seem to have a central role in the innate immunity. Such receptors are expressed in a wide range of cells of haematopoietic derivation: these include cells located in the tissues, such as dendritic cells (DC) and macrophages, but also circulating cells, such as neutrophils, eosinophils and monocytes (Doan et al., 2008a). Once the PAMPs present in the pathogens are recognised by the PRRs, the immune cells induce a cascade-type of response against the invading organism. The most common effector mechanism of the innate immune system is constituted by the elimination of the pathogen by phagocytosis (Stuart, 2005). This

phagocytic process does not have memory (i.e. it is innate) and hence, as a standardised process, it repeats itself identically upon subsequent infections.

Nevertheless, due to the extreme variability of the pathogens' molecular structures, many pathogens are capable of escaping recognition by the innate system. In this case the main line of defence is constituted by the adaptive immune system. The onset of this immune response is slower than that of the innate immune system. After recognition of the pathogen, the adaptive immune response aims to eliminate the pathogen and generate a sort of immune memory, which enables protection of the organisms from re-infections by the same pathogen. The cells of the adaptive immune system are called lymphocytes. Analogously to the cells of the innate immune system, lymphocytes are cells of haematopoietic origin and are present both in lymphoid tissue and as circulating cells in the blood and in the lymphatic circulation. Lymphocytes can be divided into B and T cells. B cells, upon encountering specific antigens, are stimulated to divide and differentiate into different subsets of cells, including plasma cells. Such plasma cells can produce high quantities of particular soluble proteins called antibodies. Antibodies are the main mediators of B cell immune responses; such immune responses are called "humoral", because the soluble antibodies are released in the blood and other fluids of the organisms. The function of antibodies is to bind specific antigenic structures, present in all pathogens. The binding of antibodies to the antigen is often sufficient to inactivate the antigen. Moreover, antibodies can activate complementary mechanisms to eliminate the pathogen. However, antibodies cannot cross the cellular membranes and hence cannot fight pathogens located intra-cellularly (Moser and Leo, 2010). Instead, T cells are active against intracellular pathogens. All the nucleated cells of the organism have the capability to expose partially digested intra-cellular proteins (in form of short peptides) at the surface of their plasma membrane. This mechanism enables exposing fragments of pathogens, which were present inside the cell, at the cellular surface. Such fragments can be recognised by specific receptors exposed by T cells, called T cell antigen receptor (TCR). This binding induces anti-pathogenic effects, which are mediated by soluble molecules (i.e. cytokines) (Moser and Leo, 2010).

### 1.1.2 Exploitation of the Immune System for Prophylactic Vaccination

The adaptive immune system is a key component of the immunogenic responses to pathogens and vaccines. The effectiveness of the adaptive immune system resides in the specificity and memory. These are essential features shared by both T and B cells. Specificity is defined as the capability of T and B cells and antibodies to individually recognise virtually any known pathogenic (or non-pathogenic) molecular structure. This is possible due to the extreme diversity of T and B cells, each expressing a unique receptor, bearing a unique configuration. Hence when an antigen enters the body for the first time, a specific lymphocyte will bind that given antigen. It has been estimated that the number of specific antigen binding sites, produced by the host, is greater than  $10^{11}$  (Hannigan et al., 2009b).

Nevertheless, the vast variety of the entire lymphocyte population implies that the relative amount of each lymphocyte will be very low. For this reason, in order to mount a strong immunogenic response upon contact with the antigen a given lymphocyte starts to multiply. Such phenomenon, called “clonal selection”, enables a given lymphocyte type to be overproduced (Burnet, 1976). This effect starts upon antigen exposure and can last the whole life cycle of the individual host. The overproduction of a specific lymphocyte that remains quiescent implies that upon a second exposure to the same antigen, a prompter and more potent immunogenic response can be elicited. This sort of “immune memory” is regularly exploited in prophylactic vaccination. For instance, exposure to a vaccine is supposed to represent the first exposure to one or more antigen belonging to a certain pathogen. Following the administration, a potent immunogenic response, characterised by T and/or B cell activation, should be elicited. As a consequence, the immunised subject will have one or a series of overrepresented lymphocytes. Such “memory cells” should be able to protect the immunised individual from harmful re-infection, upon subsequent exposure to the (otherwise virulent) pathogen (Gourley et al., 2004).

An ideal vaccine should not stimulate harmful side-effects when inducing the immunogenic and inflammatory response. At the same time it should be as good as natural pathogens in triggering potent immune responses, which includes the induction of “memory cells” (Zepp, 2010).

---

### 1.1.3 Mucosal Immunity

Mucosal membranes covering the body are constantly in contact with environmental pathogens. Physical and chemical barriers constitute a first line of defence. However, most mucosal sites are also well equipped with their own lymphoid tissue. This mucosal-associated lymphoid tissue (MALT) is considered separate and independent from the non-mucosal, so called peripheral or parenteral immune system (i.e. spleen and lymph nodes). Nevertheless, the lymphoid structures of the MALT appear similar to the one of the parenteral system. However, the two systems are not isolated and seem to constantly interact (Doan et al., 2008b).

Considering that many pathogens invade the host through mucosal routes, mucosal immune responses are considered strategically important: in fact the induction of immunity directly at the site of the entry of the pathogen can offer an excellent means of protection by vaccination. Indeed, generally strong mucosal immune responses are induced via mucosal immunisation. In contrast, parenteral immunisation often induces poor responses at the mucosal site and hence parenteral vaccination often fails in protecting the host from mucosal infections. Thus, it is clear how the development of mucosal vaccines could be beneficial for protection against pathogens that naturally infects or enter the host via the mucosal routes (McGhee et al., 1992; Neutra and Kozlowski, 2006). Furthermore, induction of immunity at specific mucosal sites can lead to protective immunity also at distal effector mucosal sites. This reflects the notions of a “common mucosal immune system”. However, this interplay between distal mucosal sites seems to be selectively compartmentalised. For example, nasal immunisation seems to evoke strong vaginal and pulmonary immunity; conversely nasal immunisation does not induce strong immunity in the gut (Holmgren and Czerkinsky, 2005). On the other hand, induction of potent systemic immunity is not only a prerogative of parenteral immunisation: in fact, mucosal immunisation can stimulate also strong and protective systemic T cell and B cell responses, including the activation of long term memory T and B cells (Lycke, 2012). In summary, parenteral vaccination often ensures strong immunogenic responses, but poor immunogenicity at mucosal sites; instead mucosal immunity can elicit both mucosal and systemic responses.

This research will focus on the mucosal delivery of antigens through oral route. Aside from the possible immunological advantages just mentioned, a series of other possible advantages related to the oral administration of vaccines will be discussed in the next Section.

## **1.2 Oral Vaccination**

### **1.2.1 Advantages of Oral Vaccination**

Vaccines are broadly regarded as one the major public health successes (Center for Disease Control (CDC), 2011). Vaccines are considered worldwide to be a cost-effective medical technology that generates broad spectrum benefits among populations of all ages (Poland and Jacobson, 2001). Nowadays vaccines are still mainly delivered by injection. However, there are several disadvantages and risks related to this route of administration. First of all, injections raise safety concerns, as the use of needles carries the risk of contamination with infectious diseases leading to transmission between patients and between patients and healthcare providers. Moreover, needle-stick injuries represent a further safety issue. These problems are particularly concerning in the developing countries, where improper and unsafe injection practices are not uncommon (Simonsen et al., 1999). Another concern about injectable vaccines is the reduced compliance with the recommended vaccination schedules. This is mainly related to the patients' acceptance of this uncomfortable and sometimes painful route of administration (Giudice and Campbell, 2006). Cost is another big disadvantage of most injectable vaccines and includes the cost of production of these sterile formulations, as well as their storage between 2 to 8 °C from manufacturing to the time of administration ("cold chain"). This clearly implies transport and cost-associated complications (Giudice and Campbell, 2006; Weir and Hatch, 2004). The need for healthcare personnel trained to deliver injections is another problem of this delivery route (Giudice and Campbell, 2006). Moreover, in the case of sudden outbreak of infectious diseases, the delivery of mass immunisation programme is intrinsically slowed by the complex administration route.

In this context, it is clear how the delivery of needle-free vaccine options could be highly desirable. Among other routes, the oral delivery of a vaccine could have the potential to

overcome all the limitations of the injectable vaccines mentioned above. Oral delivery is one of the most desirable routes of administration for patients and would not require the need of trained health care workers. Thus, oral vaccines could ensure ease of administration and higher compliance worldwide. Moreover, oral vaccines could offer a cheap needle-free option, as they would not require to be produced as sterile formulations. Additionally, plant-produced oral vaccines could potentially be stable at room temperature, eliminating the need for the “cold-chain” [(Daniell et al., 2009), discussed in 1.5.5]. As a result, the delivery of mass immunisation programmes worldwide could be more easily achieved if oral vaccines became a reality.

Despite all these advantages, the development of oral vaccines has always been limited by the presence of several physiological gastro-intestinal (GI) barriers, which often impede the delivery of the candidate vaccines to the effector sites that are responsible for the induction of protective immunogenic responses. Those gastro-intestinal barriers, which constitute a real challenge in oral vaccines design, will be examined in the next Paragraph.

## **1.2.2 Immunophysiology of the Gastro-Intestinal (GI) Tract - A Barrier to Vaccine Delivery**

### **1.2.2.1 Introduction**

The function of the gastro-intestinal (GI) tract is to digest nutrients into small molecules that can be absorbed. For example, in the case of proteins the absorption occurs after their digestion into oligo-peptide and amino acids (Jackson and McLaughlin, 2009). This mechanism prevents infection from harmful pathogens ingested, while ensuring nutrient assimilation. Obviously, such a digestive environment constitutes a barrier also to the absorption of protein-based therapeutic molecules. In fact, the harsh gastric and intestinal fluids represent severe obstacles to protein stability (Lee, 2002).

Aside from the presence of physicochemical and biochemical barriers, all the mucosal surfaces of the body, permanently in contact with the external environment, are patrolled by a highly specialised local immune system, the MALT, which constitutes almost 80% of the immunocytes of the whole body (Holmgren and Czerkinsky, 2005). The part of the

MALT located in the digestive tract is called gut-associated lymphoid tissue (GALT) and it represents on its own the largest immune system in the body, with  $10^{12}$  lymphoid cells per metre of human small intestine. In the intestine, 130 to 190 g of dietary proteins are normally absorbed daily and there are also  $10^{12}$  bacteria/g of stool colonising the gut, which potentially represents a further antigenic danger for the organism (Weiner et al., 2011). Therefore, the physiological roles of the GALT include defending the mucosal tissue and the body interior from pathogens, impeding intact ingested antigens from being absorbed and avoiding the occurrence of potentially damaging immune cascades if the antigens were absorbed (Holmgren and Czerkinsky, 2005; Neutra and Kozlowski, 2006).

Thus, to develop an oral protein-based vaccine, the challenge is to circumvent the GI barriers, as gastric and intestinal fluids could inactivate the vaccine in a similar way to the degradation of food and pathogenic proteins. Furthermore, the features of the GALT could prevent the uptake of the antigens. Finally, even though the mucosal tissue is always in a permanent condition of alert, it is also used to the presence of external microbiota. Therefore, the same vaccine, which induces strong immunogenic response when administered into sterile tissues, such as muscles, could be neglected when delivered into a tissue permanently subjected to foreign microbiota, such as the gut (Holmgren and Czerkinsky, 2005; Neutra and Kozlowski, 2006).

### 1.2.2.2 Stability of Vaccines in the Fluids of Stomach and Intestine

The physical and chemical instability typical of proteins in the gastric and intestinal fluids constitutes one of the main hurdles towards the effective delivery of vaccines through the oral route (Lee, 2002). The first physicochemical barrier encountered in the GI tract is constituted by the stomach fluid: the pH in the stomach generally ranges from pH 1 to 2.5 in normal fasted state condition (Evans et al., 1988). Furthermore, the stomach fluid is rich in the enzyme pepsin that constitutes a further biochemical barrier to proteins (Mahato et al., 2003). The intestine has a more neutral pH than the stomach, generally ranging from pH 6.3 to 7.5 (Evans et al., 1988). However, the intestinal fluid also represents a biochemical threat for therapeutic proteins' stability mainly due to the presence of pancreatic enzymes including trypsin and chymotrypsin (Mahato et al., 2003).

The stability of a protein must be evaluated both in terms of chemical and physical stability. The chemical stability is defined as the integrity of the amino acid sequence forming the primary structure of the protein; the physical stability is seen as the integrity of the three-dimensional structure, which consists of the secondary, tertiary and quaternary structure (Bilati et al., 2005). The acidic pH of the stomach can compromise the physical structure of a protein by denaturation, as well as possibly inducing oxidation, deamidation or hydrolysis in particularly sensitive proteins. The digestive enzymes present in both the stomach and intestine can chemically alter the primary structure by proteolytic degradation and as a consequence, also the secondary, tertiary and quaternary structure (Sood and Panchagnula, 2001).

### **1.2.2.3 Permeability of Vaccines in the Intestine**

#### **1.2.2.3.1 GALT Physiology**

The GALT, which contains the machinery to trigger an immunogenic response, represents the target tissue for effective oral mucosal vaccine delivery. However, the main barrier in oral protein delivery, including vaccines, still remains the low absorption of such macromolecules (Park and Kwon, 2011). Therefore, an in depth knowledge about GALT structure and function and about the closely related absorptive epithelium of the intestine is essential in order to successfully undertake oral vaccine design. The GALT is made of isolated and aggregated lymphoid follicles; in the small intestine there are clearly distinctive aggregated lymphoid follicles, called Peyer's Patches (PPs), termed after Johann Conrad Peyer, who first described them in 1677. They are major inductive sites for immune response in the gut (Neutra et al., 2001). PP are mostly located in the ileum and only a limited number are present in the rest of the small intestine. PP-like structures are also found in the colon (Cornes, 1965; Heel, 1997). The number of PP seems to increase through childhood reaching a maximum at puberty, when up to more than 200 PP in an individual have been measured (Cornes, 1965). Similarly to secondary lymphoid tissue, they are made of T and B cells: at the side of follicles (FO), which mainly consist of B cells, there are T cell-rich interfollicular regions (IFR), as shown in Figure 1.2. However, PP have some unique features of the MALT: they have only efferent and not afferent lymphatic vessels. Therefore, the possibility of circulation of antigen from secondary

lymphoid tissue to the PPs is reduced (Kunisawa et al., 2008). Furthermore, they contain a highly specialised epithelium typical of the MALT, called follicle-associated epithelium (FAE). Selective transport of antigen from the gut lumen into the PP take place mainly in this region (Owen and Jones, 1974). FAE epithelium will be described more in detail in the next Paragraph. Antigens efficiently transported through the epithelium come in contact with antigen-presenting cells (APC), mainly present as dendritic cells (DC) inside the PP. The processing and presentation of the antigen through the DC can trigger antigen-specific immunogenic responses: the position of the DC, mostly located in the subepithelial dome region (SED) (Figure 1.2), just under the FAE is strategic for the processing and presentation of the antigens to the immune cells (Kunisawa et al., 2012).

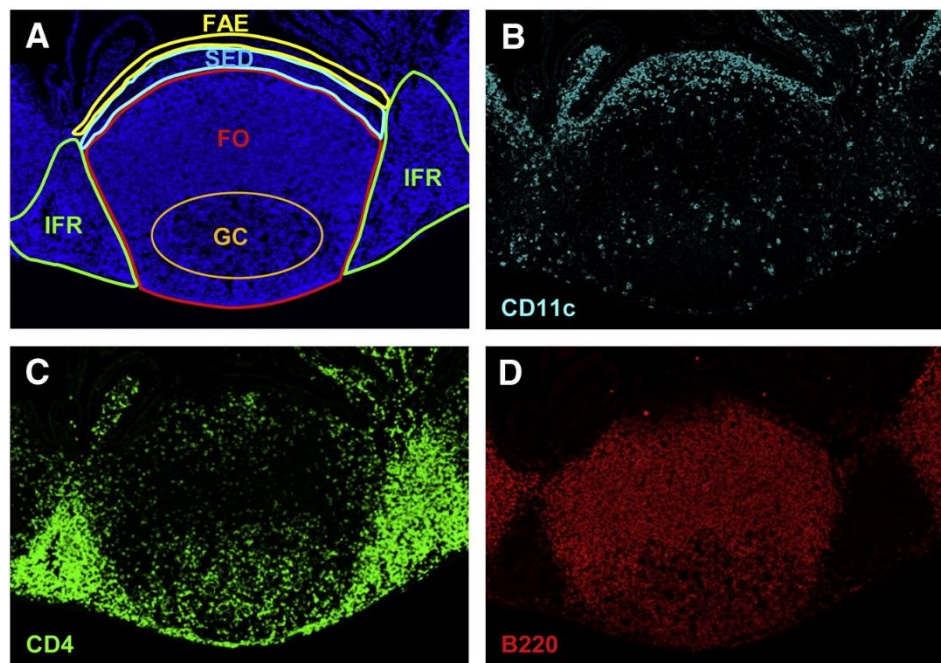


**Figure 1.2. Peyer's patches compartments and cell distribution.**

(A) 4', 6-diamidino-2-phenylindole stained PP. The contour of each region is drawn: follicle (FO), follicle-associated epithelium (FAE), germinal center (GC), interfollicular regions (IFR) and subepithelial dome region (SED); (B) Immunohistological data: staining for DC (anti-CD11c); (C) Immunohistological data: staining for T cells (anti-CD4); (D) Immunohistological data: staining for B cells (anti-B220). Image adapted from Kunisawa et al. (2012).

The mesenteric lymph nodes (MLN) appear also to play a key role in the GALT function and activation. They are considered to be an important communication link between the mucosal tissue in the gut and the peripheral lymph nodes; however, they have different organogenesis than peripheral lymphoid tissue and PP (Mowat, 2003).

### 1.2.2.3.2 FAE and M cells

Decades of research about the physiology and functions of the intestinal epithelium covering the intestinal mucosa has led to clearer understanding of such a complex tissue. The intestinal epithelium needs to allow absorption of water, ions and nutrients, but at the same time it has to act as a barrier to the large quantities of potential pathogens and macromolecules present in the gut. This obstacle to the penetration of macromolecules is provided by both physical and chemical mechanisms: first of all the epithelial cells, being connected by tight junctions, form a compact, almost impermeable, layer. Moreover, locally secreted IgA, the large glycocalix and the thick mucus layer covering the luminal side of those cells provide additional impediments to the penetration of pathogens. Despite its main function as a barrier, the intestinal epithelium must also allow the immunogenic machinery to function; this implies that macromolecules and antigens need to breach the barrier in a specific and organised manner in order to reach the intestinal immune system. The permeability of an antigen through the intestinal epithelium is considered a necessary step for the induction of protective mucosal and systemic immunity. For many years the scientific belief was that the transport of microorganism or antigens is a strict prerogative of the FAE overlying the PP: within the FAE, this unique function is accomplished by antigen-sampling microfold or membranous cells (M cells) (Nicoletti, 2000). Recently, an alternative and complementary mechanism of luminal antigen sampling, directly mediated by intestinal DC, has been proposed (Rescigno et al., 2001). However, the precise role of those DCs has not been fully determined yet and whether they are involved in the induction of immune response has not been clarified (Arques et al., 2009; Nicoletti et al., 2009). Further investigations of this antigen-sampling route are needed and to date M cells are still considered the main portal of entry for antigen presentation to the immune system.

M cells constitute 5% of the epithelial cells of the FAE in humans, with variations among other animal species (Buda et al., 2005). They have clearly distinctive characteristics which differentiate them from conventional epithelial cells: they are covered by only a thin layer of mucus and have a reduced glycocalix and short microvilli. On the basolateral side they have an invagination, forming a pocket which houses lymphocytes, macrophages and DC. M cells have also shown reduced intracellular lysosomal activity (Kraehenbuhl and Neutra, 2000). Figure 1.3 shows the main features of FAE, within PP. The function of M

cells reflects their morphological structure: M cells' main function is the transport of material from the gut lumen. The almost complete lack of mucus and short glycocalix allows easy contact with the pathogen or antigen. Thus the antigen could enter into direct contact with APCs in the basolateral pocket: the M cells' pocket provides a "short track" for the transport of the antigen to the immune cells. The reduced enzymatic activity prevents the digestion of the antigen inside the M cells, during its passage (Corr et al., 2008; Kunisawa et al., 2012; Nicoletti, 2000).

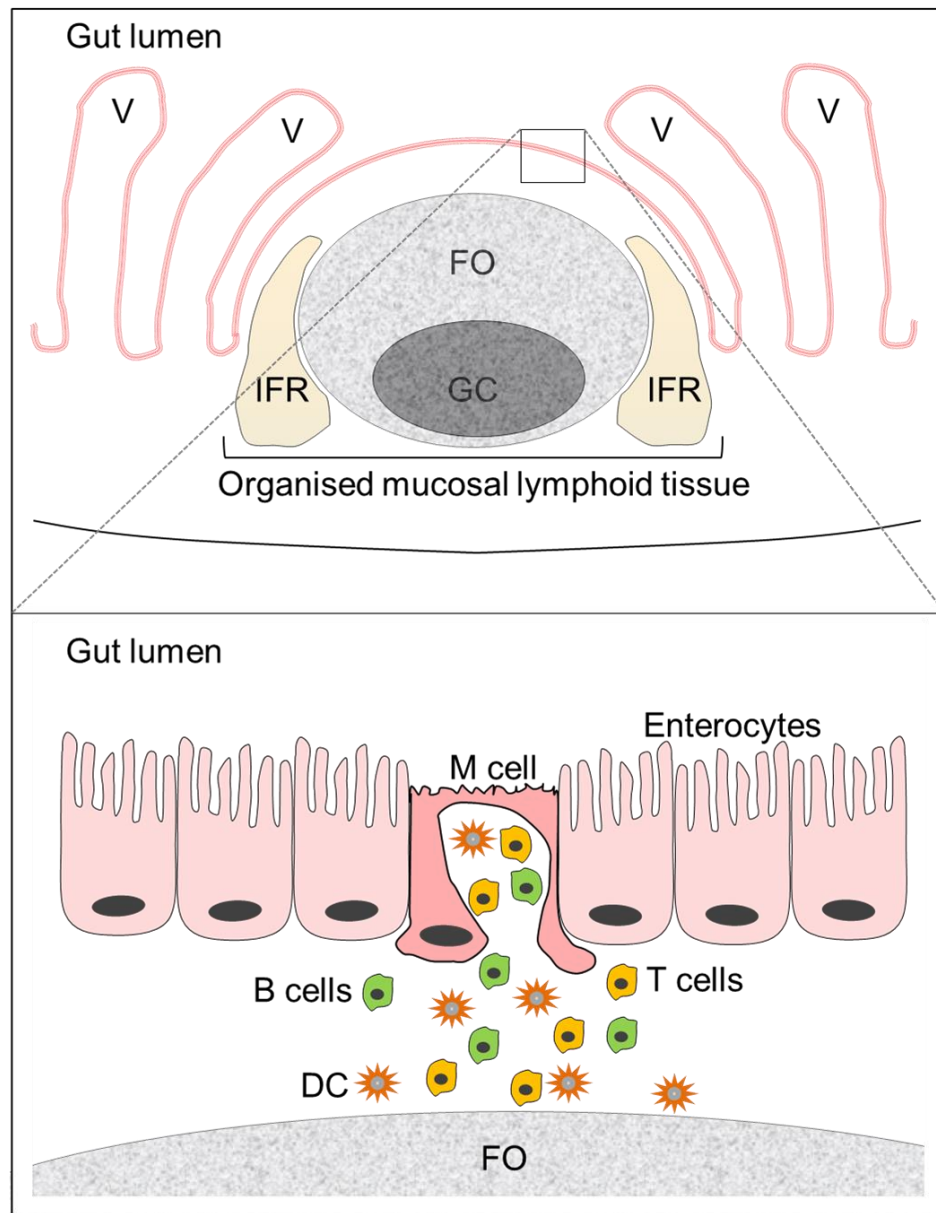


**Figure 1.3. Overview of PP compartments with focus on the epithelium.**

The upper illustration shows the structure of the PP: they form a dome-like shape, which is embedded within villi. PP contains organised mucosal lymphoid tissue. V = villus. The lower illustration is an enlarged representation of the FAE overlying the PP. The FAE is constituted by conventional enterocytes and M cells. M cells show unique features: short microvilli, basolateral pocket, intimate contact with APC, T cells and B cells.

M cells have shown efficient transport of various types of particulate substances, including latex beads, carbon particles, liposomes, bacteria and viruses (Corr et al., 2008). Conversely, the specific uptake of soluble antigens or molecules is poor (Awaad et al., 2011; Mayer et al., 2001). Based on this knowledge it is believed that trans-epithelial transport of particles or microbes does not seem strictly specific, as long as the substances

to be transported are in particulate form. The transport mechanism as well as the efficiency of transport seems to vary based on the nature of the particle transported (Des Rieux et al., 2007, 2005; Nicoletti, 2000). M cells' particularly intimate contact with APC, B and T cells suggest that they might have a greater functional involvement in the gut immunity, than just sampling antigens (Nicoletti, 2000). Moreover, the direct release of pro-inflammatory cytokines (i.e. IL-1) by M-cells is a further indication of their possible active involvement in the induction of immunogenic response in the gut (Pappo and Mahlman, 1993).

#### **1.2.2.3.3 Exploiting the M cells Gateway for Vaccine Delivery**

PPs have been named the “Achilles heel” of the intestinal barrier due to the M cells' specific ability to transport various microorganisms. This apparently negative regard given to the M cells underlines their capacity to allow the invasion of harmful enteric microorganisms into the mucosa leading to infection (Pron et al., 1998; Sansonetti and Phalipon, 1999). At the same time, this same feature can also be viewed as positive, considering the vital role of M cells in opening the gate of the immune system to therapeutics: the antigen-sampling activity can in fact be exploited in vaccine delivery for the protection against harmful pathogens (Nicoletti, 2000).

It is worth mentioning that M cell-mediated transport is particularly suitable for oral vaccine delivery, more than it is for any other therapeutic proteins. This is due to the fact that M cells' function has proved to be much more than simply antigen sampling: the housing of immunity cells in the M cell pocket allows fast and direct delivery of the candidate vaccine to the machinery capable of inducing immunogenic response. Therefore, if for other therapeutics, M cell-mediated delivery approaches can be advantageous, it could be indispensable in case of oral vaccines. In the last few years the growing understanding about M cells' formation has provided scientists with improved tools to study mucosal vaccine delivery. M cell ontogenesis is related to a series of endogenous and exogenous factors: exogenous *in vivo* short-term challenge with a non-intestinal bacterium *Streptococcus pneumoniae R36A* has been shown to increase the number of functional M cells and to enhance microparticles transport through the FAE in rabbits (Borghesi et al., 1999; Meynell et al., 1999). Similarly Raji B lymphocytes have been proven to convert undifferentiated intestinal epithelial cells into M cells (Kernéis et al., 1997), even when

Raji B and epithelial cell are co-cultured, but not in physical contact (Gullberg et al., 2000). The resulting scenario is that the immune system seems to play a role in the induction and regulation of operative M cells: this differentiation into operative M cells is induced by the same soluble cytokine produced by the host-bacteria interaction in case of bacterial challenge or by Raji B in case of co-culture with epithelial cells (Man et al., 2008). The co-culture conversion of epithelial cells has also been exploited to develop an *in vitro* model of FAE, useful for the assessment of new candidate vaccines or therapeutic proteins (Des Rieux et al., 2005; Kernéis et al., 1997).

Transport and uptake studies with particulate materials allowed the determination of the influence of the chemico-physical characteristics of the particles on M cell mediated transport:

- Nature of the material: Small molecules, such as dye, did not show PP-specific absorption (Awaad et al., 2011); small 2.5 nm dendrimers have also surprisingly shown poor absorption in PP, compared to larger size particles (Florence et al., 2000), but this result could be related to the low stability of those dendrimers in the gut (Hussain et al., 2001). Research about the FAE permeability at the interface between particles and molecules (as in the case of dendrimers) have not been further carried out and could clarify the limit of M cell sampling capacity.
- Size: size is one of the most important parameters that influence the uptake of particles by PP. Several studies over the years have demonstrated that particles ranging between 50 and 500 nm in diameter are more highly transported than larger particles (Des Rieux et al., 2006; Florence et al., 2000; Jung et al., 2000). A recent study defined a more precise optimal size: when 95, 130, 200, 340, 695, 1050 nm particles were given orally to mice, 95 nm particle showed the greatest transport in the PP (Awaad et al., 2011). These results are in accordance with Jani et al. (1990), who showed that in mice 50 nm particles were better absorbed in the PP and distributed in the body than 100 nm particles (Jani et al., 1990). The optimal range of size for PP absorption can be therefore narrowed down to 50 to 100 nm, probably with 50 nm better than 100 nm. Unfortunately there are no published data for particles smaller than 50 nm.

- Surface charge: a positive charge on the particles would seem to favour their uptake by M cells, considering the negative charge of the cell membrane. However, the mucus and ordinary epithelial cells' membranes are also negatively charged and therefore electrostatic interaction between the positively charged particles and negatively charged physiological components would be largely non-specific (Kammona and Kiparissides, 2012) and could lead to entrapment of particles by enterocytes, by mucus or by the cellular membranes of M cells. Accordingly, negative and non-ionic particles have shown better M cell-mediated transport than positively charged ones (Florence et al., 2000; Jung et al., 2000).
- Hydrophobicity/hydrophilicity balance: studies with nanoparticles have shown that hydrophobic surfaces tend to be more suitable for M cell mediated absorption, whereas more hydrophilic particles have better tropism for enterocytes (Des Rieux et al., 2006).
- Presence of targeting molecules: decorating the surface of particles with molecules targeting M cells can be a more specific way of increasing uptake and transport by M cells; increasing the specificity of M cell-mediated transport could counterbalance the unfavoured M cells/enterocytes ratio (M cells make only 5% of the epithelial cells). Several approaches have been studied: first of all, cellular glycosylation pathways have been investigated, so to be able to engineer the particles surface with lectin which could target specific sugars on the M cell surface. However, surface markers on the M cells have proved to be rather specific among animal species, making targeting studies more complicated. Other promising approaches have been based on the exploitation of the same M cell receptors to which pathogens naturally bind: bacterial surface proteins have been attached on the surface of particles in order to target M cells (Azizi et al., 2010; Brayden et al., 2005; Des Rieux et al., 2006). Similarly, other specific targets for pattern recognition receptors (PRR) of dendritic cells or macrophages have been developed (Chadwick et al., 2010).

Overall, experimental results are sometimes contradictory and vary between animal species and experimental conditions. Nevertheless, there is a general agreement in terms of optimal particle size, in the sense that smaller particles always tend to be better absorbed; however, in terms of hydrophobicity and surface charge the situation is more complicated (Des Rieux et al., 2006).

#### **1.2.2.4 Oral Tolerance vs. Immunogenic Response**

Even in cases in which the undigested vaccine could breach the intestinal barrier, another main risk of failure in oral vaccine delivery is the possibility of inducing oral tolerance, rather than protective immunogenic responses (Lycke, 2012; Mowat, 2003). This Paragraph describes how those two apparently opposite mechanisms can be developed within the same mucosal immunity machinery and what are the current approaches adopted in drug delivery in order to avoid oral tolerance.

##### **1.2.2.4.1 Mechanisms of Oral Mucosa Responses to Commensal and Foreign Microbiota**

Proteins from the diet and commensal bacteria colonising the gut in physiological conditions generally show oral tolerance: following exposure to the potential antigen, mesenchymal cells and macrophages produce prostaglandin E2 (PGE2) and epithelial cells transforming growth factor- $\beta$  (TGF- $\beta$ ) and possibly interleukin-10 (IL-10), which stimulate the maturation of DC. Consequently, those APC become able to present the antigen to naïve CD4+ T cells in the MLN or PP. These T cells switch into regulatory T cells, characterised by the production of IL-10 and interferon- $\gamma$  (IFN- $\gamma$ ) and other T helper (T<sub>h</sub>) 2-like cytokines, resulting in systemic and local tolerance. Furthermore, differentiation of the naïve CD4+ T cells into T helper (T<sub>h</sub>) 3 cells can also induce secretion of local IgA, which has several roles in the mucosal defence from pathogens and favours maintenance of the gut immune homeostasis (Mowat, 2003).

Conversely, the interaction with pathogens and their products in the gut tends to produce local inflammation: Toll-like receptors (TLRs), expressed by mesenchymal cells, macrophages and epithelial cells induce DC maturation. As a result, DCs that have taken

up the antigen in the Peyer's patch or lamina propria mature completely and produce the pro-inflammatory cytokine IL-12. Those DCs can also migrate to the MLN, where they induce differentiation of naïve CD4+ T cells into gut homing Th1 cells, which produce IFN- $\gamma$ , another pro-inflammatory cytokine (Mowat, 2003). Secretory IgA is also massively produced in case of immunogenic response to pathogens, therefore, they have an important role both in the case of tolerance and in case of immunogenic response.

Mucosal immunogenic responses and tolerance to antigens can be developed both locally and systemically. It has been hypothesised that the interplay of the MLN with PP and peripheral immune tissue allows the activation of local and systemic responses; however, the physiological mechanism behind these systemic response has not been fully understood yet (Mowat, 2003). The fact that mucosal entry routes of vaccine are able to induce not only local, but also systemic responses is an essential concept, which is often neglected in drug delivery. Oral vaccines research is often confined to vaccines against enteric diseases and instead it has also an interesting potential for vaccination against non-enteric pathogens (Wang, 2008).

#### **1.2.2.4.2 Vaccine Characteristics for the Development of Robust Immune Responses**

When discussing oral vaccines it is worth remembering that first the GI stability and second the entry of the vaccine in the effector sites are necessary prerequisites for inducing an immunogenic response: vaccine degradation or lack of absorption would therefore reduce contact with the cells of the immune system, decreasing any possible reaction and hence protection against the given pathogen. However, even if those first two major obstacles were overcome, the interaction of the candidate vaccine with the effector site of immunity in the gut would not necessarily lead to the development of strong protective immunity, as tolerance could arise (Mowat, 2003). Recently published results in this field allow the definition of the general characteristics that a vaccine candidate should have for the induction of immunogenic response:

- Antigen dose and schedule: for non-living vaccines, large and multiple doses are generally required to induce an immunogenic response (Mayer et al., 2001; Neutra and Kozlowski, 2006; Tacket and Mason, 1999); this also takes into account the

“upstream” tendency of vaccines to be poorly stable and poorly absorbed in the gut. However, it has also been reported that single high doses of antigen might lead to tolerance (Garside et al., 1995), whereas smaller, multiple doses could result in an immunogenic response (Strobel and Mowat, 1998). In the same manner low repeated doses of vaccine should induce tolerance, as may be the case with repeated ingestion of drinking water contaminated with potential pathogens, but very low doses have been shown to trigger mucosal and systemic immunogenic response (Mayer et al., 2001). It is clearly difficult to define general rules, because studies are often contradictory even with the same protein antigen: the general consensus is that each vaccine candidate should be evaluated independently in terms of dose and administration schedule.

- Antigen nature: soluble antigens have proved to be much more prone to tolerance than particulate vaccines, that instead tend to produce immunogenic responses: even in case of the same candidate antigen, the formulation of the vaccine in particulate form can abolish the development of tolerance in favour of strong immune responses (Challacombe et al., 1992; Mayer et al., 2001; O’Hagan et al., 1993). Aside from the great advantages of being taken up by M cells of the PPs, particulate vaccines with a repetitive structure can obviously be more efficient in presenting the “danger” signal to cells of the immune system (Herbst-Kralovetz, 2010; Huang, 2005). This is probably due to the similarity of those vaccines with the intrinsic nature of pathogens, which is particulate. The influence of particle size on induction of either tolerance or immunogenic response has not been directly evaluated; however the dependency of antibody production on the particle size has been evaluated, but results were different with different antigens, emphasising that case by case considerations have to be made (Des Rieux et al., 2006).

Thus, the overall picture suggests that particulate vaccines given orally favour effective immunogenic responses over tolerance. The dose and schedule of immunisation must be assessed on a case by case basis, but, considering the low bioavailability of oral vaccines, high-doses should be the first choice. As previously mentioned, protective immune responses through mucosal routes can be achieved by overcoming the three GI barriers: environmental instability of the vaccine in gut, reduced absorption and induction of

tolerogenic pathways. However, it is often difficult in cases of vaccine candidates which fail to induce protective immunity to define which one (or more) of those GI barriers was the obstacle that impeded a sufficiently strong immune response.

### 1.3 Technological Approaches for Oral Vaccine Delivery

#### 1.3.1 A Unique Class of Vaccines: Virus-like Particles (VLP)

Vaccines are biological preparations that induce protection of the body against a given pathogen. This protection is achieved by stimulation of the immune system. Live attenuated vaccines are widely considered the oldest and most effective vaccines. They are based on the use of whole viruses or bacteria, whose virulence had been attenuated (WHO, 2013). They stimulate strong humoral and cellular responses, which often enables protection against future infections. However, despite reduced pathogenicity, the pathogens, on which these vaccines are based, can still replicate and induce a mild infection soon after the vaccination. Furthermore, the good efficacy goes alongside a high incidence of side-effects, related to the reversion of the attenuated pathogen to more virulent and harmful forms (Martín et al., 2004).

On the other hand, inactivated vaccines, generated by killing the pathogen, are not able to replicate and therefore cannot restore virulence. Thus, inactivated vaccines are relatively safer, yet less effective than live attenuated vaccines (due to the inability to replicate), and several booster injections, as well as addition of adjuvants, are often required to obtain protective immunity (Liljeqvist and Ståhl, 1999; Ulmer et al., 2006; Wiedermann et al., 1990). Furthermore, as in the case of attenuated vaccines, regulatory requirements are difficult to meet, due to the fact that they are based on whole organisms (Liljeqvist and Ståhl, 1999). Alternatively, subunit vaccines obtained by extraction and purification of some of the antigens from the intact micro-organisms have been used as candidate vaccine components. Their efficacy was shown to be limited and large scale production is expensive and potentially unsafe, due to the risk of inefficient or incomplete purification and detoxification of the original pathogen (Liljeqvist and Ståhl, 1999; Ulmer et al., 2006). A promising class of vaccines is that of recombinant subunit vaccines which are composed of only some immunogenic portions of the target organism. They are expressed as

heterologous proteins in a variety of different hosts including mammalian cells, yeast, insect cells and bacteria. Subunit vaccines are safer than vaccines which are generated from whole pathogens. However, they bear only parts of the microorganism structure, therefore, their efficacy is expected to be lower than that of the whole pathogen types of vaccines and often high doses and multiple administrations are required to obtain protective immunity (Liljeqvist and Ståhl, 1999). Nevertheless, in the case of vaccines against viral pathogens, a new subclass of recombinant subunit vaccines has been shown to be highly effective. Virus-like particles (VLPs) are subunit vaccines that mimic the whole organism structure, but they do not contain the genetic material that allows the organism to replicate. As with all other subunit vaccines, VLPs are produced as recombinant heterologous proteins. However, in the case of VLPs the viral proteins naturally self-assemble into capsids in the host cell environment where they are produced. Their structure resembles the antigenic conformation and repetitive nature of the whole organism. These features allow VLPs to be as effective as inactivated vaccines, yet VLPs are also extremely safe as they cannot replicate, reverse or recombine to a more virulent form. Overall, VLPs combine efficacy of inactivated vaccines and safety of recombinant subunit vaccines (Jennings and Bachmann, 2008; Noad and Roy, 2003). The characteristics of each vaccine class is summarised in Table 1.1.

**Table 1.1. Characteristics of different classes of vaccines**

| Class of vaccine               | Ability to replicate | Overall safety** | Microorganism structural arrangement | Efficacy*** |
|--------------------------------|----------------------|------------------|--------------------------------------|-------------|
| <b>Attenuated</b>              | <i>Yes</i>           | +                | <i>Yes</i>                           | +++         |
| <b>Inactivated</b>             | <i>No</i>            | ++               | <i>Yes</i>                           | ++          |
| <b>Non-recombinant subunit</b> | <i>No*</i>           | ++               | <i>No</i>                            | +           |
| <b>Recombinant subunit</b>     | <i>No</i>            | +++              | <i>No</i>                            | +           |
| <b>Virus-like particle</b>     | <i>No</i>            | +++              | <i>Yes</i>                           | ++          |

\* *Unable to replicate, given the effectiveness of the purification and detoxification procedure.*

\*\* +, ++ and +++ indicates lowest, intermediate and highest safety profile, respectively.

\*\*\* +, ++ and +++ indicates lowest, intermediate and highest efficacy, respectively.

A relatively new and alternative class of vaccines is constituted by DNA vaccines, which are based on the transfection of a plasmid DNA into the cells of the host. The DNA containing genes that encode for an immunogenic protein of the pathogen is expressed, exploiting the translation machinery directly of the host cell. DNA vaccines could be advantageous compared to other classes of vaccines, particularly in those cases where antigenic drift of the pathogen strain rendered the more traditional vaccines less effective (Donnelly et al., 1995).

A broader description of vaccines for their general use as injectable vaccines goes beyond the purpose of the work described in this thesis. However, an examination of vaccines and VLPs used in oral delivery research will be given in the next Paragraph.

### 1.3.2 Oral Vaccine Delivery - State of Art

Recent literature reveals a rapidly growing interest in needle-free vaccine alternatives: a futuristic vision of potentially safe, effective, easily-delivered and cheap therapeutic options against many infectious diseases has widely spread among scientists in the last few

years. Oral delivery seems one of the most, if not the most, valued routes towards this objective. However, the oral route, as previously mentioned, is associated with three major challenges that could hinder effective oral vaccines delivery. Nevertheless, decades of research have allowed a deep understanding of those obstacles and have led to the development of progressively more valuable methods to overcome them. An overview of the current tools in the vaccine delivery arsenal and an analysis of the most promising and successful vaccine approaches are an essential step before attempting novel investigations.

Nowadays there are relatively few oral vaccines in the market and they are all attenuated or killed vaccines. There are a few examples of both bacterial and viral attenuated vaccines, including polio and cholera vaccines. They are known to be highly effective, but are often unstable and more importantly could raise safety concerns because the quiescent virulence can suddenly revive (Silin et al., 2007). Oral killed (or inactivated) vaccines have been shown on the other hand to be safer; however, they can still induce more or less severe side effects (Huang, 2004). Furthermore, they are generally less effective than attenuated vaccines (Silin et al., 2007). The commonalities of both approaches, relying on actual (attenuated or killed) pathogens, are the presence of robust pathogenic structures that can resist the GI harsh environment, or that can replicate in the gut (i.e. attenuated vaccines) and the presence of surface ligands that the invasive pathogen normally exploit to colonise and attack the host organism (Brayden et al., 2005; Lycke, 2012; Silin et al., 2007). All other vaccine candidates that are not based on whole (inactivated or killed) pathogens do not seem to have passed the phase I clinical trial stage (Amorij et al., 2012).

In the case of recombinant vaccines and DNA vaccines, adjuvants are often required in order to induce a strong oral immune response. Adjuvants can be categorised into three main classes: particulate adjuvants, targeting adjuvants and/or immunostimulatory adjuvants. First of all, the knowledge that the intestine is not a perfect barrier to particles has been exploited for the development of particulate carriers: a carrier is considered an adjuvant by protecting the antigen or DNA from the harsh GI condition and by enabling improved transport in the GALT (Saroja et al., 2011). Bacterial/viral carriers (Silin et al., 2007), polymeric solid micro- and nanoparticles (Chadwick et al., 2010) and vesicles (Wilku et al., 2013) have been the most investigated carriers for oral vaccine delivery.

Cellular targeting represents another adjuvant mechanism, improving the vaccine transport or presentation to the GALT. It can be achieved not only by using whole attenuated microorganisms as transporters for foreign vaccines, but also by decorating the carrier with targeting sequences for M cells, DC or macrophages [reviewed in Paragraph 1.2.2.3.3].

The third class of adjuvant is comprised of immunostimulatory adjuvants, which work by intensifying the immunogenic response. Bacterial-based adjuvants, as well as cytokines, chemokines, some plant compounds (e.g. saponins) and synthetic compounds, have been used for their immunomodulatory properties (Purcell et al., 2007; Silin et al., 2007). These adjuvants can often complement the vaccine formulation and sometimes one component bears both immunomodulatory and transporter properties: typical examples are immunostimulatory complexes (ISCOM), which have been exploited as mucosal adjuvants being at the same time carrier and immunostimulatory adjuvants (Cox et al., 2006).

In summary, the oral vaccine formulations available in the market are currently only those based on attenuated or killed pathogens. These types of vaccines have raised safety concerns over the years, causing the research focus to shift to the development of efficient subunit or DNA vaccines. These vaccines are safer and therefore are well regarded by pharmaceutical companies: safety is, in fact, a primary issue in vaccine industries, as they are the ones legally responsible for the adverse reactions of therapeutics. As a downside, they are less effective than attenuated vaccines, because they are less equipped to overcome the physiological GI barriers. Therefore, in the last few years carrier-, cell targeting- and immunomodulatory adjuvants have been investigated in order to improve subunit and DNA vaccine efficacy. It is worth remembering that the three types of adjuvants can often overlap, because good adjuvants can bear in the same structure the three components: typical examples are the saponin of the ISCOM or VLP, which will be discussed in the next Paragraph.

### **1.3.3 VLPs as Oral Vaccines**

VLPs (Paragraph 1.3.1) are ideal vaccine candidates for oral delivery as they should exhibit both the safety of subunit vaccines and the efficacy of inactivated viral vaccines. They in fact share the same viral particulate conformation of killed vaccines, but do not

carry the viral genome, and they therefore avoid the risk of reversion to virulence (Noad and Roy, 2003). They bear in the same structure the four components required for induction of potent immunogenic response:

- Antigenicity: the repetitive structure of the VLP is a high-density platform of hundreds of identical epitopes. This explains their higher intrinsic immunogenicity when compared to traditional subunit (soluble) antigens (Ludwig and Wagner, 2007).
- Carrier: as previously explained in Paragraph 1.3.2, efficient oral vaccines require the presence of a carrier that can improve the stability of the labile antigen in the harsh gastric environment and improve the intestinal transport. VLPs are self-carriers in the sense that the antigenic repetitive structure naturally forms particles. Their highly packed structure could be strong enough to survive the harsh GI environment (Herbst-Kralovetz, 2010; Huang, 2005). For example, Norwalk virus VLPs are stable at low pH and are trypsin resistant (Ausar et al., 2006; Jiang et al., 1992; O'Hagan et al., 1993). Furthermore, two plant viruses [Cucumber Mosaic Virus and Cowpea Mosaic Virus (CPMV)] have been demonstrated to be stable in simulated gastric and intestinal conditions (Nuzzaci, 2010; Rae, 2005). This suggests that VLPs of animal viruses may also be stable in the gut.
- M cell targeting: VLPs mimic the exact structure of viruses, therefore they use the same invasive mechanisms that viral pathogens exploit to infect the host. This is particularly true in the case of oral delivery of VLPs of enteric viruses: by exploiting the normal route of transmission of the pathogen, VLPs employ a sort of “natural” targeting of transporters to intestinal cells (Holmgren, 2005; Huang, 2005). It is also expected that the particulate nature of VLPs of non-enteric viruses would favour the M cell-mediated absorption. The VLP's average size of circa 50 nm seems the optimum for this purpose. *In vivo* M cell uptake of CPMV, has been recently shown (Gonzalez et al., 2009).
- Immunostimulatory: the size of most VLPs favours their uptake by the dendritic cells (DC) as the optimal size of nanoparticles to be uptaken by DC is 40 nm (Fifis et al.,

2004). Furthermore, the highly repetitive organisation of VLPs, which is different from the usual structure of the host proteins, exposes the cells of the immune system to molecular configurations typical of pathogens, called PAMPs. Those structures are recognised by TLRs and other PRRs of the host as a “danger signal” and thus trigger innate immune responses. Moreover, the presence of foreign nucleic acid in many VLPs candidates constitutes another immunostimulatory PAMP. All those characteristics of VLPs aid the development of potent immune responses (Plummer and Manchester, 2011).

VLPs have also the potential to be used as vehicles for the presentation of foreign epitopes: this adjuvant/carrier function has been also exploited for oral delivery (Niikura et al., 2002). Furthermore, certain VLPs can act as carriers for DNA vaccines (Takamura et al., 2004). To date several orally delivered VLPs have been assessed in pre-clinical studies and a few VLP candidates have entered phase I clinical trials (such as Norwalk VLP and HBsAg) (Kushnir et al., 2012).

## **1.4 Hepatitis B Core Antigen (HBcAg)**

In this Section background information regarding Hepatitis B and Hepatitis B Core Antigen (HBcAg), which is the candidate antigen used in this research, is given.

### **1.4.1 Hepatitis B Virus (HBV)**

Hepatitis B virus (HBV) is one of the major human pathogens. Chronic infection with HBV is associated with cirrhosis and primary liver cancer. It has been estimated that two billion people have been infected with HBV and every year HBV causes around 600,000 deaths world-wide (Center for Disease Control and Prevention (CDC), 2012). HBV has been ranked as the 10<sup>th</sup> leading cause of death in the world (Lavanchy, 2004). Acute HBV infection is often not lethal and individuals infected usually fully recover. However, in the case of vertical transmission from mother to neonate, there is a 90% risk that the acute infection can progress to chronic infection, which is the major cause of premature death from cirrhosis or liver cancer in 25% of the infected individuals. Instead, horizontal

transmission in adults via body fluids results in chronic infection in only circa 5% of the cases (Center for Disease Control and Prevention (CDC), 2012).

Hepatitis B belongs to the family of Hepadnaviridae; the 42 nm HBV virion is formed by an external envelope made of a lipid bilayer and three membrane proteins. The envelope surrounds an internal nucleocapsid. A 3.2 kB partially double-strand DNA is contained inside the nucleocapsid (Seitz et al., 2007). Figure 1.4 shows the structure of the HBV virion.

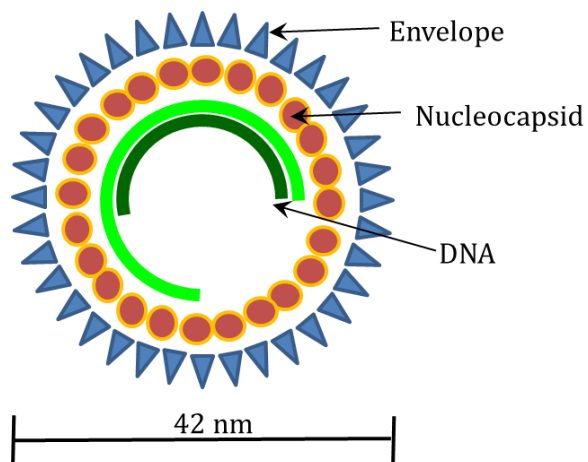


**Figure 1.4. Hepatitis B virus structure.**

Hepatitis B virus bears an external envelope forming a 42 nm shell and an internal nucleocapsid, which contains the viral partially double-stand DNA.

HBV replicates preferentially in hepatocytes. Receptor-mediated interaction of the virus with the hepatocytes results in internalisation of the virus, with detachment of the envelope and nucleocapsid release in the cytosol. Upon nucleocapsid entry into the nucleus, the viral genome is used as a template for transcription. The messenger RNAs are then translated into viral proteins in the cytoplasm, exploiting the host translational machinery. The viral proteins encoded are the envelope proteins, named Hepatitis B surface antigens (HBsAg) and the nucleocapsid protein, called Hepatitis B core antigen (HBcAg). Nucleocapsid assembly occurs in the cytosol. In the endoplasmic reticulum nucleocapsids are packed into the envelopes (Wei et al., 2010). A peculiar characteristic of HBV infection is the generation of other viral products aside from the 42 nm virion: a 22 nm subviral empty envelope shell as well as a soluble (non-particulate) form of core protein, named E antigen,

are also generated in large amounts during the infection (Jean-Jean et al., 1989; Wei et al., 2010).

### 1.4.2 Hepatitis B Core Antigen (HBcAg) Structure

Sequencing of the region of the HBV genome encoding for HBcAg allowed its expression in *Escherichia coli*, opening the possibility for a deeper understanding of this nucleocapsid antigen. Full-length HBcAg is 21 kDa monomeric protein (Figure 1.5 A), made of 183 amino acids (Pasek et al., 1979). Electron cryomicroscopy of recombinant HBcAg revealed that HBcAg monomers self-assemble into dimers which present a hammer-like shape with the handle being like a protruding spike (Figure 1.5 B). Dimers arrange into icosahedral spiky particles of two distinct subtypes (Figure 1.5 C): 34 nm particles, being the majority of the total population (circa 85%), are made of 240 HBcAg subunits, arranged as 120 dimers and with a  $T = 4$  triangulation number. The triangulation number is related to the icosahedral geometry. A second class of particles with a diameter of 30 nm was also identified: these particles consist of 180 HBcAg monomers, arranged as 90 HBcAg dimers and with a  $T = 3$  triangulation number (Birnbaum and Nassal, 1990; Crowther et al., 1994).

Further structural studies revealed two protruding  $\alpha$ -helical hairpins are connected by a loop within a monomer; the interaction of two hairpins of identical HBcAg monomers determines the formation of the spiky dimers, featuring a four-helix bundle (Böttcher et al., 1997; Wynne et al., 1999). Furthermore, two of the four cysteine residues contained in the full-length HBcAg have shown to be important for dimer stabilisation: the two Cys61 residues of identical monomers have shown to form a disulfide bridge which appears to stabilise the interaction of the hairpins of the two dimers (Wynne et al., 1999; Zheng et al., 1992). Cys183 of a monomer is also involved in a disulfide bond with the Cys183 of the other monomer of the dimer (Zheng et al., 1992). Nevertheless, Cys48 (Wynne et al., 1999) and Cys107 are present as free thiols (Zheng et al., 1992). The formation of disulfide bridges is not essential for particle formation. However, it seems to confer stability to the dimers (Wynne et al., 1999; Zheng et al., 1992).

The last 34 C-terminal amino acids of HBcAg sequence have been shown to be non-essential for HBcAg assembly into particles; however, this C-terminal arginine-rich

domain, also called protamine-like domain, was demonstrated to bind and encapsidate nucleic acids. This arginine-rich tail also confers overall positive charge to the protein (Birnbaum and Nassal, 1990; Gallina et al., 1989). A C-terminus truncated version of HBcAg, lacking the whole protamine-like domain, has been shown to assemble into particles, virtually devoid of nucleic acids and lacking the Cys183 disulfide bridge (Figure 1.5 A). The fact that the truncated version still forms particle suggests that the C-terminal arginine-rich tail is not essential for particle formation (Birnbaum and Nassal, 1990; Zheng et al., 1992). However, the C-terminus of the full-length protein seems to have an important role in particle stabilisation: in fact full length HBcAg particles subjected to different denaturing stress (i.e. high pH and SDS treatment), was shown to be more stable than truncated HBcAg versions (Birnbaum and Nassal, 1990; Newman et al., 2003).

HBcAg used in this project is a 176 amino acids deleted version of HBcAg (HBcAg $\Delta$ 176). It is a 20.2 kDa protein (Figure 1.5 A). It contains most of the protamine-like tail amino acids and is supposed to bind and encapsidate nucleic acids into its multimeric particles (Liu et al., 2010). Figure 1.5 illustrates the structure of HBcAg: the primary structure is presented as deleted versions and as full-length protein (Figure 1.5 A); the dimeric structure is also shown from two orientations (Figure 1.5 B) and finally the particulate structure is displayed in its T = 4 geometric class (Figure 1.5 C).

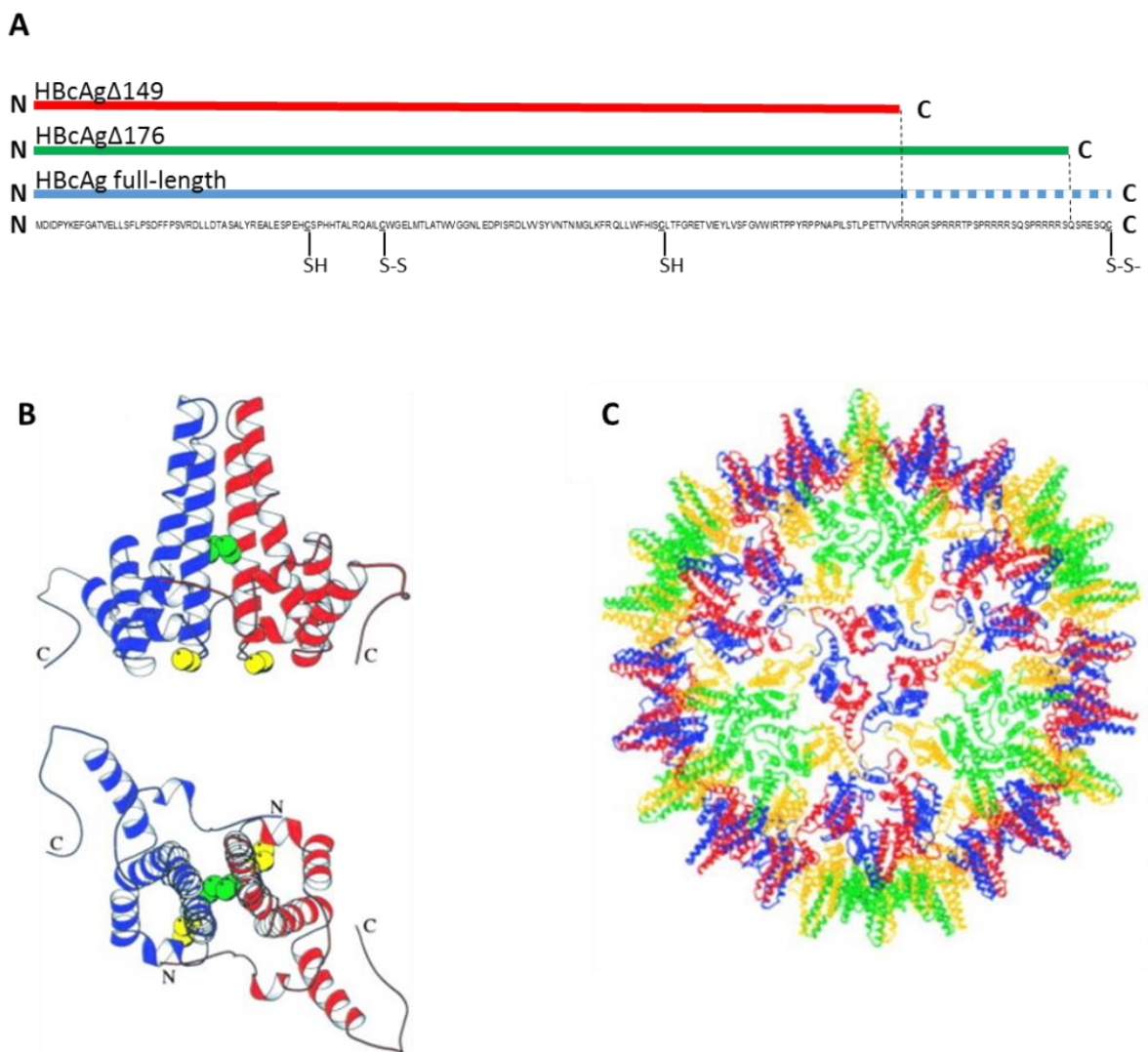


**Figure 1.5. HBcAg structure.**

(A) represents HBcAg amino acid sequence: HBcAg $\Delta$ 149 is the C-terminal deleted version, lacking the whole protamine-like domain. HBcAg $\Delta$ 176 is the C-terminal deleted version used in this study; HBcAg full-length is the naturally occurring 183 amino acids long version. The dash C-terminus indicates the protamine-like region. The four cysteine exposing free thiols or forming disulfide bridges are symbolised respectively by  $-SH$  or  $S-S$ . N = N-terminus, C = C-terminus (B) illustrates the dimeric hairpin-like structure, seen from two orientations. The green and the yellow spheres symbolise Cys61 and Cys48, respectively. (C) represents the surface of a particle bearing T = 4 geometry. The figure was adapted from Wynne et al. (1999).

### 1.4.3 Hepatitis B Core Antigen (HBcAg) as a Vaccine

Prophylactic vaccination is to date the best prevention strategy against HBV infection in humans. The current HBV vaccine is the recombinant surface protein (HBsAg) produced in yeast. It has been in the market for more than 20 years and it is produced by Merck (as

Recombivax HB) and GlaxoSmithKline Pharmaceuticals (as Engerix-B). HBV vaccine is given intramuscularly in a three-dose schedule. It is 80 to 100% effective and less than 5% of the people remain unresponsive to vaccine after receiving six doses, as they do not develop detectable anti-HBsAg antibody (Center for Disease Control and Prevention (CDC), 2012). HBV vaccine is now part of most mass-immunisation programmes worldwide: routine infant immunisation with hepatitis B vaccine was carried out in 152 countries already in 2002 (Lavanchy, 2004). Undoubtedly the current vaccine has proved to be overall effective in reducing the incidence of HBV infections worldwide. However, aside from the unresponsiveness of a small percentage of the population, this vaccine presents other drawbacks including the impracticality of the parenteral administration with a schedule of three doses, especially in developing countries (Tiwari and Vyas, 2011).

The core protein, HBcAg, has also been studied as a potential parenteral vaccine candidate. HBcAg has been shown to induce potent B and T cell responses (Milich et al., 1997, 1987a). The very strong immunogenicity of HBcAg could be related to its particulate nature. Surprisingly, HBcAg administration can also mediate anti-HBsAg antibody production. It was proposed that this capacity of eliciting anti-HBsAg responses could be the mechanism underlying the ability of HBcAg to protect against HBV infection (Milich et al., 1987b). In fact, it was shown that HBcAg could partially or fully protect chimpanzees against HBV infection (Iwarson et al., 1985; Murray et al., 1984). More recently, HBcAg has shown an immune-enhancing effect on co-delivered HBsAg upon nasal administration in animal studies (Aguilar et al., 2004; Lobaina et al., 2003). Furthermore, a phase I clinical trial has demonstrated that seroprotective anti-HBsAg antibody levels could be induced in 75% of the subjects to which the HBcAg/HBsAg formulation was co-delivered nasally (Betancourt, 2007).

Over the years, HBcAg has also earned the reputation of being an exceptionally promising carrier for foreign epitope sequences. The theory behind the use of particles as carriers for foreign antigens is based on the fact that, though soluble antigens are safe, they often fail to induce strong immunogenic response. Therefore, the conjugation of such antigens to particulate carriers can allow high density and repetitive display of the epitopes of interest on the surface of particles (Grgacic and Anderson, 2006). HBcAg VLP is considered a particularly good candidate for its use as vaccine platform for foreign antigens, because of

its extremely high intrinsic immunogenicity. HBcAg's capability of eliciting strong antibody production, inducing T cell production and mediating anti-HBsAg responses suggested that they could be exceptionally effective carrier vehicles for foreign epitopes (Milich et al., 1987b). In addition, HBcAg is non-cytotoxic and well tolerated in humans. Moreover, HBcAg has demonstrated flexibility in sustaining chemical and genetic insertions without alteration of the particulate integrity. Insertion of the foreign sequences is usually obtained by genetic insertion of foreign sequences in the loop region, which is the tip that connects the two  $\alpha$ -helix of the hairpin-like structure. Insertion of up to 55 amino acids have shown to be compatible with maintenance of the particle assembly (Whitacre et al., 2009).

#### **1.4.4 Hepatitis B Core Antigen (HBcAg) Tandem Technology**

One of the major limitations in using HBcAg as VLP platform for presentation of foreign epitopes is that large insertions in the loop region of HBcAg can be incompatible with particle assembly. This is mainly due to the fact that, within a dimer, the two loops of each monomer are very close and are both sites of insertions. For this reason, the inserted epitopes are sterically hindered with respect to each other, impeding initial dimerisation and subsequent particle formation (Nassal et al., 2008).

A research group in Leeds developed a technology to reduce this spatial obstruction on the site of the insertions (Gehin et al., 2007): genetic fusion of two HBcAg monomers through a flexible linker allowed production of a dimer-like protein as a single peptide. In this way, the two loops could be modified separately. The tandem HBcAg technologies enable having a single insertion within a dimer. This is in contrast with the double insertion, which is unavoidable when using wild-type HBcAg, where the dimer is made of two identical repeated structures. This tandem technology, by having only half of the tips of each monomeric loop bearing a foreign sequence, can significantly reduce the steric hindrance, potentially allowing larger sized insertions (Gehin et al., 2007).

## 1.5 Plants as Bioreactors for Recombinant Proteins

### 1.5.1 Introduction

“Molecular farming” is the term given to the production of pharmaceutically and commercially valuable proteins in plants (Franken et al., 1997). This description emphasises the fact that the production of valuable molecules could be as easy as the cultivation of plants. Molecular farming enthusiasts advocate that expression of recombinant proteins in plants is both easy to optimise and to scale-up. Thus, molecular farming could offer an effective means for the production of pharmaceutical and therapeutic proteins, including those whose therapeutic potential has not been evaluated due to the lack of a production system (Fischer and Emans, 2000). Historically, recombinant protein production has been mainly limited to production in bacteria, yeast, insects and mammalian cells. The main advantages for the use of plants for expression of heterologous proteins are indicated below:

- Plant ensures a higher eukaryotic synthesis pathway, analogous to those of animals cells and compatible with mammalian protein glycosylation (Cabanes-Macheteau et al., 1999; Fischer and Emans, 2000); this offers a high chance to produced full-size complex recombinant protein.
- Multimeric proteins as complex as antibodies or VLPs can be expressed in plants and the expression is often compatible with their correct folding and assembly (Ma et al., 1995; Mason et al., 1992; Thuenemann et al., 2013).
- Plant expression systems are cheap and easy to scale-up. In particular, in the case of transgenic expression, plant recombinant proteins could be farmed at agricultural scales (Fischer and Emans, 2000)
- Plant expression is virtually free from possible contamination or co-purification with human or animal pathogens or oncogenic sequences (Fischer and Emans, 2000; Ulmer et al., 2006).

- Plants can be potentially used for the development of oral vaccines [reviewed in Paragraph 1.5.5].

The first pharmaceutically relevant recombinant protein was expressed in plants in 1986. It was a form of human growth hormone expressed in transgenic tobacco (Barta et al., 1986). Since then, an extremely wide range of recombinant proteins has been produced in plants. These include therapeutic proteins such as vaccines, antibodies, cytokines, blood proteins, growth factors, therapeutic enzymes and insulin. Furthermore, many enzymes for industrial use and some biopolymers have been also produced in plants and some have already reached the market (Lico et al., 2012; Xu et al., 2012). However, only very recently, the first plant-produced biopharmaceutical has been approved for human use by the US Food and Drug Administration: this recombinant protein is taliglucerase alfa, an enzyme used for treating type 1 Gaucher's disease (Fox, 2012). Despite the huge production of recombinant proteins for human use, only one has reached the market level so far. This clearly suggests that the biggest challenge to be overcome is still the acceptance from regulatory bodies. Furthermore, persistent "industrial inertia" does not enable the switch from the conventional production systems already in place to the plant-based system, because this would require considerable initial investments (Ma et al., 2003; Rybicki, 2009).

### 1.5.2 Stable Transformation vs Transient Expression

Recombinant protein production in plants has been for long, mainly relegated to stable integration of constitutively expressed transgenes into the genome of the host plants. This production system is very easy to scale-up, because once transgenic lines are produced, the scale-up could consist of simply sowing the seeds (Fischer and Emans, 2000). In the case of recombinant protein production in transgenic plants, the fact that there is already a regulatory framework in place for GM crops and food could potentially reduce the regulatory obstacles (Spök et al., 2008). However, the generation of transgenic lines is quite a long and troublesome process and it can take up to 9 months before being able to analyse the expressed proteins.

On the other hand, transient expression of heterologous proteins in plants does not present this limitation. As the name suggests, transient expression systems are based on temporary transformation: the foreign genes are not integrated with the host chromosomes, but they are present in the nucleus where they are transcribed (Fischer and Emans, 2000). Transient expression can be used as a means of testing whether a certain protein can be efficiently expressed in a plant, as maximum expression levels can be achieved in just seven days, thereby allowing fast screening of new constructs (Sainsbury and Lomonossoff, 2008). The main disadvantage of the transient expression, compared to the stable transformation, is the relatively more difficult scalability than the stable transformation (Daniell et al., 2009)

Transient expression can be achieved in *Nicotiana benthamiana* by agroinfiltration: a simple method based on the use of *Agrobacterium tumefaciens*. This bacterium contains a tumour inducing (Ti) plasmid, in which the disease and virulence causing elements are substituted with the foreign genes of interest necessary for the expression of the recombinant protein. Agroinfiltration is achieved by simply forcing a suspension of the modified *Agrobacterium* into the intercellular spaces of the leaf lamella. The bacteria can then attach to the plant cell and transfer the gene responsible for the foreign protein expression into the cell. For small scale experiments, this can be achieved by syringe infiltration. However, this process can be easily scaled up using vacuum-agroinfiltration (Fischer et al., 2004). Large scale production of foreign proteins in plants by means of transient expression is already a reality. In fact, Medicago Inc., (Quebec, Canada) has current Good Manufacturing Practice (cGMP) facilities for production of plant-made vaccines. Medicago already produce vaccines for Phase I and Phase II clinical trials; moreover, this company proved that it was possible to produce 10 million doses of a cGMP-grade influenza vaccine in less than 30 calendar days (<http://www.medicago.com>). This achievement highlights that transient expression could be an efficient way to promptly achieve industrial scale production of novel vaccines tailored against newly emerging pandemic outbreaks.

### 1.5.3 CPMV-HT and pEAQ Expression Systems

In the past decades, transient expression of foreign proteins in plants has been mainly based on agroinfiltration or alternatively achieved using plant viral vectors. Viral vectors

exploit the capacity of plant viruses to infect plants, for the production of the heterologous protein of interest. Originally, heterologous gene sequences were included into the full viral genome; the capacity of the virus to infect the plant and to replicate was exploited for the concomitant production of the foreign protein. However, this method had several drawbacks, including the impossibility of producing large and complex heterologous proteins and the presence of recombinant, highly infectious viruses poses obvious bio-containment issues (Gleba et al., 2004).

A remarkable breakthrough in this field consisted of the coupling of agroinfiltration with the use of deconstructed viral vectors that cannot replicate (Rybicki, 2010). The use of non-replicating viral vectors that can be targeted to the nucleus of the plant cell by agroinfiltration overcomes most of the hurdles encountered with full viral vector systems. Among other expression systems, the Lomonosoff group at the John Innes centre (JIC), Norwich have focused on the development of Cowpea Mosaic Virus (CPMV)-based expression systems. CPMV contains two genomic RNAs; over several years of research, it was demonstrated that only the so called 5' untranslated regions (5'-UTRs) and 3' untranslated regions (3'-UTRs) of CPMV RNA-2, in the presence of RNA-1 and a suppressor of silencing, were essential for good levels of expression of inserted heterologous proteins. Basically, it was found that only the sequence upstream (5'-UTR) and downstream (3'-UTR) to the encoded sequences of RNA-2 were essential for the expression of an inserted heterologous genes. Hence removing most of the RNA-2 sequence, including those encoding for the actual plant virus (i.e. CPMV), was still compatible with the expression of the heterologous protein. RNA-1, responsible for the RNA-2 replication, had to also be present. The use of this highly deleted version of the viral genome did not allow the production of infectious virus, whose sequences were substituted with those for the expression of the heterologous genes. Therefore this approach solved the biocontainment issues typical of full vectors systems (Cañizares et al., 2006).

Nevertheless, a huge step forward in this technology came with the finding that the expression of the foreign protein could be enhanced by at least 10-fold by further deletions of the RNA-2 5'-UTR. The removal of two start codons, which are located upstream to the start codon for the heterologous protein, generated this huge increase in the expression

---

level. Furthermore, it was found that the higher expression was not related to increased transcription level, but to enhanced translation. From this, the name *hypertranslational* (-HT) was given to the expression system. This also obviated the need for replication, so co-infiltration with RNA-1 was not required (Sainsbury and Lomonossoff, 2008).

Soon after this technology was optimised by the development of a plasmid that could combine the high yield achievable with the CPMV-*HT*, with the possibility of easily inserting longer expression sequences and multiple insertion sites. This system, called plasmid easy and and quick (pEAQ) enables easy one-step cloning (Sainsbury et al., 2009). Figure 1.6 illustrates a schematic representation of the steps required for the preparation of pEAQ vectors usable for the transient expression of heterologous proteins by means of agroinfiltration.

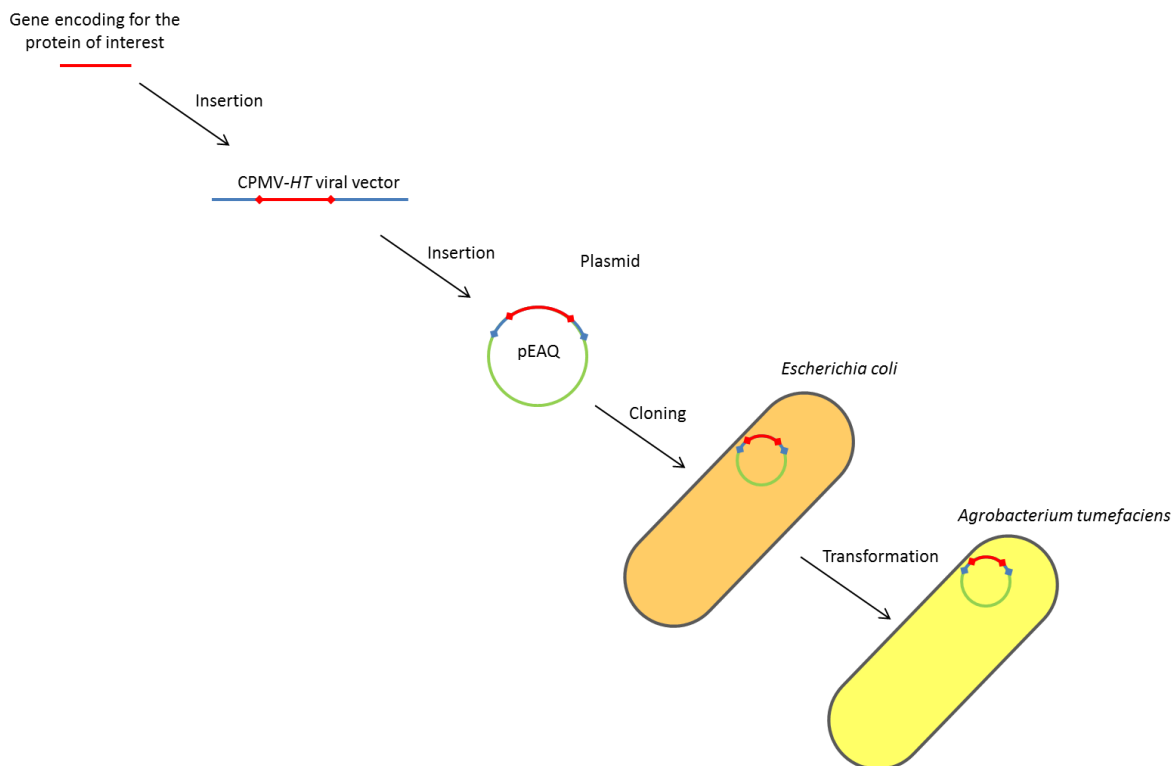


**Figure 1.6. Foreign protein expression using pEAQ-expression system.**

The gene encoding for the heterologous protein is initially inserted into the CPMV-*HT* RNA-2 sequences. Then this viral vector is inserted into pEAQ plasmid, which is subsequently cloned into *Escherichia coli*. Finally, after transformation of the plasmid into *Agrobacterium tumefaciens*, the bacterial suspension can be used for agroinfiltration.

Upon infiltration of the intercellular space of the plant leaf with the *Agrobacterium* suspension, the plasmid enables transfer of the encoding sequences to the cellular nuclei. Here the CPMV-*HT* system mediates the expression of the recombinant protein. Interestingly, this viral vector system of expression does not rely on enhanced replication or transcription of the foreign sequences, but on extremely efficient translation (Sainsbury and Lomonosoff, 2008).

In only five years from when it was first published, the CPMV-*HT* system has been used in more than 200 universities and institutes for research purposes (Prof Lomonosoff personal communication). Furthermore, it has been adopted for industrial-scale production of an Influenza hemagglutinin vaccine, which is currently used in clinical trials (D'Aoust et al., 2010).

#### **1.5.4 Transient Expression of Hepatitis B Core Antigen (HBcAg) in Plant**

HBcAg was expressed for the first time in plants by the Lomonosoff group, using a full length viral vector system. The yield achieved was variable, from circa 10 to at least 50 mg/kg of fresh weight of the leaves, depending on the viral vector used (Mechtcheriakova et al., 2006). In the same year it was demonstrated that using another expression system, HBcAg could be expressed in plant up to levels of 2.4 g/kg of fresh weight leaf tissue. The immuno-equivalence of this plant-produced HBcAg to HBcAg produced in bacteria was also demonstrated (Huang, 2006). HBcAg was finally produced also using the CPMV-*HT* system to levels of 1 g/kg of fresh weight tissue (Sainsbury and Lomonosoff, 2008). Furthermore, recombinant tandem HBcAg (described in Paragraph 1.4.4) was also expressed in plants in a particulate form. Additionally, green fluorescent protein (GFP) could be genetically inserted in the tip of the dimeric structure with this insertion being compatible with particle formation (Thuenemann, 2010).

HBcAg (HBcAg $\Delta$ 176) was produced in *Nicotiana benthamiana* throughout this study, using the viral vector CPMV-*HT* (Sainsbury and Lomonosoff, 2008), inserted into pEAQ plasmid (Sainsbury et al., 2009). Moreover, one version of the tandem construct, codifying for heterotandem core-GFP, named CoHe7e-GFP, was used in this project. The main

reason for its use was that CoHe7e-GFP consists of a fluorescent version of HBcAg and it could therefore be used as an investigation tool for bio-imaging.

### **1.5.5 Plant Oral Vaccines - the History of an Unmet Challenge**

Scientific articles on the use of VLPs for oral delivery are often also articles regarding plant oral vaccines. The concept that plant material could act as an adjuvant in the oral delivery of VLPs has been growing over the last two decades and has pushed research towards the development of plant based VLP oral vaccines. In fact VLP is a very effective recombinant vaccine strategy and its expression in plants could constitute an excellent delivery system. For instance if the vaccine is expressed in an edible plant or fruit, animals or humans could be fed with an un-purified, “ready to use”, low cost edible vaccine. This concept was introduced by Charles Arntzen in 1992 when for the first time his research group managed to express a recombinant vaccine VLP in plants (Mason et al., 1992). Over the subsequent years several important proofs of concept followed that initial intuition: by 2000 the Arntzen group had demonstrated that both transgenic tobacco and transgenic potato expressing recombinant antigens could be immunogenic if fed as oral vaccines against bacteria and viruses both in animals and humans. Protection against challenge after priming with edible vaccines was subsequently proved in animal models (Haq et al., 1995; Mason et al., 1998; Tacket et al., 2000, 1998). After those initially exciting results, several further candidate vaccines had shown promising results and at the beginning of the 21<sup>st</sup> century the edible vaccine concept reached the maximum interest, with many reviews publicising the great potential of this technology, and new concepts as “vaccine farming” became popular slogans in the scientific arena (Rybicki, 2009).

The main presumed advantages of these technologies were the so called “bio-encapsulation” of the vaccine in the plant cell wall and cellular compartments, which could allow supplementary protection to the antigen, and the heat-stable environment of the vaccine host (Walmsley and Arntzen, 2000). However, three concomitant circumstances induced a sudden regress in the enthusiasm of edible vaccines around 2002 (Rybicki, 2009):

- In 2002, maize and soybean seeds harvest in two US states were found to be contaminated with some seeds containing a transmissible gastroenteritis virus capsid protein, which a biotech company was producing for research on pig vaccines. The case was contained and stricter guidelines were reinforced thereafter (USDA, 2013).
- Research in immunology was providing more and more consistent evidence about the possibility of developing tolerance following mucosal antigen exposure (Rybicki, 2009).
- The general feeling that the regulatory bodies may not grant a license for plant vaccines for animal or human use, due to possible lack of dose and process standardisation (Rybicki, 2009).

These factors determined a general drawback after the initial excitement, because it suddenly seemed that containment measures for transgenic plants, risks of tolerance and regulatory issues could become tough hurdles to overcome. However, research on oral vaccines produced in plants continued and scientists had simply to tune their plant oral vaccine vision: in a famous interview Arntzen declared "We don't say 'edible' vaccine any more - we say 'heat-stable oral vaccines' ". It was explained that for oral vaccine development, the use of food that could enter the food chain had been abandoned and that previously non-edible plants such as *Nicotiana benthamiana* would have been used to produce vaccines. They could have been minimally processed in order to be filled into heat-stable capsule formulations. In this way contamination of the food chain could have been avoided. Furthermore, dose standardisation could have possibly led to better acceptance by regulatory bodies (Coghlan, 2005).

Over the years plant oral vaccines have often shown good efficacy in terms of antibody production: it is feasible that VLPs based on pathogens that normally survive the gut will show greater efficacy (Herbst-Kralovetz et al., 2010). Surprisingly, even HBsAg, a VLP of a non-enteric pathogen has been proven to induce a strong antibody production in mice upon ingestion of transgenic potatoes. In contrast, ingested purified HBsAg did not produce any relevant immunogenicity. It is therefore clear that the potatoes' bio-

---

encapsulation of the VLP improved the efficacy of the oral vaccine in mice (Kong et al., 2001). However, not all attempts had been successful, whereby doses of oral vaccines that are 10 to 25 times higher than the injectable ones often failed to induce immunogenic responses as strong as those induced via injection (Rybicki, 2009). Reduced oral immunogenicity can be multi-factorial, but certainly one of the main concerns remains the stability in the gut. The plant bio-encapsulation as a mean of antigen protection in the GI was shown to be rather convincing for HBsAg expressed in potatoes (Kong et al., 2001), but it has not been systematically addressed for different plants and different antigens. Recently two articles from the Walmsley group started to address more rigorously this crucial point: in this research it was assessed whether the plant material could control the release of the antigen in the gut both in mice and sheep and whether this possible delayed release could affect the oral immunogenicity of the antigen. They concluded that the choice of the plant and of the part of the plant in which the antigen is expressed influences its release in the gut, with roots releasing the vaccine more slowly than the leaves in *Nicotiana benthamiana*. However, they used a model antigen stable in the GI tract: thus both studies confirmed that there was sustained release of the vaccine in gut, but they failed in demonstrating whether the plant material actually protected the antigen (Pelosi et al., 2012, 2011a).

Not only the plant and the plant tissue chosen, but also the plant cellular compartment of expression seems to have an important role in the way the antigen is delivered into the gut: chloroplast expression has shown good potential in terms of antigen protection in the gut (Kwon, 2013). Looking at this aspect from a drug delivery point of view, the question to be answered is whether the plant cell rigid compartments could work as a sort of natural gastro-protected formulation or as a simple sustained release system. So far only the latter option has been extensively shown. In conclusion, the possible advantages and drawbacks of plant oral vaccines can be summarised as follows.

Possible advantages include:

- Heat-stability (Daniell et al., 2009; Hefferon, 2010; Penney et al., 2011).

- Cheap vaccine production and minimal formulation processing required (Daniell et al., 2009; Hefferon, 2010; Penney et al., 2011).
- Natural bio-encapsulation of the vaccine within the plant cell able to protect the vaccine from the harsh conditions of the GI tract (Huang, 2006; Lico, 2012; Paul, 2010; Zhang, 2006).
- When using agroinfiltrated *Nicotiana* plants as vaccine bioreactors, the presence of lipopolysaccharide from *Agrobacterium* or of plant alkaloid could act as a vaccine adjuvant in the GALT (Pelosi et al., 2011a).

Possible drawbacks involve:

- Dose and formulations standardisation needed for regulatory body approval of animal and human vaccines (Huang, 2008; Tiwari, 2009).
- Risk of oral tolerance (Pelosi et al., 2011b; Penney et al., 2011).
- Reduced immunogenicity compared to injectable counterparts (Rybicki, 2009).
- Need for substantial initial investments to support large scale production even for clinical trials vs the current conservative tendency of pharmaceutical companies to stick to current, well-established technologies (Rybicki, 2009; Tiwari et al., 2009).

The great potential of this revolutionary technology has quickly developed in a few years with a series of ground-breaking proofs of concept. However, the impetuous excitement and the huge expectation generated by this “trendy” vaccination option probably constituted its main setback. There was the feeling that vaccination would have become shortly “as easy as eating a banana”. Edible vaccines seemed like the heaven of vaccination. Therefore, when a series of more practical issues came out unexpectedly, the initial excitement paradoxically risked to turn in a big delusion (Rybicki, 2009). Now a more careful and critical approach towards oral plant vaccines has been established and scientists are slowly trying to address and give answers to many unsorted questions. Drug

---

delivery could somehow help in understanding the key point of the whole oral plant vaccine fundament. In order to prove this technology superior to the existing ones, it has to be demonstrated that the plant material can be an effective controlled release aid and that it can allow cheap and minimal processing. The plant oral vaccine approach could turn into a pioneering branch of drug delivery.

## 1.6 Plant-expressed Oral Hepatitis B Vaccine - Where Are We?

Hepatitis B vaccine is one of the major health successes of the last decades. However, costs and cold-chain requirements have limited its use in the most poor and remote countries in the World (Hayden et al., 2012). Furthermore, circa 5 % of the patients do not respond to the vaccine and the multi-dose vaccination regimen often reduces compliance: in developing countries the rate of HBV chronic infection still ranges between 8 and 10% (Floreani et al., 2004; Makidon et al., 2008). Another problem with systemic immunisation is that it elicits very poor mucosal protection: considering that most pathogens usually invade the organism through mucosal tissues, protection at the site of entry of the pathogen is highly desirable. A safer, cheaper, heat-stable, patient friendly vaccination technology could allow the achievement of a more efficient immunisation programme worldwide (Lebre et al., 2011). Oral delivery is generally considered the most desired route of administration and it could be also exploited for Hepatitis B vaccine (HBV). HBsAg and HBcAg have been among the most studied plant-expressed vaccine candidates for oral delivery.

When injected, plant-expressed HBsAg proved to be immunologically similar to the yeast derived HBsAg, which is marketed (Thanavala and Yang, 1995). However, the proof of concept that the plant-expression could favour the development of an oral Hepatitis B vaccine came out in 2001: in mice, gavage of raw potatoes containing transgenic expressed HBsAg resulted in higher anti-HBsAg antibodies production than yeast expressed HBsAg; transgenic potatoes induced anti-HBsAg antibodies exceeding what is considered the protective level. The use of an adjuvant proved to be necessary for the development of immunity (Kong et al., 2001). Interestingly, they showed also that parenteral priming with subimmunogenic doses followed by oral boosts enabled the development of strong immunogenicity. Thus, they suggested that the development of an oral Hepatitis B vaccine

could serve as a way to improve the efficacy of the current injectable vaccine whereby orally delivered HBsAg-expressing potatoes could be used to boost strong immunogenicity following priming with a parenteral dose.

A human clinical trial was undertaken using HBsAg expressed in lettuce. Lettuce was administered orally in three volunteers, who were not previously immunised or infected by HBV. After oral immunisation with two doses, two of the volunteers developed anti-HBsAg antibodies to a level superior to the established minimum level of protection in humans. However, the protection did not seem to last long (Kapusta et al., 1999). Subsequent clinical trials in humans have shown interesting results: previously vaccinated volunteers, ingesting three separate doses of raw potatoes expressing HBsAg, developed an increase in serum anti-HBsAg in 10 cases out of 17, with a maximum antibodies increase of 56 fold. The trial was carried out without using any adjuvant (Thanavala et al., 2005). The results obtained were encouraging and created the basis to believe that a Hepatitis B oral vaccine could be developed. In spite of those promising results, further improvements were required. Increasing the expression level in the plant tissue to be eaten and ensuring antigen stability in the gut have been proposed to be important future steps towards an efficient Hepatitis B oral vaccine (Thanavala and Lugade, 2010).

HBcAg immunogenicity is already demonstrated for parenteral administration (Paragraph 1.4.3). Furthermore, HBcAg has shown to be potentially effective in protecting against HBV when administered systemically by injection (Paragraph 1.4.3). However, its mucosal immunogenicity still needs to be established, in order to evaluate its potential as a nasal or oral vaccine, delivered on its own or in combination with HBsAg. Nasal delivery of HBcAg proved to stimulate strong specific serum IgG production (Lobaina et al., 2003) and hence it was successfully co-administered with HBsAg with the aim of developing a more potent vaccine formulation against HBV infection (Aguilar et al., 2004; Lobaina et al., 2005). Moreover HBcAg could be also used as an immunogenic carrier for foreign epitopes and hence used as a sort of adjuvant for heterologous candidate vaccines (Whitacre et al., 2009).

In terms of oral delivery, bacterial-expressed HBcAg induced lower serum specific IgG when administered orally to mice (Lobaina et al., 2003). Plant-expressed HBcAg was also

---

used for oral immunogenicity studies: five mice were primed with partially purified Hepatitis B capsids by oral gavage without any adjuvant. Two weeks after, an oral boost with the same dose was given. Four weeks after the boost, three mice out of five developed detectable specific serum anti-HBc IgG. In the following weeks, anti-HBc antibodies could be only detected in two mice out of five. Faecal IgA were detectable at week 16 only in one mouse (Huang, 2006). These data showed that partially purified plant-expressed HBcAg VLPs were only moderately immunogenic when given by oral gavage to mice. However in this study VLP was partially purified before administration: the authors speculate that higher immunogenic response could have been obtained by using raw plant material expressing HBcAg. These results taken together can raise interesting questions:

- HBcAg shows a poor/moderate oral immunogenicity. Authors consider the gastric degradation of the VLP as the main barrier (Huang, 2006). However, this is not the only barrier as there could be some intestinal obstacles hindering the oral immunogenicity of an antigen, including lack of absorption and stimulation of tolerogenic pathways. Further investigation could elucidate the actual impediment to a strong oral immunogenicity of HBcAg.
- As many protein vaccines, HBcAg might need protection from the GI instability, and plant bio-encapsulation could offer some sort of aid. However, it is not clear to which extent this natural protection could function and whether it could substitute a more sophisticated artificial pH-dependent formulation.

In conclusion a needle-free vaccine against Hepatitis B could offer a safe, cheap and patient friendly option with oral delivery still being the most desirable. HBsAg has been extensively studied; alternatively HBcAg could be investigated for mucosal protection alone or co-administered with HBsAg for a more potent protection (Lobaina et al., 2005). Preliminary results showed reduced oral immunogenicity of HBcAg, when compared to the extremely strong immunogenicity of the same antigen administered via other routes of administration. The main problem might be the GI instability of the vaccine and further studies are essential to define whether the plant bio-encapsulation or some other sort of GI protection of HBcAg could promote better survival of the antigen in the gut.

---

## 1.7 Objectives of the Research

VLPs are a new generation of recombinant vaccines, which mimic the pathogen structure. It has been proposed that such vaccines could be as effective as mucosal oral vaccines, as their compact organisation could be strong enough to withstand the harsh-gastrointestinal environment (Herbst-Kralovetz, 2010; Huang, 2005). Aside from this intrinsic robustness, the expression of VLPs in plant could enable exploitation of the natural bio-encapsulation as a sort of adjuvant: if the unpurified plant material is to be delivered orally, the VLP internalisation within the plant cell compartments could allow protection of the antigen from the extreme gastric pH and from the gastro-intestinal digestive enzymes (Mason et al., 2002). Moreover, it is believed that the VLP particulate structure could favour efficient absorption in the small intestine by the antigen-sampling epithelial M cells within the PPs (Gonzalez et al., 2009). Thus, the expression of VLPs in plant could be an effective way to deliver vaccines orally. In this study, HBcAg, as a candidate vaccine, and *Nicotiana benthamiana*, as the host plant, were used to evaluate the potential applicability of this oral plant vaccine approach. A previous study on plant-expressed HBcAg elucidated that oral administration of plant extracts containing HBcAg elicited only poor immunogenicity in mice and it was speculated that this could have been due to the gastric instability of the antigen. Hence, the authors suggested that natural plant-bioencapsulation of the antigen expressed in plant, administered as raw materials or alternatively the in-vitro bioencapsulation could have allowed better immune response upon oral administration (Huang, 2006).

In this context, the main objective of this research was that of investigating if and to what extent HBcAg VLP could withstand and overcome some of the gastro-intestinal barriers and to evaluate whether the compartmentalisation of the antigen in the plant material in which it is expressed could offer some aid to the oral delivery of HBcAg. The final objective was that of producing an oral formulation of HBcAg, exploiting its expression in plant.

Initially, a robust protocol for the routine production, extraction, purification and characterisation of plant-expressed HBcAg was established and is described in Chapter 2. Then the stability of the plant-expressed antigen in numerous bio-relevant media

simulating the GI environment was evaluated. This study was divided into two parts: the stability of purified HBcAg in simulated and natural GI fluids was evaluated in Chapter 3. Then once the intrinsic susceptibility of the antigen was defined, the aim of Chapter 4 was to test whether the raw or dried plant material expressing the VLP could offer protection to the antigen against simulated GI fluids. Moreover, the final purpose of this Chapter was to produce a dosage form that could enable effective oral delivery of stable antigen to the gut, exploiting the expression in plant. In Chapter 5, different drying approaches of the VLPs into potentially stable solid dosage forms were attempted, with the final aim of producing an oral dosage form, containing purified HBcAg. Finally, as a separate objective, in Chapter 6 the permeability of purified HBcAg in the GALT was evaluated in an *in vitro* human cell culture model and *in vivo* in mice, using a ligated intestinal loop model. The overall structure of this thesis is summarised in Figure 1.7.

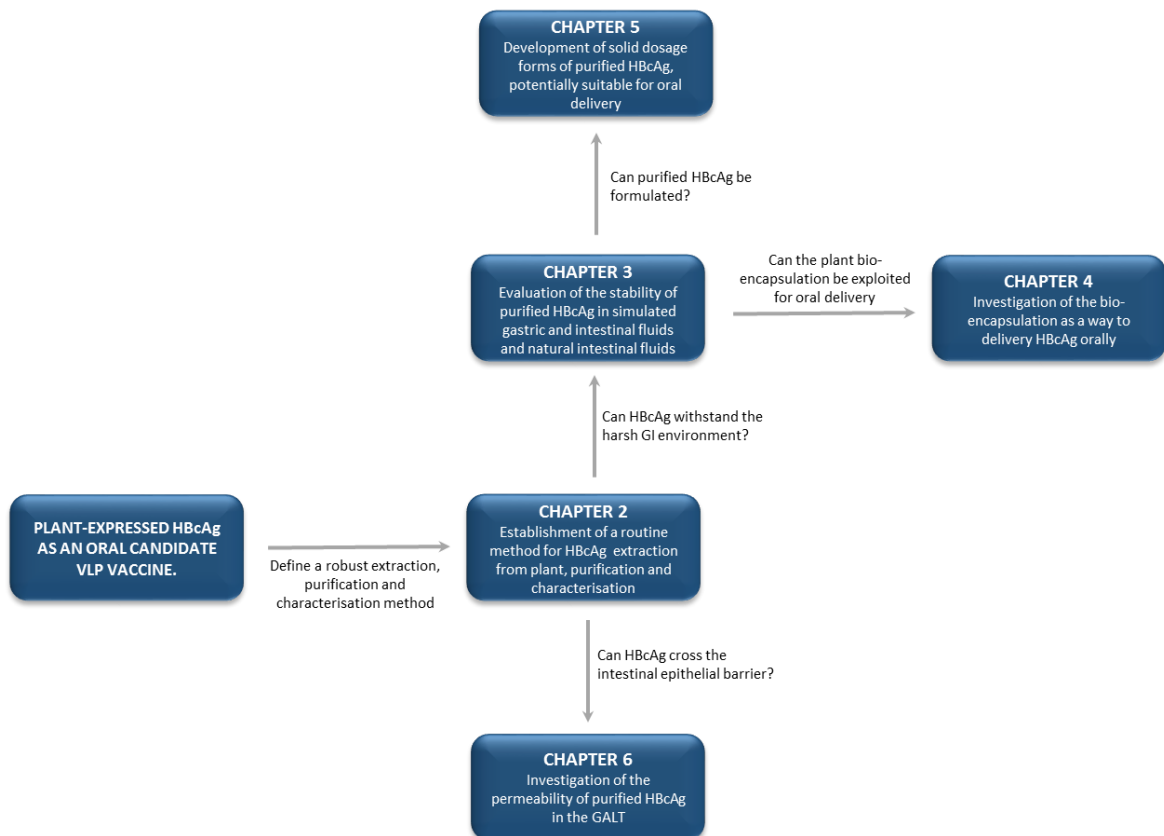


**Figure 1.7. Structure of the thesis.**

## **2 Production, Purification and Characterisation of Plant-expressed HBcAg VLP**

### **2.1 Introduction**

Hepatitis B core antigen (HBcAg) virus-like particle (VLP) was the main model vaccine used in this work. It was expressed in plants, extracted and then purified using a sucrose gradient technique. Several characterisation and quantification techniques were used including sodium dodecyl sulfate polyacrylamide gel electrophoresis (SDS-PAGE), Western blot, dot blot, transmission electron microscopy (TEM), native agarose gel electrophoresis, and direct and sandwich enzyme-linked immunosorbent assay (ELISA).

This Chapter will introduce the general materials and techniques used to extract and purify HBcAg (i.e. the major raw material in this study), and will show the results of the characterisation studies of HBcAg VLPs after harvesting.

Subsequent chapters will include descriptions of the materials and methods specifically used at those points (e.g. the formulation preparation techniques will be discussed fully in Chapters 3, 4 and 5).

### **2.2 Materials**

#### **2.2.1 Molecular Biology Media, Buffers and Solutions**

General media, buffers and solution used in this study for bacterial growth, plant agro-infiltration and protein analysis are catalogued in Table 2.1.

**Table 2.1 Media, buffers and solutions used for molecular biology experiments.**

| Name   | Recipe   |
|--|--|
| Luria Bertani (LB)                                     | 10 g/L tryptone, 5 g/L yeast extract, 10 g/L sodium chloride (NaCl) adjusted to pH 7.0   |
| MMA  | 10 mM 2-[ <i>N</i> -morpholino]ethanesulfonic acid (MES) buffer, pH 5.6 : 10 mM MgCl <sub>2</sub> , 100 μM acetosyringone  |
| Extraction buffer 1                                    | 50 mM Tris-HCl, pH 7.25 : 150 mM NaCl, 2 mM ethylenediaminetetraacetic acid (EDTA), 0.1% (w/v) Triton X-100, 1 mM dithiothreitol (DTT) (added fresh), Complete® tablet (added fresh) |
| Extraction buffer 2                                    | 10 mM Tris-HCl, pH 8.4: 120 mM NaCl, 1 mM EDTA, 0.75% (w/v) sodium deoxycholate, 1 mM dithiothreitol (DTT) (added fresh), complete tablet (added fresh)                              |
| Phosphate-buffered saline (PBS)                        | 140 mM NaCl, 15 mM monopotassium phosphate (KH <sub>2</sub> PO <sub>4</sub> ), 80 mM disodium phosphate (Na <sub>2</sub> HPO <sub>4</sub> ), 27 mM potassium chloride (KCl)          |
| Dot blot block buffer                                  | 5% (w/v) dried milk, 0.1% (v/v) Tween-20, in PBS   |
| Dot blot washing buffer                                | 0.1% (v/v) Tween-20, in PBS  |
| Western blot block buffer                              | 1% bovine serum albumin (BSA) (w/v), 1% casein (w/v), 0.05% (v/v) Tween-20 in PBS  |
| Western blot transfer buffer                           | 10.8 g/L Tris-HCl, 14.4 g/L glycine, 20% (v/v) methanol  |
| Western blot washing buffer                            | 0.05% (v/v) Tween-20 in PBS  |
| Tris/Borate/EDTA (TBE)                                 | 3.03 g/L Tris-HCl, 5.5 g/L boric acid, 2 mM EDTA   |
| Enzyme-Linked Immunosorbent Assay (ELISA) block buffer | 5% (w/v) dried milk, 0.05% (v/v) Tween-20 in PBS   |
| ELISA washing buffer                                   | 0.05% (v/v) Tween-20 in PBS  |

## 2.2.2 Antibodies and Antigens

Antibodies and antigens used for dot blot, Western blot and ELISA are listed in Table 2.2.

**Table 2.2 Antibodies and antigens used for immunodetection assays.**

| Antibody  | Antigen        | Supplier                          | Application  |
|---|----------------|-----------------------------------|--|
| Monoclonal mouse HBcAg antibody-Clone: 10E11                      | HBcAg          | Abcam                             | Dot blot: 1:5000 in Dot blot block buffer<br>Western blot: 1:5000 in Western blot block buffer   |
| Polyclonal rabbit HBcAg antibody                                  | HBcAg          | AbD Serotec                       | Dot blot: 1:5000 in Dot blot block buffer<br>Western blot: 1:5000 in Western blot block buffer<br>ELISA direct: 1:2000 in 1% (w/v) dried milk, 0.05% (v/v) Tween-20 in PBS |
| Anti-mouse HRP conjugated   | Mouse IgG      | Invitrogen or Amersham Bioscience | Dot blot: 1:5000 in Dot blot block buffer<br>Western blot: 1:5000 in Western blot block buffer   |
| Anti-rabbit HRP conjugated  | Rabbit IgG     | Promega                           | Dot blot: 1:5000 in Dot blot block buffer<br>Western blot: 1:5000 in Western blot block buffer<br>ELISA direct: 1:4000 in 1% (w/v) dried milk, 0.05% (v/v) Tween-20 in PBS |
|   | HBcAg standard | AbD Serotec                       | ELISA control and standard   |
| Monoclonal mouse HBcAg antibody- Clone: H6F5 (7E6)                | HBcAg          | AbD Serotec                       | ELISA sandwich: 1:1000 in 1% (w/v) in PBS  |
| Monoclonal mouse HBcAg Antibody HRP conjugated- Clone: H3A4 (4H5) | HBcAg          | AbD Serotec                       | ELISA sandwich: 1:1000 in 1% (w/v) dried milk, 0.05% (v/v) Tween-20 in PBS   |

### 2.2.3 Plasmids

pEAQ-*HT*-HBcAg $\Delta$ 176, pEAQ-*HT*-CoHe7e-eGFP and pEAQ-*HT*-empty binary plasmid were used (Thuenemann, 2010). Plasmid Easy and Quick (pEAQ) is the denomination given to the vector. Hypertranslatable (-*HT*) is the name given to the expression system. HBcAg $\Delta$ 176 is the construct codifying for the first 176 amino acids from the HBcAg N-terminus. CoHe7e-eGFP is the construct codifying for heterotandem core-GFP.

## 2.2.4 Other Materials Used in the Molecular Biology Studies

Complete® Protease inhibitor tablets were purchased from Roche (UK), Miracloth from Merck (UK) and dialysis tubes from Spectrum Laboratories (Europe) or from Sigma (UK). Amicon 5 and 15 mL ultrafiltration tubes were purchased from Millipore (UK). SDS-NuPAGE gels bis-tris Mini, NuPAGE MOPS buffer, NuPAGE LDS Sample Buffer and SeeBlue Plus 2 marker were purchased from Invitrogen (UK).  $\beta$ -Mercaptoethanol, Brilliant Blue R Concentrate, 3,3',5,5'-tetramethylbenzidine dihydrochloride (TMB) substrate, Rifampicin and Kanamycin were purchased from Sigma (UK). InstantBlue stain was bought from Expedon (UK), SuperSignal West Dura Chemiluminescent Substrate from Thermo Scientific (UK) and polyvinylidene fluoride (PVDF) membranes and Hyperfilm from Amersham (UK).

## 2.3 Methods

This Paragraph will introduce the molecular biology methods used in this Chapter.

### 2.3.1 Plant Expression of HBcAg and Protein Extraction

The production process of HBcAg involves three successive steps of agroinfiltration, harvesting and protein extraction. Some of the methods described derive from the general techniques used in Prof. Lomonossoff's research group [for reference (Sainsbury and Lomonossoff, 2008; Sainsbury et al., 2009)] and they were tailored to this particular research.

#### 2.3.1.1 Agroinfiltration

*Nicotiana benthamiana* plants were grown in a glasshouse at a fixed temperature of 25 °C. During winter time (October to April), 16 hours of daylight were ensured by artificial lighting. Plants were watered every afternoon. *Valmaine romaine* lettuce was grown under similar conditions. *Nicotiana benthamiana* plants were used 3 to 4 weeks after pricking out, preferentially before flowering, while *Valmaine romaine* lettuce was used 4 weeks after pricking out.

pEAQ-*HT*-HBcAg $\Delta$ 176, pEAQ-*HT*-CoHe7e-eGFP and pEAQ-*HT*-empty binary plasmid were kindly donated by Dr. Eva Thuenemann in the form of glycerol stocks. Cultures were grown in Luria-Bertani medium, supplemented with 50  $\mu$ g/mL Rifampicin and 50  $\mu$ g/mL Kanamycin, and kept in a shaking incubator at 28 °C for 48 hours. After subculturing and further 24 hours incubation, the bacteria were pelleted by centrifugation at 2000 g for 20 minutes. Pellets were subsequently drained and resuspended in freshly made MMA solutions. The suspension was left to stabilize at room temperature for 1 to 4 hours. The concentration of the bacterial suspension in MMA was then measured by Optical Density at a wavelength of 600 nm (OD600), which was approximately 4 to 5. The culture was then appropriately diluted in fresh MMA to a final OD600 of 0.4 to 0.6. This agrobacterium suspension was subsequently pressure-infiltrated into *Nicotiana benthamiana* leaves. Syringe infiltration was used to infiltrate small batches (up to 15 plants), whereas vacuum infiltration was chosen for larger batches. Four-week old *Valmaine romaine* lettuce was vacuum-infiltrated using the same agrobacterium suspension used for the infiltration of *Nicotiana benthamiana*.

For reasons of simplicity HBcAg $\Delta$ 176 will be referred to as HBcAg, hereafter.

### 2.3.1.2 Harvesting

Infiltrated leaves were harvested 6 to 7 days post-infiltration. The weight of the batch was recorded and the leaves were either extracted immediately or stored at – 80 °C. In cases of small scale experiments, when only a few leaves were infiltrated, leaf disks were prepared using a cork borer of 11 mm diameter and the rest of the leaves were discarded. *Valmaine romaine* lettuce leaves, infiltrated with the HBcAg, were harvested at 3, 5, 7 and 9 days post-infiltration in order to establish the time of maximum yield.

### 2.3.1.3 Protein Extraction

Extraction of the protein from the leaves was performed by homogenisation in three volumes of extraction buffer 1 or extraction buffer 2 (See Table 2.1). The recipes for both extraction buffers were developed by Dr. Eva Thuenemann (Thuenemann, 2010). For batches of *Nicotiana benthamiana* leaves expressing HBcAg, protein extraction was

performed throughout this study with either extraction buffer 1 or extraction buffer 2. Batches of *Valmaine romaine* leaves expressing HBcAg or *Nicotiana benthamiana* expressing HBcAg tandem-GFP were extracted using extraction buffer 2 only.

In the case of small batches, ceramic beads were added together with the leaf disks and three volumes of an extraction buffer in screw-cap tubes and homogenised using a FastPrep machine (MP Biomedicals, UK) at a speed setting of 5.0 for 40 seconds. In the case of larger scale batches, the leaves and the three volumes of the extraction buffer were blended in a Waring blender (UK) for three consecutive times, each for approximately 15 seconds. The whole extract was then cloth-filtered using a double layer Miracloth and subsequently clarified by centrifugation in order to remove most plant cell debris. Crude extracts containing HBcAg or CoHe7e-eGFP were centrifuged at 12,000 x g and 9,000 x g, respectively, for 15 minutes. In order to control the expressed protein solubility, the pellet obtained after the centrifugation was also re-suspended in LDS  $\beta$ -mercaptoethanol, boiled and used for SDS-PAGE analysis.

The clarified supernatant was used as a crude extract for further purification through sucrose density gradient. Protein extraction was always performed at 4 °C and the samples were kept on ice, before further purification. Figure 2.1 summarises the plant expression and protein extraction process.

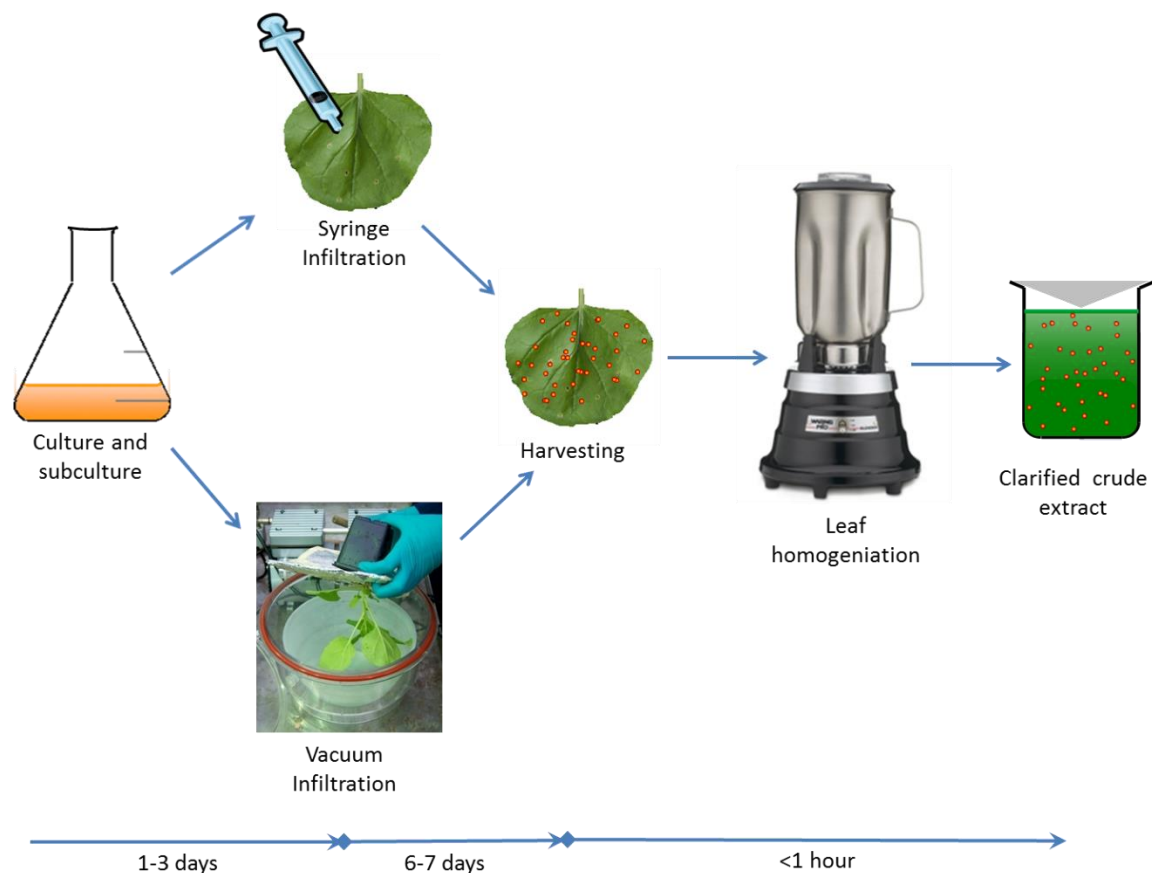


**Figure 2.1. HBcAg virus-like particles (VLP) plant expression and protein extraction.** *Agrobacterium* containing a genetically modified plasmid was grown in LB culture for 2 days and subcultured for a further day. Following infiltration either by a syringe for small batches or vacuum for large ones, the plants were incubated in the green house for 6-7 days. After harvesting, the leaves were immediately homogenised in an extraction buffer. The crude extract was then clarified by cloth filtration and subsequent centrifugation. Orange particles symbolise VLPs.

### 2.3.2 HBcAg Purification

#### 2.3.2.1 Sucrose Density Gradient

Sucrose density gradients have been used as a process for HBcAg purification (Birnbaum and Nassal, 1990). Using 10 mM Tris-HCl pH 8.4 containing 120 mM NaCl as a solvent, a 60% (w/v) sucrose solution was prepared. Subsequently, 50%, 40%, 30%, 20%, 10% (w/v) solutions were obtained by dilution of the 60% (w/v) stock solution in increasing volumes of 10 mM Tris-HCl pH 8.4 containing 120 mM NaCl. Density gradients were created in 12 or 36 mL ultra-centrifugation tubes: initially the crude extract was forced to the bottom of the tube through a needle and the sucrose solutions of increasing density were then forced

to the bottom of the tube. In this manner, the denser layer, pushed to the bottom, will lay below the less dense layers, creating a gradient whose density increases from the top to the bottom along the tube. The gradients were then centrifuged in a swing-out rotor for 2 hours and 30 minutes: a SW41Ti rotor was used at 40,000 rpm for the 12 mL tubes, whereas a Surespin 630 rotor was used at 30,000 rpm for the 36 mL tubes. After centrifugation, the tubes were pierced at the bottom, so that the sucrose gradient fractions could be collected, starting with those of highest densities. Generally, seven fractions were collected with the volume of each fraction being approximately correspondent to the volume of each sucrose solution layer. Figure 2.2 summarises the steps of the density gradient purification. In some specific cases the sucrose gradient procedure was simplified by using only 20%, 30, 40% and 50% (w/v) sucrose solutions.

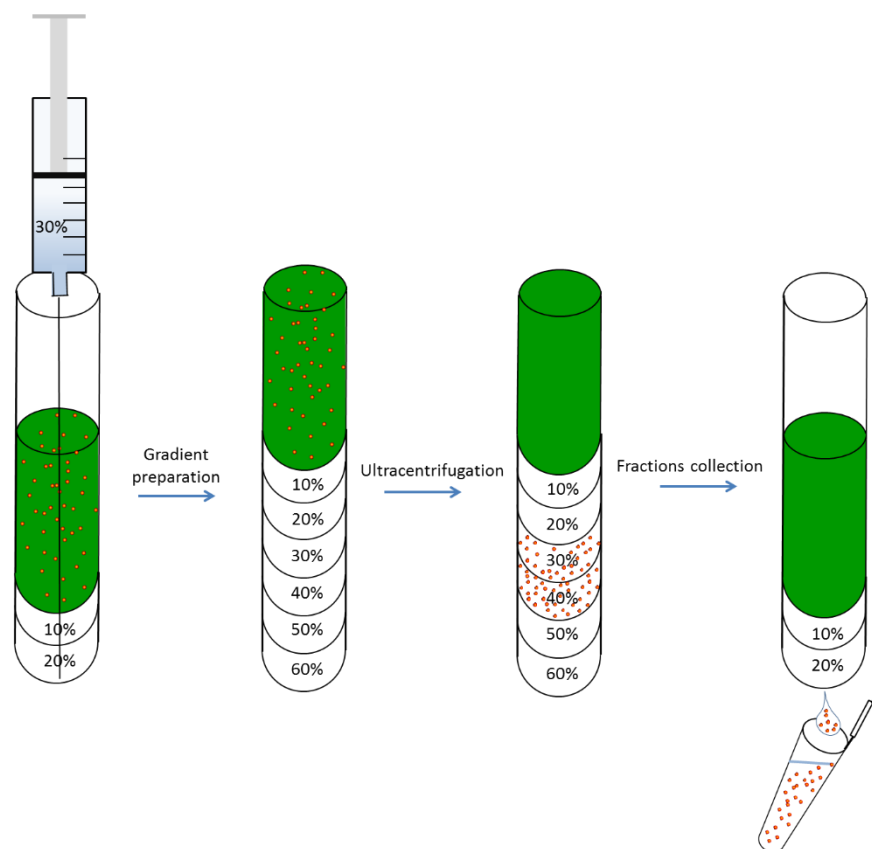


**Figure 2.2. A schematic representation of sucrose gradient purification.**

Clarified crude extract and sucrose solutions of increasing density were underlain from the bottom using a syringe. Then tubes were spun for 2 hours and 30 minutes in an ultracentrifuge, allowing VLPs separation from crude extract. Sucrose fractions were collected by piercing the bottom of the tube. Percentages represent the concentration (w/v) of the sucrose solutions, while orange particles symbolise VLPs.

### 2.3.2.2 Dialysis

Dialysis was used for the removal of the sucrose from the density gradient fractions and as a method for buffer exchange and purification. Dialysis membranes were filled with the different sucrose gradient fractions and dialysed against 10 mM Tris-HCl, 120 mM NaCl, pH 8.4 or against PBS. Small batches were dialysed using Spectrum Labs tubes with molecular cut-off of 100 kDa, while larger batches were dialysed using Sigma membranes with a molecular cut-off of 12 kDa. The different cut-off values were used because a molecular cut-off of 100 kDa was commercially available for small dialysis tube, but not for the larger dialysis membranes. However, in both cases the membrane cut-off would have allowed efficient buffer exchange and sucrose removal.

### 2.3.2.3 Ultrafiltration

Ultrafiltration was performed to concentrate the purified and dialysed HBcAg solutions: diluted HBcAg preparations were added to a 100 kDa molecular weight cut-off membrane, specifically built in ultrafiltration tubes. Centrifugation enabled small molecules to pass through the filter, while macromolecules larger than 100 kDa (such as HBcAg VLP) were concentrated. HBcAg samples were spun at 4,000 x g until the preparation was concentrated to the required volume.

## 2.3.3 Protein Qualitative Analysis

Protein qualitative analysis was carried out on purified and crude extract samples. The techniques used were sodium dodecyl sulfate polyacrylamide gel electrophoresis (SDS-PAGE), Western western blot and dot blot.

### 2.3.3.1 Sodium Dodecyl Sulfate Polyacrylamide Gel Electrophoresis (SDS-PAGE) - Coomassie Blue Staining

SDS-PAGE-Coomassie Blue Staining was used to assess the protein content of different preparations. This electrophoretic technique allows the fractionating and distinguishing of deliberately denatured proteins on the basis of their molecular weight. SDS-PAGE is a simple protein analysis method. However, it has a high detection limit (i.e. low sensitivity)

and it does not furnish information about the chemical identity of the proteins bands visualised, merely the molecular weight range (Sambrook and Russel, 2001a).

Ten, twelve and fifteen well gels were used throughout this study. Proteins were reduced and denatured by adding one volume of 3X LDS  $\beta$ -mercaptoethanol to two volumes of the samples. Samples were then boiled at 100 °C for 5 minutes. NuPAGE gels were run in 3-(*N*-morpholino)propanesulfonic acid (MOPS) buffer following the manufacturer's instructions. After electrophoresis, the protein bands were visualised by addition of Coomassie blue-protein stain for at least 1 hour. Then gels were de-stained in water for at least 2 hours before imaging. In each gel one well was always allocated to the protein marker.

### 2.3.3.2 Dot Blot

Dot blot allows identification of un-denatured proteins by interaction with specific antibodies. The sample is bound directly to the nitrocellulose (or PDVF) membrane for immunochemical recognition (Harlow and Lane, 1988). Compared to SDS-PAGE gel, it allows recognition of specific sequences of interest; however, it does not give information about the molecular weight of the protein.

Three  $\mu$ L of each sample were spotted onto PDVF membranes, using 10  $\mu$ L tips. Membranes were left to dry for 30 minutes and then blocked with the blocking buffer at 4 °C overnight. On the following day, membranes were washed once with the washing buffer in a shaker at room temperature for 15 minutes, before being incubated with the primary antibody for 2 hours. After three 15 minutes washes with the washing buffer at room temperature, the membranes were then probed with the secondary antibody for a further 2 hours. Following three subsequent washes with the washing buffer, chemiluminescent HRP substrate was used for the detection of the secondary antibody. The chemiluminescence was detected with Hyperfilm.

The blocking and washing buffers used are listed in Table 2.1, while the antibodies are listed in Table 2.2.

### 2.3.3.3 Western Blot

Western blot is a technique that allows the identification of an electrophoretically separated denatured protein band by its interaction with specific antibodies. Therefore, it combines the convenience of both SDS-PAGE and dot blot: Western blot supports immunochemical recognition of a specific antigen protein and also gives information about its molecular weight. Furthermore, Western blot offers higher sensitivity (i.e. lower detection limit) than SDS-PAGE Coomassie stained gels (Sambrook and Russel, 2001b).

SDS-PAGE gels were run as in 2.3.3.1. However, gels were not stained and were transferred to PVDF membranes immediately after the electrophoresis: the cassettes were assembled with the gel and the membrane layered between a sandwich of filter papers and sponges. Each layer was pre-wetted in transfer buffer. The electroblotting was performed at 100 V for 1 hour at 4 °C. The membranes were blocked with the blocking buffer at 4 °C overnight and were then washed once with the washing buffer in a shaker at room temperature for 15 minutes, before being incubated with the primary antibody for 2 hours. After three 15 minutes washes with the washing buffer at room temperature, the membranes were probed with the secondary antibody for a further 2 hours. Following three subsequent washes with the washing buffer, chemiluminescent HRP substrate was used for the detection of the secondary antibody bound to the membrane. The chemiluminescence was detected with Hyperfilm.

The blocking and washing buffers used are listed in Table 2.1, while the antibodies are listed in Table 2.2.

### 2.3.3.4 Fluorescence Microscopy

Fluorescence microscopy was used in order to effectively visualise the fluorescence of CoHe7e-eGFP. A 3 µL drop of circa 50 µg/mL purified CoHe7e-eGFP was dotted on a microscopy slide and directly observed on a Zeiss Axioplan microscope.

### 2.3.4 HBcAg Physical Characterisation

HBcAg assembles into virus like particles (VLPs). The physical stability of VLPs was assessed by transmission electron microscopy (TEM), native agarose gel electrophoresis and sucrose density gradient followed by qualitative or quantitative techniques.

#### 2.3.4.1 Transmission Electron Microscopy (TEM)

Samples diluted to an approximate concentration of 0.1 mg/mL were adsorbed onto hexagonal, plastic and carbon-coated copper grids, which were then washed three times by dripping of three consecutive water droplets. Then grids were negatively stained with 2% w/v uranyl acetate for 20 seconds and the stain was removed using filter paper. VLPs were imaged using a FEI Tecnal G2 20 Twin TEM with a build-in digital camera at the bottom.

TEM imaging was kindly carried out by Mrs. Elaine Barclay or by Dr. Alaa Aljabali in my presence.

#### 2.3.4.2 Native Agarose Gel Electrophoresis

Native agarose gels are protein gels that run in non-denaturing conditions; they allow the detection of intact HBcAg VLPs (Birnbaum and Nassal, 1990) and they were therefore used to determine particle integrity.

Agarose gels (1.2% (w/v)) were usually run in duplicate at 60 V for 90 minutes. One gel was stained in a bath containing a 0.5 µg/mL solution of ethidium bromide for 30 minutes and then visualised under UV light (wavelength = 302 nm). The other gel was stained with Brilliant Blue R Concentrate (Coomassie stain) for 30 minutes. The gel was then de-stained for 1 to 2 days with 20% methanol, 10% acetic acid solution. Foam bags were added in the floating solution in order to absorb the excess of the stain.

Ethidium bromide binds to nucleic acid, while Coomassie stains proteins. Therefore gels stained with ethidium bromide were used for the detection of encapsidated nucleic acid, while Coomassie stained gels were used to detect protein. Overlapping of the two stains is an indication of the presence of nucleic acid encapsidated in a protein core.

### 2.3.4.3 Sucrose Density Gradient

Sucrose density gradients were used as a purification method (Paragraph 2.3.2.1). However, sucrose density gradients coupled with other detection techniques were also used for the evaluation of the physical integrity of HBcAg VLPs. Intact particles were shown to sediment in the 30% and 40% sucrose gradient bands (Birnbaum and Nassal, 1990), therefore, analysis of these sucrose fractions using qualitative or quantitative techniques can reveal the stability of the VLPs.

In this Chapter, density gradients were followed by SDS-PAGE Coomassie stained, dot blot, Western blot or ELISA.

## 2.3.5 Protein Quantitative Analysis

One of the most commonly used techniques for the quantification of antigenic proteins is the enzyme-linked immunosorbent assay (ELISA). This method is based on the exploitation of enzyme-conjugated antibodies for the quantification of given antigens. Direct and sandwich ELISA methods have been carried out throughout this work. Direct ELISAs are usually used to quantify purified or semi-purified samples containing the antigen. Instead there is generally no requirement for antigen purity in sandwich ELISAs and this can be three to five times more sensitive than direct ELISAs (Khan, 2009).

### 2.3.5.1 Direct Enzyme-Linked Immunosorbent Assay (ELISA)

Direct ELISA was carried out following the protocol developed by Thuenemann (2010).

ELISA plates of 96-wells were coated in replicates with 50  $\mu$ L of different sample dilutions in PBS. Two-fold dilution series of known concentrations of HBcAg were used as standard references. Plates were incubated at 4 °C overnight. Preceded by three washes, the remaining protein-binding sites were blocked with the blocking buffer at 37 °C for 1 hour and 30 minutes. Following three subsequent washes with the washing buffer, each well was incubated with 50  $\mu$ L of a dilution of primary rabbit polyclonal antibody at 37 °C for 1 hour and 30 minutes. After further three washes with the washing buffer, 50  $\mu$ L dilutions of rabbit secondary antibody were added to each well and incubated at 37 °C for 1 hour

and 30 minutes. Following three subsequent washes with the washing buffer, 3,3',5,5'-tetramethylbenzidine dihydrochloride (TMB) substrate solutions, prepared as per the manufacturer's instructions, were used to elicit a colour reaction that was stopped with 1 M sulphuric acid upon visualised saturation of the standard curve (approximately 2 minutes and 30 seconds). Absorbance of the whole plate was then determined at 450 nm using a multi-well plate reader. HBcAg was quantified by reference to the emission values of the standard dilutions: the negative control emission values were subtracted from all the samples and a linear regression of the standard curve was calculated by plotting the resulting values of the known concentrations of the standard dilutions. Using the equation of the linear regression, the dilutions of the original samples were back-calculated.

The blocking and washing buffers used are listed in Table 2.1, while the antibodies and the HBcAg standard are listed in Table 2.2.

### 2.3.5.2 Sandwich Enzyme-Linked Immunosorbent Assay (ELISA)

A specific sandwich ELISA has been developed for this study. After several trials, the following protocol was established.

ELISA plates of 96-wells were coated with 50 µL of mouse monoclonal antibody [Clone: H6F5(7E6)] dilutions. Plates were incubated at 4 °C overnight. Preceded by three washes with the washing buffer, the remaining protein-binding sites were blocked with the blocking buffer at 37 °C for 2 hours. Following three subsequent washes with the washing buffer, each well was coated in replicates with 50 µL of different sample dilutions in 1% dried milk and 0.05% (v/v) Tween-20 in PBS. Two-fold dilution series of known concentrations of HBcAg were used as standard references. The plates were then incubated at 37 °C for 2 hours. After further three washes with the washing buffer, 50 µL dilutions of mouse monoclonal antibody [Clone: H3A4(4H5)] were added to each well and incubated at 37 °C for 2 hours. Following three subsequent washes with the washing buffer, TMB substrate solutions, prepared as per the manufacturer's instructions, were used to elicit a colour reaction that was stopped with 1 M sulphuric acid upon visualised saturation of the standard curve (approximately 12 minutes). Absorbance of the whole plate was then determined at 450 nm using a multi-well plate reader. HBcAg was quantified by reference

to the emission values of the standard dilutions: the negative control emission values were subtracted from all the samples and a linear regression of the standard curve was calculated by plotting the resulting values of the known concentrations of the standard dilutions. Using the equation of the linear regression, the dilutions of the original samples were back-calculated.

## 2.4 Results and Discussion

Over the last years, Prof. Lomonosoff's research group has been working on the expression of recombinant proteins in plant, using a Cowpea Mosaic Virus (CPMV)-based gene expression system (Sainsbury et al., 2010). Extremely high yields of foreign protein expression were demonstrated by the CPMV-*HT* system, which is based on the use of a deleted version of CPMV RNA-2. Among other proteins, HBcAg was also expressed using the CPMV-*HT* system up to yields of approximately 1 g/kg fresh weight (FW) tissue (Sainsbury and Lomonosoff, 2008). Such high levels of expression have opened the possibility of using this plant-based expression system for medical and pharmaceutical research purposes.

### 2.4.1 Expression of HBcAg and CoHe7e-eGFP in Plant

As described in Paragraph 2.3.1, pEAQ-*HT*-HBcAg $\Delta$ 176, pEAQ-*HT*-CoHe7e-eGFP and pEAQ-*HT*-empty binary constructs were infiltrated in *Nicotiana benthamiana* and the infiltrated leaves were harvested after 6 or 7 days. The leaf material was then weighed and blended in three volumes of the extraction buffer 2. Following cloth filtration, the crude extract was clarified by centrifugation and the resulting supernatant was separated from the precipitated pellet (insoluble fraction). The pellet was re-suspended in LDS  $\beta$ -mercaptoethanol, boiled and clarified again. Both the supernatant and the insoluble fractions were examined by SDS-PAGE, as shown in Figure 2.3. Identical SDS-PAGE gels were either Coomassie stained (Figure 2.3 A) or used for anti-HBcAg Western blot detection (Figure 2.3 B).

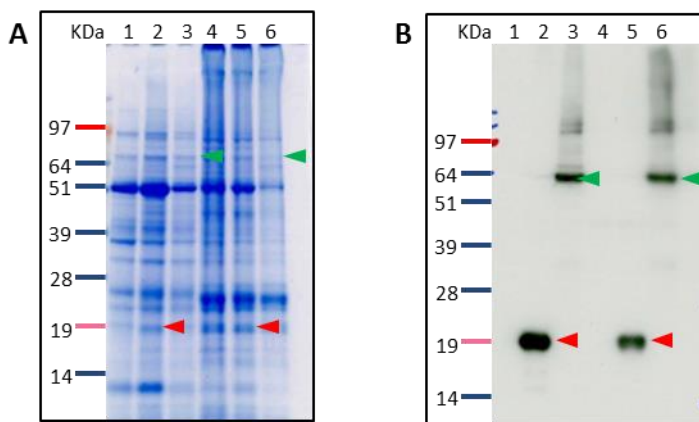


**Figure 2.3. HBcAg and CoHe7e-eGFP identification in *Nicotiana benthamiana* protein extracts.**

SDS-PAGE analysis of supernatant and insoluble fractions of crude extracts of leaves infiltrated with different constructs: (A) Coomassie stained SDS-PAGE; (B) Western blot (mouse antibody). Both gels were run identically: crude extracts of leaves infiltrated with pEAQ-HT-empty (lane 1); pEAQ-HT-HBcAg $\Delta$ 176 (lane 2); pEAQ-HT-CoHe7e-eGFP (lane 3); insoluble fractions of leaves infiltrated with the aforementioned constructs (lanes 4, 5 and 6), respectively. Arrows indicate the location of the expected bands for HBcAg (red) and for CoHe7e-eGFP (green).

Coomassie stained gel (Figure 2.3 A) illustrates the protein bands contained in the clarified crude extracts and in the insoluble fractions of plant material infiltrated with different constructs: crude extracts of leaves infiltrated with pEAQ-HT-empty (control), pEAQ-HT-HBcAg $\Delta$ 176 and pEAQ-HT-CoHe7e-eGFP are separated in lanes 1, 2 and 3, respectively; insoluble fractions of the plant material infiltrated with the aforementioned constructs are separated in lanes 4, 5 and 6, respectively. Comparing the protein bands of crude extracts of leaves infiltrated with HBcAg-based construct (lane 2) to those of the control (lane 1), it could be noted that evident bands corresponding to the HBcAg-based protein were present in lane 2, but missing in the control. This comparison offers good evidence for the expression of the recombinant protein in plant material. However, various plant protein bands, possibly having a similar size to HBcAg $\Delta$ 176 and CoHe7e-eGFP, could be seen in the control. It was therefore not possible to prove the expression of the foreign proteins solely by simple observation of this gel.

Therefore, anti-HBcAg Western blot of an identical gel (Figure 2.3 B) was examined in parallel. As expected, crude extracts of leaves infiltrated with the control pEAQ-HT-empty vector did not show any anti-HBcAg reactivity (lane 1). Instead, HBcAg was detected in the crude extract of leaves infiltrated with pEAQ-HT-HBcAg $\Delta$ 176 (lane 2, as indicated by

red arrows), as well as in the crude extract of those infiltrated with pEAQ-*HT*-CoHe7e-eGFP (lane 3, as indicated by green arrows). HBcAg $\Delta$ 176 was detected at circa 20 kDa protein band, while CoHe7e-eGFP showed a much higher anti-HBcAg band at circa 68 kDa. In conclusion, the use of Coomassie stained SDS-PAGE along with the Western blot confirmed the presence of the HBcAg and CoHe7e-eGFP in the protein extract of the infiltrated leaves.

However, insoluble fractions of crude extracts of leaves infiltrated with pEAQ-*HT*-HBcAg $\Delta$ 176 (lane 5) and pEAQ-*HT*-CoHe7e-eGFP (lane 6), showed that some of the HBcAg-based protein remained trapped in the solid pellet that formed upon centrifugation. In the case of HBcAg $\Delta$ 176, the intensity of the anti-HBcAg signal was however clearly stronger in the supernatant (lane 2), rather than in the insoluble fraction (lane 5) of the crude extract. These findings can be related to the extraction buffer in use.

When expressing a recombinant protein in plant, the buffer chosen for the homogenisation of the leaf material must be able to efficiently extract this protein into the extract solution. In contrast, incomplete extraction would result in most of the recombinant protein getting trapped in the insoluble fraction, which is pelleted upon centrifugation. A recombinant protein “stuck” in the insoluble fraction is virtually un-retrievable and it is not therefore effectively viable for further processing. Thus the choice of the extraction buffer is obviously crucial. Under the conditions of this experiment, HBcAg $\Delta$ 176 could be highly “solubilised” and only a minor fraction remained in the insoluble pellet. Instead, the amount of HBcAg-based protein in the insoluble fraction of plant material infiltrated with CoHe7e-eGFP was almost as high as the amount of the same protein “solubilised” in the extraction buffer. The efficiency of this extraction buffer, developed by Dr. Eva Thuenemann, seemed good enough to allow the use of this extraction protocol as a standard for systematic plant-production of HBcAg-based proteins used in the course of this research.

#### 2.4.2 Purification and Characterisation of Plant-expressed HBcAg VLPs

HBcAg is a circa 20 kDa immunogenic protein, whose monomers self-assemble into a virus-like particle (Birnbaum and Nassal, 1990). The purification of VLPs from the crude

extract was carried out by sucrose density gradient, exploiting the properties of HBcAg VLP structure. HBcAg tertiary structures arrange into monomers, the monomers assemble into dimers and the dimers form a VLP, which constitutes the quaternary structure (Chapter 1). Upon ultracentrifugation, these VLPs are expected to sediment in the density fractions of 30, 40, and 50% (w/v) sucrose (Birnbaum and Nassal, 1990; Broos et al., 2007; Huang et al., 2006). Most plant proteins, as well as disassembled HBcAg, are expected to remain in the supernatant, whereas aggregated particles or other agglomerates of monomers tend to migrate to the bottom of the sucrose gradient. Therefore this technique was used as a primary method for the purification of VLPs from the crude extracts. Furthermore, the knowledge that morphologically intact cores can be specifically separated by density gradient centrifugation was also used throughout this study as a systematic quality control method to assess the yield, purity, morphological integrity and antigenicity of the VLP cores. For the fraction analysis, the sucrose gradient centrifugation was coupled with different detection methods, such as Coomassie stained SDS-PAGE gel, dot blot, Western blot or native agarose gel electrophoresis. Alongside with the qualitative characterisation methods, two different quantification methods for HBcAg were assessed.

#### **2.4.2.1 HBcAg Assembly in Plant Crude Extracts - A Qualitative Approach**

Figure 2.4 illustrates the distribution of HBcAg VLPs, contained in the plant crude extract, along the density fractions of a 10 to 60% discontinuous sucrose gradient upon ultracentrifugation. After ultracentrifugation, seven fractions, each approximately corresponding to the density layers of sucrose and to the supernatant, were collected from the bottom side of the tube (Figure 2.4 A) and analysed by SDS-PAGE. Three identical gels were run in parallel using the following set up (Figure 2.4 B, C and D): lane 1 corresponds to the original crude extract; lanes 2 to 8 contains density fractions of the sucrose gradient starting from the supernatant (lane 2) to the 60% sucrose fraction (lane 8); and lanes 9, 10 and 11 were loaded with diluted samples of the commercially available HBcAg standard with HBcAg content of 20, 100 and 500 ng/well, respectively. Figure 2.4 E and F show the dot blot immunoreactivity using the monoclonal and the polyclonal antibody, respectively.

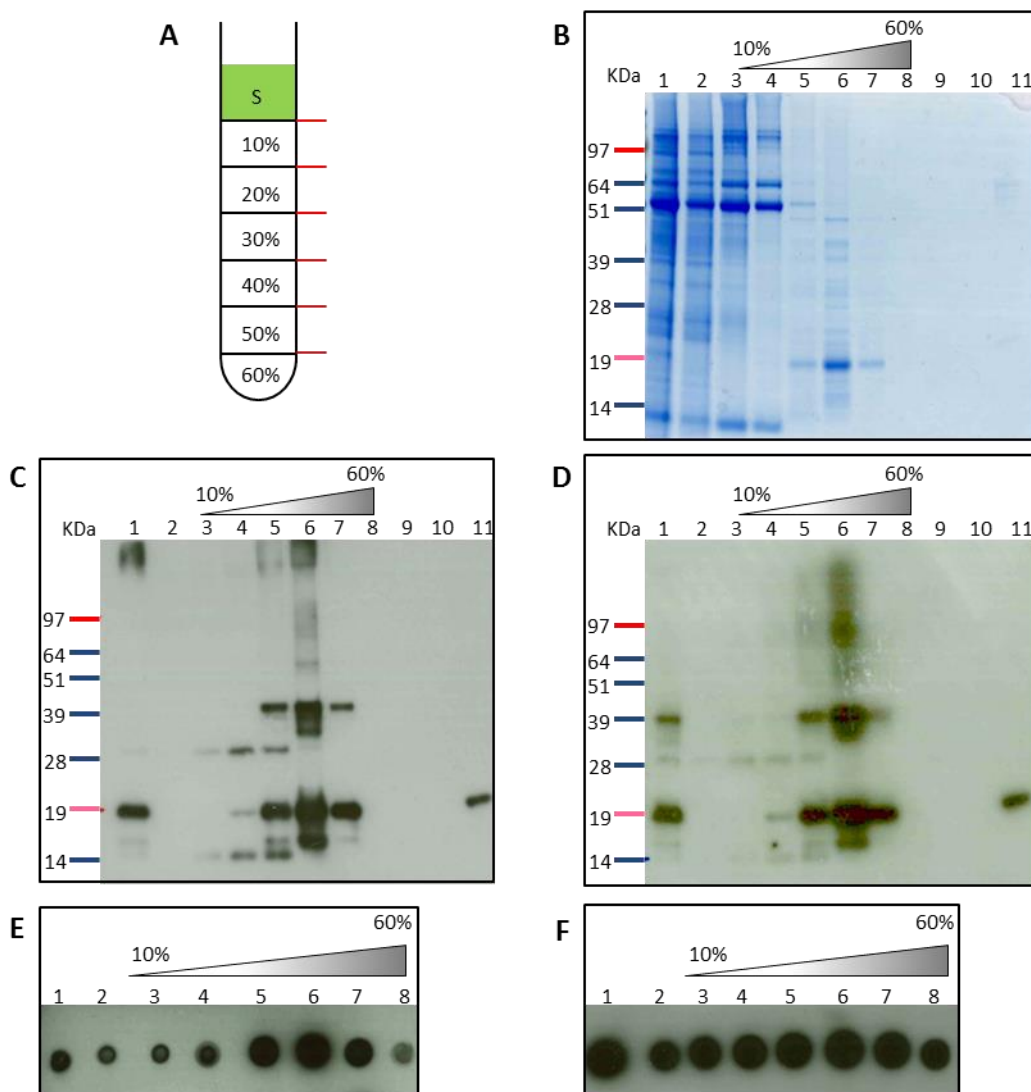


**Figure 2.4. Qualitative sucrose gradient analysis of plant crude extract.**

Crude extract of leaves of plant expressing HBCAg were layered onto 10 to 60% sucrose step gradient: (A) sucrose gradient (7 fractions from the supernatant to 60% sucrose); (B) Coomassie stained SDS-PAGE of the fractions; (C) Western blot using monoclonal antibody; (D) Western blot using polyclonal antibody. The lanes arrangement was as follows: crude extract (lane 1); supernatant (lane 2), 10 to 60% w/v sucrose fractions (lane 3 to lane 8); 20, 100 and 500 ng / well HBCAg standards (lanes 9, 10 and 11, respectively). E and F show the dot blot immunoreactivity using the monoclonal and the polyclonal antibody, respectively. The dots were spotted as follows: crude extract (dot 1); supernatant (dot 2); 10 - 60% (w/v) sucrose fractions (dot 3 to dot 8).

Coomassie stained gel (Figure 2.4 B) showed a 20 kDa band, corresponding to the size of monomeric HBCAg, in the 30, 40 and 50% (w/v) sucrose gradient fractions. The same band was, however, absent in the 60% (w/v) sucrose fraction. Most plant proteins bands remained in the supernatant and in the first two density fractions, i.e. 10 and 20% (w/v). The standard was probably too diluted and could not be detected. Proteins from the other

two gels, separated by gel electrophoresis, were transferred in PVDF membranes and probed with either anti-mouse monoclonal antibody (Figure 2.4 C) or anti-rabbit polyclonal antibody (Figure 2.4 D). The anti-HBcAg Western blots confirmed that the 20 kDa band, detected in lanes 5, 6 and 7 of Coomassie stained SDS-PAGE gel, actually corresponded to HBcAg. As expected, HBcAg was also detected in the original crude extract (lane 1) and in the most concentrated sample of HBcAg standard used as a control (lane 11). In the HBcAg-rich lanes, it is also possible to notice a persistent 40 kDa band. This band very likely denotes HBcAg dimers, which were resistant to the denaturing and reducing condition of the assay. The presence of this band corresponding to the dimer was also observed by others (Huang et al., 2006; Mechtcheriakova et al., 2006). Even larger size HBcAg multimeric structures have been detected in denaturing gel electrophoresis (Broos et al., 2007). Weaker bands of circa 15 kDa monomeric HBcAg and its dimer of 30 kDa can also be seen and they are possibly the result of partial enzymatic digestion of HBcAg by plant proteins. In the remaining samples HBcAg was not detected or only a weak signal could be detected under the experimental conditions employed.

Furthermore, the collected fractions from the sucrose gradient were also spotted onto two identical PVDF membranes, which were subsequently probed with either anti-mouse monoclonal primary antibody (Figure 2.4 E) or anti-rabbit polyclonal primary antibody (Figure 2.4 F). Dot 1 corresponds to the crude extract, while dots 2 to 8 contain density fractions of the sucrose gradient starting from the supernatant (dot 2) to the 60% (w/v) sucrose fraction (dot 8). HBcAg signal was detected in all the samples in both membranes. However, the anti-mouse monoclonal antibodies detected higher HBcAg content in the 30, 40 and 50% (w/v) sucrose fractions as compared to the other samples, whereas the rabbit polyclonal antibody seemed to detect high amounts of HBcAg in all the sucrose fractions as well as in the supernatant. The dots corresponding to the HBcAg immunoreactivity were of similar intensity in all the sucrose gradient fractions upon shorter exposure to the polyclonal antibody, suggesting that the high HBcAg concentration might have saturated the immunodetection.

A complete qualitative analysis of the sucrose gradient of the crude extract containing plant-expressed HBcAg was carried out by comparing denaturing gels either stained for protein or probed with two different specific monoclonal and polyclonal anti-HBcAg

antibodies, and with dot blots carried out in non-denaturing conditions. The first evidence is that most of the HBcAg was accumulated in the density fraction corresponding to 40% (w/v) sucrose and to a lower extent in 30 and 50% (w/v) sucrose gradient bands. This migration of the HBcAg to these high density fractions is compatible with the assembly of HBcAg into VLP (Birnbaum and Nassal, 1990; Broos et al., 2007; Huang et al., 2006). A close comparison between the monoclonal and polyclonal antibodies shows a very similar affinity of the two antibodies for HBcAg when this protein is denatured (Western blot). However, in the case of native undenatured samples as in the dot blot, the polyclonal antibody demonstrated much greater affinity for HBcAg than the monoclonal, particularly in those fraction of the sucrose gradient where partially disassembled HBcAg structures (10 to 20% (w/v) sucrose) or aggregated HBcAg (60% (w/v) sucrose) are expected. It is possible that the polyclonal antibody might have a particular affinity for a conformational epitope which is hindered by the properly assembled VLP structure and it is exposed in case of incomplete particulate formation or in case of protein aggregation. Moreover, this study allowed a first evaluation of the efficiency of the purification method: the Coomassie stained SDS-PAGE shows excellent purification and concentration of the VLPs using this sucrose gradient protocol. The crude extract (lane 1) appeared to be highly rich in plant proteins, to an extent that HBcAg, either as VLP or disassembled was not clearly detectable, possibly overlapping with the pool of plant proteins. In contrast, HBcAg VLP purified by density gradient centrifugation (lanes 5, 6 and 7) appeared well separated from the protein impurities and constituted the predominant protein band in each of these lanes. Approximately, a purity of > 90% could be estimated by visualisation of the gel.

#### 2.4.2.2 HBcAg Assembly in Plant Crude Extracts - A Quantitative Approach

The distribution of plant-expressed HBcAg in the sucrose density gradient was also quantitatively examined. Two different ELISA approaches were carried out for this purpose. This study also allowed the estimation of the total HBcAg yield. Furthermore it was possible to investigate the morphological integrity of HBcAg expressed in plant and therefore to evaluate the effective yield of VLP that can be recovered from the sucrose gradient and be used for further processing. Finally it was possible to compare the specificity of the two different ELISA methods.

Figure 2.5 illustrates a quantitative analysis of the density gradient: plant crude extracts containing HBcAg were loaded onto 20 to 50% (w/v) sucrose density gradients. After ultracentrifugation, five fractions approximately corresponding to each density layer as well as the supernatant were collected from the bottom side of the tubes and analysed by either direct (Figure 2.5 A) or sandwich ELISA (Figure 2.5 B). The amount of HBcAg in the density gradient fractions or in the supernatant was presented as mg HBcAg/kg of fresh weight (FW) of the original leaf tissue. Quantification by direct ELISA (Figure 2.5 A) revealed a total yield of the soluble HBcAg of 561 mg/kg FW, of which 44.1% was present in the 30 and 40% (w/v) sucrose density fractions and expected to correspond to intact HBcAg VLPs (Birnbaum and Nassal, 1990). HBcAg seemed predominantly detected in the supernatant of the sucrose gradient constituting 37.7% of the total HBcAg detected. Quantification of another density gradient by sandwich ELISA (Figure 2.5 B) demonstrated a total yield of the soluble HBcAg of 569 mg/kg FW, of which 75.4% was present in the 30 and 40% (w/v) sucrose density fractions. The supernatant contained only 1.9 % HBcAg of the total HBcAg detected.

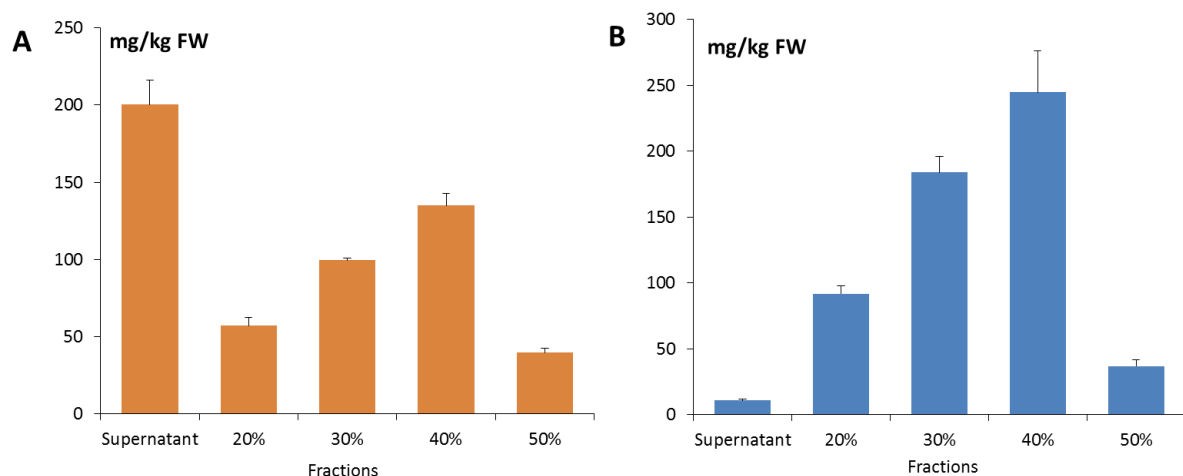


**Figure 2.5. Quantitative analysis of sucrose gradient density fractions of plant crude extract.**

Crude extracts of leaves of plant expressing HBcAg was layered onto 20 to 50% (w/v) sucrose step gradients. After ultracentrifugation, five fractions were collected from the bottom and further analysed by ELISA to quantify HBcAg distribution in these fractions: (A) direct ELISA ( $n = 3$ ); (B) sandwich ELISA ( $n = 3$ ). Error bars indicates standard deviation (SD). The amount of HBcAg is presented as mg of HBcAg/kg FW of the original tissue (y-axis) and plotted against concentration (in %) of the sucrose fractions (x-axis).

Although the total yield values obtained by the direct and sandwich ELISA were almost the same, the quantitative distribution of HBcAg through the sucrose gradient was clearly different between the two methods. This can be explained by the fact that different antibody sets were used for the two ELISAs and therefore the specificity of the two protocols could differ, potentially significantly. This hypothesis was confirmed by a simple experiment whereby purified samples of HBcAg, dialysed to remove the sucrose, were boiled for 10 minutes and analysed either by direct ELISA or by sandwich ELISA. The direct ELISA showed that boiled HBcAg maintained 75% residual anti-HBcAg immunoreactivity, when compared to the original sample. This finding together with the fact that the same polyclonal antibody used for the ELISA was also successfully used for detection in Western blot analysis of denaturing gels (Figure 2.4 D), confirmed that the polyclonal antibody has some affinity not only for conformational epitopes, but also for linearised and denatured epitopes. On the other hand, the sandwich ELISA analysis showed that boiled HBcAg lost all the anti-HBcAg immunoreactivity when compared to the native undenatured sample. This result clearly demonstrates that the use of a combination of two antibodies in the sandwich ELISA assay allowed the detection of conformationally intact particles only and it is therefore specific for VLPs.

In the light of this finding, the results of the quantification of HBcAg distribution obtained in Figure 2.4 can be re-examined and clarified: the most evident difference is that direct ELISA detected high amounts of HBcAg in the supernatant, while the sandwich ELISA, specific for VLP, did not. This suggests that the HBcAg detected in the supernatant was very likely monomeric, dimeric or a disassembled form; for this reason this HBcAg was unable to migrate down the gradient. The fact that a consistent amount of disassembled HBcAg was present in the supernatant is probably due to the incomplete formation or to the partial degradation of some of the HBcAg present in the leaf material or in the crude extract.

#### 2.4.2.3 Purified HBcAg VLP Characterisation

Using different qualitative and quantitative methods, thus far it was shown that plant-expressed HBcAg can assemble into VLP and can be separated from the more “soluble” proteins of the crude extract by sucrose gradient centrifugation. In this Paragraph, HBcAg

VLPs purified from plant-material were pooled together and further analysed, in order to characterise the integrity of the particles and to further explore the detection methods.

Plant crude extract containing HBcAg was layered onto sucrose gradient fractions for subsequent ultracentrifugation as described in the previous Paragraph. Based on the results previously shown and the knowledge that 30 and 40% (w/v) sucrose fractions should contain HBcAg VLPs (Birnbaum and Nassal, 1990; Huang et al., 2006), the purified 30 and 40% (w/v) immunoreactive fractions were pooled together and dialysed against 10 mM Tris-HCl, 120 mM NaCl buffer, in order to remove the sucrose. The sample was then examined by native agarose gel: equal amounts of HBcAg were separated by electrophoresis at 60 V for 90 minutes into 1.2% (w/v) agarose gel (Figure 2.6 A) and either stained with Coomassie stain (lane 1) or with ethidium bromide (lane 2). Coomassie is a stain for proteins, while ethidium bromide indicates the presence of nucleic acids. A clear band could be seen in the Coomassie stained native agarose gel, as well as in the ethidium bromide stained gel. The two signals appeared at equal electrophoretic mobility, strongly suggesting that the protein core, stained by the Coomassie, encapsidated nucleic acids. This is not surprising as it has been demonstrated that HBcAg contains an arginine-rich C-terminus domain, which binds non-specifically host nucleic acids (Birnbaum and Nassal, 1990; Gallina et al., 1989). The knowledge that HBcAg VLP binds nucleic acids has been exploited in the past to extensively characterise the stability and morphology of HBcAg by Coomassie or ethidium bromide stained native agarose gels (Newman et al., 2003).

The presence of VLPs was further confirmed by TEM images (Figure 2.6 B) of the dialysed 30 and 40% (w/v) sucrose gradient fractions: intact VLPs were clearly visible and their diameter (circa 30 to 35 nm) matches the size documented in the literature (Lee and Tan, 2008; Wingfield et al., 1995). From the TEM images, it was also possible to note the lack of evident agglomerates or nano-sized impurities in the sample.

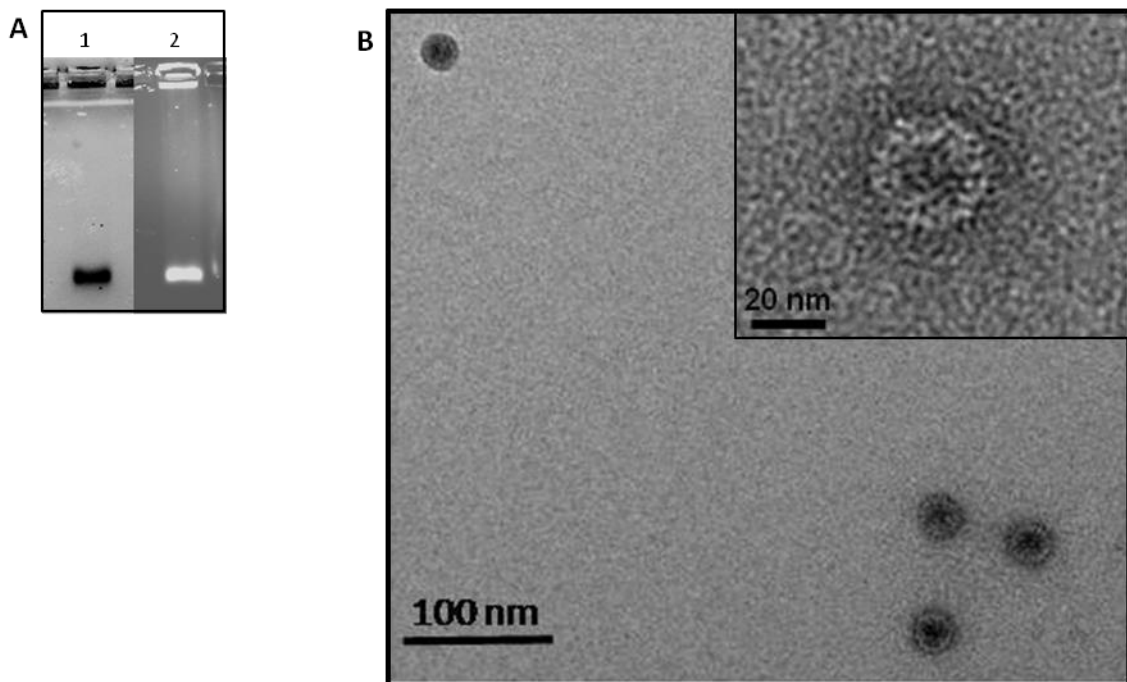


**Figure 2.6. Purified HBcAg assembled into VLP.**

Purified HBcAg samples, dialysed from 30 and 40% (w/v) sucrose gradient fractions were pooled together and analysed by: (A) native agarose gel electrophoresis, either stained with Coomassie stain (lane 1) or with ethidium bromide (lane 2), and (B) TEM images. Black scale bars and their relative dimensions are reported at the bottom of the image.

To further characterise HBcAg VLPs, purified and dialysed sucrose fractions were layered on a sucrose gradient, in order to establish the migration of purified VLPs following ultracentrifugation. The sucrose gradient fractions were analysed by sandwich and direct ELISA. Figure 2.7 A shows the distribution of the anti-HBcAg reactivity throughout the collected fractions of the sucrose gradient, detected by sandwich ELISA or direct ELISA. The data are reported as a percentage of immunoreactivity of the single density fraction as compared to the total reactivity of the sample. The sandwich ELISA, specific for VLPs, showed that 93.2% of the HBcAg particles migrated to the 30 and 40% (w/v) sucrose fractions. The fact that the purified intact VLPs migrated efficiently to the middle fractions of the sucrose gradient has been exploited in the subsequent chapters as a standard quantitative method to determine the stability of VLPs to particular conditions or manufacturing processes. In contrast, the direct ELISA detected only 73.1% of HBcAg in the 30 and 40% (w/v) sucrose fractions, and also showed certain immunoreactivity in the supernatant and the 10 and 20% (w/v) sucrose fractions. This latter signal possibly corresponded to partially degraded or breakdown forms of HBcAg. The lower specificity

of the direct ELISA for morphologically intact particles makes the use of this technique as a method to assess VLP stability complicated; for this reason the sandwich ELISA was always the technique of choice for future experiments.

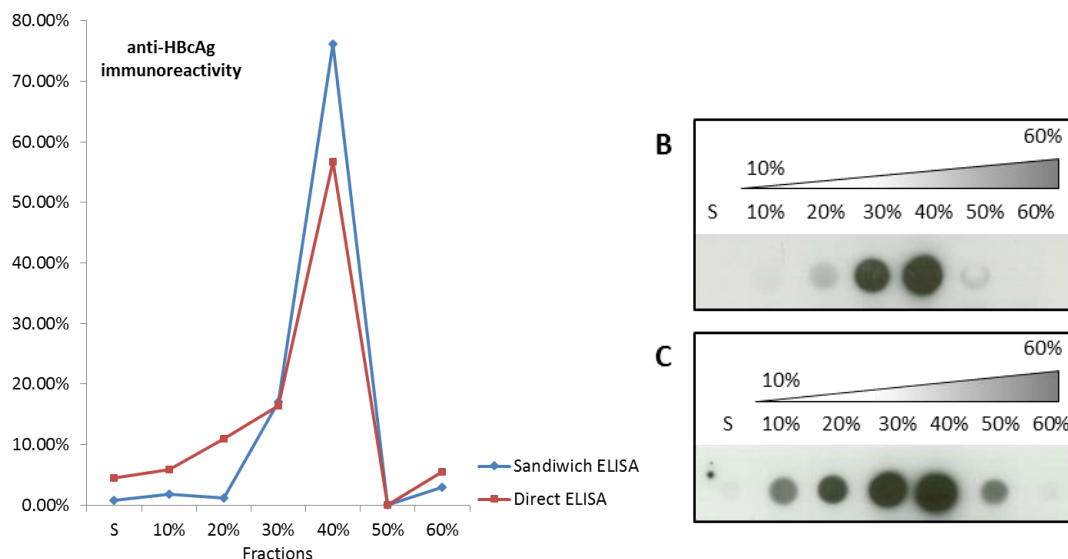


**Figure 2.7. Sucrose gradient analysis of purified VLPs.**

Purified HBcAg, obtained from pooling together the dialysed 30 and 40% (w/v) sucrose gradient fractions, were layered onto 10 to 60% (w/v) sucrose step gradients. After ultracentrifugation, seven fractions were collected from the bottom and further analysed. (A) shows the distribution of the anti-HBcAg reactivity throughout the collected fractions of the sucrose gradient, detected by sandwich ELISA or direct ELISA. The data are reported as a percentage of immunoreactivity of the single density fraction as compared to the total reactivity of the sample. (B) and (C) show the dot blot immunoreactivity using the monoclonal and the polyclonal antibody, respectively. S = supernatant; percentages indicate the respective sucrose concentration of each fraction.

The sucrose gradient was further analysed by dot blot, probing the membranes with anti-HBcAg monoclonal antibody (Figure 2.7 B) or with anti-HBcAg polyclonal antibody (Figure 2.7 C). The monoclonal antibody detected HBcAg mainly in the 30 and 40% (w/v) sucrose fractions, whereas the polyclonal antibody detected HBcAg in all fractions under study except in the supernatant and the 60% (w/v) sucrose fraction. This result reflects a similar experiment carried out on the crude extract (Figure 2.4 E and F), whereby the polyclonal antibody seemed to have a higher tropism than the monoclonal for disassembled HBcAg, present in the lighter fractions of the sucrose gradient. This result is a confirmation that the binding of VLPs to antibodies can be quite complicated. Thus, a

careful selection of the right antibody, depending on the specific application for which it is chosen, as well as a careful interpretation of the experimental results should be carried out.

#### **2.4.2.4 Preparation of Purified VLP Batches**

Batches of purified HBcAg VLPs were routinely prepared during the course of this research to be used for further processing or testing. For this purpose plant leaves were infiltrated with pEAQ-HT-HBcAg $\Delta$ 176, harvested after 6 to 7 days and homogenised with extraction buffer 2. The resulting crude extract was clarified and the supernatant was placed on the top of the sucrose density gradient. After ultracentrifugation, fractions corresponding to each density layer were collected from the bottom. Sucrose density fractions of 30 and 40% (w/v) were pooled together and dialysed against PBS or 10 mM Tris-HCl, 120 mM NaCl buffer, depending on the application. VLP preparations were then concentrated by ultrafiltration carried out at 4,000 x g for the time required. The preparation was then centrifuged at 4,000 x g for 20 minutes, in order to spin down residual impurities. After final quantification by ELISA, the purified HBcAg batches were stored in the fridge until use. Generally the purified VLPs were used within 4 to 6 weeks from production. Immediately before use, VLP preparations were appropriately diluted, depending on the application. Figure 2.8 A summarises the VLP production and purification steps described above. Samples indicated by numbers 1, 2, 3, 4, 5 were collected at different steps of the purification and further analysed.

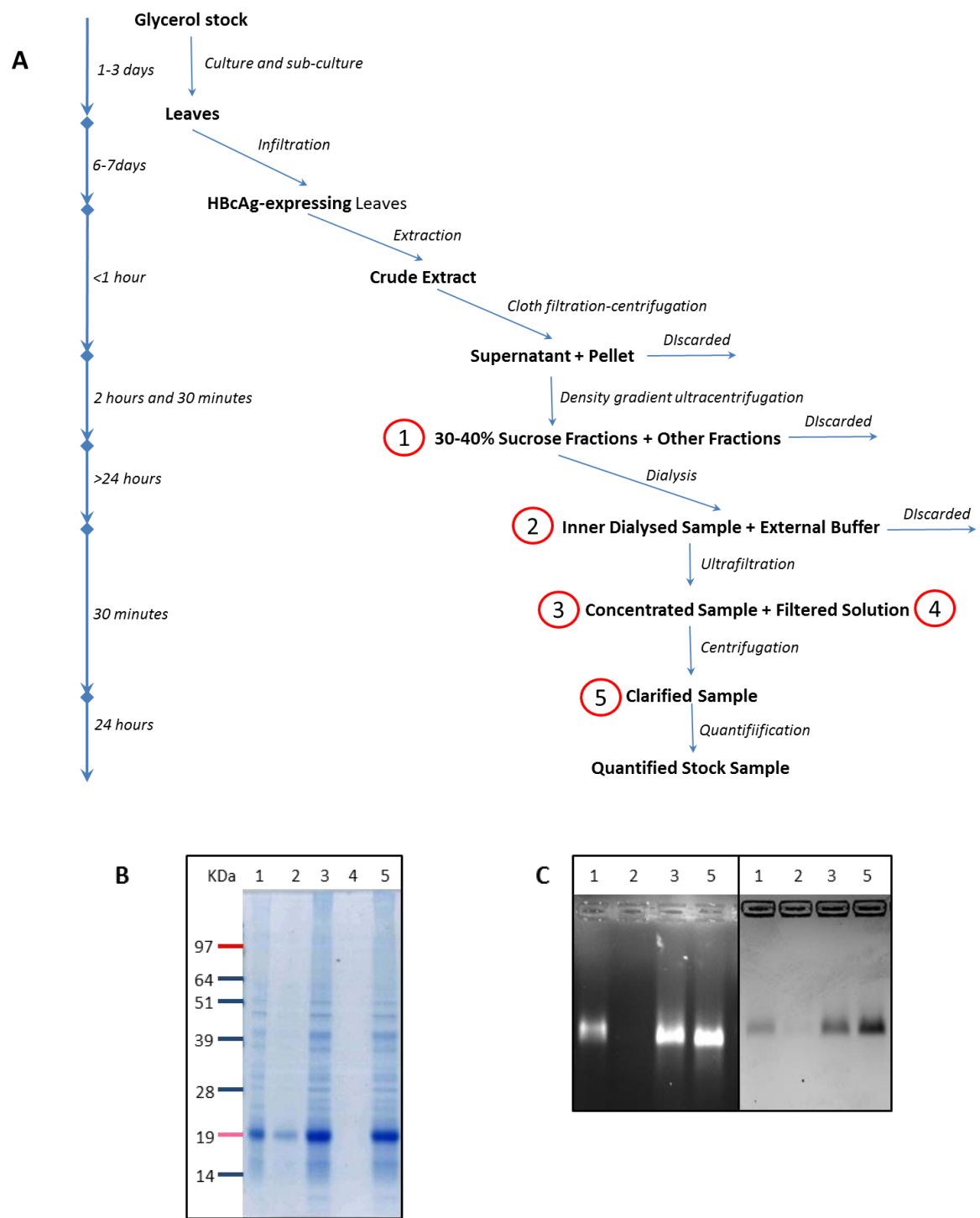


**Figure 2.8. VLP purification and concentration efficiency.**

(A) is a diagram that illustrates the VLPs production and purification steps. Samples indicated by numbers 1, 2, 3, 4, 5 were collected at different steps of the purification and further analysed. (B) shows the Coomassie stained SDS-PAGE. Lanes correspond to samples as numbered in the diagram above. (C) shows the native agarose gel electrophoresis: the images relative to the ethidium bromide stain and to the Coomassie stain are presented in the left side and in the right side, respectively. Lanes correspond to samples as numbered in the diagram above.

Figure 2.8 B illustrates a Coomassie stained SDS-PAGE relative to the different purifications steps. The 20 kDa protein band, corresponding to HBcAg, can be constantly observed in samples 1, 2, 3 and 5, indicating that HBcAg was not significantly lost during the process. Dialysis was carried out using membranes up to 100 kDa cut-off. This size of the cut-off would allow monomeric HBcAg, but not HBcAg VLP, to leak out from the membrane, proving that most HBcAg was present as VLPs. However, the sample became quite dilute upon dialysis, due to the osmotic force exercised by the sucrose solution loaded into the dialysis membrane. For this reason, the sample was subsequently concentrated by ultrafiltration. HBcAg VLP did not pass through the 100 kDa cut-off membrane as demonstrated by the fact that the HBcAg protein band was absent in the filtrate (sample 4). Furthermore, VLP did not stick to the ultrafiltration membrane: in fact it could be recovered and concentrated, as shown in sample 5.

The same samples were also separated by native agarose gel electrophoresis (Figure 2.8 C). Two identical gels were stained either by ethidium bromide (Figure 2.8 C, left side) or by Coomassie (Figure 2.8 C, right side). A discrete band can be also visualised in both native agarose gels: the band of protein staining (Coomassie-stain) and that of nucleic acid (ethidium bromide-stain) showed identical electrophoretic migration. This strongly suggests that the capsid-like structure, encapsidating nucleic acid, was stable throughout the purification. The dilution of the VLPs during the dialysis and the subsequent concentration of the sample during the concentration step are evident in the native agarose gel, as in the SDS-PAGE gel.

Overall, the downstream yield of plant-expressed intact HBcAg VLPs, extracted and purified through sucrose gradient was circa 400 mg/kg FW, as determined by sandwich ELISA. During the course of the current research, 15 plants were generally infiltrated each time and were then pooled together, extracted and purified in a single batch of six identical sucrose gradients: 15 plants correspond to circa 50 g of leaf tissue, which, after dialysis and concentration, could allow the recovery of approximately 10 mg of purified VLPs, usable for pharmaceutical research purposes. Initially, the amount of HBcAg VLPs can seem quite low, when compared to the kilograms of bulk stocks of other active ingredients available for drug delivery research purposes. However, VLP proteins are very complex and expensive macromolecules. For comparison, the price of the cheapest recombinant

HBcAg standard, sold by a global manufacturer, costs at the present day £234 for only 0.1 mg of product. It is therefore evident that the production of tens of mg of the same recombinant protein in plant, inexpensively and in less than 2 weeks starting from culturing the glycerol stock to the final protein purification, constituted a unique opportunity for this project: each 10 mg batch of purified VLPs was potentially worth about £20.000! Overall, subsequent drug delivery oriented research could have not been carried out on these proteins if such an effective expression system was not available.

### 2.4.3 Plant-expressed CoHe7e-eGFP Characterisation

In Paragraph 2.4.1, the expression of CoHe7e-eGFP in plant was shown in parallel to HBcAg expression. CoHe7e-eGFP is a construct in which the original HBcAg expression sequence was modified to allow the expression of a GFP molecule on the loop of each HBcAg dimer. Therefore, the assembly of dimers into particles generates VLPs decorated by fluorescent proteins all around its structure. The possibility of using fluorescent HBcAg particles could provide a useful investigation tool for the drug-delivery studies and bio-imaging purposes of this research.

Plant-expression and assembly of HBcAg-derived VLP, such as CoHe7e-eGFP, is not as efficient as for HBcAg wild-type (Dr. Eva Thuenemann, personal communication). Thus, before further use of CoHe7e-eGFP in the current research, it was essential to evaluate whether adequate yields of purified, properly formed CoHe7e-eGFP VLP could be achieved. For this purpose, leaves expressing CoHe7e-eGFP were homogenised in the extraction buffer 2 and the resulting crude extract was layered on the top of a 10 to 60% (w/v) discontinuous sucrose gradient. After centrifugation, fractions were collected from the bottom and analysed by Coomassie stained SDS-PAGE, as illustrated in Figure 2.9 A: lanes 1 and 2 represent the crude extract and the supernatant, respectively, while lanes 3 to 8 correspond to density fractions of sucrose concentration increasing from 10 to 60% (w/v). As indicated by the green arrow, a protein band of circa 65 to 70 kDa, matching CoHe7e-eGFP size, could be seen in lanes 1 to 7 and more markedly in lanes 5, 6 and 7. The same density gradient fractions were also spotted on two PVDF membranes, which were then probed with anti-HBcAg antibody, in order to assess HBcAg immunoreactivity along the density gradient. Figure 2.9 B and C illustrate the anti-HBcAg dot blots using

monoclonal and polyclonal antibody, respectively: dots 1 and 2 represent the crude extract and the supernatant, respectively, while dots 3 to 8 correspond to density fractions of sucrose concentration increasing from 10 to 60% (w/v). Both images confirmed that HBcAg immunodetection was observed in the supernatant and along all fractions of the sucrose gradient, except for the 60% (w/v) sucrose density layer. Most anti-HBcAg reactivity can be seen in the dots corresponding to 30, 40 and 50% (w/v) sucrose fractions. This result matches the one obtained with the SDS-PAGE gel: CoHe7e-eGFP showed good expression levels in plant, however, it was detected in most layers of the sucrose gradient. This latter observation suggested that a significant amount of CoHe7e-eGFP was not properly assembled into VLP and it was present in a variety of multimeric intermediate forms, which migrated all along the gradient. However, the almost complete lack of CoHe7e-eGFP detection in the 60% sucrose fraction implies that probably the protein did not form agglomerates.

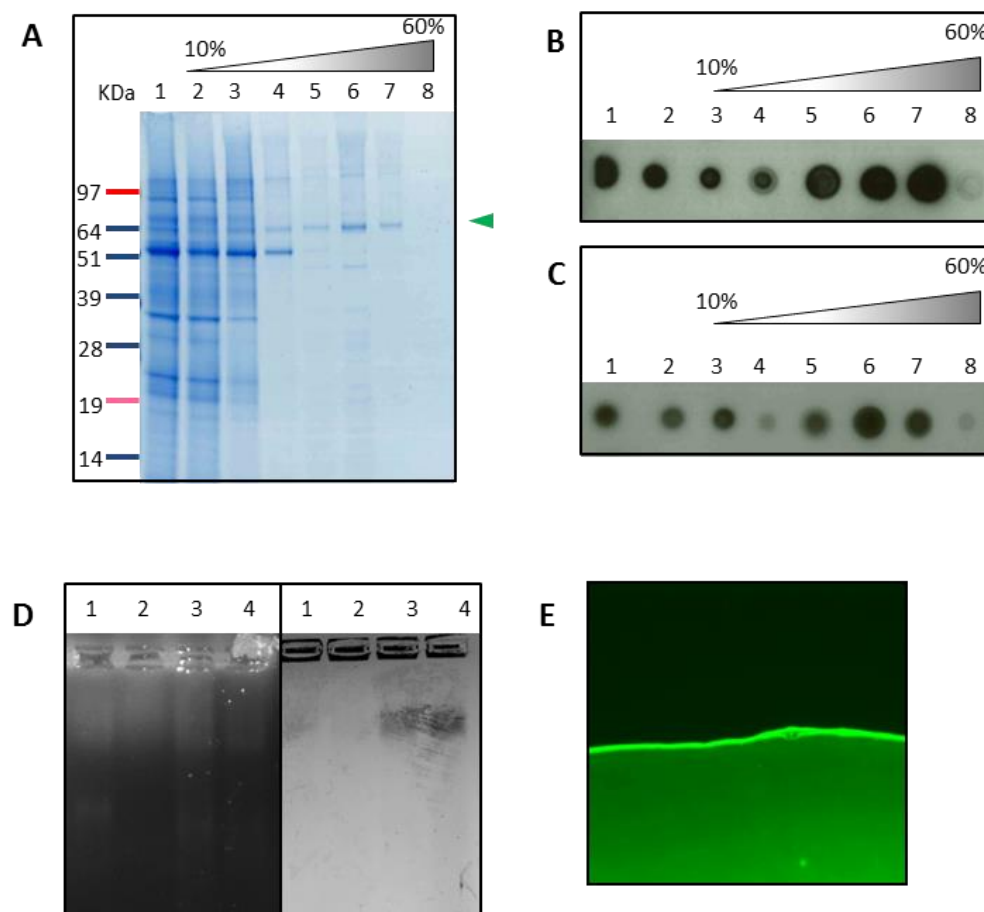


**Figure 2.9 CoHe7e-eGFP purification and characterisation.**

Crude extract of leaves of plant expressing CoHe7e-eGFP were layered onto 10 to 60% (w/v) sucrose step gradients. After ultracentrifugation, seven fractions were collected from the bottom and further analysed. (A) illustrates the Coomassie stained SDS-PAGE: crude extract (lane 1); supernatant (lane 2); sucrose density fractions of increasing concentrations of 10 to 60% w/v (lanes 3 to 8). (B) and (C) show the dot blot immunoreactivity using the monoclonal and the polyclonal anti-HBcAg antibody, respectively: crude extract (dot 1); supernatant (dot 2); 10 to 60% (w/v) sucrose (dots 3 to 8). Purified HBcAg, dialysed from 30 and 40% w/v sucrose gradient fractions were pooled together and subsequently concentrated by ultracentrifugation. Finally, the sample was clarified by centrifugation at 4,000 x g for 20 minutes before use. (D) shows the native agarose gel electrophoresis: ethidium bromide stained (left side) and Coomassie stained (right side). Pooled together 30 and 40% (w/v) sucrose density fractions, dialysed sample, concentrated sample, and final product after the last centrifugation are illustrated in lanes 1, 2, 3 and 4, respectively. (E) illustrates the fluorescence of purified CoHe7e-eGFP drops as seen using the fluorescent microscope (10x magnification).

Based on the knowledge that wild type HBcAg VLPs tend to migrate to the 30 and 40% w/v sucrose gradient fractions, CoHe7e-eGFP collected from those two fractions were pooled together, dialysed and concentrated by ultrafiltration, before a final centrifugation at 4,000 x g for 20 minutes. The presence of VLPs and their stability during each step were

assessed by native agarose gel electrophoresis: two identical gels were stained either by ethidium bromide (Figure 2.9 D, left side) or by Coomassie-stain (Figure 2.9 D, right side): lane 1 corresponds to the VLP-rich 30 to 40% (w/v) sucrose fractions collected after ultracentrifugation; lane 2 represents the same sample, after dialysis of the 30 to 40% (w/v) sucrose fractions; lane 3 relates to the dialysed sample, after being concentrated by ultrafiltration; lane 4 corresponds to the sample after the last centrifugation at 4,000 x g for 20 minutes. The ethidium bromide stained native agarose gel seemed free from nucleic acid bands, while the Coomassie-stain gels showed the presence of a very faint band in lanes 1 and 2, which seemed more marked in lanes 3 and 4. The lack of evident nucleic acid bands suggests that the particles were either too diluted or that they did not encapsidate consistent amounts of nucleic acid. Instead, in the Coomassie stained gel, the presence of a protein band whose intensity increased upon concentration by ultrafiltration, suggests that CoHe7e-eGFP did not pass through the filter being in a particulate state. Furthermore, despite its complex protein structure, CoHe7e-eGFP VLP resisted the ultrafiltration stress and could be re-suspended without getting agglomerated or stuck to the filter membrane. However, the protein band was less concentrated and more diffused compared to the ones obtained for HBcAg (Figure 2.8 B), suggesting that external charge and/or size of CoHe7e-eGFP VLP are more variable, compared to HBcAg VLP. Additionally, the yield of VLP seemed significantly lower than that of HBcAg. Furthermore, purified CoHe7e-eGFP VLP was quantified by direct ELISA (data not shown). Finally, CoHe7e-eGFP VLP drops were also observed using the fluorescent microscope. Figure 2.9 E shows the green-fluorescence of CoHe7e-eGFP VLP drop. The presence of visible fluorescence is compatible with the correct folding of the GFP portions of the VLP.

Taken together, the above results suggest that CoHe7e-eGFP was expressed in plant less efficiently than HBcAg, both in terms of yield and morphological integrity of the particles. This finding together with the fact that the CoHe7e-eGFP engineered structure differed from the naturally occurring HBcAg structure, set back the use of CoHe7e-eGFP as the first candidate VLP for further drug delivery experiments of this research, when compared to wild type HBcAg. However, despite these limitations, CoHe7e-eGFP VLP could be purified and concentrated; therefore its use was attempted for bio-imaging investigations.

#### 2.4.4 HBcAg Expression in Lettuce

The main focus of this research was the investigation of plant-expressed HBcAg VLP for the development of oral vaccines. One of the most recognised benefits of the expression of candidate vaccines in plant is the possibility of using edible plants (Walmsley and Arntzen, 2000): the prospect of producing effective edible vaccines in fruits or vegetables is extremely fascinating and has driven extensive biotechnological research in the past two decades. However, the risks of contamination of the food chain with attendant safety issues, as well as the likely difficulties in dose and formulation standardisation and possible lack of efficacy have decreased interest in edible vaccines. These aspects were discussed in Chapter 1. Aware of these limitations, the expression of HBcAg $\Delta$ 176 in an edible plant was attempted: *Valmaine romaine* lettuce was vacuum-infiltrated with an *Agrobacterium* suspension containing pEAQ-HT-HBcAg $\Delta$ 176. The infiltrated leaves were then harvested at 3, 5, 7 and 9 days post-infiltration (DPI). The leaf material was then snap-frozen and stored at - 80 °C until use. For the extraction of VLPs, the leaf material was weighed and blended in three volumes of the extraction buffer 2. Following cloth filtration, the crude extract was clarified by centrifugation: the resulting supernatant was separated from the precipitated pellet (insoluble fraction). The pellet was re-suspended in LDS  $\beta$ -mercaptoethanol, boiled and clarified again. Both the supernatant and the insoluble fraction were separated by SDS-PAGE. The gel was then used for anti-HBcAg Western blot detection. The soluble fraction was also used for sandwich ELISA quantification of HBcAg VLP.

Figure 2.10 illustrates the presence of the HBcAg in the protein extracts of the infiltrated lettuce leaves. Figure 2.10 A presents the anti-HBcAg Western blot: purified HBcAg expressed in *Nicotiana benthamiana* (lane 1); the supernatant of the crude extract of infiltrated lettuce leaves harvested at 3, 5, 7 and 9 days post-infiltration (DPI) (lanes 2, 3, 4 and 5, respectively); empty lanes (lanes 6 and 7); insoluble fraction of the crude extract of infiltrated lettuce leaves harvested respectively at 3, 5, 7 and 9 DPI (lanes 8, 9, 10 and 11). Anti-HBcAg immunoreactivity can be seen from 5 to 9 DPI in the soluble fraction. Furthermore, the quantification of HBcAg VLP by sandwich ELISA (Figure 2.10 B) showed that a maximum yield of 8.75 mg/kg of FW of the tissue was reached at 7 DPI. This result represents a proof of concept that HBcAg could be expressed in edible lettuce

using the unmodified pEAQ-*HT*- system. However, the level of expression was approximately 50-fold lower than the expression level achieved in *Nicotiana benthamiana*. For this reason the expression of HBcAg in lettuce was not carried forward for the production of bulk quantities of HBcAg throughout this project. Nevertheless it is possible to hypothesise that optimisation of the plasmid sequence for *Valmaine romaine* could boost expression to considerably higher levels.

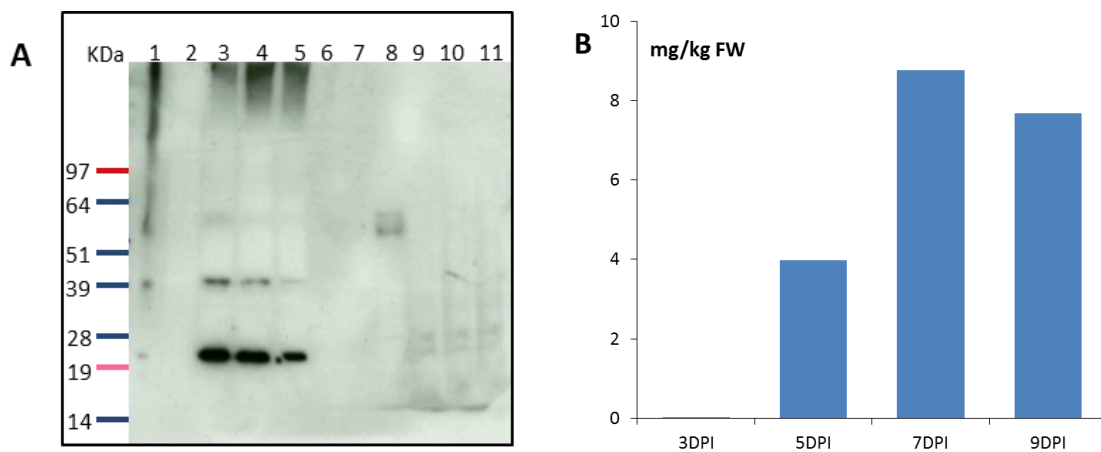


**Figure 2.10. HBcAg expression in lettuce.**  
 pEAQ-*HT*-HBcAg $\Delta$ 176 was vacuum infiltrated in *Valmaine romaine*. The infiltrated leaves were harvested at 3, 5, 7 and 9 days post-infiltration. Following extraction of the leaves' protein, the supernatant and the insoluble fraction of the crude extract were separated by SDS-PAGE. (A) illustrates the anti-HBcAg Western blot (monoclonal antibody) of the crude extracts: purified HBcAg expressed in *Nicotiana benthamiana* (lane 1); the supernatant of the crude extract of infiltrated lettuce leaves harvested at 3, 5, 7 and 9 DPI (lanes 2, 3, 4 and 5, respectively); empty lanes (lanes 6 and 7); insoluble fraction of the crude extract of infiltrated lettuce leaves harvested respectively at 3, 5, 7 and 9 DPI (lanes 8, 9, 10 and 11). (B) shows the sandwich ELISA quantification (n = 2) of the supernatant of the crude extracts at different DPI. Results are presented as mg of HBcAg/kg FW of the original tissue. DPI= days post-infiltration.

#### 2.4.5 Conclusions

In this research, plant-expressed HBcAg VLP was studied as a potentially orally active macromolecule. In this Chapter, HBcAg-based VLP, expressed in plant using the pEAQ-*HT*-system, were extensively characterised. The physical structure and immunogenicity of HBcAg in the plant crude extract were evaluated; in parallel purified HBcAg VLPs were further characterised. Additionally, the extraction, purification and concentration methods were assessed in terms of yield, purity, morphological integrity and antigenicity.

Plant-expressed HBcAg could be immunodetected. Purification of the crude extract by density gradient ultracentrifugation demonstrated that part of the expressed HBcAg could penetrate the lower density fractions of the gradient, which is compatible with the formation of VLP. HBcAg VLP could in fact be detected in the 30, 40 and 50% (w/v) fractions by Coomassie stained SDS-PAGE, Western blot and dot blot. However, a moderate amount of HBcAg, present in the less dense fractions of the sucrose gradient, did not seem to have correctly assembled into particles. The distribution of the HBcAg from the crude extract through the sucrose gradient was also quantified using two different ELISA methods. Furthermore, analysis of purified VLPs showed highly selective migration to the 30 and 40% (w/v) sucrose density fractions upon ultracentrifugation. Moreover, purified HBcAg VLPs could be detected by native agarose gel electrophoresis and could be visualised by TEM. Thus, native agarose gel, TEM, as wells as sucrose gradient centrifugation coupled to Coomassie stained SDS-PAGE, Western blot and/or dot blot proved to be effective tools for investigation of the physical stability of the VLP. These techniques would therefore be essential for the assessment of VLPs' physical stability in the following Chapters.

Moreover, the specificity and limitations of the detection methods were defined: monoclonal and polyclonal anti-HBcAg antibody could be both used for immunodetection of denatured or native samples; however, the polyclonal antibody appeared to have a better affinity for the disassembled form of HBcAg. Furthermore, sandwich ELISA was demonstrated to specifically detect intact HBcAg VLP only, whereas direct ELISA was shown to detect both undenatured and disassembled HBcAg forms. Knowing the specificities of the methods used is important for a better interpretation of the results. Finally, the purification and concentration technique proved to be effective in terms of yield and VLP stability. Overall, for standard batches of 15 plants, corresponding to 50 g of leaves, approximately 10 mg of purified HBcAg could be produced.

In parallel, CoHe7e-eGFP expression in plant was also examined. This recombinant protein is a fluorescent alternative to the wild type HBcAg, potentially usable for bio-imaging purposes. The expression of CoHe7e-eGFP proved to be significantly inferior to HBcAg in terms of yield and morphological integrity. It was demonstrated also that HBcAg could also be expressed in *Valmaine romaine* lettuce, which is, unlike *Nicotiana*

---

*benthamiana*, an edible plant. However, the yield achieved was very low, discouraging the use of this method for further studies in the present research.

Overall, this Chapter described the efficiency and limitations of the production and purification of HBcAg constructs from plant. Furthermore, the usability and specificity of the characterisation techniques were investigated. In the following Chapters, the expression, purification and characterisation techniques described here will be utilised in the investigation of the potential of HBcAg VLPs as orally vaccines.

### 3 Stability of HBcAg VLP in Bio-relevant Gastro-Intestinal (GI) Media

#### 3.1 Introduction

The harsh environment present in the stomach and intestine is the first barrier to the oral delivery of vaccines and constitutes a real challenge to the stability of therapeutic proteins, including vaccines.

The gastric fluid in the human stomach is an extremely harsh environment for physically- and chemically-labile molecules, due to the highly acidic pH and the presence of digestive enzymes. *In vitro* models of simulated gastric fluids are often used for the determination of the behaviour of therapeutic molecules and formulations under these conditions. The first systematic application of simulated gastric fluid digestion was developed to establish the digestibility of food allergens (Astwood et al., 1996). Since then such *in vitro* models have been used for the evaluation of the stability and release of different therapeutic formulations, including those of nucleic acids and therapeutic proteins (Gamboa and Leong, 2013; O'Neill et al., 2011). Several protocols have been established, in order to achieve good correlation between *in vitro* models and human gastric conditions [reviewed by (O'Neill et al., 2011)]. Three commonly used recipes are summarised in Table 3.1.

**Table 3.1. *In vitro* models of gastric fluids [adapted from(O'Neill et al., 2011)]**

| Model media                                   | Description   | Reference                    |
|---|---|------------------------------|
| Simulated gastric fluid (SGF)                 | pH 1.2 (with and without pepsin), NaCl                        | (British Pharmacopeia, 2012) |
| Fasted State Simulated Gastric Fluid (FaSSGF) | pH 1.6, pepsin and low levels of bile salt and lecithin, NaCl | (Vertzoni et al., 2005)      |
| Fed State Simulated Gastric Fluid (FeSSGF)    | Variable pH , full-fat milk, acid and pepsin                  | (Fotaki et al., 2005)        |

Simulated gastric fluid (SGF) as described in the British Pharmacopeia is the standard model mimicking fasting conditions in the stomach and can be supplemented also with porcine pepsin (British Pharmacopeia, 2012). However, Vertzoni et al. (2005) proposed a media which should more accurately simulate the fasting gastric contents; this bio-relevant

media was called Fasted State Simulated Gastric Fluid (FaSSGF): compared to the original SGF formula, in FaSSGF, the pH was increased to 1.6 and physiologically appropriate small amounts of bile salts and phospholipids were introduced. Furthermore, a different pepsin than that used in SGF was employed in FaSSGF and its concentration in the media was fixed as 0.1 mg/mL. This concentration should relate to the reported *in vivo* concentration of pepsin, after ingestion of a glass of water (Kalantzi et al., 2006; Vertzoni et al., 2005). Later in the same year, a model of gastric fluid simulating the fed condition of the stomach was also developed. The Fed State Simulated Gastric Fluid (FeSSGF) is based on the knowledge that there are postprandial pulsatile acid and pepsin secretions in humans. The initial medium is constituted by full-fat UHT milk, which contains protein, carbohydrates and fat, mimicking the composition of a complete meal. At predetermined time intervals, aliquots of HCl and pepsin are added, in order to closely simulate the *in vivo* pulsatile secretion of these two components after a meal: in this model the pH declines from pH 6.5 to circa pH 2.8 over the first 90 minutes (Fotaki et al., 2005), reflecting the physiological values observed *in vivo* after the ingestion of a meal substitute (Kalantzi et al., 2006).

Despite the improved bio-relevance of these simulated gastric fluid models, it is still difficult to completely simulate the extremely variable physiological conditions. For example, human gastric acidity was reported to range between pH 1 and 6 in fasted conditions (Efentakis and Dressman, 1990). It has been also stated that the pepsin activity in human gastric fluid can vary over 10,000 fold (Gomes et al., 2003). In this perspective, it is clear that a single standard protocol cannot fully represent this huge variability observed *in vivo*.

The small intestinal environment is, after the stomach, the second physico-chemical barrier that a candidate vaccine has to withstand upon oral administration. The intestinal fluids bear a more neutral pH compared to the gastric fluids, generally ranging between pH 6.3 and pH 7.4 (Evans et al., 1988). However, it was more recently reported that the pH can be as low as 5.5 in the duodenum (the first section of the small intestine). Moreover, even in the small intestine the variability of pH between different people can be very high (over two pH units) (McConnell et al., 2008b). Nevertheless, due to its relative neutrality, the pH of the intestine is not expected to be such an important barrier as that of the stomach for

most orally delivered vaccine formulations. However, the intestine also contains several enzymes, including trypsin and chymotrypsin, which could digest antigens. Moreover, many novel nanoparticulate protein formulations, in particular those based on vesicular carriers, such as liposomes, can also be degraded by the detergent effect of physiological levels of intestinal bile salts (Parmentier et al. 2011). Several *in vitro* models of intestinal fluids containing bile salts are available (O'Neill et al., 2011). A disadvantage of these model fluids is that they do not contain enzymes, which are likely to cause degradation of therapeutic proteins. Therefore, media containing the digestive enzymes are often used in the study of therapeutic proteins. Simulated Intestinal Fluid (SIF) described in the British Pharmacopeia (2012) is a bio-relevant medium of pH 6.8 containing porcine pancreatin, which is composed of pancreatic digestive enzymes, including most intestinal proteases (British Pharmacopeia, 2012). This model fluid is not based on the use of a single enzyme, but contains the whole pancreatic enzyme complex, and is therefore expected to be more relevant for digestion studies than those which contain a single protease (Reuter et al. 2009). Yet, it has been reported that even a pool of pancreatic endopeptidases accounts for only 1/3 of the total proteolytic activity of the intestinal fluids. Therefore, it has been suggested that *ex-vivo* studies should also be considered when assessing the stability of a protein, as the proteolytic activity of natural intestinal fluids represents the closest possible simulation of the *in vivo* scenario (Reuter et al. 2009).

In this Chapter, the GI stability of plant-expressed Hepatitis B core antigen (HBcAg) VLP, as a model candidate vaccine, was investigated. *In vitro* stability studies were carried out using bio-relevant media that simulate the different environmental conditions of the human GI tract. Furthermore *ex vivo* evaluation of the antigen stability was carried out in pig luminal intestinal fluids. The integrity of the HBcAg was investigated in terms of chemical stability of the primary structure. For this purpose the main characterisation techniques used were SDS-PAGE and Western blot. The physical stability of the capsids under gastro-intestinal conditions was also evaluated using native agarose gel electrophoresis, TEM, as well as sucrose density gradient ultracentrifugation coupled with immunodetection techniques.

The overall objective was to determine the extent to which purified HBcAg VLPs are stable under conditions simulating the gastric and intestinal environments.

## 3.2 Materials

### 3.2.1 Molecular Biology Media, Buffers and Solutions

General media, buffers and solutions used in this study for bacterial growth, plant agro-infiltration and protein analysis are catalogued in Table 2.1 of Chapter 2.

### 3.2.2 Antibodies and Antigens

Antibodies and antigen standards used for Western blot, dot blot and ELISA are listed in Table 2.2 of Chapter 2.

### 3.2.3 Enzymes and Other Materials Used for Stability Studies

The materials used for the preparation of bio-relevant media used for the incubation of HBcAg are indicated below in Table 3.2.

**Table 3.2. Components of incubation media.**

| Name  | Supplier                               |
|---|--|
| HCl   | Fisher Scientific, UK                  |
| NaOH  | Fisher Scientific, UK                  |
| KH <sub>2</sub> PO <sub>4</sub>                           | VWR (AnalR), UK                        |
| Pepsin (Ph Eur) from porcine gastric mucosa               | Sigma, UK                              |
| Pepsin ( $\geq 400$ units/mg) from porcine gastric mucosa | Sigma, UK                              |
| Pancreatin ( $\geq 3\times$ USP) from porcine pancreas    | Sigma, UK                              |
| Taurocholic acid, sodium salt hydrate, 98%                | Fisher Scientific (Acros Organics), UK |
| Lecithin (L- $\alpha$ -phosphatidylcholine)               | Sigma (Biochemika), UK                 |
| Complete Protease Inhibitor                               | Roche, UK                              |
| NaHCO <sub>3</sub>  | Sigma (Riedel-de Haën), UK             |

### 3.2.4 Pig Small Intestinal Fluids

A full-length intestine was obtained from a freshly killed pig at a local abattoir (H G Blake Costessey Ltd, Norwich, UK). The animal was processed under standard UK legislation for food-producing animals, the intestine extracted within a few hours of slaughter, transported intact to the laboratory on ice and the intestinal fluids extracted within a short time.

### 3.2.5 Other Materials Used in the Molecular Biology Studies

Materials used for SDS-PAGE, Western blot, dot blot, native agarose gel electrophoresis and ELISA are indicated in Chapter 2. Western blot and dot blot were carried out using the mouse monoclonal antibody indicated in Chapter 2, unless otherwise stated.

## 3.3 Methods

The stability of plant-expressed HBcAg VLPs in gastric and intestinal conditions was investigated by the following protocols. Each experiment consisted of incubation of VLPs in the bio-relevant media, followed by a post-incubation assessment of their physical and chemical stability using several characterisation techniques. The production and purification of HBcAg from the plant, as well as the methods used for the VLPs characterisation were described in detail in Chapter 2. Unless otherwise specified these techniques were carried out using the same protocols described in Chapter 2.

### 3.3.1 HBcAg Stability in Simulated Gastric Conditions

Simulated gastric fluid models which mimic the harsh gastric environment have been developed (British Pharmacopeia, 2012; Fotaki et al., 2005; Vertzoni et al., 2005). Despite their good bio-relevance, it is still difficult to fully simulate the conditions of the stomach fluids using a single standard protocol, as this would not be representative of the extreme variability in acid and pepsin concentrations observed *in vivo* (Efentakis and Dressman, 1990; Gomes et al., 2003). For this reason, in the current research the relative stability of HBcAg in gastro-intestinal (GI) bio-relevant media was determined not only under the standard conditions of the *in vitro* models, but also under a range of different pH values

and pepsin concentrations. This was carried out in order to obtain a better and more relevant understanding of HBcAg susceptibility to the gastric degradation.

Moreover, protein stability is often evaluated by SDS-PAGE gel, which allows the determination of the stability of the primary structure. However, it should be remembered that HBcAg is a VLP, with a complex multimeric quaternary structure. Therefore, its stability was evaluated not only in terms of chemical stability, but also in terms of physical integrity of the three-dimensional structure.

### **3.3.1.1 HBcAg Stability in Simulated Gastric Fluid (SGF) without Pepsin**

HBcAg VLPs were incubated in SGF (pH 1.2) without pepsin (British Pharmacopeia, 2012) for two hours. Following the incubation, both physical and chemical stability were investigated.

Plant-expressed HBcAg was extracted using extraction buffer 1 (Chapter 2) and purified through sucrose density gradient ultracentrifugation. VLP-rich fractions corresponding to 30 and 40 % (w/v) sucrose density bands were pooled together and were then diluted 1:5 with a solution of 80 mM HCl and 34 mM NaCl, resulting in a final pH of 1.2, matching SGF (British Pharmacopeia, 2012). The 1:5 volume ratio of HBcAg solution to SGF was chosen in order to avoid detection problems associated with highly diluted concentrations. However, at this dilution ratio the purified HBcAg solution would slightly increase the pH of the SGF. For this reason, SGF was prepared at a slightly lower pH, so that the final pH was 1.2 upon dilution, matching that of British Pharmacopoeia recipe (2012).

The HBcAg solution in SGF was incubated at 37 °C for two hours. After incubation, it was layered on the top of a pH 1.2, 10 to 45% (w/v) sucrose density step gradient. The gradient was made by preparing five concentrations of sucrose solution in HCl (pH 1.2) ranging from 10 to 45% (w/v). The migration of stable VLPs through sucrose density gradients at a more neutral pH was used as a control; for this purpose HBcAg particles from the same stock used for the SGF incubation were employed. In this case, the purified HBcAg particles were diluted 1:5 in a 10 mM Tris-HCl pH 8.4, 120 mM NaCl solution. After two hours incubation, the control sample was layered on the top of a 10 mM Tris-HCl pH 8.4,

10 to 45% sucrose density gradient. After ultracentrifugation, fractions from the sample that had been incubated at pH 1.2, as well as fractions from the control were collected. All fractions were then analysed by Coomassie stained SDS-PAGE.

In a different experiment, VLPs were incubated both at pH 1.2 and under control conditions in an identical way to the aforementioned method. Density gradient ultracentrifugation was carried out, and fractions from the sample incubated at pH 1.2 and fractions from the control were collected. These fractions were analysed by Western blot and dot blot.

### **3.3.1.2 HBcAg Stability in Simulated Gastric Fluid (SGF) without Pepsin, Followed by pH Neutralisation**

During the GI transit, a hypothetical therapeutic is subjected first to the stomach acidity and then to the more neutral pH of the intestinal environment. Therefore, it was considered important to evaluate the VLPs stability upon incubation in acid, followed by pH neutralisation to simulate the normal biological process: for instance, in case of partial or total physical instability of the VLPs in acids, the pH neutralisation might have allowed re-assembly of the VLPs structure. Therefore, in the following experiments HBcAg was first incubated in SGF without pepsin. After the incubation, the samples at pH 1.2 were neutralised and the physical and chemical stability were investigated by Coomassie stained SDS-PAGE, Western blot, dot blot and TEM.

Purified VLP preparations were incubated at pH 1.2 for two hours as described in the previous section. At the end of the two hour-incubation, the pH of the sample was neutralised by initial addition of 1 M NaOH in a drop wise manner. The neutralising agent was then switched to 0.1 M NaOH once the pH became closer to neutrality. The sample was layered on the top of 10 mM Tris-HCl, 120 mM NaCl pH 8.4, 10 to 45% (w/v) sucrose step gradient. After ultracentrifugation, fractions were collected and examined by dot blot. Moreover, a precipitate was formed at the bottom of the tube upon ultracentrifugation: it was re-suspended in 10 mM Tris-HCl, 120 mM NaCl pH 8.4 and then analysed, together with the other sucrose gradient fractions, by Coomassie stained SDS-PAGE and Western blot.

A similar experiment was performed for the assessment of the VLP physical integrity upon incubation in SGF without pepsin, followed by pH neutralisation, using transmission electron microscopy (TEM). Purified HBcAg in water was diluted 1:6 with a solution of 73 mM HCl to a final pH of 1.2. After two hours incubation at 37 °C, the pH was neutralised using aliquots of 400 mM NaHCO<sub>3</sub>. The resulting sample was used for TEM imaging.

### 3.3.1.3 HBcAg Physical Stability in Acid Without Pepsin

Considering the extreme variability in the pH of the human gastric fluid, it was considered important to evaluate the physical stability of HBcAg not only at the standard pH of SGF (British Pharmacopeia, 2012), but at a wider range of pH values likely to be encountered in the human stomach. Native agarose gel electrophoresis had been used before to assess the stability of bacterially expressed HBcAg incubated under a wide range of conditions, including different pH (Newman et al., 2003). In that research the authors also suggest that sucrose density gradient assays, measuring changes in the hydrodynamic properties, can be more sensitive for conformational changes; in contrast native agarose gel electrophoresis and TEM can constitute a more direct way to assess the particle integrity (Newman et al., 2003). For this reason, in order to define a net threshold of stability upon incubation of HBcAg at a series of different pH, the native agarose gel electrophoresis assay was considered best. This technique has a high detection limit for HBcAg compared to other techniques; hence concentrated dilutions of the antigen in the incubation media were used. In a preliminary experiment, two solutions of 100 mM HCl (pH 1) with 34 mM NaCl and 10 mM HCl (pH 2) with 34 mM NaCl were prepared. As a control, a solution of PBS was used. Purified HBcAg, dialysed in water was diluted 2:3 in each of the aforementioned acidic solutions and in PBS. After two hours incubation, each solution containing HBcAg at a different pH was loaded on the wells of an agarose gel for gel electrophoresis. The gel was then ethidium bromide stained.

In another experiment, four solutions of 10 mM HCl (pH 2) with 34 mM NaCl, 3.2 mM HCl (pH 2.5) with 34 mM NaCl, 1 mM HCl (pH 3) with 34 mM NaCl and 0.32mM HCl (pH 3.5) with 34 mM NaCl were prepared. Purified HBcAg, dialysed in water, was diluted 1:4 in each of the four acidic solutions. After two hours incubation, each solution

containing HBcAg at a different pH was loaded on the wells of an agarose gel for electrophoresis. The gel was then ethidium bromide stained and Coomassie stained.

### 3.3.1.4 HBcAg Chemical Stability in Simulated Gastric Fluid (SGF) with Different Pepsin Concentrations

The relative chemical stability of HBcAg in SGF in the presence of pepsin was evaluated. Pepsin is a protease and it can, therefore, biochemically digest the primary structure of a protein, i.e. the protein amino acid sequence. SGF with pepsin, based on the British Pharmacopeia (2012) contains 3.2 mg/mL pepsin (Ph Eur) and 34 mM NaCl at pH 1.2. However, given the extremely high variability of pepsin activity found in the human stomach (Gomes et al., 2003), it was decided to assess the stability over a wider range of pepsin concentrations, keeping the pH constant at pH 1.2. The stability of HBcAg after incubation in SGF with pepsin was evaluated by separating the residual HBcAg by SDS-PAGE. The SDS-PAGE gel was then used for immunodetection by Western blot.

A 50 mg/mL stock solution of pepsin (Ph Eur) from porcine gastric mucosa in 63 mM HCl with 34 mM NaCl was prepared and the final pH was adjusted to pH 1.2. In parallel, purified HBcAg in water was diluted 1:4 in a 67 mM HCl solution, giving a final pH of 1.2. Different aliquots from the pepsin stock (pH 1.2) were added to the VLP solution of the same pH, in order to obtain VLP samples incubated with four different concentrations of pepsin and a control with no pepsin (10, 3.2, 1, 0.5 and 0 mg/mL). After two hours incubation at 37 °C, the samples were boiled to stop the enzymatic reaction and analysed by Western blot.

For samples at lower concentrations of pepsin, a 10 mg/mL stock solution of pepsin (Ph Eur) from porcine gastric mucosa in 63 mM HCl was prepared and the pH was then adjusted to 1.2. In parallel, purified HBcAg VLP in water was added at a volume ratio 1:4 to a 67 mM HCl solution, giving a final pH of 1.2. Different aliquots from the pepsin stock at pH 1.2 were added to the VLP solution of the same pH, in order to obtain VLP samples incubated with four different concentrations of pepsin and a control (0.2, 0.1, 0.05, 0.01 and 0 mg/mL). After two hours incubation at 37 °C, the samples were boiled and analysed by Western blot.

### 3.3.1.5 HBcAg Chemical Stability in Fasted State Simulated Gastric Fluid (FaSSGF) and in Fed State Simulated Gastric Fluid (FeSSGF)

Fasted State Simulated Gastric Fluid (FaSSGF) and Fed State Simulated Gastric Fluid (FeSSGF) have been developed as bio-relevant media that can mimic closely the pre- and post-prandial conditions of the human stomach, respectively. HBcAg was tested in these two media, in order to obtain a clearer understanding of its potential use as an orally delivered therapeutic. A different source of pepsin from the one used in the previous experiments was used to prepare both FaSSGF and FeSSGF, in accordance with the original recipes described by Vertzoni et al. (2005) and Fotaki et al. (2005): pepsin ( $\geq 400$  units/mg) from porcine gastric mucosa, a raw material that contains 60 to 70  $\mu\text{g}$  of pepsin protein per mg of solid product, was used. Therefore, the calculation of pepsin concentration in the media should be performed considering not just the total solid weight, but the actual pepsin content in the solid (Diakidou et al., 2009; Fotaki et al., 2005; Vertzoni et al., 2005).

Initially, FaSSGF, containing 0.1 mg/mL pepsin, 80  $\mu\text{M}$  taurocholic acid (sodium salt), 20  $\mu\text{M}$  lecithin and 34 mM NaCl at pH 1.6 was prepared according to Vertzoni et al. (2005). FeSSGF was prepared according to Fotaki et al. (2005): full-fat UHT milk is the main component. In parallel, a pepsin stock solution of 1.83 M HCl containing 1.1 mg/mL pepsin was prepared. Aliquots of this pepsin stock were subsequently added to the milk during the incubation of HBcAg in FeSSGF, so as to mimic the pulsatile release of acid and pepsin during normal human digestion (Fotaki et al., 2005). Fifty (50)  $\mu\text{L}$  of purified HBcAg were added to 950  $\mu\text{L}$  of FaSSGF medium. Similarly another sample of 50  $\mu\text{L}$  of purified HBcAg was added to 950  $\mu\text{L}$  of full-fat milk, which was the FeSSGF starting component. The samples were then incubated at 37 °C for three hours. During the incubation the FeSSGF was supplemented with 8  $\mu\text{L}$  of the 1.83 M HCl stock solution containing 1.1 mg/mL pepsin. These additions were performed after 0, 15, 30, 45, 60, 75 and 90 minutes from the beginning of the incubation, resulting in pH and enzymatic changes over time, closely mimicking the postprandial changes observed *in vivo* (Fotaki et al., 2005). Aliquots from both the FaSSGF and FeSSGF incubations were sampled after 30, 60, 120, 180 minutes from the beginning of the incubation. The enzymatic reaction was

immediately stopped in each sample by adding one volume of 3X LDS  $\beta$ -mercaptoethanol to two volumes of the sample and subsequent boiling.

Identical samples incubated in FaSSGF in absence of pepsin and in full-fat milk in the case of FeSSGF were used as enzyme-free controls. At the end of the experiment, all the samples corresponding to different incubation time points for FaSSGF and FeSSGF were separated by SDS-PAGE gel electrophoresis, followed by Western blot using the anti-HBcAg polyclonal rabbit antibody, described in Chapter 2.

### 3.3.2 HBcAg Stability in Simulated Intestinal Conditions and Pig Intestinal Fluids

The intestine contains several enzymes, including trypsin and chymotrypsin, which could digest an antigen. Moreover, many novel nanoparticulate protein formulations, in particular those based on vesicular carriers, such as liposomes, can also be degraded by the detergent effect of physiological levels of intestinal bile salts (Parmentier et al., 2011). However, VLPs are protein-based particles and not vesicles and the conditions employed for the extraction of plant-expressed HBcAg from the leaves of *Nicotiana benthamiana*, suggest that HBcAg were stable in bile salts: in fact, the extraction buffer (described in Chapter 2) used for the extraction of VLPs from leaves, contained 0.75% sodium deoxycholate, corresponding to a concentration greater than 18 mM. Nevertheless, VLPs were intact when extracted using this extraction buffer (Figure 2.4 in Chapter 2). For a comparison the concentration of bile salts in the gut is considered to range between 0.5 mM and circa 11 mM, depending on the fasted/fed condition and on the section of intestine (i.e. duodenum, jejunum, ileum) (McConnell et al., 2008b). Thus the concentration used in extraction buffer is well above that found in the human gut.

Based on this, it was considered that the main parameter that could influence the stability of HBcAg in the intestine is the presence of digestive enzymes. For this reason, a model intestinal fluid containing digestive enzymes was required: hence Simulated Intestinal Fluid (SIF) containing pancreatin was used (British Pharmacopeia, 2012). An *ex vivo* study using pig intestinal fluids was also carried out, in order to more closely resemble the *in vivo* conditions. All digestion studies were performed over 4 hours duration, as it has been established that the small intestinal transit time in humans is almost invariably 3 to 4 hours

in most individuals, and is also not considerably influenced by the presence or absence of food (McConnell et al., 2008b).

### **3.3.2.1 HBcAg Chemical Stability in Simulated Intestinal Fluid (SIF)**

Simulated intestinal fluid (SIF) with pancreatin was prepared by mixing 7.7 mL of 0.2 M NaOH with 25 mL of a solution containing 6.8 g of K<sub>2</sub>PO<sub>4</sub> and 50 mL of water. Porcine pancreatin ( $\geq 3\times$  USP), 333 mg, was then added. The pH was then adjusted to 6.8 and the volume diluted to 100 mL with water (British Pharmacopeia, 2012). SIF without pancreatin was prepared identically, but omitting the pancreatin. Before the stability experiment, a protease inhibitor tablet was diluted in 5 mL SIF without pancreatin. This concentrated solution is 10 x more concentrated than the recommended dilution suggested by the manufacturer to ensure effective enzymatic inhibition.

For Coomassie stained SDS-PAGE and Western blot, five identical samples were prepared by dilution of purified HBcAg 1:19 in SIF. Each sample represented a different time point of HBcAg digestion in SIF: samples 1, 2, 3, 4 and 5 were incubated for 240, 180, 120, 60 and 30 minutes, respectively. A 1:19 dilution of HBcAg in SIF without pancreatin was used as a positive control. A 1:19 dilution of water in SIF was used as a negative control. The incubation temperature was set at 37 °C. Back-preparation of the five samples in reverse order (i.e. starting the reaction at different times) allowed stopping the enzymatic reaction at the same time in all the samples, immediately before processing of all samples together. For this purpose the (10 x) protease inhibitor solution was diluted 1:9 in each digestion sample.

The samples corresponding to each time point were separated in two SDS-PAGE gels. One was subsequently Coomassie stained and the other was used for Western blot.

### **3.3.2.2 HBcAg Physical Stability in Simulated Intestinal Fluid (SIF)**

For dot blot, an identical digestion experiment to the aformentioned one was carried out. The resulting digestion products at each time point and the positive control were loaded

onto six different sucrose density gradients. After ultracentrifugation, fractions from the sucrose gradients were collected and analysed by dot blot.

For detection of HBcAg by native agarose gel, higher concentrations of HBcAg were required. Therefore, HBcAg was diluted 1:9 in SIF in five samples. Each sample represented a different time point of HBcAg digestion in SIF: samples 1, 2, 3, 4 and 5 were incubated for 240, 180, 120, 60 and 30 minutes, respectively. The incubation temperature was set at 37 °C. Samples were also prepared in reverse order so that the enzymatic reaction could be stopped at the same time in all samples. For this purpose the (10 x) protease inhibitor solution was diluted 1:9 in each digestion sample and the samples were immediately cooled on ice. A 1:9 dilution of HBcAg in SIF without pancreatin was used as positive control and a 1:9 dilution of water in SIF was used as a negative control. The 5 samples and the controls were then loaded on two native agarose gels. After electrophoresis, one gel was ethidium bromide stained and the other was Coomassie stained.

For TEM imaging, HBcAg was diluted 1:6 in SIF and the sample was incubated for 120 minutes. The enzymatic reaction was then stopped by 1:9 dilution of (10 x) Protease inhibitor solution in the digestion sample. The sample was kept cool on ice. TEM imaging was carried out within two hours of the end of the incubation.

### **3.3.2.3 *Ex Vivo* HBcAg Stability in Natural Intestinal Fluid (natIF)**

Pig intestinal fluids were chosen as natural intestinal fluids (natIFs). The full-length intestine collected from the freshly killed animal was immediately transported to the laboratory and used for the collection of the luminal fluids. Firstly, the intestine was laid inside a fume-hood. The small intestine is circa 4 to 4.5 fold longer than the large intestine. Furthermore, the small intestine is considerably thinner than the colon and the luminal content is generally less viscous (Kararli, 1995; Merchant et al., 2011). After localisation of the small intestine and large intestine, the two parts were separated and the large intestine was discarded. Then, four segments of approximately the same size from the proximal to the distal small intestine were divided and luminal fluid content was collected from each of the four segments separately. Small aliquots were made and frozen at – 80 °C

until use. Digestion experiments were conducted within ten weeks of collection of the fluids.

For the SDS-PAGE analysis, aliquots from the four different segments of the small intestine were thawed and the solid content was pelleted by centrifugation at 9300 g for 10 minutes. Aliquots from the most proximal part of the intestine (i.e. duodenum) were centrifuged twice to separate the more viscous phase. The supernatants constituted the natural intestinal fluid (natIF) of this study. The four natIFs from the proximal to the distal small intestine are referred to as natIF 1, natIF 2, natIF 3 and natIF 4 for the studies detailed below. Purified HBcAg aliquots were diluted 1:19 in each of the four natIFs and incubated at 37 °C for 4 hours. At the end of the incubation, 1:3 dilutions of the four samples in water were made and then boiled to stop the enzymatic reaction. The four samples were then run on two SDS-PAGE gels. One gel was used for Coomassie staining and the other for Western blot. For a positive control, HBcAg aliquots were diluted 1: 19 in PBS. In parallel, further positive controls were created: 1:3 dilutions of the natIFs in water and LDS  $\beta$ -mercaptoethanol were boiled for 10 minutes and then cooled. Purified HBcAg was then added in the same ratio as in the digestion samples. This control allowed enzymatically inactive natIFs media to be compared to the active ones. Negative controls were also created by diluting the PBS in natIFs.

For dot blot, on the day of the experiment, purified HBcAg aliquots were diluted 1:19 in the four natIFs and incubated at 37 °C for four hours. Then, the proteolysis was stopped by the addition of 1:9 dilution of (10 x) protease inhibitor solutions in each digestion sample. For a positive control, HBcAg was diluted 1:19 in PBS. The control and the digestion samples were loaded onto five identical sucrose density gradients. After ultracentrifugation, fractions from the sucrose gradients were collected and analysed by dot blot using anti-HBcAg mouse monoclonal antibody.

### 3.4 Results and Discussion

The development of oral vaccines, which can effectively protect humans from infectious diseases, is one of the greatest challenges of today's drug delivery research. However, the natural physiology of the GI tract presents a series of obstacles to the oral delivery of

vaccines. The first barrier that a vaccine encounters subsequent to oral administration is the harsh environment in the stomach and intestine. Gastric and intestinal fluids, designed for the digestion of food, could induce chemical and physical instability of protein-based antigenic vaccines (Lee, 2002). Plant-expressed HBcAg was used in this study as a model candidate vaccine and its potential stability in the GI tract was assessed in various media simulating the GI conditions, as well as in pig intestinal fluids. The main reason for which this delivery approach could be considered particularly promising is related to the dense and compact structure of the VLPs: their morphology, in fact, is similar to that of the main component of viruses that naturally invade, survive and proliferate inside various fluids of animals or plants. Therefore, they could be resistant to relatively harsh GI environmental conditions (Huang et al., 2005).

### **3.4.1 HBcAg Stability in Simulated Gastric Fluid (SGF)**

HBcAg is a complex protein structure assembled as a VLP. The gastric fluid could interfere with the stability of HBcAg VLPs, due to the effect of pH and the presence of pepsin. These two conditions could degrade HBcAg by different mechanisms: the pH could physically denature the particles' three-dimensional structure, while the pepsin could digest the protein's primary structure. For this reason, the effect of these two different environmental factors was investigated separately. Firstly, HBcAg VLP stability was studied evaluating the denaturing effect of the SGF in absence of pepsin, i.e. the pH effect; then the enzymatic digestion of HBcAg VLP was investigated using SGF in the presence of pepsin.

#### **3.4.1.1 HBcAg Stability in Simulated Gastric Fluid (SGF) without Pepsin**

Initially the stability of plant-expressed HBcAg VLPs was investigated at the acidic pH of the SGF (1.2).

The results of these experiments are illustrated in Figure 3.1. It is worth noticing that the sucrose gradient was set up in a way to maintain its pH consistent with the incubation pH (Figure 3.1 A). This was done in order to prevent pH neutralisation of the test samples during the analysis, which could possibly have caused further conformational change of

the protein chains, thus affecting the assessment of protein stability and not giving a faithful representation of the sole effect of the acid on the VLP stability. Coomassie stained SDS-PAGE electrophoresis of the collected fractions, from the sucrose gradients at pH 8.4 (control) and at pH 1.2, shows that the acidic pH of the SGF did not cause any disruption of the primary structure of the HBcAg, which was present throughout the gel as a circa 20 kDa protein band (Figure 3.1 B). Therefore, HBcAg seems chemically stable under acidic conditions. HBcAg appeared to migrate to the bottom of the density gradient in the control sample, as indicated by the presence of the 20 kDa band only in the lanes corresponding to circa 30 and 40% (w/v) sucrose fractions (lanes 6 to 8), suggesting intact VLPs. However, in the sample incubated in SGF, part of the 20 kDa band could be seen diffused in most fractions of the sucrose density gradient (lanes 9 to 16), although the highest concentration of the protein was seen in the circa 40% (w/v) sucrose fraction (lanes 14 to 16). This result clearly suggests that the capsid structure of HBcAg VLP exhibits a certain degree of physical instability on exposure to the acidic conditions. This is based on the fact that intact particles are expected to be found almost exclusively in the 30 and 40% sucrose density fractions, as seen in the control, whereas partially disassembled VLPs may appear in the less dense gradient fractions.

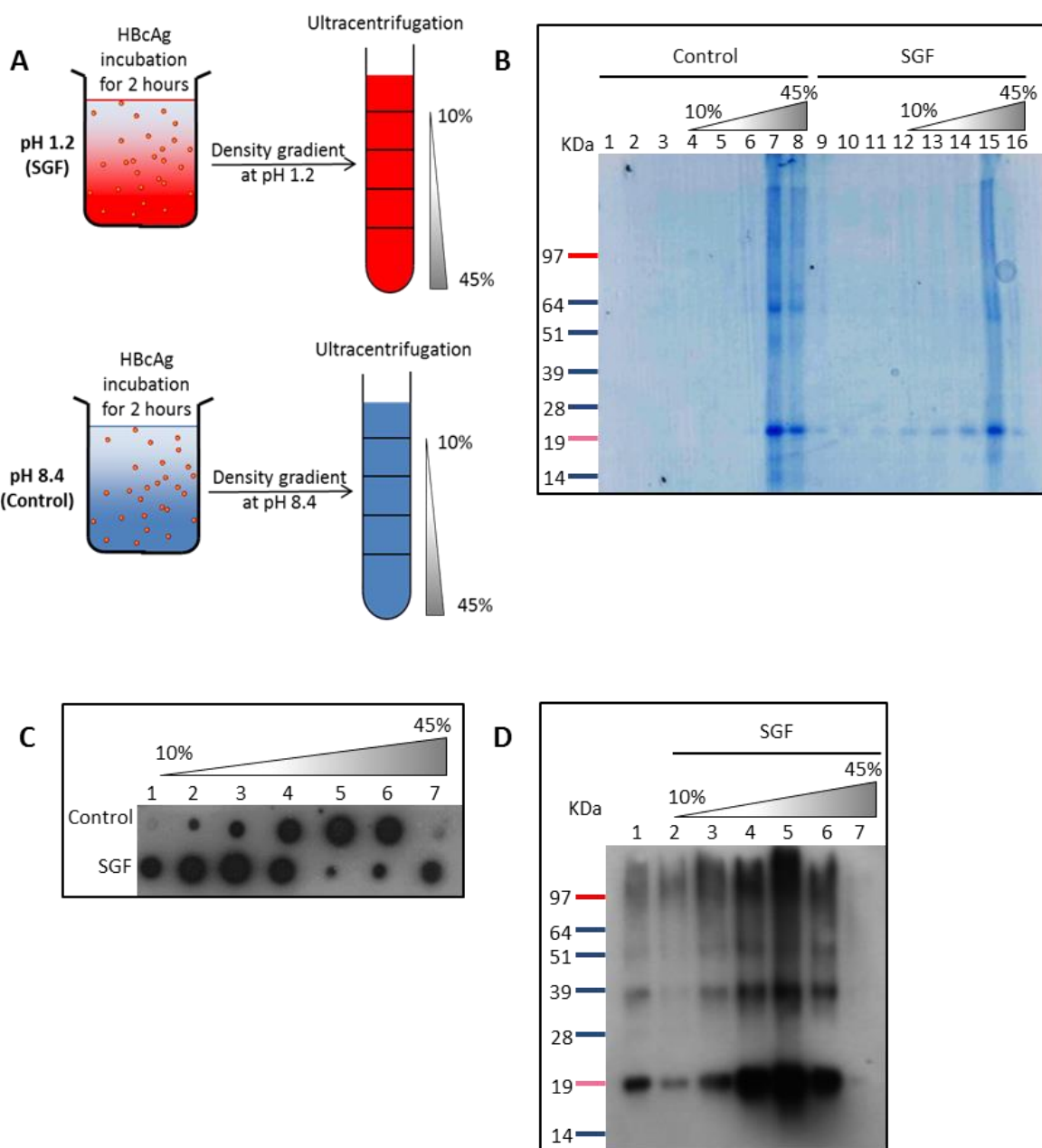


**Figure 3.1. HBcAg stability in simulated gastric fluid (without pepsin).**

(A) illustrates the setting of the experiment: purified HBcAg, dialysed from 30 and 40% sucrose gradient fractions, was incubated either in SGF (pH 1.2) or in the control, Tris buffer (pH 8.4). The content of both samples was then separated by density gradient ultracentrifugation, carried out at the respective pH. (B) shows the Coomassie stained SDS-PAGE of the fractions collected from the sucrose gradients of both the control sample and the sample incubated in SGF: supernatant (lanes 1 to 3); 10 to 45% sucrose fractions for the control (lanes 4 to 8); supernatant (lanes 9 to 11); 10 to 45% sucrose fractions for SGF (lanes 12 to 16). (C) illustrates the dot blot (polyclonal antibody) of a similar experiment: supernatant (dot 1); 10 to 45% (w/v) sucrose fractions for both control and SGF (dots 2 to 7). (D) represents the Western blot (monoclonal antibody) of the SGF fractions: supernatant (lane 1); 10 to 45% sucrose fractions (lanes 2 to 7).

The same samples were also analysed by dot blot (Figure 3.1C). In the dot blot of the control sample, most of the anti-HBcAg signal was visible in the circa 30 and 40% (w/v) sucrose fractions (dots 5 and 6). Instead, in the sample incubated in SGF, most of the HBcAg was detected in the less dense sucrose fractions (supernatant and dots 1 to 4) and at the bottom fraction of the gradient (dot 7), with a very weak signal in the circa 30 and 40% (w/v) sucrose (dots 5 and 6). This result suggests that HBcAg VLP was not physically stable in the SGF without pepsin (pH 1.2). However, the degree of instability was much more remarkable in the dot blot than in the Coomassie stained SDS-PAGE, where the HBcAg band intensity seemed most intense in the 30 and 40% (w/v) sucrose bands. Therefore, the same fractions collected from the sucrose gradient were also examined by Western blot analysis for a better understanding of this issue (Figure 3.1 D). This immunodetection technique confirmed the results of the corresponding Coomassie stained SDS-PAGE gel, where a circa 20 kDa anti-HBcAg signal could be detected mainly in 30 and 40% (w/v) sucrose fractions (dots 4, 5 and 6). In addition, weaker bands were also present in the supernatant and in the other fractions of the gradient, indicating partial disassembly of VLPs.

Taken together, these results suggest that HBcAg VLP is chemically stable in SGF in the absence of digestive enzymes, but the quaternary structure that forms the VLP shows a certain degree of physical disassembly. However, there is a discrepancy in the results depending on the technique used: the SDS-gel assays (Coomassie stained gel and Western blot) show that most of HBcAg VLPs sedimented in the 30 and 40% sucrose fractions as expected for intact VLPs, with only a moderate amount of HBcAg present in the other fractions of the gradient. This is compatible with relatively modest instability of the capsids. The instability, however, seemed much more accentuated based on the outcome of the dot blot. This difference may be attributed to the fact that HBcAg VLP is not deliberately denatured in the dot blot process as it would be in the SDS-PAGE process, therefore the antibody might have bound differently to the denatured HBcAg (in the SDS-PAGE gels) compared to the native HBcAg (in the dot blot). The different specificity of antibodies to denatured and native samples was also discussed extensively in Chapter 2. It can be speculated that the Coomassie stained SDS-PAGE gel, where the band intensity is merely proportional to the amount of protein present, and does not depend also on the

antibody affinity to the antigen, can probably be considered the most reliable method to estimate the extent of distribution of HBcAg throughout the sucrose density gradient.

The physical stability of HBcAg in SGF in the absence of pepsin was also analysed by evaluating the fate of purified HBcAg VLPs after an initial incubation at pH 1.2 and 37 °C for two hours, followed by neutralisation of the pH. The neutralised sample was layered on the top of a sucrose density gradient at pH 8.4 (Figure 3.2 A). After ultracentrifugation, the fractions from the gradient were collected and analysed. The dot blot shows that HBcAg could not be detected in any of the fractions of the sucrose gradient (Figure 3.2 B). However, a precipitate was visible at the bottom of the tube used for the ultracentrifugation of the sample. This precipitate was re-suspended and analysed by SDS-PAGE together with the other fractions from the gradient. The Coomassie stained gel (Figure 3.2 C) shows that a 20 kDa protein band corresponding to HBcAg was not present in any of the gradient fractions; however, a protein band, of a similar size to HBcAg, was visible in the re-suspended precipitate sample (lane 8). A Western blot of the same sample (Figure 3.2 C, right side) revealed anti-HBcAg immunoreactivity at a protein size of 20 kDa, confirming that the precipitate contained HBcAg monomers. The fact that HBcAg was not found in any of the fractions of the gradient indicate that HBcAg was not present as intact VLP, nor as a disassembled monomeric or multimeric form. Furthermore, HBcAg sedimentation at the bottom of the gradient suggests that possibly the monomers or dimers aggregated in some sort of cluster that could migrate through all fractions of the gradient. For a final characterisation of HBcAg in SGF without pepsin, purified HBcAg particles were incubated in SGF at pH 1.2 for two hours and then the acidity was neutralised with NaHCO<sub>3</sub>. This sample was used for TEM imaging. The TEM image (Figure 3.2 D) shows that the typical HBcAg VLP structure detected in the control sample could not be found in the acidified and neutralised sample. Instead clusters of materials could be diffusely seen in the latter. It can be hypothesised that these clusters are agglomerates of HBcAg protein.

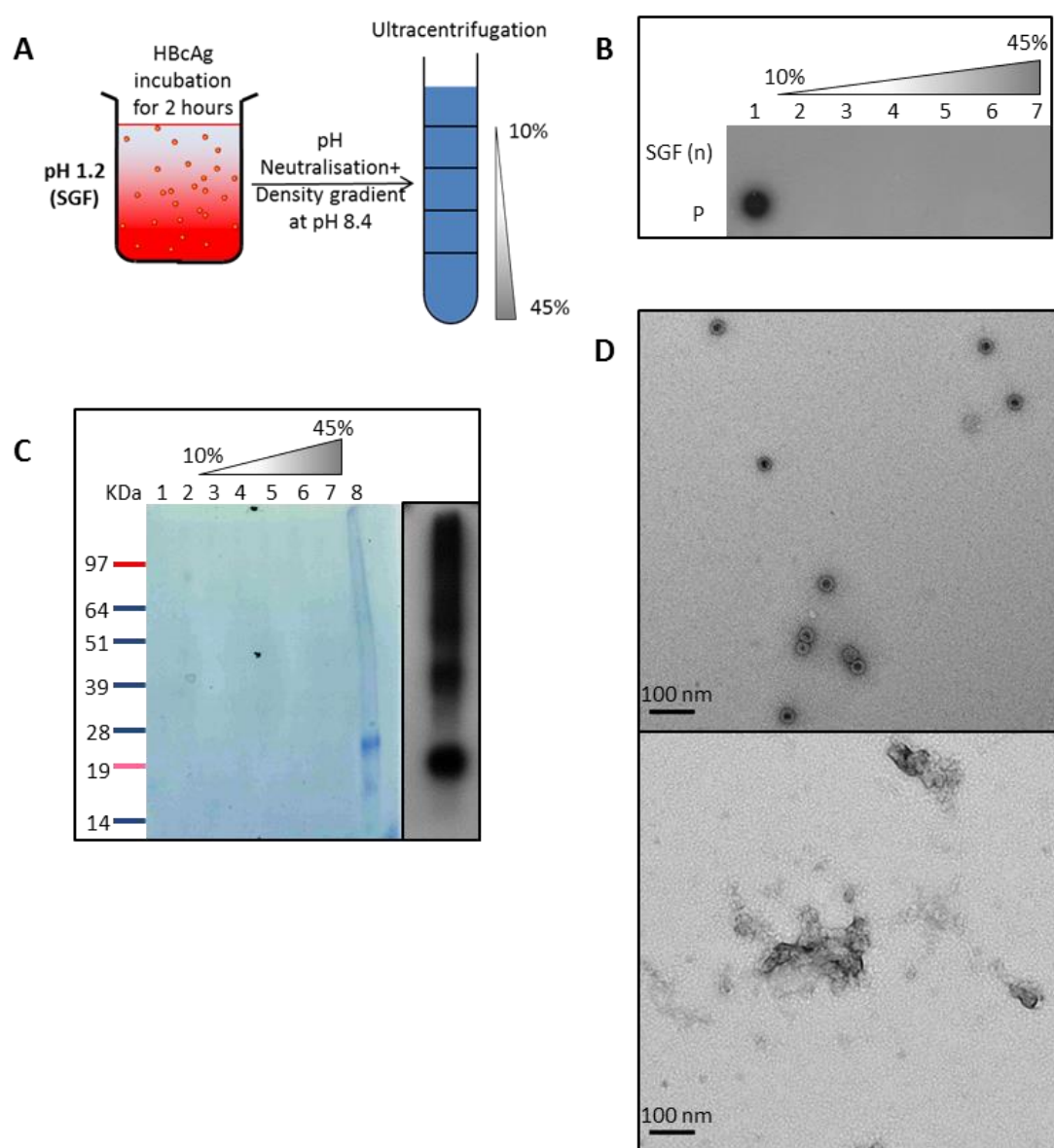


**Figure 3.2. HBcAg stability upon incubation in simulated gastric fluid (without pepsin) and subsequent neutralisation.**

(A) illustrates the setting of the experiment: purified HBcAg, dialysed from 30 and 40% sucrose gradient fractions was incubated at pH 1.2 and 37 °C for two hours and the pH was subsequently neutralised. The resulting sample was separated by density gradient ultracentrifugation. Seven fractions were collected and analysed by dot blot and SDS-PAGE. (B) shows the dot blot of the collected fractions; in the upper lane: supernatant (dot 1); 10 to 45% sucrose fractions (dots 2 to 7) and in the bottom lane P = positive HBcAg control. (C) illustrates the Coomassie stained SDS-PAGE of the sucrose gradient fractions and of the re-suspended precipitate resulting from the ultracentrifugation: supernatant (lane 1); 10 to 45% sucrose fractions (lanes 2 to 7); precipitate (lane 8). At the right side of the image the same precipitate was examined by Western blot (monoclonal antibody). (D) illustrates two TEM images: a control HBcAg sample can be seen in the top image; an HBcAg sample upon acidification in SGF and subsequent neutralisation is shown in the bottom image.

The observation that HBcAg VLPs were unstable upon acidification in SGF and subsequent neutralisation was confirmed by a similar experiment using native agarose gel electrophoresis. In this experiment, samples of HBcAg were incubated in HCl solutions of pH 1 and pH 2 and in Tris buffer (pH 8.4, control) for two hours. Then, the three samples were directly loaded on the wells of an agarose gel in Tris/Borate/EDTA (TBE) buffer. After the electrophoresis, the gel was ethidium bromide stained. It is worth remembering from Chapter 2, that HBcAg VLPs contain nucleic acids and can be separated by electrophoresis in agarose gels. Therefore, HBcAg can be identified by the presence of ethidium bromide stained nucleic acid, which is encapsidated in its VLP. The image of the agarose gel (Figure 3.3 A) reveals that in the samples incubated at pH 1 (lane 2) and pH 2 (lane 3) the band corresponding to the VLP was not present, whereas a clear band was seen in the control (lane 1). However, a strong signal was visible in the wells at pH 1 and pH 2. These results suggested that while intact VLPs in the control sample could migrate through the agarose gel, HBcAg agglomerated and remained blocked in the wells of samples incubated under acidic pH. Considering the previous finding that HBcAg seemed to agglomerate upon acidification and subsequent neutralisation, it is possible to hypothesise that HBcAg clustered when loaded in the gel, upon neutralisation by the Tris/Borate/EDTA (TBE) buffer present. This result is in accordance with Newman et al. (2003), who used native agarose gel electrophoresis to study the stability of HBcAg expressed in bacteria: it was shown that HBcAg, when incubated at pH 2 for only 30 minutes, was unstable and it remained blocked in the well (Newman et al., 2003).

A second experiment was conducted in order to establish the threshold pH for HBcAg VLP stability (Figure 3.3 B). The image of the ethidium bromide stained agarose gel (Figure 3.3 B - left side) shows the presence of nucleic acids trapped in the wells of samples incubated at pH 2 (lane 1) and pH 2.5 (lane 2), while a nucleic acid smear was visible in the sample incubated at pH 3 (lane 3). Finally a discrete band was visible in the sample incubated at pH 3.5 (lane 4). The Coomassie stained gel (Figure 3.3 B - right side) confirmed the presence of a protein smear in the sample incubated at pH 3 (lane 3); furthermore a protein band could be seen in the sample incubated at pH 3.5 (lane 4): this band showed an identical electrophoretic migration to the respective lane in the ethidium bromide gel. As seen in Chapter 2, overlapping Coomassie stained and ethidium bromide stained bands is compatible with the presence of VLP that encapsidated nucleic acids. These results suggest

that HBcAg VLP quaternary structure is physically stable upon incubation in acid at pH 3.5 for two hours. The VLP appeared only partially stable when incubated at pH 3 and totally unstable at lower pH. At pH 2 and 2.5, HBcAg seemed to agglomerate as revealed by the presence of trapped nucleic acids in the wells.

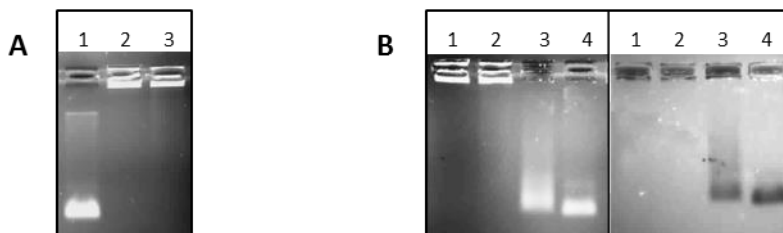


**Figure 3.3. HBcAg VLP stability in different acidic conditions.**

(A) represents an ethidium bromide stained native agarose gel where HBcAg is incubated at different pH: positive HBcAg control (lane 1); pH 1 (lane 2) and pH 2 (lane 3). (B) represents an ethidium bromide stained native agarose gel (left) and an identical Coomassie stained gel (right) where HBcAg is incubated at different pH: pH 2 (lane 1); pH 2.5 (lane 2); pH 3 (lane 3) and pH 3.5 (lane 4).

Based on these results, it is possible to think that HBcAg tends to disassemble rather than agglomerate upon incubation in acids (Figure 3.1), however, it completely agglomerates when the neutral pH is restored (Figure 3.2 and Figure 3.3). It is well known that hydrophobic interactions are responsible for the dimerization of monomers and that the residues between the amino acid 120 and 143 stabilise the dimer-dimer assembly into capsids (Metzger and Bringas, 1998; Pumpens and Grens, 1999; Wynne et al., 1999). Therefore, it can be suggested that the denaturing effect of the acid pH induces partial disruption (i.e. disassembly) of the monomer-to-monomer or dimer-to-dimer interactions responsible for proper assembly. Then, once the denaturing effect of the pH is removed by neutralisation of the pH, the same interactions, which usually keep the monomer and dimers assembled into well-defined capsids, could not be restored. Instead the subunits were driven into agglomeration. This behaviour is similar to HBcAg thermal instability: Newman et al. (2003) showed that native agarose gel electrophoresis of heat-denatured HBcAg results in nucleic acid stuck on the wells, when the gel is run at room conditions. This suggests that when HBcAg is subject to a denaturing shock (i.e. acidic pH or temperature) and then the denaturing agent is removed, the protein tends to aggregate. It can hence be suggested that as the thermal denaturation is irreversible (Wingfield et al., 1995) so is the acid-mediated denaturation.

Finally native agarose gel electrophoresis revealed that this complete loss of the physical stability upon incubation of HBcAg for two hours in acid and further neutralisation occurs at pH < 3 to 3.5.

The *in vitro* model of simulated gastric fluid adapted from British Pharmacopeia (2012) is based on two hours incubation at pH 1.2. However, the actual pH of human gastric fluid in fed state has been reported to range between 1.0 and 2.5 (Evans et al., 1988), although in some individuals the pH values can be as high as pH 5 to 6 (Efentakis and Dressman, 1990). On the base of the experiments carried out in this research, it was possible to hypothesise that HBcAg VLPs are likely to be unstable in the stomach environment of humans. More specifically, it is possible that the pH would not cause a complete disassembly of the capsid three-dimensional structure; however, the subsequent passage to a more neutral pH in the intestine could induce complete VLP disassembly and agglomeration. This would reflect the VLP particular behaviour observed here. The fact that the VLP particulate structure was lost upon incubation in media at pH values lower than pH 3 to 3.5, suggests that even though the gastric pH in the fasting state can have individual variability, HBcAg would be unstable in the fasted gastric environment in most cases. In fact this experimentally-found pH 3 to 3.5 threshold, though useful to know as an absolute stability value, is well above the usual range of pH found in the empty stomach.

#### 3.4.1.2 HBcAg Chemical Stability in Simulated Gastric Fluid (SGF) with Pepsin

The stability of purified plant-expressed HBcAg was evaluated after 2 hours incubation in SGF in the presence of pepsin, in order to model the digestive environment of the stomach. The British Pharmacopoeia (2012) formula of SGF has a fixed 3.2 g/L pepsin (Ph.Eur.) concentration; however variations of pepsin activity up to 4 orders of magnitude have been reported in humans (Gomes et al., 2003). For this reason it was decided to use other concentrations of pepsin as well as the pharmacopoeial concentration. Specifically, several aliquots of HBcAg were incubated in SGF at pH 1.2 containing pepsin at concentrations ranging from 10 g/L to 0.01 g/L. After two hours incubation, the samples were run on two SDS-PAGE gels that were subsequently used for anti-HBcAg Western blots (Figure 3.4). The Western blot shows that the 20 kDa band, present in the control and corresponding to HBcAg, was absent in the sample of HBcAg incubated in SGF containing 3.2 g pepsin/L,

i.e. the concentration specified in the British Pharmacopoeia (2012). Furthermore, some digestion of HBcAg occurred at all concentrations of pepsin. For concentrations of pepsin  $\geq 0.5$  g/L (lanes 2 to 5), no anti-HBcAg signal was clearly detected; however, for concentrations of pepsin  $\leq 0.2$  g/L (lanes 6 to 10) a circa 14 kDa band of anti-HBcAg immunoreactivity could be visualised. Only when the concentration of pepsin was as low as 0.01 g/L (lane 10) was a detectable amount of 20 kDa HBcAg present.

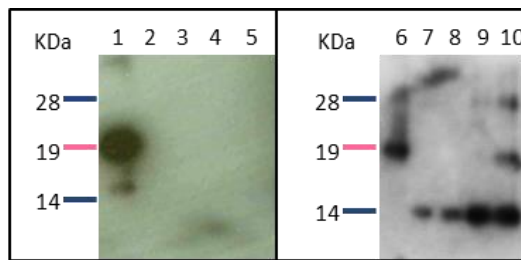


**Figure 3.4. HBcAg digestion in SGF (with pepsin).**

HBcAg was incubated for two hours in SGF containing different concentrations of pepsin. The digested samples were then analysed by Western blot (monoclonal antibody): SGF without pepsin (lane 1 and lane 6); 10 g/L pepsin (lane 2); 3.2 g/L pepsin (lane 3); 1 g/L pepsin (lane 4); 0.5 g/L pepsin (lane 5); 0.2 g/L pepsin (lane 7); 0.1 g/L pepsin (lane 8); 0.05 g/L pepsin (lane 9) and 0.01 g/L pepsin (lane 10).

This result suggests that HBcAg is extremely sensitive to chemical digestion by pepsin, not only at the pharmacopoeial pepsin concentration of SGF, but at thousands-fold lower concentrations. According to these data, it is likely that HBcAg would also be highly digested in the gastric fluid *in vivo*.

### 3.4.1.3 HBcAg Chemical Stability in Fasted State Simulated Gastric Fluid (FaSSGF) and in Fed State Simulated Gastric Fluid (FeSSGF)

The stability of purified plant-expressed HBcAg was then evaluated using the FaSSGF/FeSSGF models. The Western blot image (Figure 3.5) shows the results of HBcAg digestion in FaSSGF (Figure 3.5 - left side) and FeSSGF (Figure 3.5 - right side). On the left side of the image, it can be seen that the 20 kDa band, present in the control (lane 1), was absent after only 30 minutes of incubation in FaSSGF (lane 2). This suggests that HBcAg had been promptly digested in this medium. On the right side of the image, it can be visualised that the 20 kDa band, present in the control (lane 1), was consistently present for the first 60 minutes of incubation (lanes 2 to 3). At longer incubation times, i.e.

120 (lane 4) and 180 (lane 5) minutes, a faint anti-HBcAg signal could be detected at a protein size of circa 15 kDa. This is consistent with partial digestion of HBcAg over time. In all the lanes clear anti-HBcAg immunoreactivity corresponding to the presence of HBcAg dimers could be visualised. Dimers were visible at circa 40 kDa band for the intact protein over the first 60 minutes and circa 30 kDa for the partially digested HBcAg at 120 and 180 minutes. Samples in FeSSGF did not show a perfect electrophoretic migration due to the presence of milk in the media. The results obtained indicate that HBcAg was strongly and quickly digested in FaSSGF. However, it was digested much more slowly in FeSSGF, where incubation times as long as 180 minutes could result in a digested form of HBcAg that was still immunoreactive.

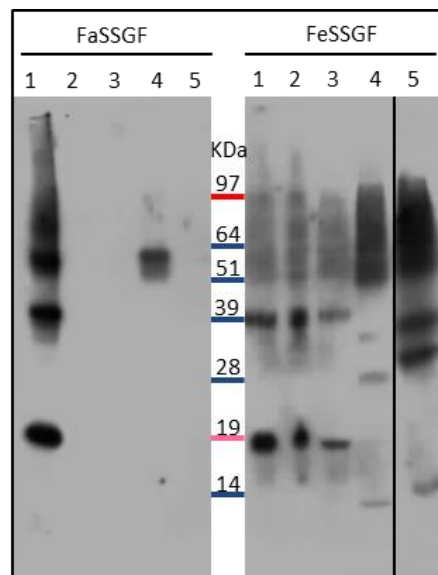


**Figure 3.5. HBcAg digestion in FaSSGF and FeSSGF.**

HBcAg was incubated in FaSSGF and FeSSGF for 180 minutes. Samples were drawn at 30, 60, 120 and 180 minutes. The digested samples were then analysed by Western blot (polyclonal antibody): positive control (lane 1), 30 minutes (lane 2), 60 minutes (lane 3), 120 minutes (lane 4) and 180 minutes (lane 5).

FaSSGF is definitely a harsher media than FeSSGF in terms of acidity; however the final concentration of pepsin in both media is comparable. Therefore, it is surprising that HBcAg was highly susceptible to digestion in FaSSGF, but it appeared to be partially stable in FeSSGF over the first 180 minutes of incubation. This result can be possibly explained by the presence of nutrient components of the milk reducing the enzymatic degradation of this candidate vaccine by being digested themselves. Intriguingly, it has already been reported that bystander proteins can protect candidate oral vaccine-ligands

against intestinal enzymatic proteolysis. Reuter et al. (2009) found that three vaccine-ligands which were normally susceptible to enzymatic degradation in simulated intestinal fluids could withstand the enzymatic digestion for at least three hours when they were co-incubated with Bovine Serum Albumin or Ovalbumin. The authors speculated that it would be advisable to administer oral vaccines, not on an empty stomach, but together with easily digestible irrelevant bystander proteins from foods. Moreover, a more recent study suggested that the formulation of an antigen in peanut butter favoured slower release and higher immunogenic responses than when the same candidate vaccine was delivered with honey and apple juice upon oral administration in mice. It was hypothesised that the protein and fat present in large quantities in the peanut butter could function as a “defensive coating” and act as a “decoy for digestive enzymes” (Pelosi et al., 2011a). The preliminary data presented here seems to support this hypothesis. Furthermore, it is reasonable to think that the presence of food in the stomach could buffer the harsh pH towards more neutral levels, allowing certain proteins to withstand the denaturation. It has been reported that after the administration of a complete nutrient drink, the neutralising effect of the meal on the pH was still apparent three and a half hours after intake (Kalantzi et al., 2006). Thus, a vaccine might possibly bypass the stomach barrier if “delivered” together with a meal, which is expected to act as a decoy for enzymes and simultaneously buffer and dilute the gastric fluid for hours.

### 3.4.2 HBcAg in Intestinal Fluids: An *In Vitro* and *Ex Vivo* Stability Approach

The second barrier that HBcAg could encounter upon oral administration is the harsh environment of the small intestine. In the following experiments the ability of HBcAg to withstand the intestinal digestive environment was investigated from two angles: firstly HBcAg was incubated in an *in vitro* model of intestinal fluid containing pancreatic enzymes. Then a more bio-relevant study was carried out using natural small intestinal fluids from pig, in order to closely mimic the *in vivo* scenario. It is worth remembering that HBcAg is a complex protein bearing an organised particulate quaternary structure. Therefore, in these stability experiments not only the chemical digestion was investigated, but also the influence of digestion on the maintenance of the VLP’s particulate structure, i.e. the physical stability was evaluated.

### 3.4.2.1 HBcAg Stability in Simulated Intestinal Fluid (SIF)

The two gels relative to the chemical stability of HBcAg incubated in SIF are shown in Figure 3.6. The Coomassie stained gel (Figure 3.6 A) shows that the circa 20 kDa band, seen in the positive control (lane 1) and corresponding to HBcAg, slightly overlaps with a much fainter band of the same size in the negative control (lane 2). For this reason, careful consideration is required when interpreting these results. At all incubation times, it appears that HBcAg was partially digested into slightly shorter proteins. In particular the more prominent digestion residual appeared at a circa 17 kDa protein band. The intensity of this band seems to increase proportionally with the incubation time in SIF. These results were confirmed by the Western blot, which shows that the strongest anti-HBcAg signal in the samples incubated in SIF (lanes 3 to 7) was the circa 17 kDa band. However, a series of anti-HBcAg bands of intermediate sizes between the full-length and the 17 kDa version were present in smaller quantities. As expected a circa 20 kDa band, corresponding to indigested HBcAg is seen in the positive control (lane 1) and no bands are present in the negative control (lane 2).

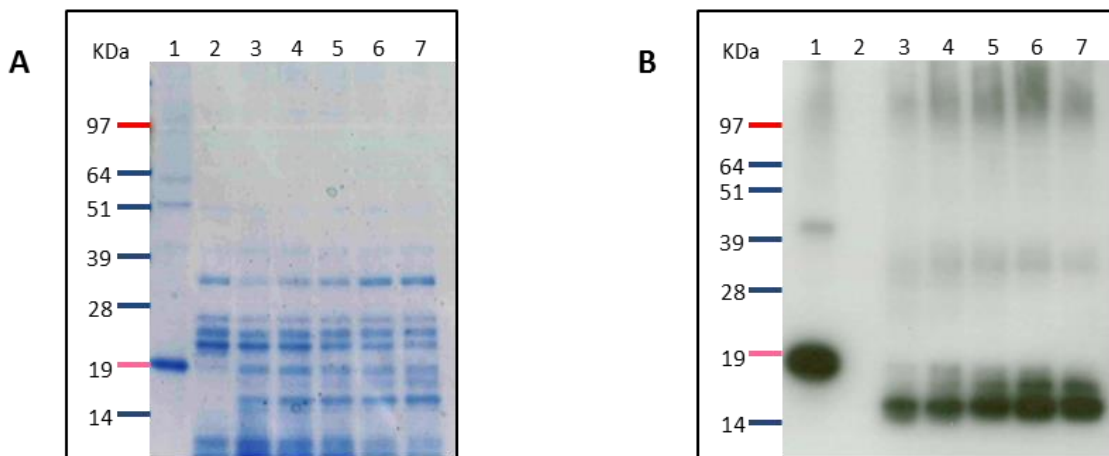


**Figure 3.6. HBcAg Chemical Stability in SIF.**

Aliquots of purified HBcAg were incubated in SIF with pancreatin for different time intervals. All the resulting digestion samples were analysed by SDS-PAGE. HBcAg was also incubated in SIF without pancreatin as a positive control; whereas a dilution of water in SIF with pancreatin was used as a negative control. (A) shows the Coomassie stained SDS-PAGE and (B) shows the Western blot (monoclonal antibody): positive control (lane 1); negative control (lane 2); 30 minutes (lane 3); 60 minutes (lane 4); 120 minutes (lane 5); 180 minutes (lane 6); 240 minutes (lane 7).

These results suggested that HBcAg was highly digested by the pancreatic enzymes of SIF. However, the main detectable product of this digestion was not smaller than circa 17 kDa. Considering that the anti-HBcAg mouse monoclonal primary antibody used has specificity for the first N-terminal 10 amino acids, it is evident that the digestion is expected to have only occurred at the C-terminus. In contrast, digestion of the N-terminal would have resulted in loss of affinity of HBcAg to this given antibody, resulting in a lack of immunoreactivity.

The above results demonstrated that HBcAg was digested to a smaller protein after exposure to SIF. However, SDS-PAGE gels are carried out on denatured proteins (the denaturation being part of the processing for the gel electrophoresis), thus they can give information only about the stability of the primary structure. It was therefore necessary to define whether this chemical digestion maintained or disrupted the physical three-dimensional structure of the VLP.

Figure 3.7 illustrates the effect of the incubation of HBcAg in SIF with pancreatin on its physical stability. The dot blot (Figure 3.7 A) represents the HBcAg sedimentation upon ultracentrifugation of the samples undergoing the proteolytic treatment. Irrespective of the incubation time in SIF with pancreatin, most HBcAg immunoreactivity could be visualised in dots corresponding to the 30 and 40% (w/v) sucrose fractions, as in the undigested VLP positive control. This result suggests that HBcAg maintained its particulate form after digestion. This result was confirmed by native agarose gel electrophoresis (Figure 3.7 B). HBcAg incubated in SIF (lanes 2 to 7) showed electrophoretic migration almost identical to that of the untreated VLP of the control sample (lane 1). Finally TEM imaging (Figure 3.7 C) indicates that VLPs were still present after incubation of HBcAg in SIF with pancreatin for 120 minutes. These results taken together strongly suggest that HBcAg was partially digested upon treatment in SIF; however the digestion did not seem to interfere with physical stability of the VLPs.

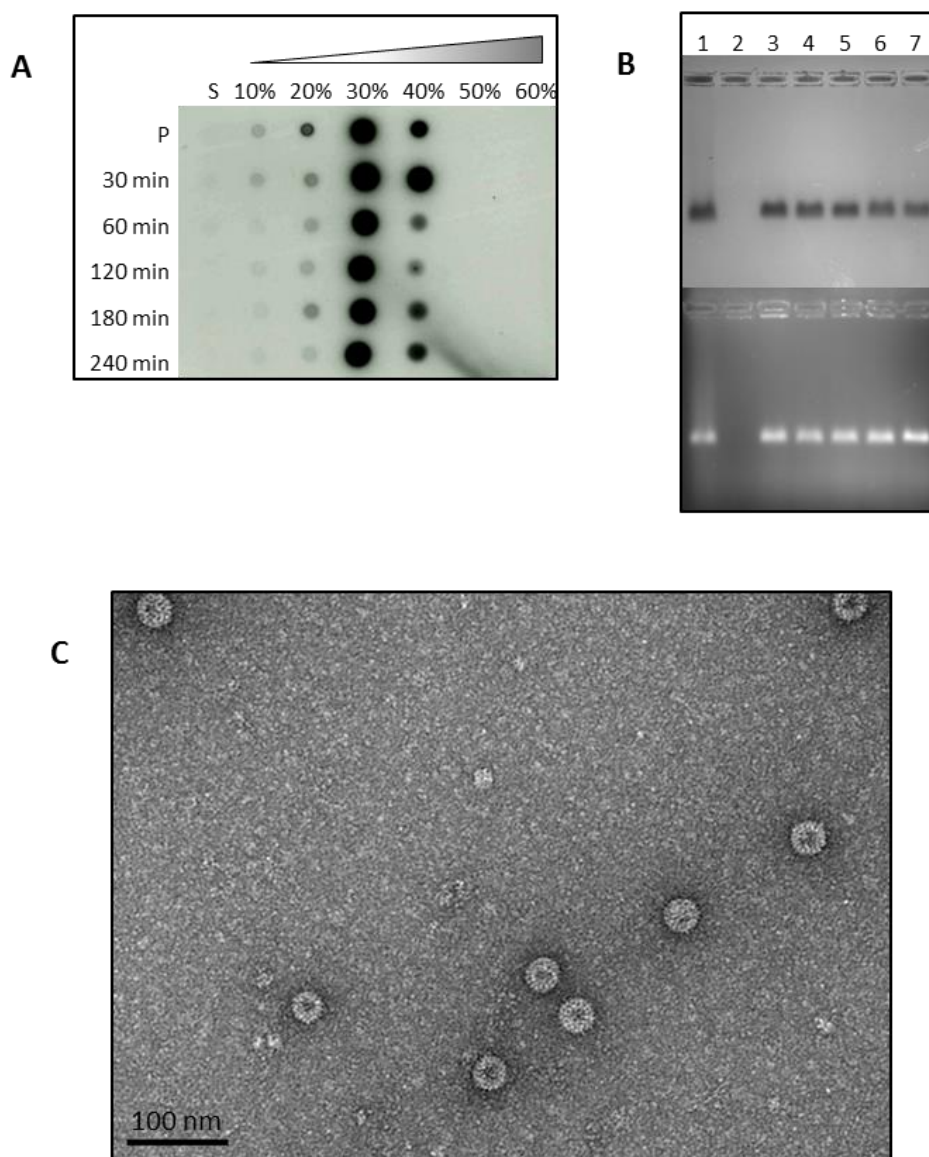


**Figure 3.7 HBcAg Physical Stability in SIF.**

Aliquots of purified HBcAg were incubated in SIF with pancreatin for different time intervals. All the resulting digestion samples were either separated by density gradient centrifugation and analysed by dot blot, or directly examined by native agarose gel electrophoresis or TEM imaging. HBcAg was also incubated in SIF without pancreatin as a positive control; whereas a dilution of water in SIF with pancreatin was used as a negative control. (A) shows the dot blot (monoclonal antibody): percentages indicate the approximate concentration of the sucrose density fraction (S = Supernatant), while incubation times are listed vertically (P = Positive). (B) shows the native agarose gel: positive control (lane 1); negative control (lane 2); 30 minutes (lane 3); 60 minutes (lane 4); 120 minutes (lane 5); 180 minutes (lane 6); 240 minutes (lane 7). (C) shows a TEM image of HBcAg incubated in SIF with pancreatin for two hours.

The pancreatin present in the SIF contains several pancreatic proteases, including trypsin, chymotrypsin and elastase, which could potentially digest antigens. Interestingly, it was reported in a virology study, that HBcAg, expressed in *Xenopus* oocytes, was partially digested into smaller proteins upon incubation in trypsin: the main residue was a circa 17 kDa protein, but several intermediate forms ranging between 17 and 21 kDa were also detected, corresponding to different cleavage sites for trypsin at the C-terminus. However, the most striking finding was that intact capsids were digested only at the C-terminus and that this digestion did not affect the particle assembly (Seifer and Standring, 1994). It is worth remembering that HBcAg bears in its monomeric structure a C-terminal tail arginine-rich domain. This domain is not essential for the assembly and stabilisation of the monomers into a VLP (Chapter 1). Intriguingly, it was demonstrated that the trypsin digests only these C-terminus sequences, which were “non-essential” for the particle assembly. The authors suggested that these C-terminal regions are accessible to the enzymatic attack, while the other possible cleavage sites are relatively sequestered inside the VLP structure. Another important finding of the aforementioned research is that the maximal trypsin cleavage was achieved after only 8 minutes of incubation and that the addition of fresh protease or longer incubation times up to 8 hours did not increase the extent of specific digestion (Seifer and Standring, 1994). The results obtained in the current research in SIF with pancreatin strongly suggest that the main pancreatic enzyme involved in the digestion of HBcAg is trypsin. In fact the intestinal bio-relevant media used determined a similar pattern of digestion to that suggested in the study, described by Saifer and Standring (1994).

Putting all these results into the wider context of oral delivery strongly suggest that HBcAg VLPs, though partially digested, could still withstand the harsh intestinal environment maintaining the particulate morphology and immunogenicity. In fact it was found that all the major epitopes mediating T- and B-cell responses are not found in the C-terminal arginine rich region (Vanlandschoot et al., 2003), which is digested by the trypsin. It is fascinating to ascertain that once again structures, whose design is the result of thousands years of evolution, have been naturally equipped to resist extreme environmental conditions. For instance, in this case only sequences that are non-essential for the stability and immunogenicity were digested, while the particle “scaffold” remained intact.

### 3.4.2.2 *Ex Vivo* HBcAg Stability in Natural Intestinal Fluids (natIFs)

Despite the fact that pancreatic enzymes are the main proteases in the intestine, it has been recently reported that pancreatic proteases only partially contribute to the total intestinal enzymatic activity in animal models (Reuter et al., 2009). Therefore, the stability of HBcAg in natural intestinal fluid (natIF) of pig was investigated, in order to complement the *in vitro* model.

The whole pig small intestine was excised in four parts of approximately same length and natIFs were collected from the resulting four sections and named natIF 1, natIF 2, natIF 3 and natIF4 from the proximal to the distal regions. For evaluating the extent of digestion, HBcAg was incubated in each of these natural media at 37 °C for 4 hours and the fate of HBcAg was subsequently evaluated. Figure 3.8 shows the Coomassie stained SDS-PAGE, Western blot and the dot blot of the density gradient ultracentrifugation relative to this study. After the 4 hours incubation, the samples were diluted in water, boiled and loaded on gels for SDS-PAGE. The dilution step of samples in water was required, based on a preliminary experiment that showed that the very high protein content of the natIF did not result in good electrophoretic separation of bands when undiluted. As a negative control, natIF diluted in water was used. Positive controls, including a dilution of HBcAg in PBS and a dilution in previously boiled, and thus enzymatically inactive, natIFs were used. After electrophoresis one of the two gels was Coomassie stained while the other was used for Western blot. The Coomassie stained gel showed a faint 20 kDa band corresponding to HBcAg in the positive control in PBS (lane 1). However, it was difficult to identify HBcAg in the other samples containing natIFs due to the very high content of proteins of various sizes. Nevertheless, the Western blot of the same samples showed that anti-HBcAg immunoreactivity was detected at circa 20 kDa in all positive controls where natIFs had been previously inactivated (lanes 2 to 5). In contrast, for the actual digestion samples where active natIFs were present (lanes 6 to 9), HBcAg was mainly visible at circa 16-17 kDa band. The intensity of the band was the highest in natIF 1 (lane 6) and reached a minimum in natIF 2 (lane 7), then it gradually increased in natIF 3 (lane 8) and natIF 4 (lane 9). In natIF 4 a weak 20 kDa band was also present, probably corresponding to intact HBcAg. As expected, no bands were seen in the negative controls (lanes 11 to 14).

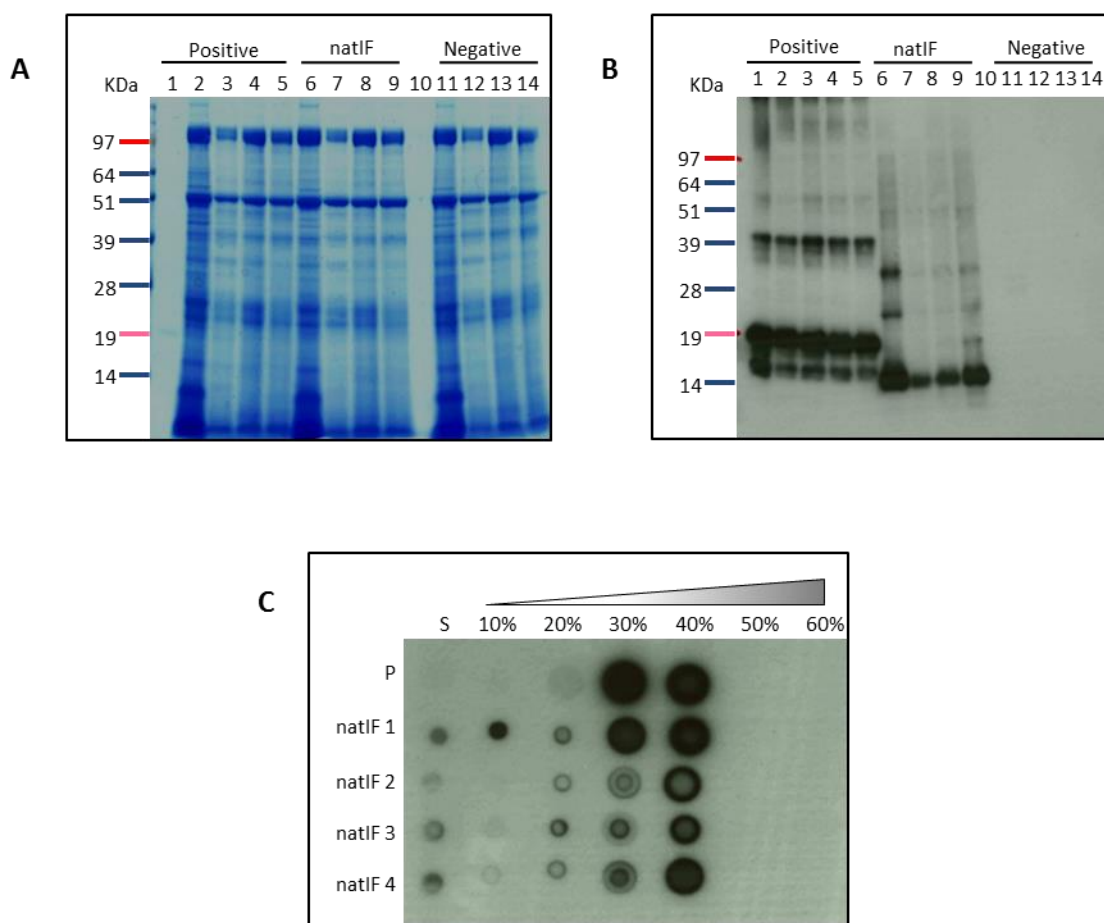


**Figure 3.8. *Ex vivo* HBcAg Stability in pig intestinal fluids.**

Stability studies were carried out in four NatIFs collected from pig, named natIF 1, natIF 2, natIF 3, natIF 4 from the proximal to the distal small intestine, respectively. HBcAg was incubated in each of the aforementioned media at 37 °C for four hours. (A) and (B) represent the Coomassie stained SDS-PAGE and Western blot (monoclonal antibody), respectively. The two gels were run identically: HBcAg in PBS (lane 1); HBcAg in inactive natIF 1 to natIF 4 (lanes 2 to 5, respectively); HBcAg in natIF 1 to natIF 4 (lanes 6 to 9); empty lane (lane 10); PBS in natIF 1 to natIF 4 (lanes 11 to 14). (C) shows the dot blot (monoclonal antibody) of fractions collected from sucrose density gradient ultracentrifugation of different HBcAg samples incubated in each of the aforementioned NatIFs. The sucrose concentrations corresponding to density fractions collected are indicated horizontally; the incubation samples analysed are indicated vertically. P = positive (HBcAg in PBS); S = Supernatant.

In a similar experiment samples were not boiled, so they could maintain their native physical structure. However, the enzymatic reaction was stopped at the end of the digestion study by adding a protease inhibitor solution. Sucrose density gradient ultracentrifugation was then carried out in parallel for the four samples, corresponding to the digestion of HBcAg in the four NatIFs, and for the control sample of HBcAg in PBS. After ultracentrifugation, fractions approximately corresponding to the original sucrose solutions

loaded were collected and analysed by dot blot. Figure 3.8 C shows that anti-HBcAg immunoreactive dots were found mainly in the 30 and 40 % (w/v) sucrose fractions, typical for intact HBcAg VLP, in the positive control. For samples digested in the natIFs, HBcAg was still detected mainly in the 30 and 40% (w/v) sucrose density fractions; however, some immunoreactivity was also present in the less dense fractions of the gradient.

In the light of these results, the stability of HBcAg in natIFs can be discussed both in terms of chemical and physical stability. HBcAg incubated *ex vivo* in pig intestinal fluids was chemically digested mainly to the shorter, circa 16 to 17 kDa, form that matched the size of HBcAg resulting from the *in vitro* digestion in the SIF with pancreatin. This suggests that despite the fact that the intestinal natural fluids have a much wider pool of proteases than just the pancreatic proteases used *in vitro* (Reuter et al., 2009), the main product of HBcAg digestion appears to be the same.

However, comparing the anti-HBcAg signal between the positive control and the HBcAg sample incubated in the enzymatically active natIFs, a decrease in the overall band intensity can be observed for the *ex vivo* samples, especially those samples incubated in natIF 2 and natIF 3. Such remarkable loss of HBcAg was not observed upon incubation in SIF with pancreatin, suggesting that a more aggressive chemical digestion occurred in the natural fluids than in SIF. Furthermore, differences in HBcAg digestion in the different natIFs collected from different parts of the small intestine could be possibly explained by the fact that the enzymatic activity is higher in the duodenum (proximal segment), where the pancreatic juice is released, than in the ileum (distal segment). A decrease in enzymatic activity on moving from the duodenum to the ileum has been demonstrated in humans, with only 22% of trypsin activity being preserved in the ileum compared to the duodenum (Whitcomb and Lowe, 2007). The increase in HBcAg stability on moving from natIF 2 to natIF 3 and then natIF 4 is therefore consistent with the intrinsic enzymatic activity of each intestinal segment. However, the fact that HBcAg is much more stable in natIF 1 than in natIF 2 was surprising. This result could be related to the ductal pancreatic physiology in pigs. It has been reported that the pancreatic duct in pigs enters the duodenum in the second, descending part of the duodenum. Furthermore it was found that pigs can have an accessory pancreatic duct that opens into the third part of the duodenum (Ferrer et al.,

2008). In the current experiment the natIF 1 is constituted by the very proximal luminal fluid of the duodenum, possibly upstream from the pancreatic ducts, which discharge the pancreatic load in the second and third part of the duodenum. This could explain the lower degradation of HBcAg in natIF 1 compared to natIF 2. Moreover, it could be observed that natIF 1 fluid was remarkably thicker and more viscous than the other three natIFs fluids. The viscous content might have partially sheltered HBcAg from enzymatic digestion.

In terms of physical stability of HBcAg in pig small intestinal fluids, the dot blot detected some minor anti-HBcAg signal in the less dense fraction of the gradient and thus suggested that partial disassembly took place upon incubation of HBcAg natIFs. However most of the immunoreactivity was still detected in the 30 and 40% fractions of the gradient, where usually intact VLPs are found. It is also worth noticing that the intensity of dots' signal was moderately weaker in the natIFs than in the control, indicating partial HBcAg loss. This latter consideration is in accordance with what was seen in the Western blot.

It can be concluded that HBcAg appeared chemically unstable upon incubation in pig intestinal fluids. However, these data also suggest that the principal digestion products were still immunoreactive and that HBcAg was still mainly present as a VLP.

### 3.4.3 Contextualisation and Relevance of the Findings

The aim of this Chapter was to gain a better understanding of the stability of purified plant-expressed HBcAg in the gastro-intestinal (GI) tract. For this purpose, several *in vitro* bio-relevant models simulating the GI conditions, as well as pig intestinal fluids, were used as incubation media for HBcAg. The stability of the antigen was investigated in terms of chemical digestion of HBcAg primary structure and physical stability and integrity of the VLP structure. The outcomes suggested that HBcAg was generally unstable in conditions simulating the human stomach in the fasting state, as a result of both physical instability in the harsh acidic pH and prompt enzymatic digestion by pepsin. However, improved chemical stability of HBcAg upon incubation in gastric fed state conditions was also suggested. Moreover, it was reported that the average stomach pH can remain  $> 3.5$  for the first three hours after a meal (Kalantzi et al., 2006). Therefore, based on the finding that HBcAg was found to be physically stable upon two hours incubation at pH 3.5, it can be

---

expected that the VLP structure could be potentially physically stable at the pH of the fed stomach.

Furthermore, it was found that HBcAg was promptly digested in the *in vivo* and *ex vivo* simulations of the intestinal condition. However, it remained physically stable upon digestion and maintained its most immune-relevant antigenic determinant. Therefore, it is possible to hypothesise that if these results were closely correlated to the *in vivo* scenario, HBcAg could circulate through the human small intestine notwithstanding major degradation. These findings can help interpret previous findings: previous research showed that HBcAg could elicit only weak immunogenicity upon oral administration in mice and it was speculated that exposure to the gastric environment could have resulted in either major chemical degradation or particulate disassembly (or both) before the VLP could enter into contact with the mucosal surfaces of the intestine (Huang et al., 2006). This assumption is supported by the current work and strongly suggests that HBcAg gastric instability, both in terms of chemical digestion and physical disassembly, can constitute a major obstacle to HBcAg oral delivery. The oral immunogenicity of a candidate vaccine is the result of the intrinsic ability of the antigen to efficiently cross the several GI barriers on its way down through the gut, including pH and enzymes. The current findings can be an important step towards understanding the complex oral immunogenicity of HBcAg.

Investigations into the chemical stability of two plant viruses in simulated gastric conditions have been previously carried out. However, in these studies, the physical stability of the virus was not evaluated (Nuzzaci et al., 2010; Rae et al., 2005). In the current research a more systematic approach was adopted: the gastro-intestinal barriers were evaluated separately, analysing firstly the pH influence and then the enzymatic degradation. Furthermore, the fate of the VLP was evaluated not only in terms of chemical digestion of the primary structure, but also in terms of the stability of the three-dimensional quaternary structure. In addition, a wide range of different conditions of the gastric fluids was employed to account for the extremely high variations of pH and pepsin activity in the human stomach (Efentakis and Dressman, 1990; Gomes et al., 2003), so that more representative conclusions regarding the fate of HBcAg VLPs in the stomach could be drawn. Finally, it was recently reported that the use of simulated intestinal fluids to assess antigen stability is not the most efficient means to simulate the *in vivo* conditions.

Therefore, it was proposed that the use of intestinal fluids from animals could be a more efficient way to simulate the *in vivo* scenario in humans (Reuter et al., 2009). Based on this knowledge, it was decided to flank the results of HBcAg stability in the routinely used simulated intestinal fluids, with the evaluation of its stability upon incubation in natural intestinal fluids of pig.

Overall, this Chapter presents a deep investigation into HBcAg stability in GI bio-relevant conditions. In addition a systematic method for the effective assessment of VLP stability was developed, possibly adaptable to other VLP candidates for oral use.

### 3.5 Conclusions

HBcAg gastric stability was investigated using *in vitro* models of gastric fluids. HBcAg was demonstrated to be physically unstable at gastric pH, showing a peculiar behaviour where it appeared only slightly unstable upon acidification, but showed major aggregation upon subsequent neutralisation. Furthermore, HBcAg could be highly digested by biologically relevant concentrations of pepsin at the simulated gastric pH. However, HBcAg appeared to be relatively more stable at pH > 3.5 and under conditions mimicking the fed state of the stomach. In simulated intestinal fluids, HBcAg was shown to be highly digested, selectively at the C-terminal arginine-rich tail, which is not essential for the maintenance of the particulate structure, nor essential for HBcAg immunogenicity. Finally, more bio-relevant studies relative to the intestinal stability were carried out by incubating HBcAg *ex vivo* in pig intestinal fluids. HBcAg seemed to be subjected to a similar digestion pattern to that seen in simulated intestinal fluids; however, slightly harsher digestion occurred, leading to partial antigen recovery. Furthermore, a minor amount of the VLP seemed to have been physically disassembled.

Taken together, these findings suggest that HBcAg would be very likely unstable in the stomach, but fairly stable in the intestine upon oral administration. Therefore, it can be suggested that oral delivery of HBcAg VLPs to the mucosal absorption sites could possibly be achieved if the antigen could be protected from the gastric environment. In the following two Chapters different approaches towards the development of oral formulations of HBcAg have been investigated.

## 4 Exploitation of the Expression in Plant for Oral HBcAg Delivery

### 4.1 Introduction

One of the most claimed advantages of the expression of recombinant vaccines in plant is the potential use of this technology for the development of oral vaccines. In other words, the use of plants as green bioreactors for the production of vaccines might allow an oral administration of raw plant material or more probably minimally processed plant formulations (Mason et al., 2002). This could result in a huge reduction in purification and formulation costs. Moreover, the expression of the vaccine within the plant cellular compartments could act as a sort of bio-encapsulation: it is in fact thought that such entrapment within the plant cell wall could confer protection of the vaccine from gastro-intestinal (GI) degradation, if administered orally (Pelosi et al., 2011a; Walmsley and Arntzen, 2000).

In Chapter 3 the intrinsic stability of HBcAg exposed to bio-relevant GI media was investigated and the results are summarised in Table 4.1.

**Table 4.1. HBcAg stability in bio-relevant GI fluids (summary of Chapter 3)**

| Media  | Chemical Stability                     | Physical Stability   | Impact on immunogenicity  |
|--|--|--|---|
| <b>Simulated Gastric Fluids</b>                |  |  |   |
| Gastric pH                                     | Stable                                 | Partially denatured - agglomeration upon pH neutralisation (i.e. intestinal passage) | VLP chemically and physically unstable and hence loss of immunogenicity |
| Enzymatic digestion                            | Degraded                               | Chemical digestion incompatible with VLP stability                                   |   |
| <b>Simulated and Natural Intestinal Fluids</b> |  |  |   |
| Enzymatic digestion                            | Selectively digested at the C-terminus | Chemical digestion compatible with VLP stability                                     | VLP physically stable and immunogenicity maintained                     |

Based on this knowledge, HBcAg could represent a suitable candidate to study the effect of the plant bio-encapsulation on the oral delivery of the antigen: the leaves-mediated

delivery of the antigen in simulated gastric and intestinal media could be evaluated. Moreover, given the intrinsic antigen instability in the bio-relevant gastric media, it could be assessed whether HBcAg entrapment within plant leaves could somehow protect it from degradation and denaturation.

In this research project, *Nicotiana benthamiana* was used as a platform for HBcAg expression. This plant is one of the most extensively used in molecular farming: it is particularly suited for transient expression, because it can be easily agroinfiltrated and it grows quickly (Conley et al., 2011). Nevertheless its potential use for oral administration is somehow contradictory. In some cases *Nicotiana benthamiana* leaves are regarded as the most promising candidate for the production of oral vaccines (Clark and Pazdernik, 2011; Coghlan, 2005): this plant is non-edible, offering a considerable advantage for its exploitation as a recombinant protein expression host, as there is no risk of contamination of the food chain. In contrast, other authors believe that the presence of alkaloids within *Nicotiana benthamiana* makes it unsuitable for oral delivery. For this reason, a bio-engineered alternative version of *Nicotiana tabacum* (a closely related species to *Nicotiana benthamiana*), containing very low amounts of alkaloids has been developed. This low-alkaloids tobacco was fed for 30 days to mice at concentrations as high as 20% (w/w) of the diet and it was perfectly tolerated (Menassa et al., 2007). More recently, alkaloids-free *Nicotiana* hybrid species were created: in this case even the subcutaneous administration to mice of crude extract from the leaves did not induce any toxicity (Ling et al., 2012). These low or free alkaloids *Nicotiana* versions could certainly constitute a good alternative for the possible production of oral vaccines in plants. Nevertheless, it is reasonable to think that even wild-type *Nicotiana benthamiana* could be sufficiently tolerable upon oral administration: the simple observation that *Nicotiana tabacum* leaves are chewed regularly without apparent acute toxicity suggests that the ingestion of only few tens of milligrams of *Nicotiana benthamiana* plant material, for one-off oral vaccine administrations, should not lead to any acute side effect.

The aim of this Chapter was to exploit the leaf material for the oral delivery of HBcAg. Several aspects had to be addressed. First of all the fresh plant material containing the antigen had to be efficiently processed into an unpurified pre-formulation, which could retain stable HBcAg VLP. The second objective was to evaluate the effect of the plant bio-

encapsulation on the delivery of the antigen in simulated GI fluids, so to understand whether this natural delivery system could allow release of the entrapped antigen and whether it could offer some protection against the antigen degradation in the GI. The last objective of this Chapter was to exploit the antigen expression in plants to produce a simple and potentially cheap oral formulation that could effectively protect HBcAg from the GI degradation.

## 4.2 Materials

### 4.2.1 Molecular Biology Media, Buffers and Solutions

General media, buffers and solutions used in this study for bacterial growth, plant agro-infiltration and protein analysis are catalogued in Table 2.1 of Chapter 2.

### 4.2.2 Antibodies and Antigens

Antibodies and antigens standards used for Western blot, dot blot and ELISA are listed in Table 2.2 of Chapter 2.

### 4.2.3 Enzymes and Other Materials Used for Stability and Release Studies

The materials used for the preparation of bio-relevant media used for the incubation of HBcAg are indicated in Chapter 3.

### 4.2.4 Other Materials Used in Molecular Biology Studies

Materials used for SDS-PAGE, Western blot, dot blot, native agarose gel and ELISA are indicated in Chapter 2.

### 4.2.5 Excipients Used for the Formulation of Tablets

Alpha-lactose monohydrate ( $\alpha$ -lactose monohydrate) is the most widely used filler excipient for tablets. Its main characteristics are good compactability, solubility in water, lack of hygroscopicity and a fairly non-reactive character (Alderborn, 2007).  $\alpha$ -Lactose

monohydrate imparts mechanical strength to tablet formulations. It was purchased from Sigma-Aldrich (UK) in a reagent grade and used as received.

Microcrystalline cellulose (MCC) is considered a good tablet former and it is extensively used as a filler in solid pharmaceutical formulations (Alderborn, 2007). The type of MCC used in this study is Avicel PH 101 and it was obtained from FMC BioPolymer (UK) and used as received.

Partially gelatinized starch bears swelling properties that causes the tablet to rupture when in contact with a liquid. It was therefore used here as a disintegrant. Moreover partially gelatinized starch also functions as a binder in wet granulation formulations. It was purchased from Colorcon (UK) as the grade Starch 1500 and used as received.

Magnesium stearate is usually used to reduce friction between the tablet and the punches during the formation and ejection of the tablet. It was therefore used as a lubricant. It was purchased from Aldrich (UK) and used as received.

#### **4.2.6 Excipients Used for the Coating of Tablets**

Eudragit L 100 is a polymer that dissolves at  $\text{pH} > 6$ . It is a copolymer of methacrylic acid and methyl methacrylate. It is commonly used for enteric coating of oral formulations with fast dissolution in the small intestine (Eudragit, 2011). Eudragit L 100 was kindly donated by George-William Smith (Evonik Industries, UK) and used as received.

PlasACRYLT20 is a blend of anti-tacking agent and plasticiser added to the coating suspension (Evonik Industries, 2013). It was also kindly donated by George-William Smith (Evonik Industries, UK) and used as received.

Triethyl citrate (TEC) is a commonly used plasticiser added to the coating suspension. It was purchased from Sigma Aldrich (UK) and used as received.

Ammonia ( $\text{NH}_3$ ) used for the partial alkaline-neutralisation of the Eudragit L 100 was bought from Fisher Scientific (UK) as 35% solution in water and diluted to 1 M before use.

## 4.3 Methods

In this Paragraph, different methods of processing of the plant material expressing HBcAg are described. Furthermore, the characterisation of the formulated plant material will be defined. Finally, the protocols used to assess the stability of HBcAg, as well as its release from the formulation are also explained. Molecular Biology techniques were carried out as described in Chapter 2, unless otherwise stated.

### 4.3.1 Oven-drying

Oven-drying is a simple desiccation method commonly used in food and pharmaceutical industry. It has been used in the past for the drying of plant-expressed vaccine candidates (Lee et al., 2003).

*Nicotiana benthamiana* leaves were infiltrated with pEAQ-HT-HBcAgΔ176 as described in Chapter 2. Infiltrated leaves were harvested 6 to 7 days post-infiltration, weighed and spread on a tray. The tray was then incubated in oven at 40 °C or 50 °C for 5 days to dry the leaves before being collected. Alternatively when smaller batches were needed, after harvesting, leaf disks were prepared using a cork borer of 11 mm diameter and they were also oven dried at 40 °C or 50 °C for 5 days. After drying, the leaves or the leaf disks were kept in glass vials sealed with parafilm and stored in fridge (2-8 °C).

#### 4.3.1.1 In Process Dehydration of Oven-dried Leaves

Gravimetric analysis (GA) was used as a method to assess the water loss from the leaves due to dehydration during oven-drying. Circa three grams of wild type (wt) *Nicotiana benthamiana* fresh leaves were cut into approximately 1 to 2 cm pieces, which were equally distributed into three identical glass bottles. The total weight of the glass bottles as well as their empty weight was recorded immediately. Then the bottles were incubated in an oven at 40 °C for 6 days. During the drying process, the total weight of the bottles was measured at different time intervals, in order to assess the water loss over time. The weight loss during the drying corresponds to water evaporation.

### 4.3.2 Freeze-drying

Freeze-drying is a commonly used drying technique for the preparation of parenteral formulations. It is extensively used for the formulation of proteins and other bio actives, as it usually ensures high stability of the active ingredient. It has also been used for the production of fast-dissolving tablets; furthermore, it is widely used in the food industry. Freeze-drying is based on the sublimation, i.e. conversion from ice into vapour without passing through the liquid state. This phase transition is possible only at very low pressure conditions (Abdul-Fattah et al., 2007). In this Chapter, freeze-drying was used as a drying method for the leaves expressing HBcAg.

*Nicotiana benthamiana* leaves were infiltrated with pEAQ-HT-HBcAgΔ176 as described in Chapter 2. Infiltrated leaves were harvested 6 to 7 days post-infiltration, weighed and laid on a tray for subsequent freeze-drying in a Wizard 2.0 freeze drier (VirTis, USA). For the thermal treatment step, the shelf temperature was initially set at - 60 °C for 360 minutes and was then reduced to the lowest possible temperature (maximum freezing mode) for 240 minutes to achieve maximum freezing. After this phase, the primary drying was carried out at a chamber pressure of 180 millitorr with sequential temperature steps of 180 minutes, using the following order: - 45, - 35, - 25 and - 15 °C; this was followed by further drying steps at a chamber pressure of 180 millitorr with sequential temperature steps of 240 minutes: 5, 15, 20 and 25 °C.

After freeze-drying, the leaf material was usually ground into powder using a Waring blender (UK). Alternatively disks from leaves expressing HBcAg were prepared using a cork borer of 11 mm diameter. The leaf disks were freeze-dried using the aforementioned protocol. Freeze-dried leaves or leaf disks were stored in glass vials sealed with parafilm and stored in fridge (2-8 °C). Freeze-dried samples were generally used within 4 weeks from production.

### 4.3.3 Thermogravimetric Analysis (TGA)

Thermogravimetric analysis (TGA) measures changes in mass, resulting from chemical or, sometimes, physical processes, as a function of temperature or isothermally as a function of time (Galwey and Craig, 2007). It is a simple and quick technique used for the

measurement of weight loss. Among other uses in drug delivery, TGA is commonly used for the measurement of the water content of a given drug or excipient. TGA was performed using a Hi-Res TGA 2950 (TA Instruments, Newcastle, USA).

The residual water content of the oven-dried and freeze-dried wild type (wt) *Nicotiana benthamiana* leaf material was measured by weight loss due to sample dehydration. Dried leaves were ground into powder using a Waring blender (UK) and the resulting powder was used. Samples ( $n = 3$ ) were loaded into open aluminium pans and heated from 30 °C to 110 °C at a heating rate of 10 °C/minute, and then were held (isothermally) at 110 °C for 30 minutes. The weight change was calculated as a measure of residual moisture content. Statistical differences in residual moisture content between the different drying techniques were calculated using a 2-tailed T-test.

#### **4.3.4 HBcAg VLP Stability upon Oven- and Freeze-drying of Leaves**

The stability of HBcAg within the leaf material upon oven-drying and freeze-drying was evaluated using the commonly used detection methods already described throughout this thesis. The chemical stability was evaluated by Coomassie stained SDS-PAGE and Western blot, while the physical stability of the VLP was assessed by density gradient ultra-centrifugation, followed by collection of fractions and dot blot analysis. Finally, HBcAg VLP overall stability was also quantified by sandwich ELISA.

##### **4.3.4.1 HBcAg VLP Chemical and Physical Stability: A Qualitative Investigation**

*Nicotiana benthamiana* leaves were infiltrated with pEAQ-HT-HBcAgΔ176. Three leaves from the same plant were harvested 7 days post-infiltration. Four leaf disks were prepared from each of the three leaves using a cork borer of 11 mm diameter. Three disks, one from each of the three leaves, were pooled together. This was done to minimise differences in expression levels. Each of the four collected samples was subject to a different treatment protocol: the first was frozen at – 80 °C, the second was freeze-dried, the third was oven dried at 40 °C for 5 days and the fourth was oven dried at 50 °C for 5 days. The preparation protocol is summarised in Figure 4.1.

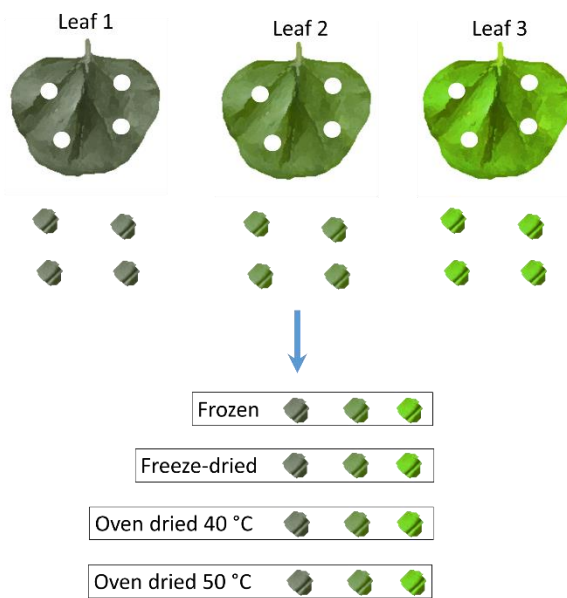


**Figure 4.1. Preparation of leaf disks for different treatments.**

Four disks from each of three leaves expressing HBcAg were prepared. Three disks, one from each of the three leaves, were pooled together and either frozen, freeze-dried, oven dried at 40 °C or 50 °C.

The oven-drying and freeze-drying were carried out as mentioned in the previous Paragraph. At the end of the 5 days the freeze-dried disks, the disks oven-dried at 40 °C and those oven-dried at 50 °C were used for protein extraction. Frozen disks (stored in the freezer at - 80 °C) were thawed and used as a positive control. After extraction, small aliquots from the four crude extracts were run on two SDS-PAGE gels; then one was Coomassie stained, while the other was used for Western blot. The physical stability of the VLP was evaluated by layering the same four crude extracts on the top of different 10 to 60% (w/v) sucrose step gradients. After ultracentrifugation seven density fractions were collected from the four gradients and analysed by dot blot. The gradient containing the crude extract from the leaf material previously stored at - 80 °C was used as a control.

#### 4.3.4.2 HBcAg VLP Stability: A Quantitative Measurement

The four crude extracts obtained from samples stored at - 80 °C, from freeze-dried and oven-dried (both at 40 and 50 °C) samples were also quantified by sandwich ELISA. The amount of HBcAg resulting from the extraction of the frozen sample was considered as the total extractable HBcAg. Therefore, the quantified HBcAg resulting from the extraction of the oven-dried and freeze-dried samples was calculated as a percentage ratio to the total

HBcAg extracted from the frozen material. Statistical significance was calculated using a 2-tailed T-test.

#### **4.3.5 Delivery of Bio-encapsulated HBcAg in Simulated GI fluids**

In this Paragraph, the methods used for the investigation of the effect of the plant bio-encapsulation on the protection and release of HBcAg in simulated GI fluids are described.

##### **4.3.5.1 Freeze-dried Bio-encapsulated HBcAg in Simulated Gastric and Intestinal Fluids**

In this study the delivery of HBcAg from freeze-dried leaves in SGF and SIF fluids in presence and absence of enzymes was evaluated. Simulated gastric fluid (SGF) was prepared according to the British Pharmacopeia (2012): SGF without pepsin was prepared as a pH 1.2 HCl, 34 mM NaCl solution; in parallel SGF with pepsin was prepared similarly, yet 3.2 g/L pepsin was added. SIF with and without pancreatin were prepared as in Chapter 3. One mL aliquots from SGF with and without pepsin and SIF with and without pancreatin were used for the stability-release study. Fifteen (15) mg of freeze-dried material were added to each of the four 1 mL media aliquots. The samples were then incubated at 37 °C for 2 hours and frequently vortexed. At the end of the incubation the solid material was separated from the supernatant by centrifugation of the sample at 12,000 g for 5 minutes. The supernatant was immediately boiled to stop the enzymatic reaction, while the pellet was re-suspended in LDS β-mercaptoethanol, boiled and clarified again. Both the supernatant and the re-suspended precipitate of samples incubated in SGF with and without pepsin and in SIF with and without pancreatin were separated by SDS-PAGE gel for subsequent anti-HBcAg Western blot detection.

##### **4.3.5.2 Delivery of Bio-encapsulated HBcAg in Intestinal Fluids, after Pre-incubation in Gastric Fluids**

The delivery of HBcAg from differently processed plant material was evaluated by incubating leaf disks in SGF, followed by subsequent incubation of the same plant material in SIF. This experiment was performed in order to see if the plant material could protect or

not the labile HBcAg against SGF and to evaluate if the antigen could be released in either SGF or SIF.

Three leaves expressing HBcAg were collected and three disks were prepared from each leaf. Then three disks, one from each of the three leaves, were pooled together and freeze-dried, oven-dried at 40 °C or frozen at – 80 °C. On the day of the experiment, fresh SGF with pepsin and SIF with pancreatin were prepared. The freeze-dried, oven-dried and frozen samples were incubated in 5 mL of SGF at 37 °C for 2 hours and were frequently vortexed. After this initial pre-incubation, SGF was carefully drained and the leaf material was collected with tweezers and incubated in 0.75 mL SIF for further 4 hours. Twenty five (25)  $\mu$ L aliquots were collected after 30 minutes, 2 hours and at the end of the 4 hours incubation. The residual leaf material was pelleted by centrifugation, re-suspended in LDS  $\beta$ -mercaptoethanol, boiled and clarified again. A control was prepared by incubating a fourth group of frozen leaf disks in SIF, without pre-incubation in SGF. Aliquots of 25  $\mu$ L were also collected at the same predetermined time points. Finally, the 30 minutes, 2 hours and 4 hours incubation and re-suspended pellet samples collected from the frozen, freeze-dried, oven dried and control disks were loaded on two SDS-PAGE gels, separated by electrophoresis and the gels were used for anti-HBcAg Western blot.

A similar experiment was carried out for sandwich ELISA quantification. Freeze-dried, oven-dried and frozen leaf disks were incubated in 1 mL SGF with pepsin at 37 °C for 2 hours and were frequently vortexed. After this initial pre-incubation, SGF was carefully drained and the leaf material was collected with tweezers and incubated in 1 mL SIF without pancreatin for further 4 hours. One hundred (100)  $\mu$ L aliquots were collected after 30 minutes, 2 hours and at the end of the 4 hours. The residual leaf material was re-suspended, homogenised in extraction buffer and clarified again. Finally, the collected samples were quantified by sandwich ELISA. For control, identical batches of frozen, freeze-dried and oven-dried disks from the same leaves used for the experiment were homogenised in extraction buffer and the total HBcAg content was calculated from these crude extracts. In this way the amount of HBcAg present in the supernatant and in the re-suspended pellets upon incubation of leaf disks in SGF/SIF could be calculated as a ratio to the total HBcAg content of disks, made from the same leaves.

#### 4.3.6 Formulation of Tablets

Tablets are by far the most commonly used pharmaceutical dosage form. They are solid unit dosage forms obtained by the compression of powder: the coherence of the powder into compact form is promoted by bond formation during the compression. There are three main stages during the tableting: die filling, tablet formation and tablet ejection. Such a sequence, also called the compaction cycle, results in formation of tablet units. Two types of tablet presses are available: single-punch presses and multi-station (rotary) presses. In the case of single-punches presses one die and an upper and lower punch are present. The powder is generally filled in a feeding shoe, which is positioned over the die; movement of the feeding shoe allows the powder to flow into the die. The lower punch position determines the quantity of powder filled into the die; therefore the lower the punch is positioned the higher will be the weight of the final dosage form. The tablet is generated by the compression of the powder in the die due to the descent of the upper punch. The lower punch which is stationary during the compression moves upwards at the end of cycle, determining the ejection of the tablet. Tablets can be obtained either by direct compression of powder, or via wet granulation. Granules have usually better flowability and mixing homogeneity properties than powders used for direct compression. Furthermore, they generally elicit good compactibility. On the other side, direct compression is a faster and cheaper production method and it is more suitable for moisture sensitive actives (Alderborn, 2007).

In this research, tablets were produced by direct compression of freeze-dried plant material, together with other excipients for compression. The freeze-dried leaves expressing HBcAg were carefully ground into powder and used as a natural matrix containing the active ingredient. The tablet formulation consisted of 69% (w/w) lactose monohydrate, 10% (w/w) ground freeze-dried leaf material, 10% (w/w) microcrystalline cellulose, 10% (w/w) pre-gelatinised starch and 1% (w/w) magnesium stearate. All ingredients except the magnesium stearate were blended together using a mortar and pestle, and then the lubricant was added. Given the small scale nature of the experiments (5-10 g of powder), tablets were produced using manual cycles; the powder mix was loaded into a Manesty E-2 single station tablet press (Manesty Machines Ltd., Liverpool, UK) and was compressed using round 7 mm diameter, plain, normal concave punches. The

powder was loaded for each single tablet using a spatula. Each batch of tablets consisted usually of 25 to 40 single dosage forms. The weight target for each dosage form was circa 175 mg.

### 4.3.7 Physical Characterisation of Tablets

#### 4.3.7.1 Weight Uniformity and Hardness Tests

An essential parameter in the characterisation of tablets is the evaluation of the mass uniformity of tablets within a batch. To test uniformity, 20 tablets from the same batch, were weighed individually. After calculation of the mean weight, compliance with the British Pharmacopeia specifications was checked: for tablets with mean weights between 80 and 250 mg, no more than two units can deviate by more than 7.5% and none by more than 15% from the average weight (British Pharmacopeia, 2012).

Another important characteristic of tablets is the hardness: sufficient hardness is essential so that the tablets can bear handling and further processing, i.e. coating, packaging and transport, without being damaged. The hardness generally influences the disintegration and hence the dissolution profile of the dosage form; for a given powder mix, normally, enhanced hardness coincides with slower disintegration and dissolution. It should be noticed that the term “hardness”, commonly used in pharmaceutical industry and hence used here, should be more correctly defined as “resistance to crushing”. The hardness of the tablets was assessed using an Erweka TBH 28 apparatus (Erweka GmbH, Germany). The hardness of 3 tablets from each batch was measured in kilo-ponds (kp) and the mean value was calculated.

#### 4.3.7.2 Disintegration Time Test

The disintegration of tablets is important to ensure reproducibility of the therapeutic effect, therefore, it should be as consistent as possible within a batch. The disintegration test was carried out by placing one single tablet in one of the tubes of the basket of a Copley DTG 2000 apparatus with disks (Copley Scientific Ltd., Nottingham, UK). The basket was then immersed in water at 37 °C. The time required for the disintegration of each tablet was recorded and the mean value for three tablets was measured. The disintegration of

uncoated tablets should occur within 15 minutes according to British Pharmacopeia (2012). However, generally most immediate-release conventional tablets disintegrate within 5 minutes or less.

#### 4.3.8 Coating of Tablets

Oral dosage forms are often coated for different purposes: the coating can protect the active ingredient from environmental conditions, i.e. moisture and light, or it can mask the taste of certain active ingredients, or it can simply give a better appearance to tablets. However, one of the most important reasons for coating tablets is to modify the release of the active drug from the dosage form. Modified release formulations can be classified as prolonged released dosage forms and delayed release dosage form (British Pharmacopeia, 2012). Delayed release of the active is often achieved using enteric coated dosage forms. Such formulations are used for the protection of the gastric mucosa from an irritant active ingredient and for the targeted release in a pre-determined area of the intestine. However, one of the main aims of enteric coating is the stabilisation of gastro-labile drugs (Balamuralidhara et al., 2011). Film coating is usually performed by spraying a polymeric dispersion or solution onto a tablet surface. The formation of a single layer of coating on the surface of an oral dosage form is the result of multiple repeated sequences, starting with droplet formation, contact, spreading, coalescence and evaporation (Dewettinck and Huyghebaert, 1998). In this research, tablets were film coated using an aqueous dispersion of Eudragit L 100, a commercially available polymer that is soluble at  $\geq$  pH 6 (Eudragit, 2011).

##### 4.3.8.1 Preparation of Coating Dispersion

The preparation of the coating dispersion is based on the available guidelines of the company producing the polymer for the enteric coating. Eudragit L 100 is a co-polymer of methacrylic acid and methyl methacrylate, hence it is highly rich in carboxylic groups. Suspensions of such polymers in water can be re-dispersed to form a nano-sized latex. This is obtained by the addition of small quantities of  $\text{NH}_3$  or other alkali that partially neutralise the carboxylic groups, enabling the formation of latex-like dispersions. Creation of such a colloidal dispersion is essential for the subsequent film formation. Furthermore plasticisers

have to be added to the aqueous dispersion in order to enable the formation of a flexible film at relatively low temperatures. However, the addition of a plasticiser can lead to formation of sticky or rubbery coating. Thus, anti-tacking agents are also added in the aqueous dispersion, to counteract this tendency (Eudragit, 2011).

The preparation of the coating dispersion was carried out in a beaker under continuous stirring; the excipients were added in the order indicated in Table 4.2. Two protocols with different stirring times were carried out and named protocol 1 and protocol 2, respectively. The respective stirring time in each phase of the formulation re-dispersion are specified in Table 4.2.

**Table 4.2. Formulation of the coating dispersion.**

| Ingredient         | Function                 | Weight | Stirring time                   |
|--------------------|--------------------------|--------|---------------------------------|
| Water              |                          | 53 g   |                                 |
| Eudragit L 100     | Polymer                  | 10 g   | 15 minutes                      |
| 1M NH <sub>3</sub> | Alkali                   | 5.6 mL | 2 hours (1)<br>Overnight (2)    |
| TEC                | Plasticiser              | 4.5 g  | 90 minutes (1)<br>Overnight (2) |
| PlasACRYL T20      | Anti-tacking/Plasticiser | 5 g    | 15 minutes (1)<br>2 hours (2)   |

#### 4.3.8.2 Fluid-bed Coating

A laboratory scale, top spray fluidised bed coater (Mini Coater/Drier 2, Caleva Process Solutions Ltd, UK) was used for coating the tablets. In this fluid-bed processing, pre-heated air is forced into the bottom of the coating chamber, where the unit dosage forms are placed. This warm stream of air keeps the substrate fluidised and enables the applied coating to be dried. The coating dispersion mixed with atomised air is sprayed from the top via a nozzle. The main parameters that can be controlled are fan speed, bed temperature, pump speed and atomised air pressure of the nozzle. Figure 4.2 summarises the coating process carried out with the fluid-bed coater used in this study.

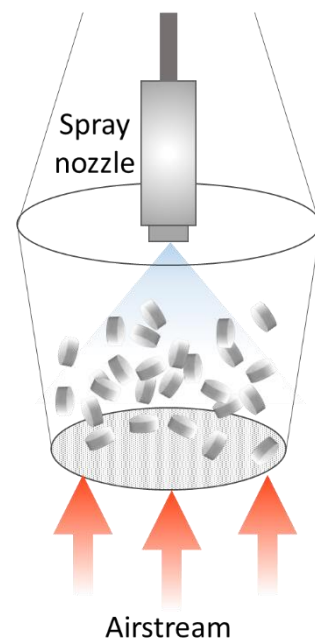


**Figure 4.2. Fluid-bed coating.**

A warm airstream from the bottom, keeps the substrate (i.e. tablets) fluidised in the coating chamber. A nozzle, located above the tablets sprays atomised droplets of coating liquid onto the tablets surface. The airstream enables the coating to dry.

Tablets were coated with the Eudragit L 100 dispersion. The air stream from the bottom of the chamber was set at a temperature of 30 °C. Nine to twelve (9 to 12) tablets per batch were placed in the coating chamber. The coating process was performed at a pump rate of 1% (1.03 rpm), with an atomization pressure set at 0.6 bar and the fan speed was kept at 80%. After coating, the tablets were left in the coater (bed temperature = 30 °C) for 10 minutes to dry. Post-drying (curing) was performed by placing the coated tablets in a hot air oven at 40 °C for 2 hours. The final coating thickness is expressed in terms of percentage total weight gain (TWG), which is the difference in the weight of tablets prior to and at the end of the coating process divided by the initial weight of tablets.

#### 4.3.9 Dissolution-Stability Test of the Enteric-coated Tablets

Dissolution tests are routinely used in the pharmaceutical field for the determination of the dissolution profile of solid dosage forms in GI bio-relevant media; such tests provide important information regarding the likely biological activity of the drug and can predict the *in vivo* performance of oral formulations (Wang et al., 2009).

The British Pharmacopeia (2012) specifications for delayed-release formulations indicate that the dosage form should be pre-incubated for 1 or 2 hours in an acidic medium, followed by incubation in buffer solution, preferentially at pH 6.8. At least two specification time points should be used: one at the end of the incubation in acid and the other after a pre-set time in the second media (British Pharmacopeia, 2012). For the current study, it was chosen to pre-incubate the samples in SGF with pepsin (pH 1.2), followed by incubation in SIF without pancreatin (pH 6.8). Samples were drawn only from the second medium and quantified by ELISA. Samples were not drawn from the SGF because HBcAg is a gastro-labile active, and hence any given amount of antigen, released from the formulation into SGF, would be promptly denatured and digested, becoming undetectable (Chapter 3). SIF without pancreatin was used, as pancreatin could have degraded the antibodies used in the ELISA assay and it was not well known whether the short version of HBcAg resulting from enzymatic digestion could be correctly measured by the ELISA assay.

#### 4.3.9.1 Preparation of the Dissolution Media

Dissolution media were prepared in 1 L volumetric flasks according to British Pharmacopeia (2012). The single components were weighed, transferred into the flask and dissolved in distilled water under continuous stirring. The final pH was calculated using a calibrated pH meter and was adjusted using HCl or NaOH when needed.

SGF was prepared by dissolving 2 g of NaCl and 3.2 g of pepsin (Ph. Eur.) in distilled water. Then circa 80 mL of 1M HCl was added, the pH was adjusted to pH 1.2 and the volume was diluted to 1 L.

SIF was prepared by mixing of 77 mL of 0.2 M NaOH with a solution of 250 mL KH<sub>2</sub>PO<sub>4</sub> under continuous stirring and the volume was brought to 250 mL. Then the pH was adjusted to pH 6.8 by further addition of 0.2 M NaOH aliquots. Finally, the volume was diluted to 1 L.

#### 4.3.9.2 Dissolution Method

Dissolution tests were performed using a BP Apparatus I (Copley Scientific Ltd., Nottingham, UK). Three vessels were used and each was filled with 300 mL of SGF. The bath temperature was fixed at  $37 \pm 0.5$  °C and the paddle rotation speed was maintained at 50 rpm. Three coated tablets were weighed separately and one tablet was added into each vessel. After 2 hours incubation, the paddles were stopped, the media were discarded and the tablets were preserved by passing the content of vessels through a sieve. Tablets were then added to vessels containing 300 mL of SIF and incubated for further 6 hours. One (1) mL samples were collected after 30 minutes, 1, 2, 4 and 6 hours from the beginning of the incubation in SIF. Samples were filtered through 0.2  $\mu$ m membrane filters and kept on ice until the end of the dissolution test. Finally, the samples were quantified by indirect and sandwich ELISA. The dissolution studies were conducted in triplicate and the average drug release  $\pm$  SD was calculated. The results are expressed as cumulative percentage drug release versus time profiles.

For control purposes, the total HBcAg content in the tablets was evaluated by adding three coated tablets in three different vessels of the dissolution bath containing 300 mL SIF without pancreatin. After 6 hours incubation, 1 mL samples were collected and filtered. The HBcAg content of these samples was also quantified by direct and sandwich ELISA.

The release of HBcAg in SIF without pancreatin, after pre-incubation in SGF, was measured as a percentage ratio to the total HBcAg released in the control vessels where the tablets were incubated in SIF without pancreatin only.

#### 4.3.10 Imaging of Uncoated and Coated Tablets

Coated and uncoated tablets were imaged by optical light microscopy and Scanning Electron Microscopy (SEM).

##### 4.3.10.1 Light Microscopy

Light microscopy was used for the visual examination of coated and uncoated tablets. A microscope (Leica DM LS2, Leica Microsystems UK Ltd) connected to a digital camera

(JVC colour video camera, TK-C1481BEG, Victor company of Japan Limited, Thailand) were used.

#### **4.3.10.2 Scanning Electron Microscopy (SEM)**

Scanning Electron Microscopy (SEM) is a microscopy technique that allows three dimensional imaging of surfaces at high resolution (Kaminskyj and Dahms, 2008). In this work the surface morphology of tablets was examined. Using double-sided tape, the tablets were mounted onto stubs and coated with gold using a Polaron SC7640 sputter gold coater manufactured by Quorum Technologies. The gold coating was generally 15 nm thick. The imaging was carried out in a high vacuum environment. Images were taken using a JEOL JSM5900 LV SEM (Japan), mounted with a tungsten filament with an acceleration voltage of 5–20 kV. Images were taken with the kind assistance of Bertrand Leze, the laboratory chief technician in School of Environmental Sciences at the University of East Anglia.

### **4.4 Results and Discussion**

The expression of antigens in plant has the potential to provide the candidate vaccine with a natural adjuvant: it is in fact hypothesised that the bio-encapsulation of the antigen within the plant cell could protect the antigen from GI degradation (Mason et al., 2002). Furthermore, the plant material containing the vaccine could be exploited to produce minimally processed, non-sterile pharmaceutical oral formulations, potentially cheap to be produced (Penney et al., 2011; Walmsley and Arntzen, 2000). In this Chapter, the processing of *Nicotiana benthamiana* leaves into a dry solid form, as well as the evaluation of the stability of HBcAg upon drying were evaluated. Furthermore the effect of the plant bio-encapsulation on the stability and release of HBcAg in simulated GI fluid was investigated. Finally, an oral formulation of plant vaccine, potentially stable in the GI environment was developed.

#### **4.4.1 Drying of *Nicotiana benthamiana* Leaves Expressing HBcAg**

The drying of *Nicotiana benthamiana* leaves expressing HBcAg using different drying methods was examined in this Paragraph. Initially the dehydration and the residual

moisture content were checked, and then the stability of the antigen upon drying was investigated.

#### 4.4.1.1 Drying of *Nicotiana benthamiana* Leaves: Dehydration and Residual Moisture Content

The first step toward the development of a plant-based oral candidate vaccine was to process the leaf material expressing the vaccine into a dry form that could be possibly ground into powder. For this purpose freeze-drying and oven-drying were chosen as desiccation techniques. Initially the drying time in oven was evaluated. Then the different drying methods were compared in terms of water content remained after the process, so to define the most suitable drying method in terms of residual moisture content.

In a preliminary study the water loss from *Nicotiana benthamiana* leaves was evaluated during the oven-drying process at 40 °C, over 6 days incubation. Figure 4.3 illustrates the weight loss accounted as water loss during this process as a function of time in days. This figure shows that rapid water loss seemed to have occurred in the first day and then it slowly levelled up till the third day. Only circa 0.2% water was further removed from the third to the sixth day.

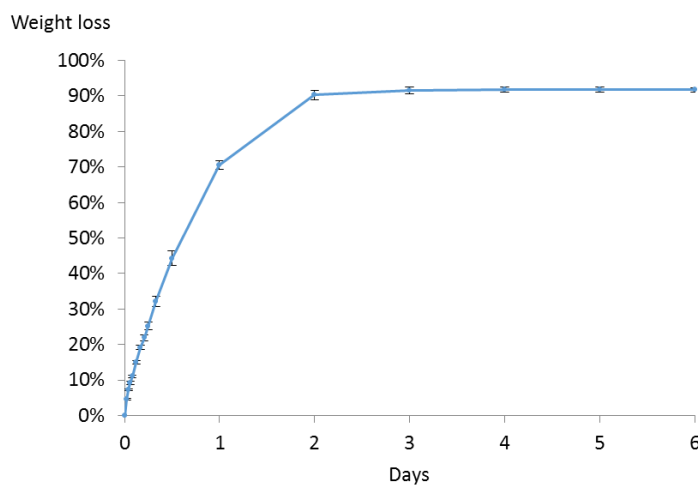


**Figure 4.3. In process Gravimetric Analysis (GA) of oven-dried leaves.**

Cut pieces of *Nicotiana benthamiana* leaves were oven-dried at 40 °C. During the drying the weight loss ( $n = 3$ ) was measured and then it was plotted against time (days). Error bars indicates SD.

Based on this result 3 to 4 days of oven-drying at 40 °C is expected to be sufficient to achieve maximum water removal under the experimental conditions used. This relatively short drying time might have been due to the small sized batch (3 g) used in this experiment. Nevertheless, it is reported that tomato fruit expressing VLPs and transgenic clover expressing an antigen had been previously oven-dried: the tomato fruit was dried for 2 weeks in a chemical hood with a final drying step in oven at 37 °C for 24 hours (Zhang et al., 2006); the transgenic clover was oven-dried in oven at 50 °C for 5 to 7 days (Lee et al., 2003). Based on the previous references and considering that batches larger than 3 g might be used in future experiments, it was thought that a longer drying period of 5 days at 40 °C might be needed and was therefore always carried out.

Then three different drying methods were compared in terms of residual moisture of the leaf material. For this purpose *Nicotiana benthamiana* leaves were either oven-dried at 40 °C for 5 days, oven-dried at 50 °C for 5 days, or freeze-dried. At the end the dried leaves were ground into powder using a blender (Waring, UK) and the residual moisture content of these leaf powders was measured by TGA. The results obtained are shown in Table 4.3.

**Table 4.3. A summary of the residual moisture content (%) of oven- and freeze-dried leaf material (mean  $\pm$  SD) as measured by TGA.**

| Drying method                | Oven-drying at 40 °C for 5 days | Oven-drying at 50 °C for 5 days | Freeze-drying   |
|------------------------------|---------------------------------|---------------------------------|-----------------|
| Moisture content (%) (n = 3) | 6.21 $\pm$ 0.69                 | 6.80 $\pm$ 0.42                 | 6.24 $\pm$ 1.59 |

The residual moisture content in the desiccated leaf samples was very similar for the three drying methods. As expected, the T-test revealed no significant difference between the values obtained. It can therefore be concluded that oven-drying at 40 °C, oven-drying at 50 °C and freeze-drying were comparable in terms of their drying efficiency. However another essential parameter in the processing of plant-expressed vaccines is the physio-chemical stability of the labile antigen upon drying. Therefore, the three drying protocols were compared in terms of stability of the HBcAg VLP next.

#### 4.4.1.2 Stability of HBcAg VLP upon Oven- and Freeze-drying of Leaves

The evaluation of the stability of proteins upon drying can be quite complex: in fact different processing conditions can influence both chemical and physical integrity of the active ingredient (Abdul-Fattah et al., 2007). HBcAg VLP is a multimeric protein, where the effectiveness as an immunogen is dependent both on the chemical stability of the primary structure and on the physical stability of the particle in terms of tertiary and quaternary structure. In Chapter 2 it was shown that both chemical and physical integrity could be investigated using molecular biology techniques. In this Paragraph, these techniques were used for the assessment of the stability of HBcAg within the leaf material upon oven- and freeze-drying of the leaves. Frozen disks containing HBcAg were used as a positive control: it was in fact demonstrated that HBcAg VLP could withstand at least three freeze-thawing cycles, without significant stability loss (Nath et al., 1992). Therefore HBcAg can be considered totally stable when frozen.

Frozen, freeze-dried or oven dried at 40 and 50 °C leaf disks containing HBcAg were homogenised with the extraction buffer and the crude extracts were used for Coomassie stained SDS-PAGE, Western blot and sucrose density gradient ultracentrifugation followed by analysis of the fractions by dot blot. The results are shown in Figure 4.4. In the Coomassie stained denatured gel (Figure 4.4 A), it was not possible to obtain clear information about HBcAg, as the bands due to the plant proteins did not allow selective recognition of HBcAg in all the lanes. However, it could be noticed that the intensity of the bands due to the plant proteins was the strongest for the frozen (lane 1), followed by the freeze-dried (lane 2), oven-dried at 40 °C (lane 3) and then oven-dried at 50 °C (lane 4) leaves. This suggests that generally the plant proteins were more stable when freeze-drying was used and less stable when the leaves were oven-dried, especially at the higher temperature. The Western blot (Figure 4.4 B) revealed that the 20 kDa immunoreactive band corresponding to HBcAg was present in all samples stored at the different conditions. Furthermore, major degradation products were not visible. This indicates that HBcAg was chemically stable within the plant material processed by freeze-drying (lane 2) and oven-drying (lanes 3 and 4). However, the HBcAg signal intensity seemed lower for the oven-dried samples, in particular for the one dried at higher temperature, suggesting moderate HBcAg loss during this process.

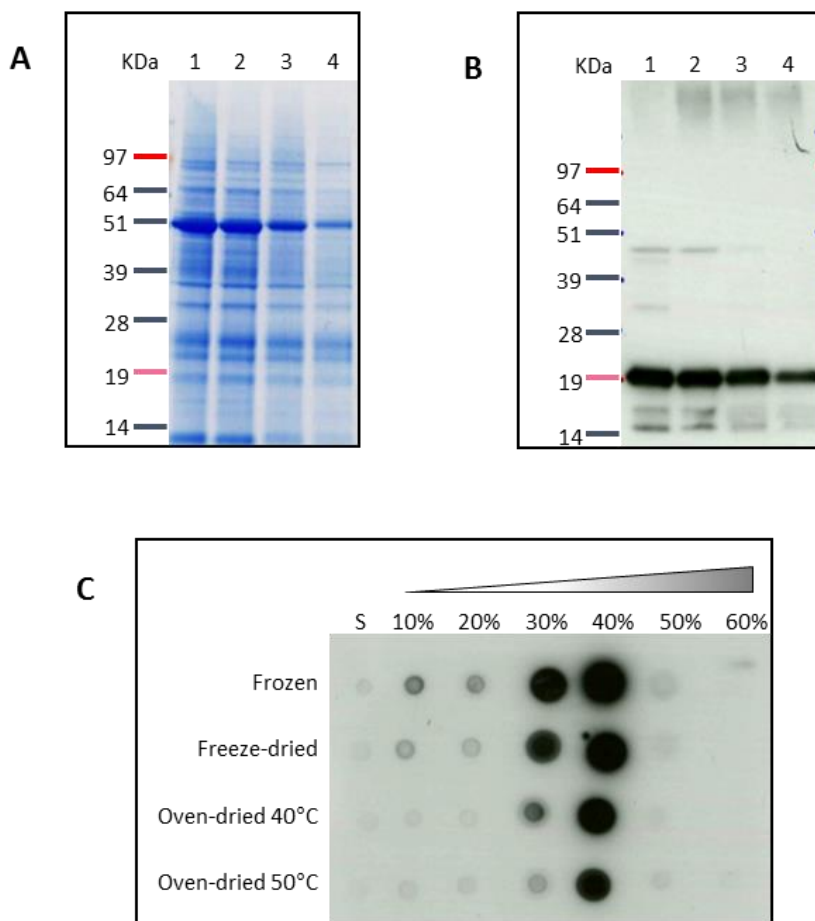


**Figure 4.4. Stability of unpurified plant-expressed HBcAg upon drying of leaves.**

Leaf disks from fresh leaves expressing HBcAg were stored either at -80 °C (control) or freeze-dried, oven-dried at 40 °C for 5 days, or oven-dried at 50°C for 5 days. Then the crude extract from the control and from the differently desiccated leaf material was analysed by Coomassie stained SDS-PAGE, Western blot and sucrose density gradient ultracentrifugation followed by dot blot. (A) illustrates the Coomassie stained SDS-PAGE and (B) the Western blot (monoclonal antibody); in both cases: frozen (lane 1), freeze-dried (lane 2), oven dried at 40°C for 5 days (lane 3), oven dried at 50 °C for 5 days (lane 4) leaf material. (C) shows the dot blot (monoclonal antibody) of the density gradient fractions. The different drying processes are indicated vertically, while approximate sucrose fraction concentrations are indicated horizontally. S = supernatant

Then the same crude extracts were separated by density gradient ultracentrifugation and seven fractions corresponding to different sucrose concentrations were collected. Analysis of these fractions by dot blot (Figure 4.4 C) shows that most of the anti-HBcAg immunoreactivity was present in fractions corresponding to 30 and 40% (w/v) sucrose both in the case of oven- and freeze-dried samples, as well as in the frozen control sample. Based on the fact that intact VLPs tend to sediment in the 30 and 40% (w/v) sucrose fractions, it can be suggested that the drying process did not interfere with the stability of

VLPs within the leaves. All together these results indicated that unpurified plant-expressed HBcAg was chemically and physically stable upon freeze- and oven-drying, even though a moderate HBcAg loss could be observed in the case of oven-drying. This latter observation was more pronounced at higher drying temperatures, i.e. greater loss occurred at 50 °C than at 40 °C.

For a more quantitative investigation, the stability of HBcAg within the leaves upon drying using different methods was also evaluated by sandwich ELISA. Figure 4.5 illustrates the results of the ELISA: in the case of the freeze-dried leaf material 87.7% of HBcAg could be recovered compared to the frozen sample; instead only 56.5% and 43.9% HBcAg could be retrieved after the oven-drying at 40 and 50 °C for 5 days, respectively. The values obtained with the oven-drying at different temperatures were not statistically different ( $p > 0.05$ - 2-tailed T-test). The sandwich ELISA developed in this research (Chapter 2) was specific for intact VLP, hence the quantified HBcAg in this assay should correspond to intact HBcAg only. The ELISA results therefore suggest that the most efficient drying method in terms of stability of the active ingredient was the freeze-drying, followed by oven-drying at 40 and 50 °C.

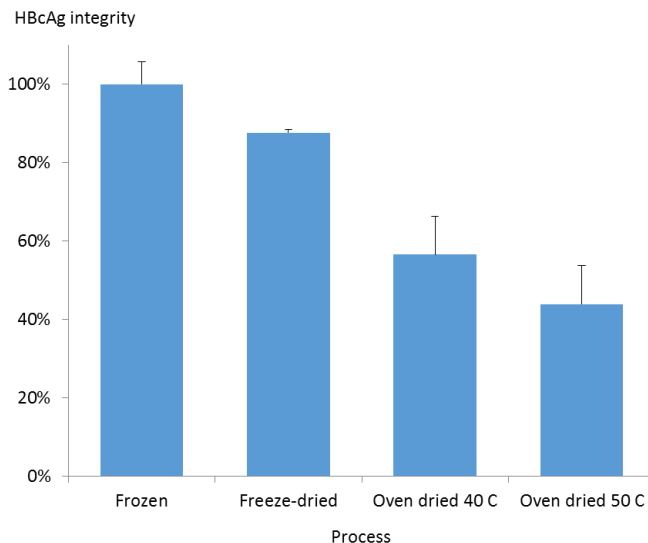


**Figure 4.5. Quantitative evaluation of HBcAg stability upon drying of leaves.**

Four 11 mm leaf disks were prepared from each of three leaves expressing HBcAg. Four sets each of three disks, pooled from different leaves, were either frozen, freeze-dried, oven-dried at 40 °C or oven-dried at 50 °C. After the drying, the samples were used for protein extraction and the content of HBcAg in these extracts was measured by sandwich ELISA ( $n = 3$ ). Error bars indicates SD. The frozen sample was used as a control and the stability of HBcAg is presented as a percentage ratio to the control.

In this Paragraph, it was evaluated whether plant material expressing HBcAg could be exploited to produce a dry material usable for further pharmaceutical processing. Drying of the leaf material was achieved by freeze-drying and oven-drying. The two methods did not show any relevant difference in residual moisture content of the dried leaves, suggesting similar efficiency in terms of desiccation. However, freeze-drying was proven to offer better protection of HBcAg than oven-drying did.

Nevertheless, the level of HBcAg VLP stability measured upon drying of leaves using the three drying methods is quite impressive. For comparison a similar study can be mentioned (Pniewski et al., 2011), where lettuce leaves containing Hepatitis B surface antigen (HBsAg) were freeze-dried and the stability of HBsAg after freeze-drying was evaluated. In that case most of the VLPs were lost upon drying, with less than 0.3% of the total HBsAg content being left in the lyophilised sample. A comparison of the HBsAg content in the freeze-dried sample to that present in the crude extract of fresh leaves (more than 50% VLP/total HBsAg content) suggests almost complete physical instability of the VLPs upon freeze-drying (Pniewski et al., 2011). In another similar study, the stability of two other HBsAg proteins upon freeze-drying of the leaves was also evaluated: in this case the

VLPs content ranged between 13.2 and 95.9%, depending on the expression group of transgenic plants used (Pniewski et al., 2012). In the light of these comparisons, the results obtained in the current research on HBcAg are remarkable: in fact after drying most HBcAg seemed to be still present as VLPs, as indicated by the fact that most of the antigen banded in the 30 and 40% (w/v) fractions of the density gradient. Furthermore, the sandwich ELISA specific for intact VLPs confirmed high levels of stability of the VLPs upon drying of leaves.

A final consideration can also be made by comparing the gravimetric analysis with the HBcAg quantification. The weight loss upon drying was > 90% of the original weight; in the HBcAg stability experiment it was found that 87.7% and 56.5% of the VLP were stable upon freeze-drying and upon oven-drying at 40 °C, respectively. This more than 10-fold reduction in the weight of leaf material, combined with the considerable stability of VLPs suggests that the concentration (w/w) of the antigen in the leaf sample could be increased up to 10-fold with drying. This antigen concentration in the leaf tissue could offer evident advantages in terms of dosing of the oral formulation. Furthermore, it could also be an advantage for storage of the leaf material for production scaling-up purposes.

#### 4.4.2 Delivery of Bio-encapsulated HBcAg in Simulated GI fluids

One of the main advantages of vaccine expression in plant is the potential oral administration of raw or minimally processed plant material containing the antigen, as the inclusion of the antigen within the plant cell wall holds the promise of protecting the vaccine against digestion in the gut (Walmsley and Arntzen, 2000). Despite the great potential and some initial encouraging results (Pelosi et al., 2012, 2011a), it is still unclear if, and to what extent, plant bio-encapsulation can effectively protect the antigen against digestion and then release the antigenic cargo in the target area of the intestine, where it can be absorbed. Therefore, the fate of plant bio-encapsulated HBcAg in SGF and SIF was investigated in this work, in order to assess the effect of the plant material on the stability and delivery of the antigen into the bio-relevant media.

Initially, samples of freeze-dried plant material containing HBcAg were incubated in SGF with or without pepsin and in SIF with or without pancreatin at 37 °C for 2 hours. The

supernatant was collected at the end of the two-hour incubation of the samples in the four different media. Furthermore, the residual solid plant material was precipitated by centrifugation and the pellet obtained was re-suspended in LDS  $\beta$ -mercaptoethanol. This protocol allowed a separate evaluation of release and stability aspects of the plant expressed antigen in different media. The supernatant of samples incubated in SGF and SIF without enzymes gave information about HBcAg release. Conversely, the HBcAg detected in the supernatant of samples incubated in SGF and SIF with enzymes was that remaining after both release and digestion, as for any given amount of HBcAg released into the medium, at least some digestion would have occurred. On the other hand, the analysis of the pellets could explain whether some unreleased antigens were segregated in the plant material and whether this possible segregation could allow antigen protection against digestion in the presence of enzymes. The four supernatants and the four re-suspended pellets, resulting from incubation in the SGF with and without pepsin, and SIF with and without pancreatin were run on SDS-PAGE gel. The gel was then used for anti-HBcAg Western blot immunodetection. This image, illustrated in Figure 4.6, shows that a 20kDa anti-HBcAg signal was present in the supernatant of samples incubated in SGF (lane 1) and SIF (lane 3) in absence of enzymes. However, upon incubation in SGF with pepsin (lane 2) and SIF with pancreatin (lane 4), HBcAg was undetectable. No protein was detected in lane 2, but a circa 16 to 17 kDa immunoreactive band could be visualised in SIF with pancreatin (lane 4). In the re-suspended pellets it was possible to observe similar results to those obtained with the supernatants (lanes 1 to 4). However, the bands did not look as sharp, due to the high concentration of plant material that impeded good electrophoretic migration and band resolution.

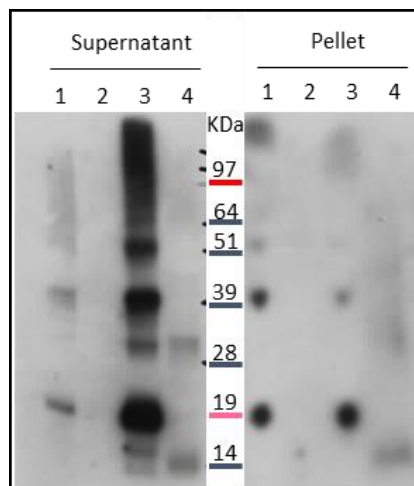


**Figure 4.6. Delivery of HBcAg from freeze-dried plant material into SGF and SIF.** Freeze-dried plant material containing HBcAg was incubated in different bio-relevant media. The fate of HBcAg upon incubation was evaluated by examination of the supernatant and of the re-suspended residual solid leaf material by anti-HBcAg Western blot (poyclonal antibody). The left part of the image shows the supernatants, while the right part relates to the re-suspended pellets. In both cases: SGF without pepsin (lane 1), SGF with pepsin (lane 2), SIF without pancreatin (lane 3) and SIF with pancreatin (lane 4).

Taken together these results suggest that HBcAg was not completely trapped in the plant cell and was partially released into the media during the two hours of incubation, as indicated by the detection of “soluble” HBcAg in the supernatant of samples incubated in SGF and SIF without enzymes. However, such premature release implies a lack of protection; in fact free antigens in the media were digested when pepsin and pancreatin were present in SGF and SIF, respectively. The pattern of digestion was the same as seen with purified HBcAg in Chapter 3, where HBcAg was digested to an undetectable product in SGF; while it was only digested to a shorter 17 kDa protein in SIF. Examination of the results obtained with the pellets revealed that part of the HBcAg remained entrapped in the plant material, as indicated by the fact that some HBcAg could be detected in the pellets of samples incubated in SGF and SIF without enzymes. However, the fact that even the HBcAg contained in the pellet was digested in presence of enzymes, suggests that although the leaf matrix retained some HBcAg, it could not prevent the enzymes from coming into contact with the antigen, determining partial or complete digestion in the case of incubation in SIF and SGF, respectively. Overall, these results indicate that freeze-dried unpurified HBcAg within the leaf material was partially released in the simulated gastric and intestinal media; moreover, part of the antigen remained in the solid residual leaf

material. However, this segregation in the leaf cellular compartments did not prevent the enzymatic degradation.

In another experiment, the leaf material containing HBcAg, previously frozen at – 80 °C, freeze-dried or oven-dried, was pre-incubated in SGF with pepsin at 37 °C for 2 hours. Then the solid leaf content was carefully removed and incubated in SIF with pancreatin for a further 4 hours. Aliquots of the supernatant during the SIF incubation were drawn and the final solid content was centrifuged forming pellets, which were re-suspended. This *in vitro* model of incubation in SGF and subsequently in SIF mimics the gastric transit and the passage to the intestinal fluids. The sampling from SIF incubation medium would be indicative of the antigen release in target areas of the gut, i.e. small intestine, where absorption is expected to take place. The supernatant aliquots and the pellets were then examined by Western blot. Moreover the influence of processing on the delivery of antigen in the bio-relevant media simulating both gastric and intestinal conditions could be also evaluated. As a control, frozen leaf material containing HBcAg was incubated in SIF with pancreatin, without pre-incubation in SGF. This enabled the examination of the release in the simulated small intestinal environment, devoid from the parameter of the gastric instability.

The image of the Western blot, shown in Figure 4.7, revealed that HBcAg was always undetectable in the supernatant of SIF incubated with frozen, freeze-dried or oven dried samples (lanes 1 to 3 of each sample) when the leaf material was pre-incubated in SGF. However, a circa 16 to 17 kDa version of HBcAg was present in the re-suspended pellets of frozen, freeze-dried and oven dried samples (lane 4 of each sample). The intensity of this band seemed higher for the frozen, followed by the oven-dried and then the freeze-dried leaf material. The result obtained in the control, where the plant material was not pre-incubated in SGF, revealed that HBcAg was present in the supernatant as a 17 kDa band (control lanes 1 to 3). Furthermore a strong HBcAg signal was also present in the pellet (control lane 4).

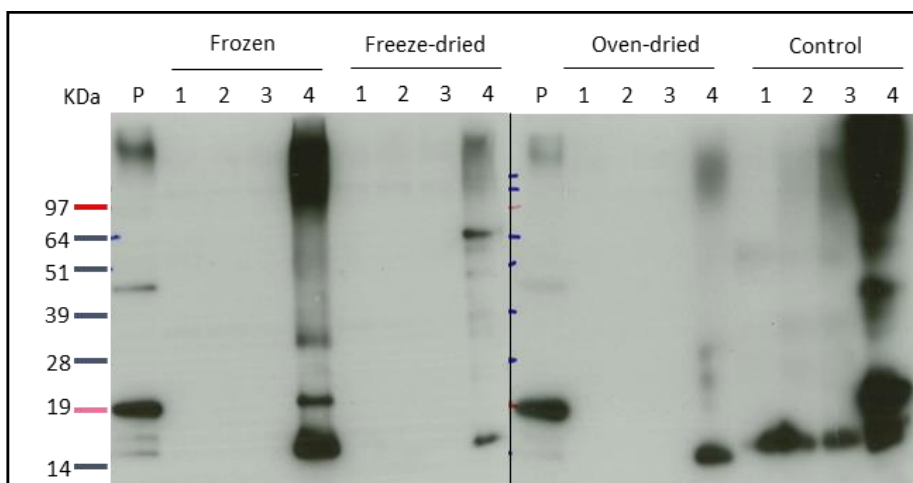


**Figure 4.7. Delivery of HBcAg from processed plant material upon incubation in GI simulating media.**

Frozen, freeze-dried and oven-dried leaf disks containing HBcAg were pre-incubated in SGF with pepsin for 2 hours and were subsequently incubated in SIF with pancreatin for further 2 hours. Aliquots from the supernatant in SIF were drawn after 30 minutes (lane 1), 1 hour (lane 2) and 2 hours (lane 3) for examination by anti-HBcAg Western blot (monoclonal antibody). The residual leaf solid content was pelleted and then re-suspended at the end of the incubation (lane 4). As a control, frozen leaf disks were incubated in SIF, without a pre-incubation in SGF. P = positive control of HBcAg in PBS.

The comparison of the control sample with all the other samples that were pre-incubated in SGF indicates that the pre-incubation resulted in premature release and subsequent instability of HBcAg and hence determined the apparent absence of HBcAg in SIF. Furthermore the re-suspended solid leaf pellets contained only small amount of HBcAg. In contrast, a considerable amount of HBcAg was released in SIF of the control sample that was not pre-incubated in SGF and was also present in the re-suspended pellet. These results taken together suggest that the up-stream passage of leaf material containing the antigen in the gastric environment could determine HBcAg degradation. In Chapter 3, it was shown that HBcAg was highly unstable in SGF, and the results of this study suggest that the entrapment of HBcAg in the plant material could not protect this antigen that was intrinsically unstable in SGF.

A similar experimental design was carried out for ELISA quantification. Frozen, freeze-dried and oven-dried leaf disks were pre-incubated in SGF with pepsin for 2 hours and then the leaf material was incubated in SIF without pancreatin for a further 4 hours. Samples were drawn during the SIF incubation. At the end of incubation period, the

residual leaf material (pellet) was re-suspended in the extraction buffer, without adding reducing or denaturing agent and without boiling the sample. Furthermore another batch of frozen, freeze-dried and oven-dried disks, made from the same leaves as the incubation samples, was used for protein extraction and total HBcAg quantification. This was done in order to compare the residual amount of HBcAg after SGF-SIF incubation, with the total amount of HBcAg present in the leaf tissue. At the end of the *in vitro* assay, the HBcAg content in the frozen, freeze-dried and oven-dried samples collected during the SIF incubation as well as the re-suspended pellets was measured by sandwich ELISA. Two differences in the assay design can be noticed as compared to the last experiment. First, SIF without pancreatin was used, as pancreatin could have degraded the antibodies used in the ELISA assay and it was not well known whether the short version of HBcAg resulting from enzymatic digestion could be correctly measured by the ELISA assay. Second, the re-suspended pellets from the residual leaf material was kept in the native, undenatured state, because sandwich ELISA is specific for native HBcAg VLP preparation, as shown in Chapter 2 (page 68-70) .

The ELISA suggested that HBcAg was undetectable in the SIF supernatant of frozen, freeze-dried and oven-dried leaf samples pre-incubated in SGF. However, a weak HBcAg immunoreactivity could be measured only in the leaf material (pellet), re-suspended after the incubation in SIF. The comparison of the total HBcAg content in untreated leaf material with the residual amount of HBcAg contained in the pellets of disk pre-incubated in SGF and then in SIF, revealed that circa 0.2% of the total HBcAg could be recovered in case of oven-drying and less than 0.05% (practically undetectable) in frozen and freeze-dried leaf material. In this experiment a precise quantification would have been difficult: in fact, even though the re-suspended samples were used undiluted for the ELISA assay, only a weak immunoreactivity, close to that of the background, could be measured. Essentially, HBcAg was digested during the pre-incubation of the leaf in SGF, regardless of the drying method.

Bio-encapsulated plant-vaccine systems designed for oral delivery should ideally protect the vaccine in the stomach and release it in the small intestine, where absorption takes place. Overall, the three assays carried out in this Paragraph consistently suggest that the leaf tissue does not constitute a perfect barrier for HBcAg from the external bio-relevant

---

media in which the material is incubated. Generally, HBcAg showed to be partially released from the plant material where it was expressed and once released the antigen was completely exposed to the medium, resulting in complete digestion of HBcAg in SGF and partial digestion in SIF. However, despite this undesired prompt release of the antigen from the plant material, if the residual HBcAg entrapped in the plant cell compartments could have remained protected from the harsh gastric environment, it could be possible that this small amount of HBcAg could be slowly released from the leaf tissue in distal segments of the upper GI. Nevertheless, the Western assays (Figure 4.6 and Figure 4.7) revealed that the HBcAg entrapped in the leaf material had been digested upon incubation just as the HBcAg already released. This suggests that the digestive enzymes could get into and attack the HBcAg entrapped inside the leaf tissue. Moreover, the use of differently processed plant material, i.e. frozen, freeze-dried or oven-dried, did not result in substantial differences. In conclusion, it can be hypothesised that the bio-encapsulation of HBcAg in *Nicotiana benthamiana* leaves would not be able to efficiently protect such a labile antigen from enzymatic degradation.

Interestingly, it was recently suggested that upon oral administration of an antigen expressed in the leaves of *Nicotiana benthamiana* in mice and sheep, the antigen was mainly released in the stomach. In contrast, it was found that the expression of the same antigen in the roots of the plant resulted in a slower release of the antigen in the intestine (Pelosi et al., 2012, 2011a). Therefore, it was hypothesised that in case of labile antigens the expression in leaf might have not been the most-suitable approach (Pelosi et al., 2011a), as prompt release of the antigen in stomach could have caused premature degradation. Indeed, data from the current research suggest that the bio-encapsulation of HBcAg, which is a gastric-labile antigen, did not prevent its release in the simulated gastric media and did not allow protection of the antigen. It is possible to speculate, as suggested by Pelosi et al. (2011a), that the expression of gastric-labile antigens in more fibrous plant parts, such as roots, could allow better gastric protection upon oral administration of the plant material. However, doubts remain about whether a tightly protected antigen within fibrous plant material could be released in the small intestine at all: if premature release negates any benefit of antigen incorporation within the plant, too efficient entrapment of the antigen within plant material could imply that the antigen does not get released at all in the gut. Therefore a balance between protection and release should be established on a case

by case approach, finely tuning the choice of the plant material to the antigen used (Pelosi et al., 2012). Nevertheless, it appears somewhat implausible that naturally occurring plant parts could act as an impermeable coat that protects a candidate vaccine till a certain area of the gut (i.e. stomach or upper small intestine), and then allow sudden and complete release of the same antigen in distal absorption areas, therefore enabling some sort of targeted delivery.

In this study it was also evaluated whether differently processed plant material could show different outcomes in terms of antigen protection against harsh simulated GI media. The fact that HBcAg was mainly either prematurely released or digested, in all cases, did not allow an optimal comparison. However examination of the residual pellets based on both the Western blot (Figure 4.7) and the ELISA suggests that oven-dried plant material seemed to better protect the antigen from the GI media than freeze-dried plant material. This agrees with previously established results, where air-dried tomato fruit expressing Norwalk virus VLP could induce higher antibodies production than freeze-dried fruit upon oral administration in mice (Zhang et al., 2006). It was suggested that the air-drying could have better preserved the fruit cellular structure, therefore enabling greater protection of the antigen. This could explain the slightly higher residual content of HBcAg in the oven-dried leaf material which remained after the incubation in simulated GI media, compared to the content in freeze-dried leaf material. Nevertheless, the relative amount of this residual HBcAg in the plant tissue was minimal in both cases, suggesting that the use of processed *Nicotiana benthamiana* leaves for oral protection of HBcAg would be inconvenient regardless of the drying process employed.

#### **4.4.3 Development of an HBcAg VLP Enteric-coated Tablet Formulation**

Previous findings of this work showed that HBcAg was highly unstable at gastric pH and was digested in bio-relevant gastric media containing pepsin. This strongly suggested that the harsh gastric environment would provide a major limitation to the oral delivery of HBcAg. Furthermore, it was also found that bio-encapsulation in leaf tissue did not protect the antigen against gastric degradation. Therefore, it was decided to develop a gastro-protected formulation that could shelter the sensitive antigen from the highly denaturing and digestive environment of the stomach. In the following Paragraph the development of

a plant-based film coated tablet formulation of HBcAg VLP and the testing of such a formulation are described.

#### 4.4.3.1 Preparation of Tablets

One of the main aims of this work was to exploit the expression of HBcAg in plant to produce an oral formulation of the VLP that could protect the antigen from the harsh GI environment. The expression in plants could be used as a simple approach for producing reasonably large quantities of minimally processed plant material formulations containing the antigen. Plant-expressed HBcAg VLP was demonstrated to be highly stable upon freeze-drying of the leaves. It was decided to use such processed plant material as the raw active material in the development of the tablet formulation, rather than to extract the antigen from the plant and then to formulate it directly. The primary function of the leaf tissue in this approach was to protect the VLP upon drying. Moreover, the homogeneous distribution of a very low dose active in oral formulations can be difficult to achieve: a suggested dose of HBcAg could be in the range of tens of micrograms and an easily handleable tablet will be at least 100 mg in weight, giving an active content of less than 0.1%. The direct use of the relatively bulky freeze-dried plant material, where HBcAg is already naturally distributed, could help to reduce these homogeneity issues.

*Nicotiana benthamiana* leaves expressing HBcAg were freeze-dried and ground into powder. Then a blend of the leaf powder with other excipients (the formulation is described above in Paragraph 4.3.4) was compressed into tablets. Figure 4.8 shows light microscopy images of the intact tablets (Figure 4.8 A) and a cross-section of a tablet (Figure 4.8 B).

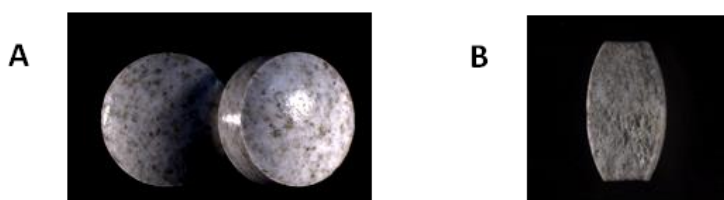


**Figure 4.8. Images of uncoated tablets.**

Light microscopy images of uncoated tablets (x 0.63 magnification). (A) illustrates an image of two intact uncoated tablets. (B) shows an image of a section of an uncoated tablet.

Tablets were characterised in terms of weight uniformity, hardness and disintegration time: the data are shown in Table 4.4. The weight uniformity and the disintegration time values were well within the limits of British Pharmacopeia (2012). Overall, the blend of powder containing the freeze-dried leaf material could be efficiently used for direct compression of tablets. Neither capping nor lamination occurred during the process and the physical characteristics of the tablets were within typical ranges.

**Table 4.4. Physical characterisation data for plant-based tablets (mean  $\pm$  SD)**

| Parameter | Weight uniformity<br>(mg, n = 20) | Hardness<br>(kp, n = 3) | Disintegration time<br>(minutes, n = 3) |
|-----------|-----------------------------------|-------------------------|---|
|           | 164.8 $\pm$ 4.47                  | 8.6 $\pm$ 0.73          | 4.26 $\pm$ 0.08                         |

#### 4.4.3.2 Enteric Coating of Tablets

It was previously suggested that the freeze-dried leaf tissue containing HBcAg, would not be able to protect the antigen against the harsh gastric condition. For this reason it was decided that the tablets containing the VLP, naturally bio-encapsulated in the freeze-dried plant material, required to be coated with a gastro-resistant polymer. Eudragit L 100, a copolymer of methacrylic acid and methyl methacrylate, is a commonly used excipient for the formulation of gastro-resistant coating for tablets. This polymer is rich in carboxylic groups, which are unionised at acidic pH, making the polymer water-insoluble. However, neutralization of the pH induces deprotonation of the carboxylic acid groups and formation of carboxylate anions. The formation of these carboxylate salts at neutral pH renders the polymer water-soluble. This pH-dependent solubility of Eudragit L 100 can be exploited for preparation of enteric coated oral formulations, which are soluble only at  $\geq$  pH 6 (Eudragit, 2011) and thus for targeting the delivery to a specific part of the gut. Film coats of Eudragit L 100 are impermeable at the gastric pH and dissolve in the small intestine, where the pH ranges from pH 5.5 to pH 7.5 (McConnell et al., 2008b).

The preparation of the coating dispersion was performed according to the manufacturer's guidelines. Briefly, the Eudragit L 100 powder was mixed with water, then small aliquots of NH<sub>3</sub> were added in order to partially neutralise the carboxylic groups of the polymer.

The mixture was stirred for 2 hours to enable the re-dispersion of Eudragit L 100 into a nano-size latex-like form. Then triethyl acetate (TEC), a plasticiser, was added and the mixture was stirred for further 1 hour and a half. Finally, PlasACRYLT20, an anti-tacking agent, was included in order to reduce the stickiness of films in the final product. This re-dispersion method was named protocol 1. The resulting coating dispersion was used to coat the tablets made of the freeze-dried leaf tissue expressing HBcAg. The coating was performed up to a final 15% total weight gain (TWG). During the coating process, some dust developed in the coater chamber. After the coating, optical microscopy and SEM imaging were performed to examine the film formation: Figure 4.9 shows images of the coated tablets and of a tablet surface. The optical microscopy image shows the section of a coated tablet (Figure 4.9 A). SEM images of the surface revealed the presence of evident cracking on the surface of the coating (Figure 4.9 B and C). Ultimately the deposition of the polymer on the tablets seemed to have formed a brittle and cracked coating rather than a homogeneous and flexible film as expected.

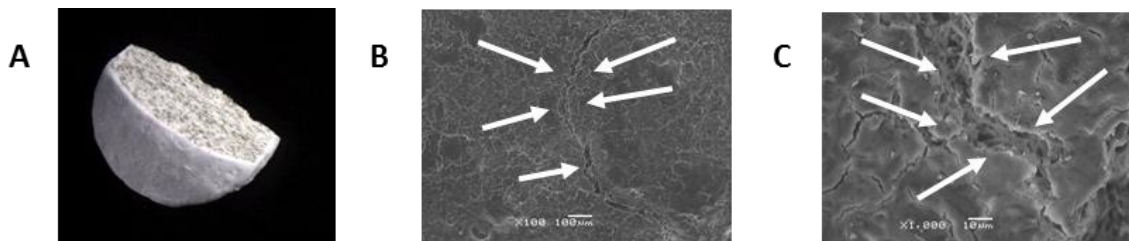


**Figure 4.9. Imaging of tablets coated using the short re-dispersion protocol.**  
Eudragit L 100 dispersions were prepared according to protocol 1 and were used to coat tablets made of freeze-dried material expressing HBcAg VLP. The surface of the coated tablets was examined by microscopy. (A) illustrates an optical microscopy image of a section of a coated tablet (0.63x). (B) and (C) show SEM images of the surface of another coated tablet (100 and 1000x, respectively). White arrows indicate the major sites of cracking.

Pseudo-latex formation and plasticisation are considered essential for the formation of a flexible film (Eudragit, 2011). In this case the poor film formation, indicated by the presence of a dusty and cracked coating, suggested that the Eudragit L 100 re-dispersion into a latex-like form had not been efficient and that the plasticisation was not effective. Thus, the re-dispersion protocol was modified (protocol 2), increasing the stirring time post-addition of NH<sub>3</sub> and TEC from circa 2 hours to overnight. This was done to ensure enough time for complete re-dispersion of the pseudo-latex and to allow homogeneous

distribution of the plasticiser within the supposedly nano-size particles of the polymer latex. The resulting dispersion of the polymer was then used to coat another batch of tablets up to 14% TWG. Figure 4.10 illustrates different images of the coating. An optical microscopy image of a section of a coated tablet (Figure 4.10 A) shows the formation of a more transparent film than the one produced using the coating protocol 1 (Figure 4.9 A), hence suggesting better re-dispersion of the polymer particles into a colloidal state. A closer examination of the coating in the SEM images revealed the presence of a smooth surface, without evident cracking (Figure 4.10 B and C). It can be suggested that the longer time allowed for pseudo-latex dispersion and for plasticisation in protocol 2 favoured the formation of a much more flexible and plasticised film coating, than when protocol 1 was used.

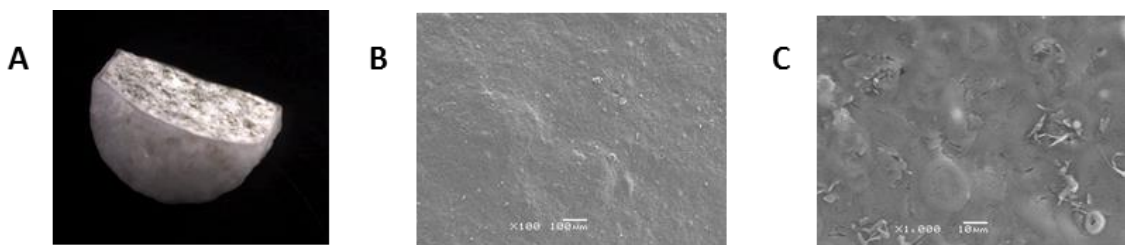


**Figure 4.10. Imaging of tablets coated using the long re-dispersion protocol.**

Eudragit L 100 dispersions were prepared according to protocol 2 and were used to coat tablets made of freeze-dried material expressing HBcAg VLP. The surface of the coated tablets was examined by microscopy. (A) illustrates an optical microscopy image of a section of a coated tablet (0.63x). (B) and (C) show SEM images of the surface of another coated tablet (100 and 1000x, respectively). The surface appears free from crackings.

The functionality of the film obtained with both protocols was investigated by assessing the gastro-resistance of such formulations in dissolution tests. To test the formulation, freshly prepared SGF with pepsin was used as the dissolution medium for the first 2 hours and was then replaced by freshly prepared SIF without pancreatin for an additional 6 hours. Three tablets coated using the re-dispersion protocol 1 formed evident cracking and the tablet cores swelled upon imbibition of the SGF with pepsin medium. This dissolution test was therefore interrupted, because it was evident that the coating was permeable to the acidic media and allowed penetration of SGF inside the tablet core. In conclusion, this coating formula failed to provide protection to the formulation against the gastric conditions. The lack of functionality of this coating matches with the brittle and cracked

appearance seen in the previous images (Figure 4.9). It is therefore possible to hypothesise that the poor film formation and the already present cracks on the dry coating favoured the penetration of medium and swelling of the tablets, resulting in further cracking of the coating.

The tablets coated using protocol 2 were also evaluated by dissolution test. Each of three coated tablets were added to one vessel containing SGF with pepsin and incubated for 2 hours at 37 °C. During this phase the coating appeared intact and the tablets did not show any sign of swelling. Then the tablets were drained using a sieve and carefully swapped into SIF without pancreatin. Aliquots were drawn after 30 minutes, 1, 2, 4 and 6 hours during the incubation in SIF without pancreatin. In parallel three tablets from the same batch were also incubated in three vessels containing SIF without pancreatin, without previous incubation in SGF with pepsin. These tablets were used as a control to calculate the total HBcAg content within the dosage form, assuming that complete stability would be observed in SIF without pancreatin, due to almost neutral pH and to the absence of enzymes. For this purpose an aliquot from each vessel was drawn after 6 hours incubation. At the end of the dissolution test the content of HBcAg in all the aliquots collected was measured by sandwich and direct ELISA.

Figure 4.11 illustrates the result from the dissolution test: HBcAg release is presented as percentage ratio from the total HBcAg content measured for the control tablets. During the first 2 hours incubation in SGF with pepsin samples were not collected, because any antigen released would have been undetectable, due to the instability of the antigen in SGF with pepsin, as demonstrated in Paragraph 4.4.2. Quantification by direct ELISA revealed that most of HBcAg was released within the first hour of incubation in SIF without pancreatin and then the presence of HBcAg in the media seemed to reach a plateau, corresponding to circa 90% release. A maximum of 91.4% ( $\pm 4.3\%$ ) HBcAg release was measured after 6 hours of total incubation (corresponding to 4 hours in SIF without pancreatin). Moreover, quantification by sandwich ELISA showed a similar release profile: 87.1% ( $\pm 9.6\%$ ) HBcAg VLPs were released after 6 hours of total incubation. The difference in results between the maximum release obtained with the two methods is not statistically different ( $p > 0.05$ - 2-tailed T-test) and might be related to the different

specificity of the two assays: the sandwich ELISA detects only native VLP, while the direct ELISA measures the native as well as the denatured forms of HBcAg.

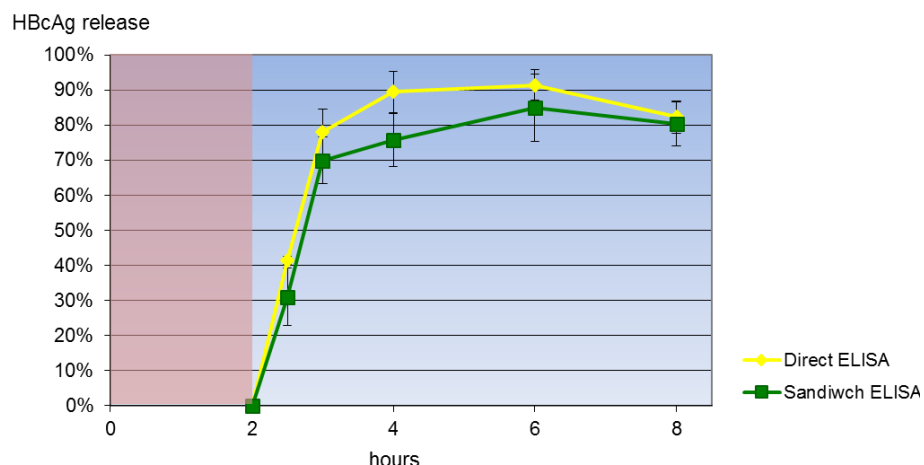


**Figure 4.11. Gastro-resistance of the enteric coated formulation.**

Tablets were coated with a dispersion of Eudragit L 100 up to 14% TWG. The release of HBcAg from tablets ( $n = 3$ ) was tested by pre-incubating the formulations for 2 hours in SGF with pepsin (red), followed by a further 6 hours in SIF without pancreatin (blue). Samples from SIF without pancreatin were collected at different times. The total HBcAg content within the formulation was evaluated by a control dissolution test of tablets ( $n = 3$ ) from the same batch in SIF without pancreatin. Quantification was carried out by sandwich and direct ELISA. Error bars indicates SD. The release is presented as percentage ratio between the measured HBcAg and total HBcAg content in the formulation.

The fact that HBcAg could be detected by sandwich ELISA suggests that the HBcAg was present as intact VLP. It was shown in Chapter 2 that the sandwich ELISA used in this work is specific for undenatured HBcAg VLPs. The total content of HBcAg VLP for the control tablet incubated only in SIF without pancreatin was 24.4 ( $\pm 2.3$ )  $\mu$ g per tablet ( $n = 3$ ). Although comparisons between two different antigens are difficult to make, it can however be mentioned that the current Hepatitis B vaccine, based on Hepatitis B surface antigen (HBsAg) is given by injection in 5 to 20  $\mu$ g doses, depending on the formulation (Center for Disease Control and Prevention (CDC), 2012). Hence, the HBcAg content in the tablets produced here is in the same range as that used in current Hepatitis B injectable vaccines, containing HBsAg.

These results taken together demonstrate that the enteric coated formulation was effective in protecting the particulate antigen against the simulated gastric media and allowing the release of HBcAg VLPs in SIF. It is worth remembering that this assay is not a typical dissolution test, as the quantified release of HBcAg is not resulting only from the

dissolution of the formulation, but also from the possible digestion and denaturation of HBcAg during the pre-incubation in SGF. Therefore, it is likely that while circa 90% HBcAg was protected within the enteric formulation, the remaining 10% was degraded by the pre-incubation in SGF. Overall, taking into account the complexity of the HBcAg macromolecular structure and the extremely high intrinsic instability of HBcAg VLP in SGF (Chapter 2), the level of protection obtained with this enteric coated formulation was remarkable.

#### 4.4.4 Contextualisation and Relevance of the Findings

The overall aim of this Chapter was to define how and in which way the expression of a candidate vaccine in plant could be an advantage for the development of an oral formulation. One of the presumed advantages of the expression of antigen vaccines in plant is the potential protection against the harsh GI environment offered by the plant bio-encapsulation (Walmsley and Arntzen, 2000). In contrast, the results from this work suggest that the expression of HBcAg in *Nicotiana benthamiana* leaves neither protect HBcAg VLPs, nor prevent their release upon incubation in simulated GI media. However, these findings cannot be generalised, as the use of more stable antigens or the use of different plant parts for the antigen expression could generate different results, as suggested by Pelosi et al. (2011a, 2012). In that case, it was found that upon oral administration of *Nicotiana benthamiana* leaves containing a candidate antigen in animal models the antigens were prematurely released in the stomach, compared to other plant parts that allowed slower release and protection in the gut (Pelosi et al., 2012, 2011a). However, from a drug delivery point of view, it appears improbable that a plant tissue, able to tightly seal the antigen within its cellular compartments during the gastric transit and then promptly release it in the target area to be absorbed, could be found.

Once the instability of the HBcAg within plant material to the gastric media was established, a tablet formulation was produced using the plant material as the source of the antigen, i.e. without any further antigen purification. The formulation was coated, in order to protect the labile antigen from gastric degradation. This formulation was shown to be functional in protecting HBcAg against SGF incubation, yet allowed the release of HBcAg in SIF. Given the fact that dissolution tests are usually predictive of the *in vivo* behaviour,

it is possible to hypothesise that such a formulation would be able to protect HBcAg from the harsh gastric environment and then release the antigen in the small intestine, where the absorption could take place.

Although the leaf material did not directly confer gastric-protection to the antigen, the use of freeze-dried plant material expressing the candidate vaccine did however offer other advantages. First, the minimal processing, involving mainly the freeze-drying step of the raw plant material expressing the antigen, is potentially simple and extremely economical. Furthermore, the leaf tissue acted as a sort of natural lyoprotectant, conferring stabilisation to HBcAg VLP upon freeze-drying. This eliminated a series of technological hurdles generally encountered in the drying of many purified labile proteins (Abdul-Fattah et al., 2007). Finally, the reproducibility in yield of recombinant protein within different crude extracts, typical of this expression system in plant (Sainsbury and Lomonossoff, 2008), indicate that the protein is uniformly dispersed within the leaf tissue. Moreover the homogeneity of HBcAg content within tablets, measured in the dissolution test in this study, suggests even distribution also in the final formulation. Hence the plant material could act as a sort of natural bulking excipient, reducing the dose homogeneity issue, typical of low dose active oral formulations.

Despite the aforementioned advantages of preparing oral vaccines formulations from minimally processed plant material, a few issues still remain to be solved, including the standardisation of the dose and dose homogeneity within large batches of plant material, as well as the study of the long-term stability of the dry formulations (Pelosi et al., 2011b; Tiwari et al., 2009).

The main *in vitro* models used to assess HBcAg VLP stability in this Chapter and in Chapter 3 are the standard British Pharmacopeia models of gastric and intestinal fluids. These models are standard receipes commonly used to mimick the far more complex GI fluids composition. In the last few years, state of art models, that are supposed to better simulate the gastric (i.e. model gut-Institute of Food Research Norwich) and small intestinal (i.e. TNO Pharma, Netherlands) physiology, have been developed. However, these models are very costly and have very low throughout. Moreover it is questionable whether such standardised *in vitro* protocols could be ever able to closely mimick the

extremely variable GI environment (McConnell et al., 2008b). On this basis it can be proposed that the biological relevance of the current studies about the GI stability of plant-expressed HBcAg VLP could be only enhanced with *ex vivo* studies using animal GI fluids or even better with *in vivo* experiments.

#### 4.5 Conclusions

In this Chapter the expression of HBcAg in plants was exploited for the development of stable dry oral formulations. Firstly, it was shown that *Nicotiana benthamiana* leaves expressing HBcAg can be dried using different methods, including freeze-drying and oven drying at different temperatures. The different drying methods showed the same drying efficiency in terms of residual moisture content. Moreover, HBcAg VLP showed to be physically and chemically stable upon freeze- and oven-drying, using qualitative techniques. A more quantitative investigation showed that better preservation of HBcAg VLP could be achieved by freeze-drying, followed by oven-drying at 40 °C and then by oven-drying at 50 °C.

Then it was examined whether the natural bio-encapsulation of HBcAg in the leaf material could offer protection against digestion in simulated GI media. The results obtained strongly suggest that the *Nicotiana benthamiana* leaves did not protect HBcAg against the degradation in SGF and SIF. Furthermore the different processing of the plant material, either freeze- or oven-dried, did not seem to improve the protection of the antigen from the external media. Finally, given the fact that freeze-drying of the leaves expressing HBcAg favoured higher antigen stability compared to oven-drying, freeze-dried leaves were used for the production of a prototype “green” tablet formulation. Tablets could be prepared by direct compression of a blend of freeze-dried leaf expressing the VLP, mixed with other excipient for compression. These tablets were characterised in terms of weight uniformity, hardness and disintegration time, showing values typical of standard immediate release dosage forms. Then the tablets were coated using Eudragit L 100, which is a polymer used for the formulation of gastro-resistant dosage form. Optimisation of the latex-like re-dispersion time and the plasticisation time enabled the formation of a flexible and homogeneous film coating that proved to be functional in protecting the formulation in SGF in presence of pepsin. The coated tablets were tested for 2 hours in SGF with pepsin

and then for further 6 hours in SIF with pancreatin. Approximately 90% of the total HBcAg VLP present in the formulation could be released undigested and undenatured within the first 4 hours of incubation in SIF.

Overall the key message of this Chapter is that even though *Nicotiana benthamiana* leaves expressing HBcAg did not offer protection against the degradation in simulated GI fluids, the expression in plant could overcome a series of technological obstacles towards the formulation of an effective oral dosage form. Firstly, the challenge of drying a pharmaceutical protein could be simply overcome by directly drying the leaf material expressing HBcAg. In addition, the expression in plants can solve the dose homogeneity issue and this plant tissue could function as natural tablet filler. Finally, a potentially cheap and simple prototype oral formulation of HBcAg VLP that is able to protect the antigen from the gastric degradation was produced, exploiting the expression of the antigen in plant.

## 5 Formulation Development of Purified HBcAg VLPs Potentially Usable for Oral Delivery

### 5.1 Introduction

In Chapter 3 it was shown that purified HBcAg VLP could not withstand incubation in simulated gastric fluids. However, HBcAg maintained its particulate structure and immunogenicity upon incubation in simulated and animal intestinal fluids. Chapter 4 showed that the natural bio-encapsulation of HBcAg in the leaves of *Nicotiana benthamiana* could not protect the antigen from gastric degradation, but that the plant material could be exploited to develop a “green” tablet formulation. This solid oral dosage form was then film coated with a pH-dependent polymer. The coated tablets demonstrated gastro-protective properties, enabling the protection of HBcAg in simulated gastric conditions and the release of the antigen in simulated intestinal media. In this Chapter, the development of a dry solid dosage form of purified HBcAg as an alternative to the “green” formulation is described.

The drying of pharmaceutical proteins is considered particularly challenging, due to their complex macromolecular structure, which can render them susceptible to chemical and more frequently physical instability upon drying. Typical drying methods for proteins are based on solvent evaporation or sublimation, with freeze-drying and spray drying being the most widely used among other techniques (Abdul-Fattah et al., 2007). However, only liquid sterile formulations of VLP-based vaccines for parenteral use are commercially produced (Vicente et al., 2011). Therefore to date, extremely limited literature on the formulation of purified VLPs in solid dosage forms is available. Nevertheless, only very recently, the growing interest in the new generation of vaccines is pushing research towards the development of stable dry formulations for parenteral and non-parenteral use (Lang et al., 2009; Shenoy and Robinson, 2009; Watts and Smith, 2011). Interestingly, Chen et al. (2010) showed that dry formulations of Hepatitis B surface antigen (HBsAg) could be produced by spray drying; the formulations produced showed good in-process and long-term stability. Moreover, they elicited comparable antibody production to that of a commercially available liquid HBsAg formulation upon reconstitution of the powder and intra-peritoneal injection in mice. Furthermore, in another study it was also shown that the Norwalk VLPs could be formulated into spray dried forms for intranasal delivery: sucrose

gradient sedimentation studies suggested that VLPs were fairly stable upon spray drying. Immunisation studies in mice proved that the spray dried formulation was at least as potent as an alternative liquid formulation (Velasquez et al., 2011).

In this Chapter, different approaches for the drying of purified HBcAg VLPs, including desiccation, oven drying, spray drying, spray-freeze-drying and freeze-drying were studied. The final aim of this study was producing a solid formulation potentially usable for oral delivery.

### **5.1.1 Granulation**

The process of granulation consists of producing granules, generally usable for the compression of tablets. In wet granulation, powders are processed into multiparticulate granules by mixing the dry powder with a binder (or granulation) solution. A wet mass is created by mixing the dry components with the binder solution and once the granules are formed, the solvent is removed by drying, generally in an oven (Summers and Aulton, 2007).

In the current study, preliminary trials of producing granules containing HBcAg VLP was carried out, drying the granules by desiccation. The desiccation process is a very low cost drying process; however, the desiccation of biopharmaceuticals carries a higher risk of denaturation of the active compared to the drying obtained by spray drying and freeze-drying. This is mainly related to the nature of the desiccation process relying on slow heat induced water evaporation (Amorij et al., 2008).

### **5.1.2 Spray Drying and Spray Freeze-Drying of pH Responsive Microparticles**

Microencapsulation is considered to be the inclusion of an active within particles ranging from 50 nm to 2 mm. One of the applications of this technique is the production of polymeric controlled release dosage forms for oral delivery (Singh et al., 2010). The production of enteric microparticles, which are supposed to prevent premature drug release in the gastric environment and allow selective release in the intestine, has been attempted by means of solvent evaporation, coacervation and spray drying. (Alhnan et al., 2011;

Dong and Bodmeier, 2006; Kendall et al., 2009). Typically, solvent evaporation and coacervation methods rely on the use of high concentrations of organic solvents. However, organic solvents in prolonged direct contact with the antigen could not be used for the fabrication of microparticles in this study. In fact purified HBcAg VLPs were shown to be unstable upon incubation in high concentrations of organic solvent, i.e. methanol, ethanol or acetone (data not shown). Spray drying of microparticles compared to other microencapsulation techniques allows the production of formulations in a quick single step process, without using or with only minimal concentration of organic solvents (Alhnan et al., 2011; Año et al., 2011; Pastor et al., 2013); hence spray drying was the technique of choice.

Spray drying consists of the atomisation of a feed liquid into a hot air-stream, which induces prompt drying of the atomised droplets into dry powder. This technique is relatively cheap and easy to scale-up (Abdul-Fattah et al., 2007). Año et al. (2011) have shown that killed *Vibrio cholerae* used as a vaccine candidate could be effectively formulated within Eudragit microparticles by spray drying. This microparticles production method simply relies on the spray drying of an Eudragit suspension, containing the vaccine candidate. This process is carried out at a relatively low temperature; it might therefore be potentially applicable to heat-labile ingredients, such as VLPs. A more complex technique for microparticles production was described by Alhnan et al. (2011). This method relies on the solubilisation of the Eudragit aqueous suspension, where the active ingredient (i.e. prednisolone in their studies) could be intimately mixed within the polymer solution, resulting in the formation of spray dried microparticles, in which the active is finely dispersed and incorporated in the polymeric matrix. This novel method enabled the production of particles of good spherical morphology compared to previous attempts. Moreover, the microparticles showed remarkable gastro-resistant properties and targeted gastro-intestinal delivery of prednisolone, used as a model drug (Alhnan et al., 2011).

Spray freeze-drying is a recently developed method for production of particles, which combines spray- and freeze-drying. Generally, in this technique a feed solution containing the active ingredient and pharmaceutical excipients is sprayed into a bed of liquid nitrogen; upon contact with the liquid nitrogen the atomised droplets freeze. Finally, freeze-drying of the frozen droplets in a conventional freeze-drier allows complete ice-water removal from

the particles. Among other applications, spray freeze-drying has been used recently as a method for enteric microsphere production (Niwa et al., 2009).

Both techniques, i.e. spray drying and spray freeze-drying, have been previously used for the formulation of enteric microparticles for oral targeted delivery (Alhnan et al., 2011; Año et al., 2011; Niwa et al., 2009). However, the formulation of VLPs into enteric coated microspheres produced either by spray drying or by spray freeze-drying had never been attempted. The observation that HBcAg VLPs are totally unstable in acidic media simulating the gastric fluids (Chapter 3) makes them a challenging candidate for the development of enteric microparticles.

### **5.1.2.1 Stability of Proteins within Microparticles - Encapsulation Efficiency**

Drying of proteins with complex physical three-dimensional structure is one of the main challenges in drug delivery. During spray drying, a protein is exposed to heat and atomisation stress (Abdul-Fattah et al., 2007). Several proteins have been shown to be vulnerable to this process, while others could withstand spray drying, maintaining good native structure (Amorij et al., 2008; Chen et al., 2010). The process parameters, the choice of stabilisers and the intrinsic physicochemical properties of the protein, influence protein instability upon spray drying. Spray freeze-drying could be more expensive and difficult to scale-up than spray drying. However, spray freeze-drying is considered a safer drying method for particularly labile proteins; compared to the heat evaporation typical of the spray drying, the ice removal by sublimation upon spray freeze-drying might favour protein stability (Abdul-Fattah et al., 2007; Niwa et al., 2009). Nevertheless, in spray freeze-drying the freezing stress and the liquid atomisation could also induce protein instability (Abdul-Fattah et al., 2007; Amorij et al., 2008).

Encapsulation efficiency is defined as the active entrapment within a particulate carrier formulation. However, in the case of spray dried proteins this parameter is not merely related to the amount of protein that remains confined within the microparticles, but it is also associated with the maintenance of the protein's native structure. Therefore, the encapsulation efficiency of a protein should be effectively considered as the percentage

ratio of physiochemically stable protein that remained entrapped within the microparticles (Li et al., 2000).

### 5.1.3 Freeze-drying of Biopharmaceutical Proteins

A general overview of freeze-drying was given in Chapter 4. Freeze-drying is the most widely used technique for the preparation of dry parenteral formulations (Abdul-Fattah et al., 2007). Furthermore, it is also considered the most common method for production of solid forms of pharmaceutical proteins. Preparation of freeze-dried solid formulations of a protein can result in much longer stability than the liquid counterpart (Wang, 2000). One of the main obstacles in the freeze-drying of proteins is the possibility of in-process protein instability, due to the freezing or to the subsequent dehydration process (Abdul-Fattah et al., 2007; Amorij et al., 2008). The de-hydration process removes water from the system that can possibly lead to loss of water-protein hydrogen bonds, resulting in instability of the native structure of the protein. The protein instability during the freezing and/or dehydration can often be avoided by using stabilisers that prevent protein denaturation. Those stabilisers whose function is that of protecting the protein from freezing are called cryoprotectant, while those that protect the protein during the dehydration are called lyoprotectant (Wang, 2000). However, such stabilisers when freeze-dried can confer high hygroscopicity to the final product. In particular, excipients, such as many sugars, that are in the amorphous state at the end of the freeze-drying process are often extremely hygroscopic and they can crystallise into more thermodynamically stable forms upon absorption of water. This physical state instability is dependent on the storage condition and it is not desired as it usually compromises protein stability (Wang, 2000). Therefore, a good compromise between in-process protein stabilisation and maintenance of the physical state is sought when developing a novel solid formulation of a biopharmaceutical protein.

Freeze-drying of HBcAg VLP was attempted with the aim to produce a solid formulation that could be potentially processed into an oral dosage form (i.e. filled into capsules).

## 5.2 Materials

### 5.2.1 Excipients Used for Wet Granulation

Polyvinyl pyrrolidone (PVP) is an inert, synthetic polymer consisting of a linear chain of 1-vinyl-2-pyrrolidinone groups. It is generally used as bulking and stabilising agent in parenteral formulations and as a granulation binder in oral dosage forms (Akers, 2002; Cutt et al., 1986). PVP K 30 was bought from Sigma (UK) and used as received. The K-value is an index of the mean molecular weight (Folttmann and Quadir, 2008): PVP K 30 corresponds to a molecular weight of 40,000. The chemical structure of this polymer is shown in Figure 5.1.

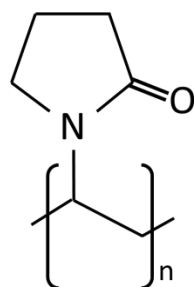


**Figure 5.1. Chemical structure of PVP.**

Hydroxypropyl methylcellulose (HPMC), also called hypromellose, is a semi-synthetic polymer of cellulose. HPMC's structure can be seen in Figure 5.2. It is a polymer widely used as excipient for oral formulations. Low viscosity grades are generally employed as binders for wet granulation (Akers, 2002). HPMC E15 LV was obtained from Colorcon (UK). In the HPMC classification, the initial letter identifies the ratios of hydroxypropyl and methyl substitution of the cellulose. The number in the middle indicates the viscosity. The last suffix indicates the specificity of the product. Therefore in the case of HPMC E15 LV “E” indicates a 28 to 30% methoxy-substitution and 7 to 12% hydroxypropoxy-substitution (see Figure 5.2); “15” indicates the viscosity in milliPascal-seconds, measured at 2% (w/v) concentration of the polymer in water at 20 °C; “LV” indicates the low viscosity type of the product.

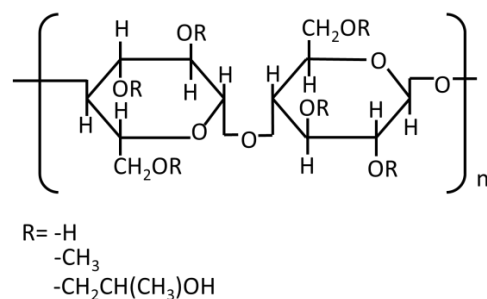


**Figure 5.2. Chemical structure of HPMC.**

### 5.2.2 Excipients Used for the Microencapsulation Studies

Eudragit L30 D55, Eudragit L 100 (introduced in Chapter 4) and Eudragit S 100 are copolymers of methacrylic acid and methyl methacrylate. They are commonly used for enteric coating of oral formulations for targeting dissolution in the small intestine (Eudragit, 2011). Table 5.1 describes the main characteristics of the Eudragit polymer used, including molecular structure, molecular weight, solubility and acid value. The acid value is the amount of alkali required for the complete neutralisation of the acid groups contained in 1 g of the polymer (Eudragit, 2011).

**Table 5.1. Eudragit polymers characteristics**

| Polymer  | Molecular structure   | Molecular Weight (g/mol) | Solubility | Acid value (mg KOH/g) |
|----------|---|--------------------------|------------|-----------------------|
| L 30 D55 | <p>The molecular structure of Eudragit L 30 D55 is shown as a repeating unit. It consists of a methacrylic acid (MA) unit linked to a methyl methacrylate (MMA) unit. The MA unit has a CH<sub>2</sub> group, a C=O group, and an OH group. The MMA unit has a CH<sub>3</sub> group, a C=O group, and an OC<sub>2</sub>H<sub>5</sub> group. The repeat unit is enclosed in brackets with a subscript 'n=1'.</p> | 320,000                  | > pH 5.5   | 315                   |
| L 100    | <p>The molecular structure of Eudragit L 100 is shown as a repeating unit. It consists of a methacrylic acid (MA) unit linked to a methyl methacrylate (MMA) unit. The MA unit has a CH<sub>2</sub> group, a C=O group, and an OH group. The MMA unit has a CH<sub>3</sub> group, a C=O group, and an OCH<sub>3</sub> group. The repeat unit is enclosed in brackets with a subscript 'n=1'.</p>                | 125,000                  | > pH 6     | 315                   |
| S 100    | <p>The molecular structure of Eudragit S 100 is shown as a repeating unit. It consists of a methacrylic acid (MA) unit linked to a methyl methacrylate (MMA) unit. The MA unit has a CH<sub>2</sub> group, a C=O group, and an OH group. The MMA unit has a CH<sub>3</sub> group, a C=O group, and an OCH<sub>3</sub> group. The repeat unit is enclosed in brackets with a subscript 'n=2'.</p>                | 125,000                  | > pH 7     | 190                   |

The three polymers differ in their intrinsic solubility: Eudragit L 30 D55, Eudragit L 100 and S 100 are soluble at pH > 5.5, > 6 and > 7, respectively. Therefore, such polymers are commercialised to direct the delivery of encapsulated actives to different areas of the gut: L30 D55, L 100 and S 100 are supposed to target the release of the active in the duodenum, in the jejunum and in the ileum/colon, respectively (Eudragit, 2011).

Eudragit L 30 D55 (liquid dispersion), L 100 (powder) and S 100 (powder) were kindly donated by George-William Smith (Evonik Industries, UK).

Other materials used for the microencapsulation studies are described in Chapter 3.

### **5.2.3 Excipients Used for the Freeze-drying Studies**

Different stabilisers and bulking excipients were used in the freeze-drying. The function of this class of excipients is to provide structure and to possibly stabilise proteins upon freeze-drying (Wang, 2000). Glycine was purchased from Fisher (UK),  $\alpha$ -lactose monohydrate and  $\alpha$ -trehalose dihydrate from Sigma (UK) and D-mannitol from Sigma (Germany).

## **5.3 Methods**

### **5.3.1 Wet Granulation**

Preliminary trials for producing granules containing HBcAg VLP were carried out. Given the small scale of the experiments, the wet granulation was performed manually mixing the dry powder and the binder solution using a mortar and pestle. HBcAg was added in the binder solution and, after sieving of the wet mass, the granules were dried in an oven or in a desiccator.

Before the granulation experiment, plant-expressed HBcAg was purified and quantified by sandwich ELISA, according to Chapter 2. Six granulation protocols were carried out, in order to compare the stability of HBcAg upon granulation, using lactose-based or lactose-free dry powder formulations, PVP or HPMC as the binder in the granulation solution and drying either in an oven or in a desiccator. Table 5.2 summarises the granulation protocols.

**Table 5.2. Granulation protocols.**

|                          | Protocol 1      | Protocol 2           | Protocol 3      | Protocol 4           | Protocol 5      | Protocol 6      |
|--------------------------|-----------------|----------------------|-----------------|----------------------|-----------------|-----------------|
| <b>Dry powder</b>        | Lactose formula | Lactose-free formula | Lactose formula | Lactose-free formula | Lactose formula | Lactose formula |
| <b>Binding solution*</b> | PVP             | PVP                  | PVP             | PVP                  | HPMC            | HPMC            |
| <b>Drying method</b>     | Oven            | Oven                 | Desiccator      | Desiccator           | Oven            | Desiccator      |

\*Added as aqueous solution during granulation.

Two formulations of dry powders were prepared: one containing 7.9 g of  $\alpha$ -lactose monohydrate mixed with 1 g of microcrystalline cellulose and 1 g of pre-gelatinised starch. The other was a lactose-free formula prepared by mixing 7.5 g of microcrystalline cellulose with 2.4 g of pre-gelatinised starch. Two different binding solutions were used: one solution contained 8.5% (w/v) PVP and 26  $\mu$ g/mL HBcAg in PBS; the second solution was made of 5% (w/v) HPMC and 85  $\mu$ g/mL HBcAg in PBS. Wet massing was carried out using a small mortar and pestle and by gradually mixing 2 g of the dry powder with 0.56 mL of PVP solution or 0.29 mL of HPMC solution. After complete mixing, the wet granules were sieved through a 2 mm sieve. The granules were then dried overnight in an oven at 45 °C or at room temperature in a closed container pre-equilibrated with  $P_2O_5$ , to give an atmosphere of almost 0% RH.

After overnight drying, 100 mg aliquots of the granules produced according to the six different protocols were weighed and dispersed in 10 mL PBS. The residual HBcAg VLP content in the dispersion was measured by sandwich ELISA and calculated as a percentage ratio to the total HBcAg VLP added to the binder solution, prior to the granulation. The calculated residual HBcAg VLP content represents a measure of HBcAg stability upon the granulation process.

### 5.3.2 Formulation of HBcAg Containing Microparticles

In this Paragraph the production of HBcAg VLP pH-responsive microparticles, by spray drying and spray-freeze drying, and the characterisation and tests performed on these macroparticles are described.

#### 5.3.2.1 Stability Pre-formulation Assessment

Both methods used for microparticles production, described by Año et al. (2011) and by Alhnan et al. (2011), were initially taken as a reference in this study for the production of gastro-resistant formulations of HBcAg VLP microparticles.

The feed solution to be spray dried had to contain a Eudragit polymer, either in solution [as in Alhnan et al. (2011)] or dispersed as a suspension [as in Año et al. (2011)], and HBcAg VLP; however, it was unknown whether the antigen could remain intact upon incubation with the polymer mixtures. Therefore, a preliminary screening was conducted, where the antigen and the polymer solutions (or dispersions) were co-incubated for 2 hours. Four aqueous Eudragit formulations were created: Eudragit L 30 D55 was prepared as a dispersion, while Eudragit L 100 and S 100 were solubilised by addition of alkali, allowing neutralisation (i.e. ionisation of the carboxylic groups of the polymer), thus increasing its aqueous solubility. The preparation methods for the three Eudragit polymers are illustrated in Table 5.3.

**Table 5.3. Eudragit re-dispersion.**

| Polymer         | Weight/Volume                      | Dilution                                      | Final Polymer concentration | -COOH neutralisation     | Physical state |
|-----------------|------------------------------------|---|-----------------------------|--------------------------|----------------|
| <b>L 30 D55</b> | 0.1 mL dispersion<br>(30% w/v)     | Undiluted                                     | 30%                         | Circa 0%<br>(circa pH 3) | Dispersion     |
| <b>L 30 D55</b> | 0.33 mL<br>dispersion (30%<br>w/v) | Water to 3.33 mL                              | 3%                          | Circa 0%<br>(circa pH 3) | Dispersion     |
| <b>L 100</b>    | 100 mg powder                      | Water + 0.65 mL 1M<br>NH <sub>3</sub> to 5 mL | 2%                          | 100%<br>(to pH 8.5)      | Solution       |
| <b>S 100</b>    | 100 mg powder                      | Water + 0.4 mL 1 M<br>NH <sub>3</sub> to 5 mL | 2%                          | 100%<br>(to pH 8.5)      | Solution       |

Then 2  $\mu$ L of 0.5 mg/mL purified HBcAg was diluted in 198  $\mu$ L Eudragit L 30 D55 dispersion or Eudragit L 100 and S 100 solutions and incubated for two hours at room temperature (25 °C). Finally, the residual HBcAg in the incubation samples was measured by sandwich ELISA and calculated as ratio to an identical dilution of HBcAg in PBS used as a control.

### 5.3.2.2 Spray Drying Process

Spray drying was carried out using a Büchi 191 Mini Spray Dryer (Büchi, Labortechnik AG, Flawil, Germany) with a standard 0.7 mm nozzle.

In the case of Eudragit L 100, 800 mg Eudragit were re-dispersed in 20 mL of water under stirring, then 5.2 mL of 1M NH<sub>3</sub> and 3.2 mL of ethanol were added and the volume was brought to circa 39 mL with water. Finally, 150  $\mu$ L of a solution of 1.5 mg/mL HBcAg was added and the volume adjusted to 40 mL with water. This was done in order to minimise the contact of HBcAg with the diluted ethanol. For Eudragit S 100, 800 mg of polymer were re-dispersed in 20 mL of water under stirring, then 3.2 mL of 1M NH<sub>3</sub> and 3.2 mL of ethanol were added and the volume was brought to circa 39 mL with water. Finally, 150  $\mu$ L of a solution of 1.5 mg/mL HBcAg was added and the volume adjusted to 40 mL with water. The two mixtures of Eudragit L 100 and S 100 containing HBcAg were spray dried separately. Each feed solution was pumped continuously at a rate of 5% (circa 2 mL/min) and 360 L/h of compressed air for atomization. The inlet air temperature was set at 88 °C.

At the end of the spray drying process, the harvested microparticles were weighed. The yield of the spray drying process was calculated as a percentage ratio between the mass of harvested microparticles and the mass of solid content in the feed solution.

The removal of residual ammonia was carried out by vacuum evaporation: half of the harvested batch of microparticles produced with Eudragit L 100 and S 100 were loaded in a Wizard 2.0 freeze drier (USA). The shelf temperature was then set at 40 °C and a vacuum of 200 millitorr was applied for 12 hours.

### 5.3.2.3 Spray Freeze-drying Process

Feed solutions of 2% (w/v) Eudragit were obtained by dispersion of the polymer in water and addition of alkali. To prepare Eudragit L 100 dispersion, 400 mg Eudragit were re-dispersed in 10 mL of water under stirring; then 2.6 mL of 1M NH<sub>3</sub> were added; finally 60 µL of 2.4 mg/mL HBcAg solution were added and the volume was brought to 20 mL with water. For Eudragit S 100, 400 mg of polymer were re-dispersed in 10 mL of water under stirring; then 1.6 mL of 1M NH<sub>3</sub> were added, followed by 60 µL of 2.4 mg/mL HBcAg solution. Finally, the volume was brought to 20 mL with water. Spraying was performed using the Büchi 191 Mini Spray with a standard 0.7 mm nozzle with the drying chamber removed. The feed solutions were pumped continuously at a rate of 25% and 250 L/h of compressed air for atomization into a tray containing a bed of liquid nitrogen, positioned horizontally circa 25 cm beneath the nozzle opening. Then the tray was immediately loaded in the Wizard 2.0 freeze drier, the shelf of which had been pre-cooled. For the thermal treatment step the shelf temperature was set at – 60°C for 180 minutes. After this phase, the primary drying was carried out at a chamber pressure of 200 millitorr with sequential temperature steps of 120 minutes, using the following order: – 45, – 35, – 25, – 15, – 5, 5, 15 and 20 °C. For the final drying and ammonia removal the shelf temperature was set at 35 °C and a vacuum of 200 millitorr was applied for 6 hours.

### 5.3.2.4 Characterisation of the Eudragit Particles

Eudragit particles containing HBcAg were characterised by SEM and FT-IR. The encapsulation efficiency and the gastro-protection were also evaluated. Four formulations, consisting of Eudragit L 100 and S 100 particles produced by spray drying and spray freeze-drying were used for the characterisation.

#### 5.3.2.4.1 SEM

Examination of the morphology of the Eudragit L 100 and S 100 particles was carried out by SEM imaging. This technique was performed as described in Chapter 4.

#### 5.3.2.4.2 Fourier Transform Infra-Red (FTIR) Spectroscopy

Fourier Transform Infra-Red (FTIR) spectroscopy is a technique used for the detection of functional groups in molecular structures. It is based on the absorption of infra-red (IR) radiation of specific wavelengths by different functional groups. It can therefore be used to identify structural changes of certain materials upon processing. FTIR can be used to determine the residual ammonium content in the Eudragit microparticle (Alhnau et al., 2011). An IFS-60/S Fourier transform infrared (Bruker Optics, UK) was used. For each sample a total of 16 scans were determined at a resolution of  $4\text{ cm}^{-1}$ . Spectra were analysed using OPUS software (version 6.0). The IR spectrum was plotted as percentage of transmittance rather than absorbance. Wavenumbers are the reciprocal of the wavelength and have the units of  $\text{cm}^{-1}$ . The stretching of the N–H bond corresponded to a wavelength of  $1525\text{--}1550\text{ cm}^{-1}$ .

#### 5.3.2.4.3 Encapsulation Efficiency

The encapsulation efficiency of the spray dried and spray freeze-dried microparticles was calculated as the percentage ratio between the actual content of stable HBcAg VLP present in the Eudragit microparticles and the theoretical content of HBcAg VLP in the microparticles. For the calculation of the HBcAg present in the formulation, 10 mg of microparticles were dissolved in 10 mL of 50 mM Tris buffer (pH 8.0) and the HBcAg content in the solution was then measured by sandwich ELISA. The theoretical content corresponded to the amount of quantified HBcAg VLP added to the feed solutions before spray drying and spray freeze-drying.

#### 5.3.2.4.4 Gastro-protective Properties of Particles

The protection of HBcAg formulated within the Eudragit particles was assessed by pre-incubation of the particles in simulated gastric fluids (SGF), followed by evaluation of the HBcAg release in alkaline conditions. The pre-incubation in SGF was intended to mimic the gastric passage in humans.

For this assay 5 mg of each Eudragit particulate formulation was incubated in 5 ml of SGF with pepsin (preparation as described in Chapter 4) at  $37\text{ }^{\circ}\text{C}$  for 2 hours with frequent

vortexing. Then 1.025 mL of 160 mM Na<sub>2</sub>CO<sub>3</sub> were added to neutralise the acidity (final pH 8.5), allowing complete dissolution of the pH-responsive particles. In parallel, control samples were made by dissolution of identical Eudragit formulations in 3.025 mL of 50 mM Tris buffer (pH 8.0). Upon complete dissolution of the particles the content of HBcAg was measured by sandwich ELISA. HBcAg protection was calculated as percentage ratio between the HBcAg content in the samples pre-incubated in SGF and the HBcAg measured in the control samples.

### **5.3.3 Freeze-drying**

Freeze-drying was also investigated as a drying method for purified HBcAg.

#### **5.3.3.1 Stability of HBcAg upon Freeze-drying with Different Excipients**

In this Paragraph HBcAg was freeze-dried together with different stabilisers and the physical stability of HBcAg VLP in the re-suspended freeze-dried material was investigated by density gradient sedimentation and by native agarose gel electrophoresis.

##### **5.3.3.1.1 Freeze-Drying**

Separate aliquots of fifty (50)  $\mu$ L of 3 mg/mL purified HBcAg in PBS were mixed with 2 mL of 4% solutions of glycine, lactose, mannitol and trehalose in PBS. The four resulting solutions were freeze-dried in a Wizard 2.0 freeze drier (VirTis, USA). For the thermal treatment step, the shelf temperature was set at – 60 °C for 360 minutes, followed by 240 minutes of maximum freezing, a phase through which the shelf temperature was reduced to the lowest possible temperature. After this phase, the primary drying was carried out at a chamber pressure of 180 millitorr with sequential temperature steps of 180 minutes, using the following order: – 45, – 35, – 25 and – 15 °C; this was followed by further drying steps at a chamber pressure of 180 millitorr with sequential temperature steps of 240 minutes: 5, 15, 20 and 25 °C. Secondary drying was set at 25 °C for 60 minutes.

##### **5.3.3.1.2 Density Gradient Sedimentation of Re-suspended Freeze-dried HBcAg**

Immediately after freeze-drying, 25 mg from each of the four dry formulations were re-suspended in 2.5 mL PBS. A positive control was created by diluting 15.6  $\mu$ L of 3 mg/mL

purified HBcAg in 2.5 mL PBS. The four re-suspended solutions and the control were loaded on the top of five 10 to 60% (w/v) sucrose density gradients. After 2 hours and 30 minutes ultracentrifugation at 41,000 rpm in a SW41-Ti rotor, the five sucrose gradients were fractioned and the collected density fractions were examined by either sandwich ELISA or dot blot using the monoclonal antibody. The sucrose density gradient method and the detection techniques are described in Chapter 2.

#### **5.3.3.1.3 Native Agarose Gel Electrophoresis of Re-suspended Freeze-dried HBcAg**

Given the lower sensitivity of the native agarose gel method, more concentrated HBcAg freeze-dried formulations had to be prepared, compared to those used for the ELISA and dot blot. Separate aliquots of 150 µL of 3 mg/mL purified HBcAg in PBS were mixed with 1 mL of 4% solutions of glycine, lactose, mannitol and trehalose in PBS. The four resulting solutions were freeze-dried as in 5.3.3.1.1. Then 10 mg of each freeze-dried product was re-suspended in 250 µL PBS. The resulting solutions were loaded on the wells of two agarose gels. After electrophoretic separation, one of the gels was stained with ethidium bromide, while the other was Coomassie stained. The method used for native agarose gel electrophoresis is described in detail in Chapter 2.

#### **5.3.3.2 Thermal Analysis of Freeze-dried Excipients**

The thermal properties of the excipients used as potential stabilisers during the freeze-drying were examined by modulated temperature differential scanning calorimetry (MTDSC) and by thermogravimetrical analysis (TGA). HBcAg VLP was not present in the formulations studied. However, as in the antigen stability studies (Paragraph 5.3.3.1), HBcAg was present at an excipient: protein ratio of only 535:1, the antigen effect on the thermal behaviour of the excipients was considered marginal.

##### **5.3.3.2.1 Modulated Temperature Differential Scanning Calorimetry (MTDSC)**

Differential Scanning Calorimetry (DSC) is the most widely used thermo-analytical technique employed in the study of pharmaceutical products. Generally, the process is based on heating or cooling a sample and then calculating the temperature and energy

associated with significant endothermic or exothermic thermal events and heat capacity changes of the material investigated (Craig and Reading, 2007). Heat flux DSC instruments are based on applying identical linear heating signals to the sample and to a reference (usually an empty pan) present in the same crucible. In this type of DSC the temperature difference between the sample and the reference changes during thermal events and it is recorded as a difference in heat flow between them. The heat flow changes are generally expressed as a function of time. Modulated Temperature Differential Scanning Calorimetry (MTDSC) is a type of heat flux DSC, in which a sinusoidal heating signal is applied on top of the linear heating signal. This method enables the separation of kinetic and thermodynamic events, which is sometimes difficult to achieve with conventional DSC, and overlapping or weak thermal events may be more easily distinguished.

In this study, four separate 4% (w/v) solutions of glycine, lactose, mannitol and trehalose in PBS were prepared and then 2 mL samples of each formulation were loaded into a glass vial and freeze-dried, using the same process parameters indicated in Paragraph 5.3.3.1. After freeze-drying, one vial of each of the glycine, lactose, mannitol and trehalose formulations was stored for 5 days in a pre-equilibrated desiccator over  $P_2O_5$  (in an environment with virtually 0% RH). Four identical vials were stored for 5 days in a pre-equilibrated desiccator over NaCl (giving an environment of 75% RH). After the incubation at the different storage conditions, the thermal behaviour of the eight samples was assessed using a Differential Scanning Calorimeter (2920, TA Instruments, Newcastle, USA) in MTDSC mode. Samples were carefully weighed (2 to 5 mg) into pinhole aluminium pans then scanned between  $-30\text{ }^{\circ}\text{C}$  and  $250\text{ }^{\circ}\text{C}$ , with modulation temperature amplitude of  $\pm 0.212\text{ }^{\circ}\text{C}$ , modulation time of 60 s and an underlying temperature ramp rate of  $2\text{ }^{\circ}\text{C}/\text{minute}$ . Before the experiments, the temperature and cell constant of the DSC instrument were calibrated with indium, n-octadecane and tin, while the calibration of the heat capacity was performed with aluminium oxide in modulated mode. Three analyses were performed for each sample. The thermograms were plotted as total heat flow, reversed heat flow and non-reversed heat flow.

### 5.3.3.2.2 Thermo Gravimetric Analysis (TGA)

Thermo Gravimetric Analysis (TGA) was carried out for the same samples analysed by DSC, in order to evaluate water loss and possible sample degradation. The samples were loaded onto aluminium pans and were heated from 25 °C to 200 °C at a heating rate of 10 °C/minute. The sample dehydration was calculated as the weight loss between 30 °C and 110 °C. Each sample was assessed in triplicate and the water loss was calculated as an average of the three measurements

## 5.4 Results and Discussion

In the vaccine development process, along with the discovery of new antigens, the design of suitable formulations is another extremely challenging task (Borde et al., 2012). For oral administration of vaccines, the gastro-intestinal instability is one of the major issues to be overcome and another is the development of a suitable oral dosage form. In fact for the development of a solid oral dosage form, the antigen has to remain stable throughout the formulation and manufacturing process, which includes protein drying. It is well documented that the preservation of the physicochemical stability of pharmaceutical proteins upon drying represents another challenging area of today's drug delivery research (Abdul-Fattah et al., 2007). In the case of VLPs this task is complicated by its complex quaternary structure: it is in fact reasonable to think that the physical stability issue would be greater with complex macromolecules made of hundreds of monomers, such as VLPs, than with smaller biopharmaceutical macromolecules, such as monomeric proteins or peptides. In this study, different approaches for developing solid dosage forms of purified HBcAg were investigated.

### 5.4.1 HBcAg Stability upon Granulation – Preliminary Study

When considering the development of an oral dosage form, tablets represent the most typical and widely used type of formulation. Furthermore, tablets represent a suitable substrate for coating with gastro-protective films when gastro-protection is required, as for HBcAg VLPs. A potential formulation of HBcAg into tablets would probably contain a few tens of µg of active ingredient, which would constitute < 0.1% of the weight of the whole tablet. This formulation falls into the category of very low-dose active ingredient

and thus in this case the dose homogeneity in the oral dosage forms becomes a formulation development hurdle. Wet granulation is often used to overcome this issue of oral dosage forms and prevent the segregation often seen in direct compression powder mixtures. In wet granulation, granules are prepared by mixing the dry ingredients (drug and excipients) of the formulation with a binder solution and then the solvent (generally water) is removed to produce roughly spherical granules, containing a roughly homogenous mixture of the ingredients. For very low dose actives, the drug may be dissolved in the binder solution, promoting homogeneity within the granule. The dried granules can then be compressed into tablets. In this way segregation and inefficient mixing of the low-dose actives can be limited (Wan et al., 1992). Based on this knowledge, a preliminary study was carried out, in which HBcAg VLP was dissolved in the binder solution used for the formulation of granules.

Table 5.4 summarises the six granulation protocols and illustrates the residual HBcAg stability upon granulation measured for each protocol. The antigen stability is presented as a percentage ratio to the total HBcAg VLP added to the binder solution used for the granulation. Less than 25% HBcAg could be recovered in all six formulations, suggesting high HBcAg VLP instability. As an exact quantification was not intended for this preliminary screening, the tests were not carried out in triplicate; therefore these data are only indicative of a trend. Comparing the relative stability of the specific protocols it appears evident that the presence of HPMC (protocols 5 and 6) in the binder solution seems to stabilise the VLP more than PVP (protocols 1 to 4) did. Furthermore, the presence of  $\alpha$ -lactose monohydrate in the formulation of the granules seemed to favour antigen stability (protocols 1 and 3), compared to the lactose-free formulation (protocols 2 and 4). Finally, drying in a desiccator seemed to have allowed higher VLP stability than oven-drying in all cases.

**Table 5.4. HBcAg stability upon granulation.**

|                                    | Protocol 1 | Protocol 2   | Protocol 3 | Protocol 4   | Protocol 5 | Protocol 6 |
|------------------------------------|------------|--------------|------------|--------------|------------|------------|
| <b>Dry powder</b>                  | Lactose    | Lactose-free | Lactose    | Lactose-free | Lactose    | Lactose    |
| <b>Binding solution</b>            | PVP        | PVP          | PVP        | PVP          | HPMC       | HPMC       |
| <b>Drying method</b>               | Oven       | Oven         | Desiccator | Desiccator   | Oven       | Desiccator |
| <b>HBcAg VLP stability (n = 1)</b> | 5.1%       | 2.3%         | 5.6%       | 3.9%         | 14.2%      | 20.4%      |

The greatly reduced stability observed upon granulation is probably related to the drying method. Despite the fact that PVP and HPMC, often used as protein stabilisers (Wang, 2000), were dissolved in the binder solution together with the VLP, the final stability of the antigen was remarkably low. An analysis of the drying process suggests that the long drying time, typical of the desiccation process, often generates phase separation between stabilisers and active ingredient, resulting in low stability of biopharmaceutical protein (Amorij et al., 2008). In addition, the fact that the liquid containing the VLP was not directly dried from liquid into solid, but the liquid was present as moisture adsorbed to the dry components of the granules, probably further slowed the drying process, resulting in further instability. Finally, as the HBcAg was spread within the wet mass of excipient during the granulation, this resulted in an extremely large air-liquid interface area: it is well documented that a large air-liquid interface area is one of the main causes of protein instability upon drying (Abdul-Fattah et al., 2007). However, drying pharmaceutical proteins in an oven or in a desiccator would be much cheaper than using spray drying or freeze-drying (sublimation) methods, therefore, the risks of instability could be counterbalanced by the low cost of this application (Amorij et al., 2008). Nevertheless, the high HBcAg instability observed in this experiment discouraged taking this approach any further. An alternative approach would be to produce the wet mass of granules as described in this section and then perform the drying by means of vacuum desiccation or by freeze-drying. In this case, the overall process would become more expensive, losing the advantage of using such an alternative approach. It was instead considered wiser to try a completely different approach, potentially able to warrant higher stability of the antigen upon drying.

### 5.4.2 Preparation of Eudragit Particles by Spray Drying and Spray Freeze-Drying

This Paragraph describes the production of HBcAg VLP enteric microparticles by spray drying and spray freeze-drying. The challenges presented by these processes were two-fold: the first hurdle would have been to ensure the stabilisation of the physical, three-dimensional stability of protein in the dry state (i.e. in the microparticles). Second, the microparticles had to provide efficient gastro-protection.

#### 5.4.2.1 Spray Drying Process

Both methods of production, described by Año et al. (2011) and by Alhnán et al. (2011), were initially taken as a reference for the production of gastro-resistant formulations of HBcAg VLP microparticles. Año et al. (2011) prepared the formulations mixing their active (i.e. inactivated *Vibrio cholerae*) in Eudragit dispersions, while Alhnán et al. (2011) mixed the active (i.e. prednisolone) in neutralised Eudragit solutions. Hence, a preliminary assessment was made as to whether the antigen would remain intact upon incubation with either of the polymer mixtures (i.e. dispersion or solution).

Table 5.5 describes the re-dispersion protocol and the stability of HBcAg in the dispersion or solution of the polymer. Measurements of HBcAg VLP stability by sandwich ELISA indicated that the antigen was not stable in the dispersion of Eudragit L 30 D55, even when the polymer was diluted to 3 % (w/v). However, HBcAg was more stable in 2% polymer solution of Eudragit L 100 and S 100, obtained from the neutralisation with alkali of the carboxylic group of the polymers.

**Table 5.5. HBcAg stability in Eudragit.**

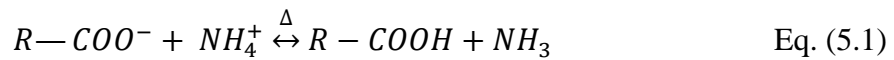
| Polymer  | Polymer concentration | -COOH neutralisation     | Physical state | HBcAg stability (n = 2) |
|----------|-----------------------|--------------------------|----------------|-------------------------|
| L 30 D55 | 30%                   | Circa 0%<br>(circa pH 3) | Dispersion     | Undetectable            |
| L 30 D55 | 3%                    | Circa 0%<br>(circa pH 3) | Dispersion     | Undetectable            |
| L 100    | 2%                    | 100%<br>(to pH 8.5)      | Solution       | 82.6%                   |
| S 100    | 2%                    | 100%<br>(to pH 8.5)      | Solution       | 56.3%                   |

This result strongly suggests that the highly acidic environment of the Eudragit L30 D55 dispersion was not compatible with VLP stability. This is in accordance with Chapter 3, where it was shown that HBcAg is unstable at pH lower than 3-3.5. However, the increase in pH, resulting from the addition of ammonia solutions to solubilise the polymer, also enabled higher antigen stability.

As HBcAg VLPs were unstable in the polymeric dispersion, the approach described by Año et al. (2011) was obviously not carried forward. Instead, as aforementioned, the enteric microparticles produced by Alhnán et al. (2011) were produced by spray drying of Eudragit solution, obtained by neutralisation of the carboxylic groups. This was supposed to improve particle morphology and functionality (Alhnán et al., 2011); however, in the current study, this formulation approach offered another advantage. The more neutral pH of the final polymer solution could allow mixing the labile antigen with Eudragit, while maintaining adequate VLP stability (Table 5.5).

Thus, the feed solution to be spray dried was formulated by dissolving 2% (w/v) Eudragit L 100 and S 100 in neutralising alkali, containing 8% ethanol. Purified HBcAg VLPs were added to the solution just before the experiment. At the end of the process the powder was collected and weighed. The yield of the processes corresponded to 25.3% and 21.6% of recovered solid product for Eudragit L 100 and S 100 microparticles, respectively. The relatively low yield obtained was related to the very low batch size of the experiments.

Alhnán et al. (2011) suggested that enteric microparticles can elicit better GI targeting properties if a post-spray drying heat treatment is performed. Spray drying of Eudragit, where the carboxylic acid groups are present in their ammonium salt form, would result in the formation of microparticles in which the polymer is still present in the salt form. Therefore, such an ionised polymeric matrix would promote water uptake in acidic gastric fluids, basically allowing contact of the acidic media with the active dispersed in the polymer matrix. This would induce premature drug release and possible instability in the acidic media. This problem was overcome by post-spray drying heating of the microparticles: the heat treatment at 70 °C favours ammonia evaporation and therefore restoration of the carboxylic acid as shown in the Eq. (5.1) (Alhnán et al., 2011).



Such heat treatment was shown to improve the gastro-resistant properties of the microparticles upon incubation at pH 1.2 (Alhnau et al., 2011). In the current work, the restoration of the unionised carboxylic groups in the microparticles was not carried out by heating at 70 °C as this could have affected the VLP stability; instead, the microparticles were incubated in the freeze-drier at 40 °C for 12 hours at a pressure of 200 millitorr. Then the microparticles were analysed by FTIR, in order to determine the residual ammonium content in the Eudragit microparticles. In Figure 5.3, FTIR spectra of Eudragit L 100 microparticles (Figure 5.3 A) and of Eudragit S 100 microparticles (Figure 5.3 B) before and after the post-spray drying treatment are shown. In both cases the spectrum reveals that the heat and vacuum treatment in the freeze-drier enabled effective removal of the ammonia, visible as a peak at circa 1550 cm<sup>-1</sup>, corresponding to N–H bond stretching.

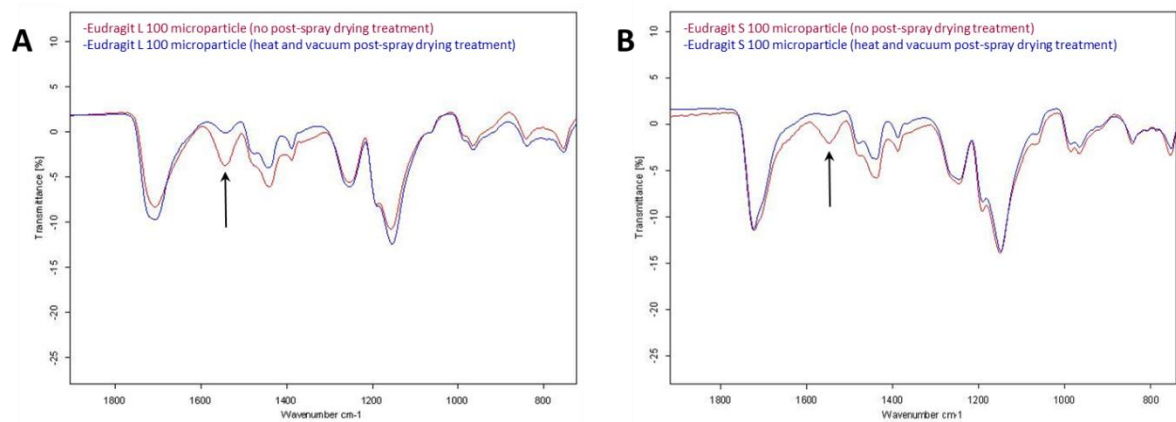


**Figure 5.3. FTIR spectra of Eudragit microparticles.**

Eudragit L 100 and S 100 microparticles containing HBcAg VLP were produced by spray drying. The collected particles were incubated at 40 °C and a pressure of 200 millitorr for 12 hours in order to remove ammonia. (A) illustrates the FTIR Spectra of Eudragit L 100 microparticles before and after the post-drying treatment, while (B) shows the FTIR Spectra of Eudragit S 100 microparticles before and after the post-drying treatment. The ammonium peak is indicated by an arrow at circa  $1550\text{ cm}^{-1}$ .

The regeneration of the unionised carboxylic acids of the polymer upon the heat and vacuum treatment (Figure 5.4) is thought to make the microparticles less hydrophilic, as compared to the ammonium salt form present in the untreated microparticles. This should reduce the water uptake of the polymer in the acidic gastric fluids, therefore enabling better protection of the HBcAg VLP present within the polymer matrix.

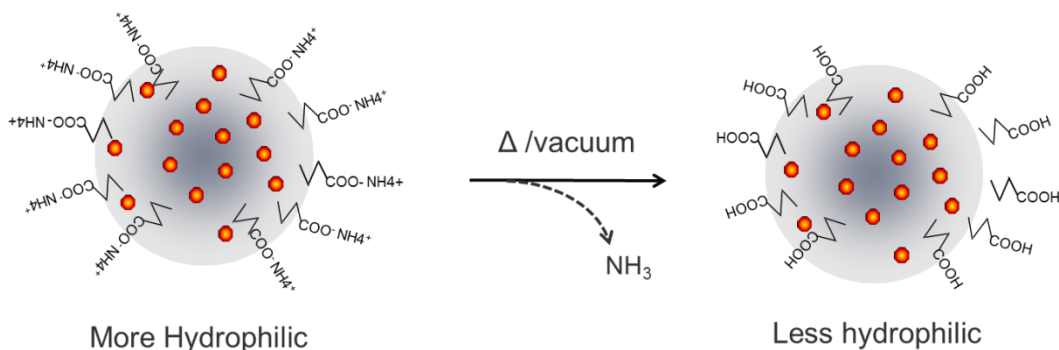


**Figure 5.4. Schematic representation of the effect of heat and/or vacuum treatment on Eudragit microparticles.**

Eudragit microparticles were highly rich in carboxylate salts when collected from the spray drier. Post-processing heat and vacuum treatment allowed ammonia removal and restoration of carboxylic acid moieties within the polymer. This final unionised form of the polymer is less hydrophilic than the ionised one. HBcAg VLPs are represented as orange particles dispersed in the grey-coloured polymeric matrix.

Further characterisation of the microparticles was performed together with that of particles produced by spray freeze-drying in Paragraphs 5.4.2.3 and 5.4.2.4.

#### 5.4.2.2 Spray Freeze-drying Process

Spray freeze-drying has been demonstrated to be particularly suitable for heat labile proteins (Rogers et al., 2002). Considering the extremely complex physical architecture of VLPs and also given the high instability of HBcAg upon desiccation seen when granulation was attempted, the spray freeze-drying of enteric particles could represent a judicious choice for maintaining the native protein structure of the particles. For comparison purposes the Eudragit L 100 and S 100 feed solution formulas were maintained similar to those used for the spray drying. The feed solutions were sprayed through the nozzle of a conventional spray drier and the atomised droplets were directly frozen into liquid nitrogen. The drying was completed in the freeze drier. At the end of the process, a post-drying step consisting of a further 6 hours incubation at 35 °C and 200 millitorr pressure was added in order to remove the residual ammonia from the Eudragit polymer and restore the unionised carboxylic groups, similarly to the procedure followed for the spray drying of the microparticles. At the end of the process, the dry polymeric particles were collected; however such particles showed high electrostatic forces, rendering the collection very difficult. Therefore, only part of the material could be recovered; for this reason the yield could not be calculated.

The spray freeze-dried particles were then characterised together with the spray dried microparticles.

#### 5.4.2.3 SEM Imaging of Eudragit Particles

The morphology of the spray dried and spray freeze-dried microparticles was examined by SEM imaging. Images of the Eudragit microparticles produced by spray drying are illustrated in Figure 5.5. Microparticles produced with Eudragit L 100 showed a fairly spherical and regular shape (Figure 5.5 A and B) and microparticles produced with Eudragit S 100 also appeared spherical and were of regular shape (Figure 5.5 C and D). In both cases the particle size was generally between 1 and 5 µm in diameter.

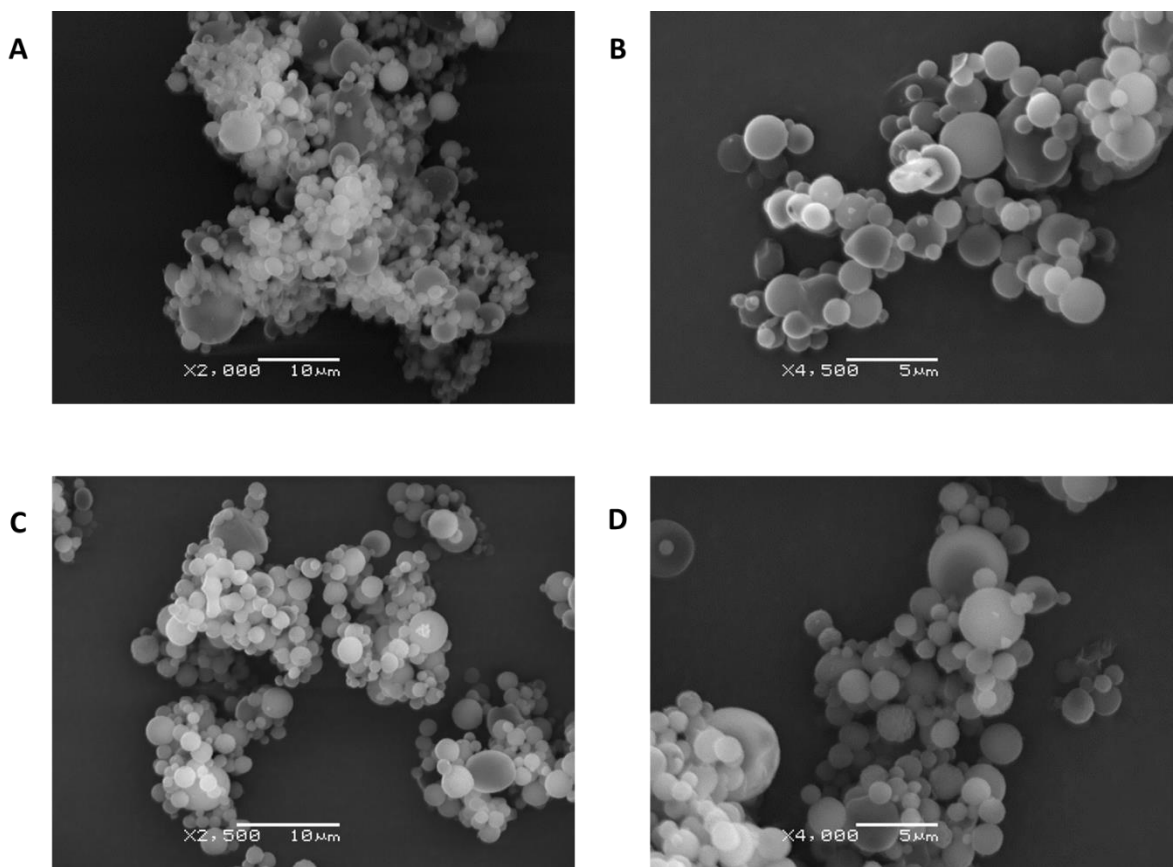


**Figure 5.5. SEM images of Eudragit spray dried microparticles containing HBcAg.** Eudragit microparticles, containing HBcAg VLP, were produced by spray drying and then examined by SEM. (A) and (B) illustrates two SEM images of Eudragit L 100 microparticles (2000x and 4500x, respectively). (C) and (D) show two SEM images of Eudragit S 100 microparticles (2500x and 4000x, respectively).

Eudragit microparticles containing HBcAg produced by spray freeze-drying were also examined by SEM, as shown in Figure 5.6. Microparticles produced with Eudragit L 100 have a spherical shape, however, their size seemed highly irregular (Figure 5.6 A, B and C). Furthermore, the microparticles appeared highly porous, showing a spongy structure. Microparticles produced with Eudragit S 100 looked similar, though they seemed to have slightly more regular spherical shape (Figure 5.6 D, E and F). The microparticles were fairly brittle, especially in the case of Eudragit L 100 microparticles, which might be due to their high porosity and could explain their irregular shape. The size of Eudragit L 100 and Eudragit S 100 microparticles seemed to range from fragments as small as a few microns to spherical particles of 100  $\mu\text{m}$  in diameter.

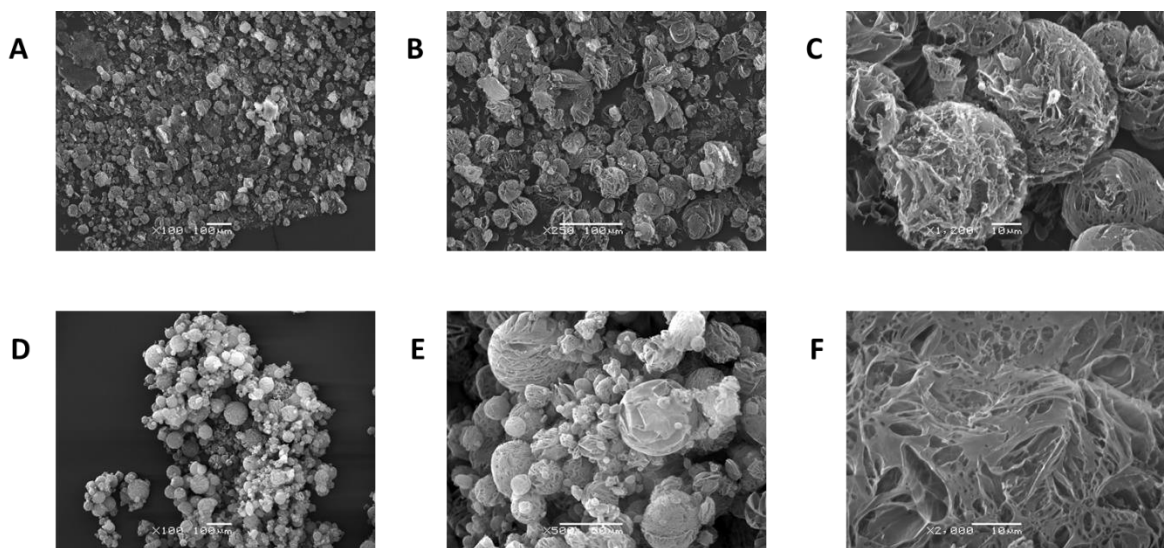


**Figure 5.6. SEM images of Eudragit spray freeze-dried microparticles containing HBcAg.**

Eudragit microparticles, containing HBcAg VLP, were produced by spray freeze-drying and then examined by SEM. (A), (B) and (C) illustrates three SEM images of Eudragit L 100 microparticles (100x, 250x and 1200x, respectively). (C), (D) and (F) show three SEM images of Eudragit S 100 microparticles (100x, 500x and 2000x, respectively).

The fact that the microparticles produced by spray drying have a smooth surface, while the ones produced by spray freeze-drying are extremely porous, is not surprising. In spray drying, the solvent in the atomised droplets is quickly evaporated, while the solute migrates to the surface till a point when saturation occurs and a crust of solute forms on the surface (Abdul-Fattah et al., 2007). The formation of such crust is likely to confer a smooth appearance to the dried microparticle. Instead, in spray freeze-drying the droplets are snap-frozen into liquid nitrogen maintaining their original shape and size and the water in the form of ice is removed by sublimation. In this process, the saturated solutes maintain the original droplet frame and the ice water sublimates through the cavities, giving the typical “honeycomb” appearance to the final microparticles (Niwa et al., 2009).

#### 5.4.2.4 Encapsulation Efficiency and Gastro-Protective Properties

Table 5.6 illustrates the results of the HBcAg encapsulation efficiency and gastro-protection for the Eudragit L 100 and S 100 microparticles, produced by spray drying and by spray freeze-drying. The encapsulation efficiency was in all cases  $> 65\%$ ; however, the HBcAg release from the formulations after pre-incubation in SGF was  $< 15\%$  in all the formulations. Moreover, it seems that Eudragit spray dried microparticles could elicit

better HBcAg protection than those produced by spray-freeze drying and that microparticles produced with Eudragit S 100 were more effective than L 100 in preventing antigen degradation in SGF.

**Table 5.6. Microparticles encapsulation efficiency and gastro-protection (%, mean  $\pm$  SD; n = 3).**

| Microparticles type        | Encapsulation efficiency (%) | Gastro-protection-HBcAg Release (%) |
|----------------------------|------------------------------|-------------------------------------|
| <b>Spray drying</b>        |                              |                                     |
| L 100                      | 81.1 ( $\pm$ 4.7)            | 6.0 ( $\pm$ 1.2)                    |
| S 100                      | 65.5 ( $\pm$ 6.9)            | 11.3 ( $\pm$ 0.9)                   |
| <b>Spray freeze-drying</b> |                              |                                     |
| L 100                      | 72.9 ( $\pm$ 4.2)            | 2.7 ( $\pm$ 0.7)                    |
| S 100                      | 76.3 ( $\pm$ 2.4)            | 4.1 ( $\pm$ 0.5)                    |

The results obtained in terms of encapsulation efficiency suggest that HBcAg VLPs could withstand the spray drying and spray freeze-drying process, being effectively entrapped within the microparticles and mostly maintaining their native structure. This indicates that HBcAg could resist the heat stress, evaporation and atomisation during spray drying and the snap-freezing, atomisation and sublimation during the spray freeze-drying. Although Eudragit L 100 and S 100 are not commonly used as stabilising excipients in drying processes, they proved effective in entrapping the protein in its native form.

Nevertheless, the results relative to the release of HBcAg VLP under more basic pH, after 2 hours of pre-incubation in SGF, suggested that the enteric formulation offered limited gastric protection. The sandwich ELISA used in this assay detects only native HBcAg VLPs, therefore, it should be assumed that the circa 90% of HBcAg that was not recovered was either degraded or denatured during the SGF pre-incubation. It is probable that despite the fact that the microparticles produced remained intact, i.e. undissolved, during the acid incubation, they did not succeed in sheltering the inner part of the microparticles. The observation that such a high amount of VLP was degraded suggests that not only the surface of the microparticles was in contact with the acidic media, but also the internal matrix. This hypothesis is strongly supported by a study on Eudragit microparticles, in which the gastric burst of different actives from enteric microparticles was evaluated.

Small therapeutic molecules with different molecular weight were encapsulated within Eudragit S 100 microparticles by a solvent evaporation method and then the release of the active from the microparticles in acid media was investigated. Interestingly, a correlation between the molecular weight and the release of the active from the microparticles was found: generally molecules  $< 300$  Da were subjected to premature release in acid, compared to larger molecules, which were retained within the microparticles. It was suggested that the microparticles have a network microstructure that allowed molecules smaller than  $< 300$  Da to move out from the microparticulate matrix during the incubation in acid. This indicated that the acidic media could penetrate inside the microparticles and dissolve the small molecules, which were diffused out through the microparticles' pores (Alhnan et al., 2010). Therefore, there is a strong suggestion that Eudragit microparticles, although insoluble in acidic media, are not impermeable to them. The Eudragit particles are composed of a fine matrix, which can be penetrated by the acidic media. In this regard, large molecules are not protected by the acidic media, but they merely remain trapped within the microparticles, until these dissolve in alkaline media. Hence, an acid-labile product is likely to be degraded even when incorporated in an Eudragit particle.

In such a context, the results of the current study suggest that HBcAg VLPs were efficiently encapsulated within the microparticles, however, the acidic medium could penetrate the formulation and come into contact with the encapsulated antigens, probably allowing its denaturation. As a result, only a reduced amount of native protein could be retrieved. The fact that spray dried microparticles could protect the antigen to a higher extent than spray freeze-dried microparticles, obviously suggests that the smoother surface of the spray dried product (Figure 5.5) was less permeated by the denaturing SGF, compared to the "honeycomb", spongy-like structure of the spray freeze-dried microparticles (Figure 5.6). Furthermore, as the Eudragit L 100 polymeric chain contains double the amount of carboxylic groups than the S 100, which instead is richer in esters, implies that the Eudragit L 100 is more hydrophilic than the S 100. This suggests that Eudragit L 100 could induce more water uptake during the incubation in acid and therefore could result in greater HBcAg instability than Eudragit S 100.

Nevertheless, the relative low gastric protection achieved must be contextualised to the extremely high intrinsic instability of HBcAg in acid gastric fluids. For comparison it can

be mentioned that HBcAg, either purified or within the plant leaf, was completely degraded when incubated in SGF with or without pepsin (Chapter 4). Thus, the observation that circa 10% of native HBcAg VLP within the microparticles could resist degradation upon 2 hours incubation in SGF indicates that the formulation could remarkably improve the stability of such a sensitive antigen. However, the superior levels of enteric protection obtained with the coated tablets in Chapter 4 could not be achieved with the microparticles. In this regard, Professor Abdul Basit (University College London) suggested that the stabilisation of acid labile proteins in the gastric environment might require a thicker and more impermeable layer of protection, than that offered by the microparticulate matrix (personal communication).

Overall, it can be concluded that despite the fact that spray drying of Eudragit solutions containing HBcAg VLP enabled formation of microparticles containing stable VLPs, such microparticles provided only limited gastric protection to the antigen. It was hypothesised that the small size of the microparticles, combined with their porosity, allowed contact of the acid medium with the VLP during 2 hours incubation in SGF and hence led to the major degradation observed. In the case of spray freeze-drying the extremely porous structure of the microparticles further reduced HBcAg gastric protection.

### 5.4.3 Freeze-Drying

In this study freeze-drying was used for the production of HBcAg solid formulations, potentially usable for oral delivery. Four different formulations were tested in order to find the most suitable excipient that could stabilise the VLPs during the freeze-drying process and also maintain a stable physical state over time upon storage in different conditions. The aim was to find a suitable freeze-dried form that could be potentially processed into a dosage form for oral delivery (i.e. enteric coated tablets or capsules).

#### 5.4.3.1 Stability of Purified HBcAg upon Freeze-drying with Different Excipients

Figure 5.7 shows the stability of HBcAg in the re-suspended freeze-dried formulations. Figure 5.7 A represents the quantification of HBcAg VLP in the density gradient fractions of the re-suspended solid formulations of the antigen in glycine, lactose, mannitol and

trehalose. The immunoreactivity was calculated as a percentage ratio to the total HBcAg, present in the control and corresponding to the amount of HBcAg in each formulation prior to freeze-drying. In the control sample HBcAg VLPs were found mainly in the 30 and 40% (w/v) density bands, as typical for native HBcAg VLP (Birnbaum and Nassal, 1990). In the case of glycine and mannitol reduced immunoreactivity could be seen in the 30 and 40% (w/v) bands compared to the control. Instead in the case of lactose, the overall HBcAg detection was similar to that of the control, though more HBcAg was present in the 30% (w/v) band and less in the 40% (w/v) fraction. In the case of the trehalose, the presence of HBcAg in the density bands corresponding to intact HBcAg seemed intermediate between mannitol and lactose. Moreover, the HBcAg yield for each formulation was also calculated as the amount of HBcAg VLP present in the 30 and 40% (w/v) density fractions, compared to that of the control: 101.7%, 58.8%, 40.9%, 30.4% of HBcAg VLPs could be recovered in the lactose, trehalose, mannitol and glycine formulations, respectively.

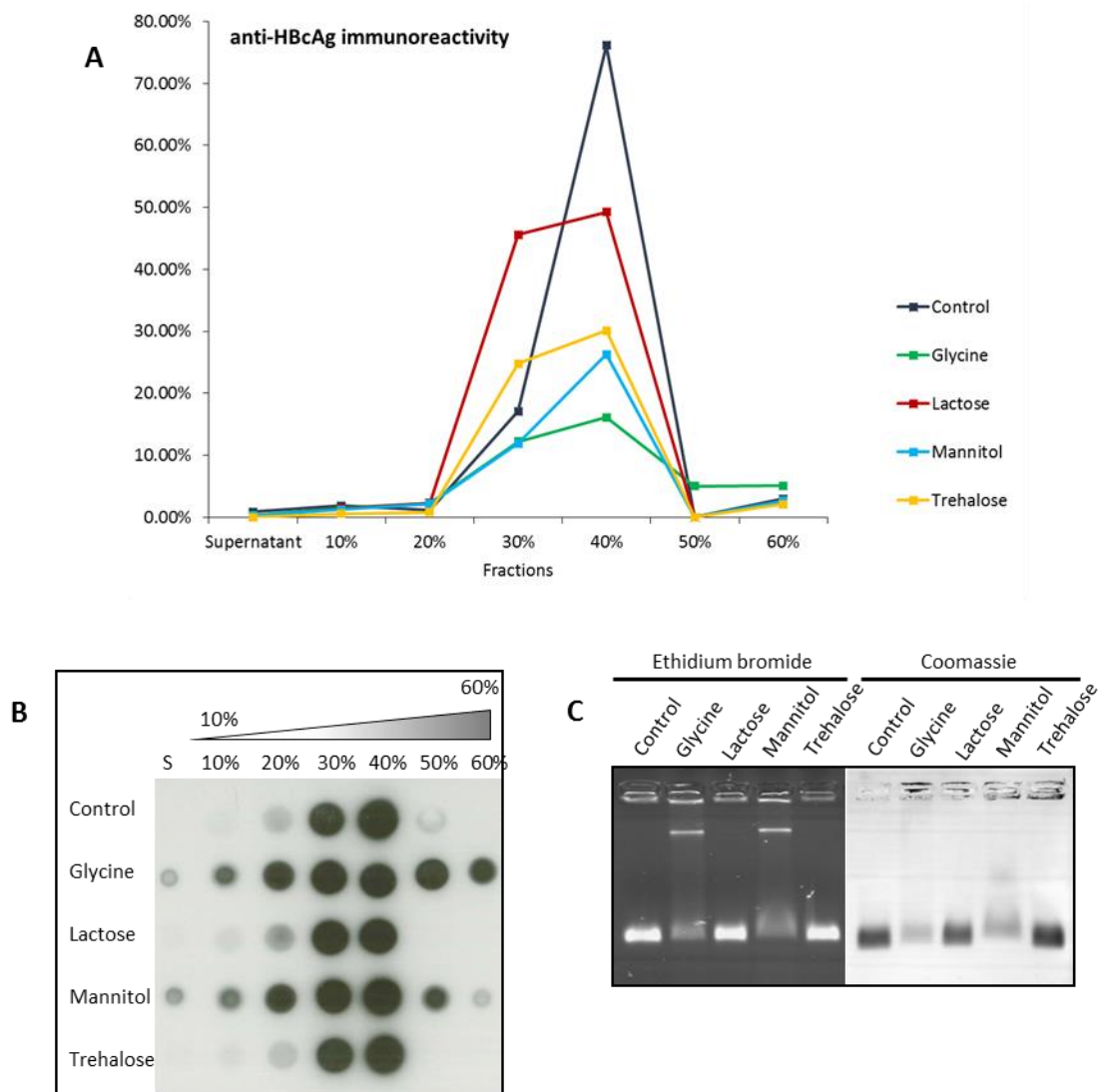


**Figure 5.7. Stability of HBcAg freeze-dried with different excipients.**

HBcAg was mixed with separate solutions of glycine, lactose, mannitol and trehalose in PBS. The four solutions were freeze-dried. After freeze-drying, the formulations were re-suspended and either separated by density gradient sedimentation or used for native agarose gels. Solutions of HBcAg in PBS were used as controls. (A) illustrates the sandwich ELISA quantification of the density gradients' fractions relative to the glycine, lactose, mannitol and trehalose freeze-dried formulations. HBcAg immunoreactivity is calculated as a percentage ratio to the total HBcAg present in the control. (B) shows the dot blot (monoclonal antibody) of the density gradients' fractions relative to the glycine, lactose, mannitol and trehalose freeze-dried formulations. (C) illustrates the ethidium bromide stained (left) and Coomassie stained (right) native agarose gel of the four re-suspended formulations.

Figure 5.7 B illustrates the distribution of HBcAg through the gradient, analysed by dot blot. This assay clearly shows that most anti-HBcAg immunoreactivity was present in the 30 and 40% (w/v) bands, corresponding to intact VLPs, in the control, the lactose and the

trehalose samples. However, in the case of glycine and mannitol samples, HBcAg could also be detected in other fractions of the gradients, corresponding to disassembled form of the antigen (supernatant, 10, 20% w/v) and to agglomerates (50 and 60% w/v). Figure 5.7 C illustrates native agarose gels, ethidium bromide stained and Comassie stained, of the four freeze-dried re-suspended formulations. In both gels VLP bands corresponding to that of the control, could be seen in both lactose and trehalose formulations. Instead in the case of glycine and mannitol the bands seemed more faint and smeared.

The sandwich ELISA assay is specific for native HBcAg VLP, while the monoclonal antibody used in dot blot and also used for the Western blot is able to detect denatured HBcAg. Therefore, the analysis of the sucrose gradients with both methods is complementary. The sandwich ELISA results provide evidence that HBcAg VLPs were mostly stable upon freeze-drying using lactose as a stabiliser. Decreasing HBcAg stabilisation was obtained, respectively, in the trehalose, mannitol and glycine formulations. In addition, the dot blot suggested that HBcAg VLPs were partially disassembled and agglomerated in the glycine and mannitol formulations, while HBcAg present in the lactose and trehalose formulations was mainly present as VLPs. Finally, the native agarose gel, which allows the detection of intact VLP encapsidating nucleic acids, confirmed the partial instability of the glycine and mannitol formulations observed in the previous assays.

HBcAg is stable upon several freeze-thawing cycles (Nath et al., 1992). Therefore, the main stability obstacle during the freeze-drying process of HBcAg remains dehydration. Stabilisers that act as lyoprotectants could therefore stabilise HBcAg during this process. Lactose and trehalose are two disaccharides often used as lyoprotectants in the freeze-drying of proteins. Upon freeze-drying these lyoprotectants tend to form an amorphous phase, which can act as a “water substitute” during the drying, forming hydrogen bonds with the protein and stabilising the protein (Abdul-Fattah et al., 2007; Costantino et al., 1998; Wang, 2000). Glycine and mannitol are instead often used as freeze-drying excipients, mainly as bulking agents, rather than lyoprotectants: this is due to the fact that they tend to crystallise upon freeze-drying and therefore dry as a stable crystalline form (Pyne et al., 2003). Crystalline components are not available in the glassy state as a substitute to the solvate water around the protein, hence they often elicit poorer protein

stabilisation than amorphous stabilisers (Wang, 2000). It is therefore not surprising that higher HBcAg VLP stability could be achieved using lactose and trehalose, than using glycine and mannitol. It can be supposed that the lactose and trehalose formulations contained higher amorphous components, thus enabling better VLP stabilisation. In the next Paragraph, the thermal analysis of the freeze-dried formulations is described in order to better evaluate the effect of the physical state of the lyoprotectant on the HBcAg stability upon freeze-drying. Furthermore, the thermal analysis will help to elucidate which formulation bears a more stable physical state under different humidity conditions.

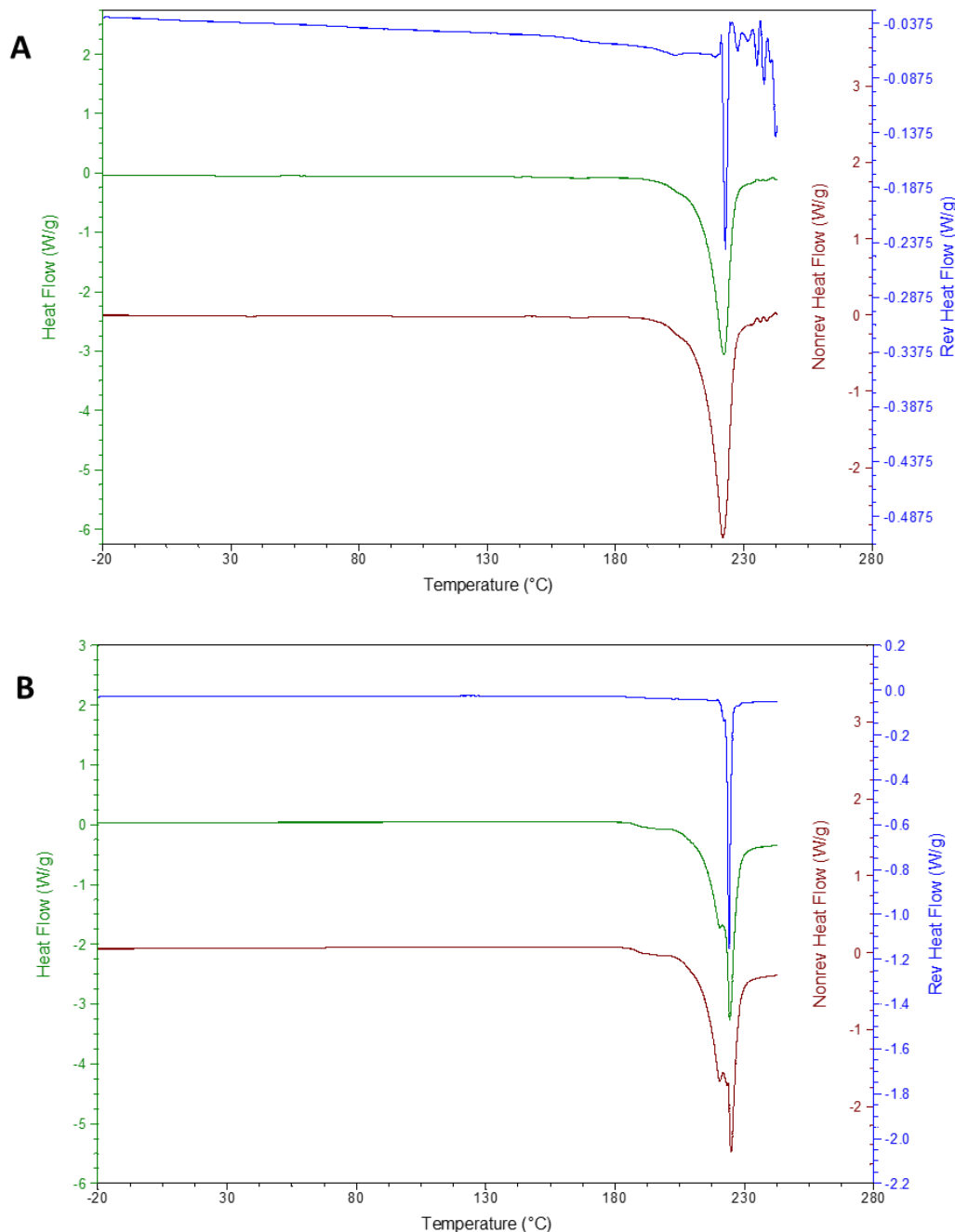
#### 5.4.3.2 Thermal Analysis of Freeze-dried Excipients

The freeze-dried material produced in this study could be further processed into an oral dosage form. For this purpose, the freeze-dried material should maintain a stable physical form during processing and storage under ambient conditions to prevent denaturation of the biopharmaceutical protein (Wang, 2000). Therefore, the evaluation of the stability of the physical form of the excipients used in the freeze-dried formulations is particularly relevant in this context. Moreover, such a study can also elucidate the relationship between HBcAg stabilisation and physical state of the stabiliser in the different formulations.

The surface water loss (assessed by TGA) and the relevant thermal events (extrapolated from the MTDSC thermograms) of freeze-dried "placebo" glycine (i.e. without the antigen) after storage at the two different humidity conditions are summarised in Table 5.7; the MTDSC thermograms are also showed in Figure 5.8. The surface water loss measured was similar for the glycine samples stored at 0% RH and 75% RH. Moreover, the MTDSC thermograms relative to the glycine samples stored at 0% RH (Figure 5.8 A) and 75% RH (Figure 5.8 B) show a weak endothermic phase transition at 166.5 °C and 192.8 °C, respectively, and a similar sharp peak at circa 220 °C. This profile is the typical profile of  $\gamma$ -crystalline form: this polymorph, being metastable, shows a characteristic phase transition that can range between 165 °C and 201 °C from the  $\gamma$ - to the  $\alpha$ -form (Perlovich et al., 2001). Sublimation and decomposition of the heat induced  $\alpha$ -form occurs at 210 to 250 °C (Yang et al., 2008). These results suggest that the freeze-dried glycine was present as  $\gamma$ -form regardless of the storage condition.

**Table 5.7. Summary of TGA/MTDSC thermograms of freeze-dried glycine (mean  $\pm$  SD, n = 3)**

| <b>RH (%)</b> | <b>Surface water loss (%)</b> | <b>Phase transition (<math>^{\circ}</math>C)</b> | <b>Sublimation and decomposition (<math>^{\circ}</math>C)</b> |
|---------------|-------------------------------|--|---|
| <b>0%</b>     | 0.26 ( $\pm$ 0.09)            | 166.5 ( $\pm$ 0.1)                               | 216.3 ( $\pm$ 0.2)  |
| <b>75%</b>    | 0.18 ( $\pm$ 0.05)            | 192.8 ( $\pm$ 1.2)                               | 220.5 ( $\pm$ 1.9)  |

**Figure 5.8. MTDSC thermograms of freeze-dried glycine.**

Freeze-dried glycine was stored at 0% RH or at 75% RH for 5 days and then analysed by MTDSC: (A) and (B) show the thermograms relative to 0% RH and 75% RH conditions, respectively.

Freeze-dried lactose surface water loss and main thermal events after storage at the two different humidity conditions are summarised in Table 5.8 and the MTDSC thermograms are shown in Figure 5.9. The freeze-dried lactose stored at 0% RH contained 1.74 % ( $\pm$  0.31) surface water. Moreover, the sample (Figure 5.9 A) shows a possible glass transition at circa 65 °C, but this transition was not clear and hence could not be reliably measured. However, for exclusion the freeze-dried lactose was suggested to be amorphous: in fact the  $\alpha$ -lactose forms are easily recognisable from a dehydration event at circa 135 to 155 °C, which is accompanied by water loss (Listiohadi and Hourigan, 2009). The MTDSC thermogram and the TGA of the freeze-dried lactose stored at 0% RH did not show such thermal event and the related water loss. Moreover, the  $\beta$ -anhydrous form typically contains very low surface water (Listiohadi and Hourigan, 2009), far lower than that measured for the freeze-dried lactose stored at 0% RH. Hence the latter sample is likely to be amorphous lactose. Instead the freeze-dried lactose stored at 75% RH (Figure 5.9 B) showed a re-crystallisation peak at 135 °C in the MTDSC thermogram, resulting in 4.65% weight loss, measured by TGA. This loss perfectly matches the stoichiometric loss of one molecule of water in each molecule of the lactose in the  $\alpha$ -monohydrate form, usually occurring at circa 135 to 155 °C (Buckton et al., 1998; Listiohadi and Hourigan, 2009). Therefore, both TGA and DSC plots strongly suggest that the freeze-dried lactose stored at 75% RH was the  $\alpha$ -monohydrate form.

**Table 5.8. Summary of TGA/MTDSC thermograms of freeze-dried lactose (mean  $\pm$  SD, n = 3).**

| RH (%) | Surface water loss (%) | Glass transition (°C) | Dehydration (°C) | Water loss at dehydration (%) | Melting point and decomposition (°C) |
|--------|------------------------|-----------------------|------------------|-------------------------------|--------------------------------------|
| 0%     | 1.74 ( $\pm$ 0.31)     | 67.6 ( $\pm$ 4.2)     | -                | -                             | > 185                                |
| 75%    | 0.31 ( $\pm$ 0.62)     | -                     | 135 ( $\pm$ 0.0) | 4.65 ( $\pm$ 0.06)            | > 185                                |

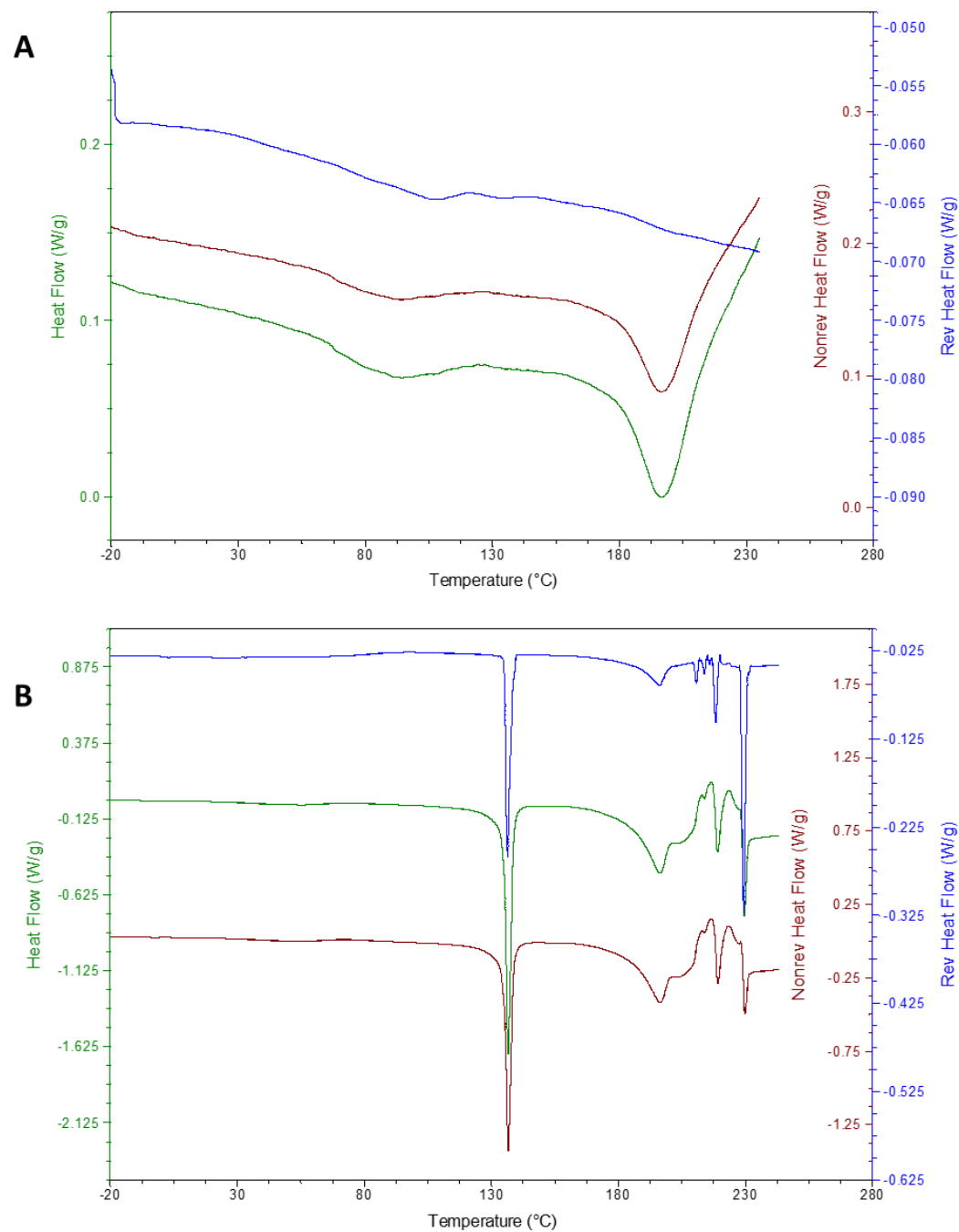


**Figure 5.9. MTDSC thermograms of freeze-dried lactose.**

Freeze-dried lactose was stored at 0% RH or at 75% RH for 5 days and then analysed by MTDSC: (A) and (B) show the thermograms relative to 0% RH and 75% RH conditions, respectively.

It is well documented in the literature that lactose solutions in water or salt mixtures when freeze-dried usually result in the formation of amorphous lactose, which is metastable and highly hygroscopic. Freeze-dried amorphous lactose tends to absorb moisture when it is exposed to humidity; the water acting as a plasticiser lowers the glass transition

temperature to a point where it matches the storage temperature. At this point lactose re-crystallises, losing the sorbed water; this process is temperature, time and water content dependent (Fakes et al., 2000; Herrington, 1934; Omar and Roos, 2007a; Roos, 2009). For instance, it was demonstrated that different freeze-dried lactose samples re-crystallised from the amorphous state at room temperature (22 to 23 °C) within 24 hours: amorphous freeze-dried lactose samples recrystallized when stored at RH > 44%, whereas amorphous freeze-dried lactose-salt mixtures recrystallized at RH > 54.4%. Moreover, storage at 76.1% RH resulted in re-crystallisation after only 3 to 4 hours (Omar and Roos, 2007a, 2007b). This is in accordance with the current study in which the freeze-dried lactose-PBS mixture produced by freeze-drying was in the amorphous state when stored at 0% RH and in the crystalline state when stored at 75% RH for 5 days, probably due to re-crystallisation of the metastable amorphous form. The influence of this phase transition process on the stabilisation of protein formulations will be discussed later.

The surface water loss and relevant thermal events of freeze-dried mannitol stored at 0% and 75% RH are detailed in Table 5.9 and the MTDSC thermograms are illustrated in Figure 5.10. The TGA and MTDSC analysis appeared very similar for the two storage conditions, suggesting that the mannitol form produced upon freeze-drying remained stable regardless of the storage condition. A first endothermic peak at 145.8 °C and 148.9 °C can be visualised for the samples stored at 0% RH and at 75% RH, respectively. Moreover, a second endothermic peak is present at 156.6 °C and 155.3 °C for the 0% RH and at 75% RH samples, respectively (Figure 5.10 A and B).

**Table 5.9. Summary of TGA/MTDSC thermograms of freeze-dried mannitol (mean  $\pm$  SD, n = 3).**

| RH (%) | Surface water loss (%) | 1 <sup>st</sup> Melting point (°C) | 2 <sup>nd</sup> Melting point (°C) |
|--------|------------------------|------------------------------------|------------------------------------|
| 0%     | 0.29 ( $\pm$ 0.17)     | 145.8 ( $\pm$ 3.8)                 | 148.9 ( $\pm$ 1.7)                 |
| 75%    | 0.23 ( $\pm$ 0.07)     | 156.6 ( $\pm$ 1)                   | 155.3 ( $\pm$ 0.1)                 |

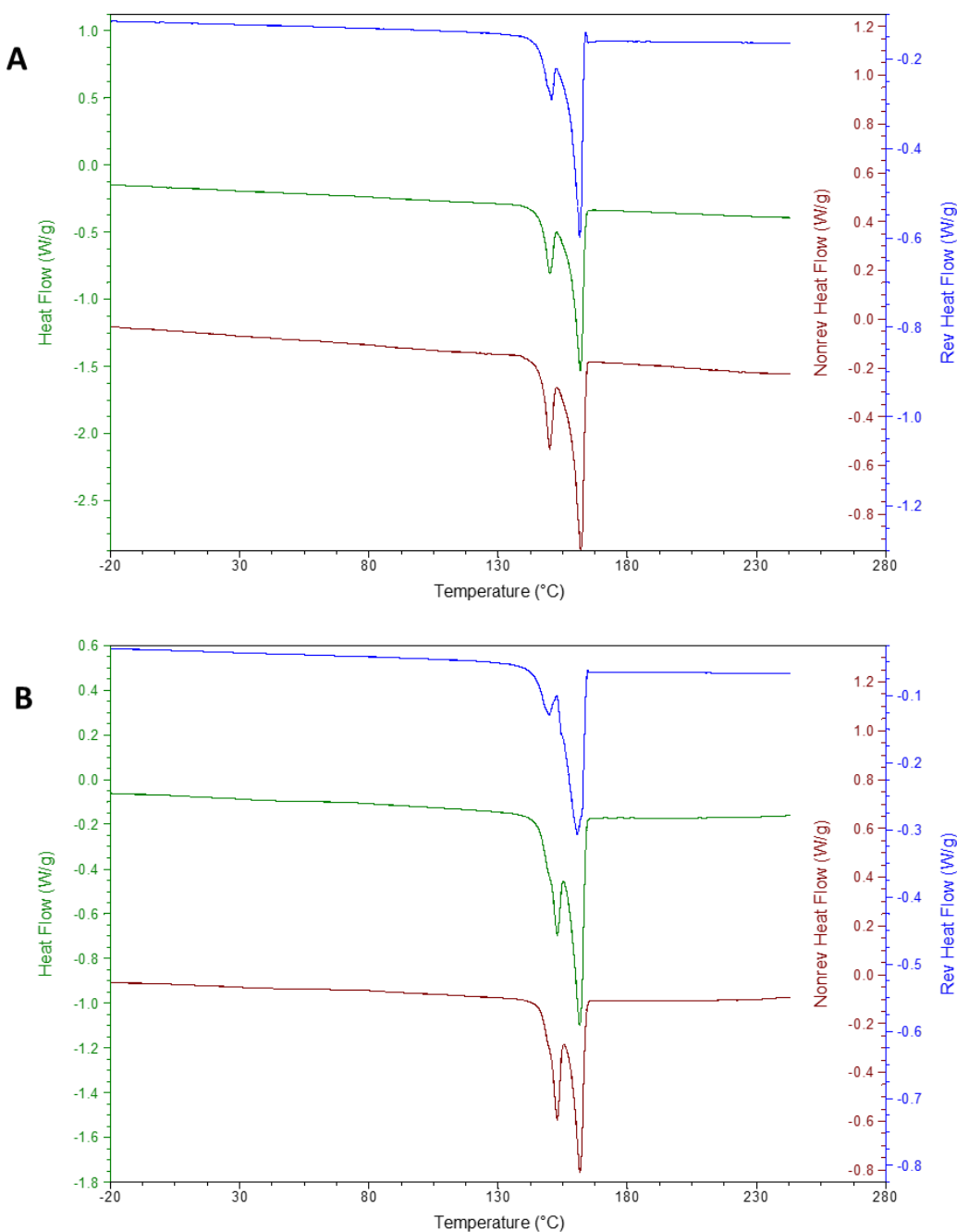


**Figure 5.10. MTDSC thermograms of freeze-dried mannitol.**

Freeze-dried mannitol was stored at 0% RH or at 75% RH for 5 days and then analysed by MTDSC: (A) and (B) show the thermograms relative to 0% RH and 75% RH conditions, respectively.

There was no loss of water measured by TGA at either of these two temperatures, suggesting that these thermal events were not associated with loss of water or crystallisation, but corresponded to the melting of anhydrous crystalline forms. Specifically, the first melting point could be attributed to the presence of  $\delta$ -mannitol, while

the second peak could correspond to the eutectic melting point of the  $\alpha$ - and  $\beta$ -mannitol polymorphs (Liao et al., 2007; Telang et al., 2003). The fact that the freeze-drying generally results in the formation of  $\alpha$ ,  $\beta$  and  $\delta$ -mannitol mixtures has already been reported; moreover, extensive thermal analysis studies suggested that the ratio between these three polymorphs is highly dependent on the mannitol concentration in the solution and on the freezing rate (Kim et al., 1998).

The surface water loss and the most important thermal events of freeze-dried trehalose stored at 0% RH and 75% RH are summarised in Table 5.10 and the MTDSC thermograms are illustrated in Figure 5.11. The two thermograms of the samples stored at 0% RH (Figure 5.11 A) and at 75% RH (Figure 5.11 B) showed very different profiles. The main thermal event of freeze-dried trehalose stored at 0% RH is a glass transition observed between 56.5 °C and 78.2 °C in the three replicates examined here. The glass transition was consistent with the presence of amorphous trehalose. However, based on the data included in McGarvey et al. (2003), the glass transition temperature seen here is slightly lower than that expected for the water content measured by TGA. This could most likely be explained by the presence of PBS in the current formulation, as this buffer has shown to lower the trehalose glass transition temperature in a concentration-dependent manner (Sitaula and Bhowmick, 2006).

**Table 5.10. Summary of TGA/MTDSC thermograms of freeze-dried trehalose (mean  $\pm$  SD, n = 3).**

| RH (%) | Surface water loss (%) | Glass transition (°C) | Dehydration (°C)  | Water loss at 1 <sup>st</sup> Melting dehydration point (°C) (%) | 1 <sup>st</sup> Melting point (°C) | 2 <sup>nd</sup> Melting point (°C) |
|--------|------------------------|-----------------------|-------------------|--|------------------------------------|------------------------------------|
| 0%     | 2.03 ( $\pm$ 0.27)     | 63.8 ( $\pm$ 12.5)    | -                 | -  | -                                  | -                                  |
| 75%    | 0.57 ( $\pm$ 0.3)      | -                     | 95.4 ( $\pm$ 1.4) | 8.94 ( $\pm$ 0.32)   | 124.6 ( $\pm$ 0.0)                 | 204.5 ( $\pm$ 1.2)                 |

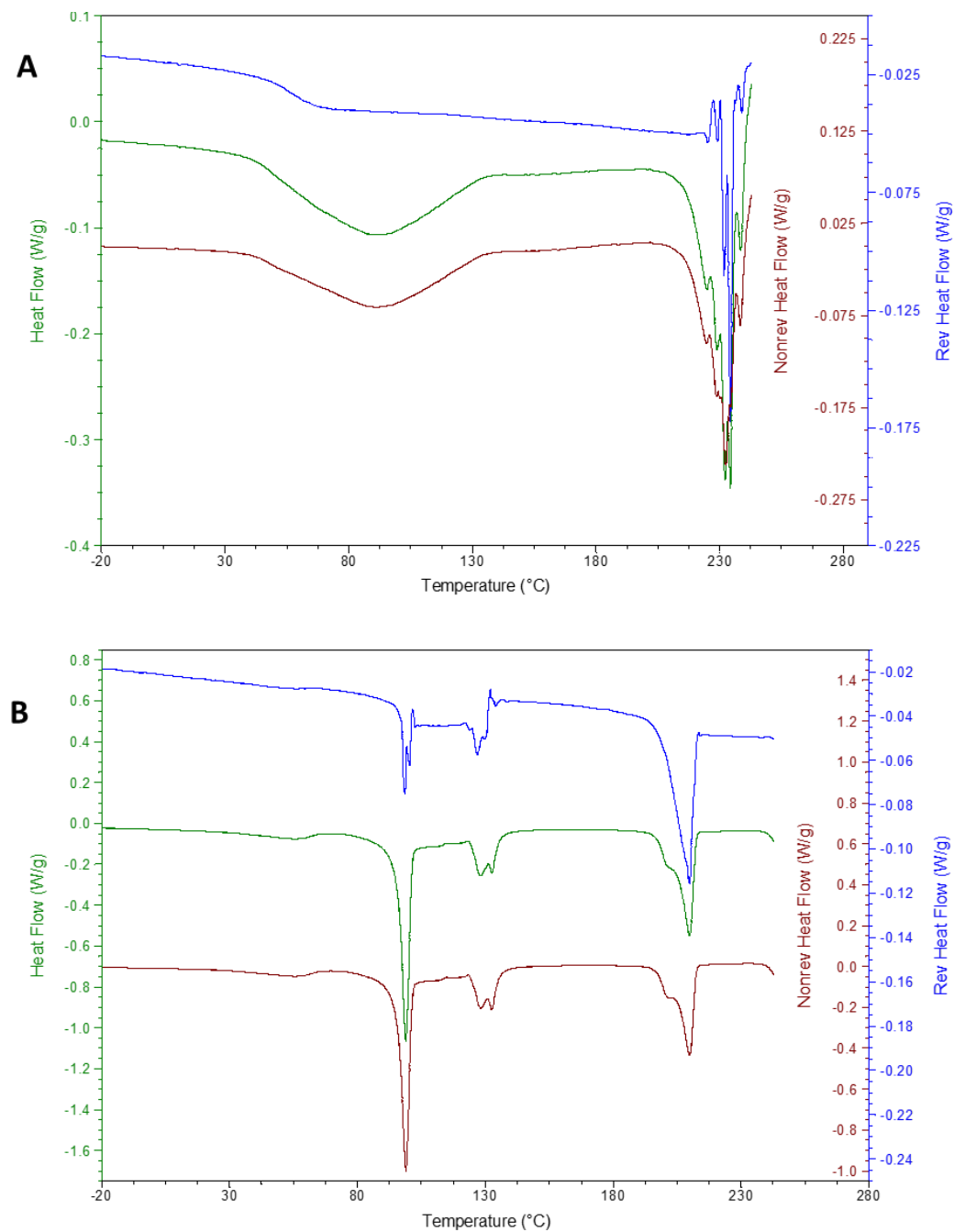


**Figure 5.11. MTDSC thermograms of freeze-dried trehalose.**

Freeze-dried trehalose was stored at 0% RH or at 75% RH for 5 days and then analysed by MTDSC: (A) and (B) show the thermograms relative to 0% RH and 75% RH conditions, respectively.

The thermal plot of the trehalose stored at 75% RH (Figure 5.11 B) suggests that trehalose was mainly present in a crystalline form. The endothermal peaks seen at 95.4 °C, 124.6 °C and 204.5 °C could correspond to the typical plot of the dihydrate trehalose form, as proposed in the work of McGarvey et al. (2003). However water loss at dehydration,

measured by TGA, was 8.94% ( $\pm$  0.32) and hence it was slightly lower than the 9.5% water loss, theoretically assigned to the loss of two molecules of water for a molecule of trehalose in the dihydrate form. This might suggest that a minimal percentage of the freeze-dried trehalose was present in a different form.

The main observation from the freeze-dried trehalose study is that, similarly to the lactose, the trehalose tended to remain amorphous upon storage at 0% RH, while it was present in a crystalline form upon storage at 75% RH. This strongly suggests that re-crystallisation occurred upon exposure to high moisture level. This is in accordance with what was extensively documented by others: amorphous trehalose has in fact shown to re-crystallise in a humidity and time-dependent manner (Fakes et al., 2000; Heljo et al., 2012; Hunter et al., 2010; Iglesias et al., 1997), where re-crystallisation of freeze-dried trehalose occurred at 43% RH in 500 hours of incubation and in less than 2 hours when the trehalose was stored at 60% RH (Heljo et al., 2012).

Overall, the thermal analysis results suggest that freeze-dried lactose and trehalose stored at 0% RH were amorphous, while glycine and mannitol, stored at the same conditions were present in a crystalline form. These results strongly suggest that the higher stabilisation offered by lactose and trehalose in the freeze-dried HBcAg VLP formulations (Paragraph 5.4.3.1) was due to the lyoprotecting effect of these excipients that freeze-dried as amorphous solids. This is in accordance with the principle that such excipients act as a “water substitute” for proteins by fulfilling the hydrogen bonding requisites, necessary to maintain stability (Carpenter and Crowe, 1989; Wang, 2000). Considering the in-process stability, lactose and trehalose might therefore seem ideal protein stabilisers.

Nevertheless, storage of the four excipients at 75% RH resulted in re-crystallisation of the metastable lactose and trehalose forms; in contrast both glycine and mannitol seemed to maintain their physical form. Re-crystallisation of amorphous excipients is one of the biggest complications in protein formulation development. In other words, the use of excipients in their amorphous state has been shown to stabilise protein formulations, however, crystallisation of the amorphous excipient upon storage can lead to undesirable protein aggregation and denaturation (Costantino et al., 1998; Wang, 2000). As the crystallisation process is moisture and temperature dependent, this phenomenon can

possibly be avoided by storing the formulation at low RH and temperature (i.e. sealed vials, storage in the fridge). However, the aim of this Chapter was to produce solid bulk materials containing stable forms of HBcAg VLPs that could be further processed into a solid dosage form. In this context, excipients that are so susceptible to temperature and humidity would not be ideal for further pharmaceutical processing under ambient conditions. For this reason crystalline excipients, such as glycine and mannitol probably would be more suitable, as they are more stable upon exposure to temperature and humidity. Nonetheless, crystalline excipients failed to stabilise HBcAg VLP upon freeze-drying, when compared to lactose and trehalose (Paragraph 5.4.3.1). It can be proposed that the ideal candidate excipients should stabilise the protein during the freeze-drying and at the same time maintain a stable physical form upon storage. Therefore, neither the amorphous excipients (i.e. lactose and trehalose) nor the crystalline ones (i.e. glycine and mannitol), as used in this study, would be real “winners”.

As a final remark it should also be underlined that lactose, being a reducing sugar, has the potential to react with primary and secondary amino groups of proteins via the Maillard reaction, leading to visible browning of the solid dosage form and to the formation of complexes able to destabilise proteins. However, the use of reducing sugars can be contemplated when these are the best stabilisers available (Akers, 2002; Wang, 2000). Therefore, their use should be assessed on case-by-case, balancing the requirement for immediate stabilisation of the protein and long-term product stability.

#### 5.4.4 Contextualisation and Relevance of the Findings

The conventional drying methods for drying biopharmaceutical proteins are spray drying, or more commonly freeze-drying (Abdul-Fattah et al., 2007). However, while there is broad research on the processing of proteins into dry formulations to be used for parenteral administration (Abdul-Fattah et al., 2007; Vehring, 2008; Wang, 2000), there is much narrower knowledge about the production of dry protein formulations for oral use. This is probably due to the fact that most protein-based therapeutics are still mainly delivered by injection. In this Chapter, the production of an oral dosage form of purified HBcAg VLP was investigated. Furthermore, given the high instability of this antigen in the gastric condition (Chapter 3), an ideal oral formulation of HBcAg should be gastro-protected. The

---

main hurdles to be overcome seemed the protein stabilisation and processing into a pharmaceutically stable dosage form.

Initially, drying by desiccation was attempted, as, despite the possible instability of the biopharmaceuticals when drying by desiccation, this risk could be counterbalanced by the low cost of such a process (Amorij et al., 2008). Therefore, HBcAg was mixed with the binder solution used for the wet granulation of drug-excipients mixtures ultimately used for compression. However, 80 to 95% of HBcAg VLPs were unstable upon drying of the wet mass in the oven or desiccator. For a term of comparison, it can be mentioned that when an engineered *Lactobacillus lactis* strain was mixed with the binder liquid used for the production of pellets by extrusion-spheronisation, 99% of the bacterial viability was lost (Huyghebaert et al., 2005b). Therefore, it can be suggested that the stabilisation of large biopharmaceutics requires more than a simple granulation process, generally suitable for processing of small molecules.

As an alternative approach spray drying, which is often a method of choice for the production of therapeutic proteins, was used. Moreover, by spray drying the VLPs with a pH responsive polymer, the antigen should be encapsulated into a pH-dependent microparticulate carrier. Thus, in a one-step process a gastro-protected formulation of the candidate vaccine should be produced. Furthermore, such small particles could be easily administered by gavage to small animals in *in vivo* studies, whereas conventional gastro-resistant oral dosage form (i.e. tablets or capsules) would be too big to be administered by gavage. Eudragit microparticles were successfully produced using this method and remarkably high encapsulation efficiency and antigen stability were achieved. However, the microparticles did not allow effective gastro-protection in simulated gastric fluid (SGF). Similarly, production of microparticles by spray freeze-drying did not enable effective gastro-protection. The outcome of these experiments underlines that both spray drying and spray freeze-drying techniques and the use of Eudragit are compatible for the stabilisation of the HBcAg VLP in the dry state. However, the morphology of the microparticles did not allow gastro-protection of such an acid and pepsin labile biopharmaceutical. Based on this research and on the evaluation of the morphology and functionality of Eudragit microparticles performed by Kendall et al. (2008), it can be concluded that pH-responsive particles cannot impede the medium-active contact, when

the formulation is incubated in acidic fluids. Hence, it can be suggested that this microencapsulation technique is not suitable for the protection of highly labile therapeutics from acid or pepsin. However, the pH-responsive microparticles could be used for intestinal targeted delivery of molecules, which are intrinsically gastro-stable.

Finally, freeze-drying of glycine, lactose, mannitol and trehalose solutions was used for the stabilisation of HBcAg VLP in dry state. In this case it was shown that the lactose and trehalose, which freeze-dried in their amorphous form, acted as good lyoprotectants and stabilised HBcAg VLP more than glycine and mannitol, which were present as crystalline solids. Despite the good in-process stabilisation that lactose and trehalose offered, further thermal studies elucidated that these excipients could be subjected to uncontrolled crystallisation if exposed to humidity. This would be unacceptable from a regulatory point of view as the physical structure of a formulation has to remain mainly unchanged; moreover this could cause destabilisation of the protein (i.e. HBcAg VLP) (Costantino et al., 1998; Wang, 2000). In case of a formulation for parenteral administration, the use of a lyoprotectant, which can be freeze-dried in the amorphous state, could be contemplated, as the dry product could be stored inside sealed vials. However, for further processing of the solid cake into solid dosage forms, moisture and temperature could become a problem for the stability of the biopharmaceutical. For instance, it has been reported that a bioengineered *Lactobacillus lactis* strain was formulated into a freeze-dried formulation, using skimmed milk as a lyoprotectant. The freeze-dried product was then compressed into mini-tablets. In order to prevent sticking of the dry powder all the handling was carried out at 20% RH. Despite this, the bacterial viability was only 15% immediately after the production of the tablets and dropped to complete viability loss after 1 week storage at 60% RH. The authors suggested that coating of a such hygroscopic formulation could have been difficult and incompatible with the bacterial viability (Huyghebaert et al., 2005b). The same research group obtained better results by using the freeze-dried material for the preparation of enteric coated capsules. However, this dosage form was still extremely sensitive to moisture and temperature (Huyghebaert et al., 2005a). These studies taken together suggest that freeze-dried formulations of labile biopharmaceutics are difficult to be processed, due to the intrinsic hygroscopicity and instability of the lyophilised material.

It can therefore be concluded that the production of a freeze-dried solid cake of amorphous excipients containing HBcAg VLPs can be an excellent approach for the drying of such a complex multimeric protein. Moreover, further processing of the lyophilised form into a gastro-protected solid dosage form could be contemplated; however, care must be taken in processing and storage of the material in controlled humidity and temperature conditions, in order to avoid excessive moisture absorption or undesired excipient crystallisation.

## 5.5 Conclusions

This Chapter offered an investigative screening into the stability of HBcAg upon drying for the potential development of oral formulations of this antigen. Mixing of HBcAg in the binder liquid used for the formulation of granules resulted in remarkable loss of antigenicity and hence it discouraged using this method for the drying of HBcAg VLPs. As an alternative, pH-responsive microparticles containing intact HBcAg VLPs were produced by spray drying and spray freeze-drying: the microparticles appeared regular and of spherical shape and enabled 65 to 81% encapsulation of native VLPs. However, incubation of the microparticles in simulated gastric fluid (SGF) resulted in a major loss of antigenicity, suggesting that the microparticles were permeable to the acidic media. Finally, HBcAg was freeze-dried using different stabilising excipients. Excipients that freeze-dried as glassy solids allowed good stabilisation of the VLP during the lyophilisation process. However, thermal studies revealed that, as typical for amorphous sugars, such formulations can be subjected to re-crystallisation. Therefore, it was suggested that the stability of the freeze-dried cakes upon further processing into oral dosage forms would require handling and storage in controlled humidity and temperature conditions.

Overall, the results from this Chapter confirm that in the case of enteric formulations of multimeric proteins (i.e. HBcAg VLP), the formulation of the protein into a stable dry form is only the initial challenge. Ensuring effective gastro-protection (i.e. in the microencapsulation), as well as sufficient stability of the formulation upon further processing into oral dosage forms (i.e. in the freeze-drying) can constitute more complex downstream hurdles. In this regard, it should be highlighted that film-coated gastro-resistant tablets using the freeze-dried plant-material expressing HBcAg were more effective and convenient formulations, as described in Chapter 4.

## 6 HBcAg Intestinal Permeability - an *in vitro* and *in vivo* Approach

### 6.1 Introduction

In the previous Chapters the ability of HBcAg VLP to survive the first gastro-intestinal (GI) barrier, i.e. the harsh GI environment, was evaluated. The influence of plant bio-encapsulation on the oral delivery of the antigen was also assessed. Then the formulation of HBcAg VLPs into solid dosage forms usable for oral delivery was investigated, using raw plant material expressing the antigen or using the purified antigen. In this Chapter, the ability of HBcAg to cross the second GI barrier, commonly considered the intestinal impermeability to macromolecules (Park et al., 2011), was evaluated.

VLPs differ from other, more extensively studied nanocarrier antigen-loaded oral vaccine candidates, as in VLPs the antigens self-assemble into particles, acting as self-carriers (discussed in Chapter 1). This is an obvious advantage in terms of formulation, because it eliminates the technological hurdles related to the active encapsulation, release and characterisation studies typical of nanoparticulate systems. Furthermore the high density of antigen display on the surface of VLPs is very likely to exhibit a more effective interaction with the Antigen-presenting cells (APC) and with cells of the immune system (Huang et al., 2004; Ludwig and Wagner, 2007; Noad and Roy, 2003; Plummer and Manchester, 2011). In addition to these unique advantages, VLPs, as all other nanoparticulate approaches, are generally subjected to higher absorption than small “soluble” antigens (Des Rieux et al., 2006). For these reasons VLPs could represent a promising oral candidate vaccine.

In this Chapter, the absorption of HBcAg VLPs in the Gut-associated lymphoid tissue (GALT) was investigated and is discussed. Intestinal absorption of various substances can be evaluated using cell culture models. In particular, a human colon carcinoma cell line, called Caco-2, has been shown to spontaneously differentiate into enterocytes when grown in culture; such enterocytes have functional and morphological features similar to those of small intestinal enterocytes (Hidalgo et al., 1989; Meunier et al., 1995). Due to these unique characteristics, Caco-2 cell mono-layers mounted on inserts' membranes have been extensively used as a model system to study the small intestinal absorption of drugs (Artursson, 1990; Hilgers et al., 1990; Yee, 1997). This can be an optimal method for

assessing the permeability of small molecules, which are generally well absorbed by the conventional absorptive epithelium of the small intestine (Le Ferrec et al., 2001). However, macromolecules, such as most vaccines, and nanoparticles are very poorly absorbed orally (Donovan et al., 1990). Therefore a model of solely Caco-2 enterocytes presents great limitations for the assessment of macromolecules' absorption and it does not offer a reliable physiological simulation. In this context a human model that includes the presence of M-cells of the Follicle-associated epithelium (FAE) was developed (Gullberg et al., 2000). M cells physiologically function as specialised transporters of antigens and nanoparticulate matters and they strategically overlay the immune system of the gut, playing a crucial role in delivering particulate matter for presentation to the underlying immune cells. Thus it is evident that a model including the FAE is much more appropriate for studies on oral vaccines and particulates (Gamboa and Leong, 2013).

### 6.1.1 Human FAE Uptake Assay

The FAE covering the Peyer's patches (PP) could be exploited by microorganisms and therapeutic candidates to breach the otherwise "impermeable" intestinal barrier. Based on the observation that M cell formation seems to be regulated by the stimulation of immune cells, Kerneis et al. (1997) developed an *in vitro* model of FAE using cell cultures. This model is based on the intercalation of mouse PP lymphocytes into Caco-2 epithelial monolayers. Lymphocytes had been shown to induce morphological and functional changes in the epithelial cells, consistent with the morphological transformation of undifferentiated enterocytes into M cells. This modelled FAE provided enhanced microorganism and particle sampling ability, when compared to the enterocytes mono-layer (Kernéis et al., 1997). In an updated model, the mouse B cells, used in the original model, were substituted with human Raji B lymphocytes and the functionality of the system was validated (Gullberg et al., 2000). This new version, which relies on an entirely human co-culture system, would more closely represent the physiology of human FAE and would therefore be more relevant for oral delivery studies. The assay is based on growing Caco-2 cells on normally oriented Transwell inserts: upon confluence of the cells into a tight mono-layer, Raji B lymphocytes are seeded at the bottom of the wells in a co-culture. The formation of M cells is considered to be completed after 4 to 6 days of co-culturing (Gullberg et al., 2000).

### **6.1.2 *In vivo* Ligated Intestinal Loop Model**

Before the advent of cell culture systems of the gut epithelium, the main technique to study the local intestinal absorption of bacteria, viruses or nanoparticles for oral vaccine research, involved direct injection of the formulations into surgically ligated small intestinal loops in animal models (Brayden et al., 2005). Several animal species have been used for this assay and different surgical procedures have been developed. The main advantage of this model over other more conventional oral administration techniques is that these intestinal ligated loop experiments can give absorption information, devoid from the potential limitation of the upstream GI instability and dilution. Therefore, this assay exclusively limits the investigation to the intestinal absorption (Gamboa and Leong, 2013). It is however clear that this cannot be considered an administration method, but it can only be used as an experimental model.

In this Chapter, the human *in vitro* cell culture model and a ligated small intestinal loop mice model were used in order to evaluate the absorption of the VLPs.

## **6.2 Materials**

### **6.2.1 Molecular Biology Media, Buffers and Solutions**

General media, buffers and solutions used in this study for bacterial growth, plant agro-infiltration and protein analysis are catalogued in Table 2.1 of Chapter 2.

### **6.2.2 Antibodies and Antigens**

Antibodies and antigens standards used for sandwich and direct ELISA are listed in Table 2.2 of Chapter 2. Antibodies used for immunohistochemistry (IHC) studies are presented in Table 6.1.

**Table 6.1 Antibodies used for immunohistochemistry (IHC) studies.**

| Antibody  | Antigen     | Supplier        | Application   |
|---|-------------|-----------------|---|
| Polyclonal rabbit<br>HBcAg antibody                   | HBcAg       | AbD Serotec, UK | IHC: 1:20 in 5% (v/v) FCS in PBS  |
| Anti-rabbit IgG<br>Alexa Fluor® 488<br>Host: Donkey   | Rabbit IgG  | Invitrogen, UK  | IHC: 1:250 in 5% (v/v) FCS in PBS<br>(Co-incubated with Anti-mouse<br>CD11c)            |
| Anti-rabbit IgG<br>Alexa Fluor® 594<br>Host: Donkey   | Rabbit IgG  | Invitrogen, UK  | IHC: 1:250 in 5% (v/v) FCS in PBS   |
| Anti-mouse CD11c<br>Alexa Fluor® 647<br>Host: Hamster | Mouse CD11c | AbD Serotec, UK | IHC: 1:50 in 5% (v/v) FCS in PBS<br>(Co-incubated with Anti-rabbit<br>Alexa Fluor® 488) |

### 6.2.3 Human FAE Model Components

This Paragraph will list the materials used in the cell culture model.

#### 6.2.3.1 Cell Lines

Human colon carcinoma Caco-2 cells and Human Burkitt's lymphoma Raji B were obtained from the American Type Culture Collection (ATCC). Both cell lines were mycoplasma free.

#### 6.2.3.2 Cell Culture Media, Chemicals and Plates

Dulbecco modified Eagle's minimal essential medium (DMEM), Roswell Park Memorial Institute (RPMI) 1640 medium, L-glutamine, penicillin/streptomycin, non-essential amino-acids, sodium pyruvate and trypsin/EDTA (0.25% w/v) were purchased from Sigma (UK) and used as received. Fetal bovine serum (FBS) was bought from Invitrogen Gibco (UK). Transwell inserts (6.5 mm diameter, 3.0  $\mu$ m pore size) were purchased from Corning Glass, Costar (UK).

### 6.2.3.3 Experimental Instruments

The electrical resistance system (Millicell-ERS) was bought from Millipore (UK).

### 6.2.4 *In vivo* Loop Study Materials

Isoflurane (Isoflo) was bought from Abbott Laboratories (UK). Microslides Superforst Plus Blue were purchased from VWR International (UK). CelLytic<sup>TM</sup> MT, Protease Inhibitor Cocktail and Anti-rabbit IgG-FITC antibody in goat were purchased from Sigma (UK). Silgard 184 silicon elastomer was bought from Dow Corning (Belgium). Saponin (8 to 25%) was bought from Sigma (UK). All materials were used as received.

## 6.3 Methods

This Paragraph briefly describes both the human FAE uptake assay and the *in vivo* VLP uptake assay and the methods used for the quantification of VLP in both models. Fluorescent microscopy and immunohistochemistry studies are also described.

### 6.3.1 Transport of HBcAg VLPs through the Human FAE Model

#### 6.3.1.1 *In vitro* Human FAE Culture

Caco-2 cells were cultivated in 75 mL plastic flasks in a medium composed of DMEM and supplemented with 10% (v/v) FBS, 1% (v/v) non-essential amino-acids, 1% (v/v) penicillin/streptomycin and 1% (v/v) sodium pyruvate, at a temperature of 37 °C and CO<sub>2</sub> level of 5%. The medium was refreshed every 2 to 3 days. The confluence of the cells at the bottom of the flask was monitored using an optical microscope: when circa 80% of confluence was reached, Caco-2 cells were subcultured. This cell passage was performed every 4 to 5 days: the media was removed and the cells were incubated in 5 mL trypsin/EDTA for 5 to 10 minutes for trypsinisation. When the Caco-2 cells were fully detached from the bottom of the flask, they were immediately spun on a centrifuge rotor at 1000 g for 5 minutes and the pellet was then re-suspended in fresh DMEM medium and split into four new flasks. Raji B cells were grown in 75 mL plastic flasks in RPMI medium supplemented with 10% (v/v) FBS, 1% (v/v) L-glutamine and 1% (v/v) penicillin/streptomycin at 37 °C and 5% CO<sub>2</sub> level. Raji B cells suspensions were

---

subcultured by splitting the cultures at a ratio of 1:10 and replenishing with fresh media every 5 to 7 days.

Caco-2 cells were used between the 55<sup>th</sup> and 63<sup>rd</sup> passages, following a previously described protocol (Des Rieux et al., 2005; Gullberg et al., 2000; Man et al., 2008). Upon 80% confluence, Caco-2 cells harvested by trypsinisation were re-suspended in fresh medium and  $5 \times 10^5$  cells in 200  $\mu\text{L}$  of medium were seeded onto the upper face of Transwell inserts. The cells were cultured on the filters in an incubator at 37 °C and 5% CO<sub>2</sub> and the medium was changed on alternate days. The formation of a tight cellular mono-layer was assessed by monitoring transepithelial electric resistance (TEER) throughout this period using Millicell-ERS. After 10-11 days,  $1 \times 10^6$  Raji B cells in a suspension of a total volume of 600  $\mu\text{L}$  were added to the lower chamber of the Transwell and incubated at 37 °C and 5% CO<sub>2</sub> level. The medium in the co-culture was refreshed daily: all the medium was changed in the apical side of the insert, while only half of the medium was replenished each time in the basolateral side, taking good care not to remove Raji B cells mostly sedimented at the bottom. The co-culture was maintained for 4-5 days prior to transport experiments. The maintenance of integrity of the cell mono-layer was monitored by TEER measurements. Corresponding Caco-2 mono-cultures were prepared identically; however, the Raji B cells were not added.

### 6.3.1.2 VLP Transport

HBcAg VLPs were used for this assay: plant expressed HBcAg VLPs were extracted from the leaves, purified through sucrose gradient, dialysed against PBS and concentrated into a stock suspension (described in Chapter 2). The stock suspension was quantified by ELISA, diluted in PBS to the desired concentration and filtered through 0.22  $\mu\text{m}$  membrane filters. Finally the VLPs suspension was used for the transport studies.

TEER values of the mono-layers were monitored before and after the experiments. The lower compartment of the Transwells containing mono- and co-cultures was washed with sterile PBS. After 15 minutes equilibration, the medium from the apical inserts was removed and replaced with 100  $\mu\text{L}$  HBcAg suspensions of different concentrations or PBS, and 600  $\mu\text{L}$  of fresh PBS were added to the basolateral compartments. Three Transwells

were used for each concentration in order to obtain a biological triplicate ( $n = 3$ ) for both the co-culture (FAE mono-layer) and the control mono-culture (conventional absorptive epithelium mono-layer). Transwell plates were kept in an incubator at a temperature of 37 °C and 5% CO<sub>2</sub> level. The content of the basal compartments was sampled after three hours of incubation. HBcAg content of the samples, collected from the basolateral side, was quantified by sandwich ELISA.

Cell culture set-up of the human FAE and its functional relevance for transport studies have been summarised in Figure 6.1.

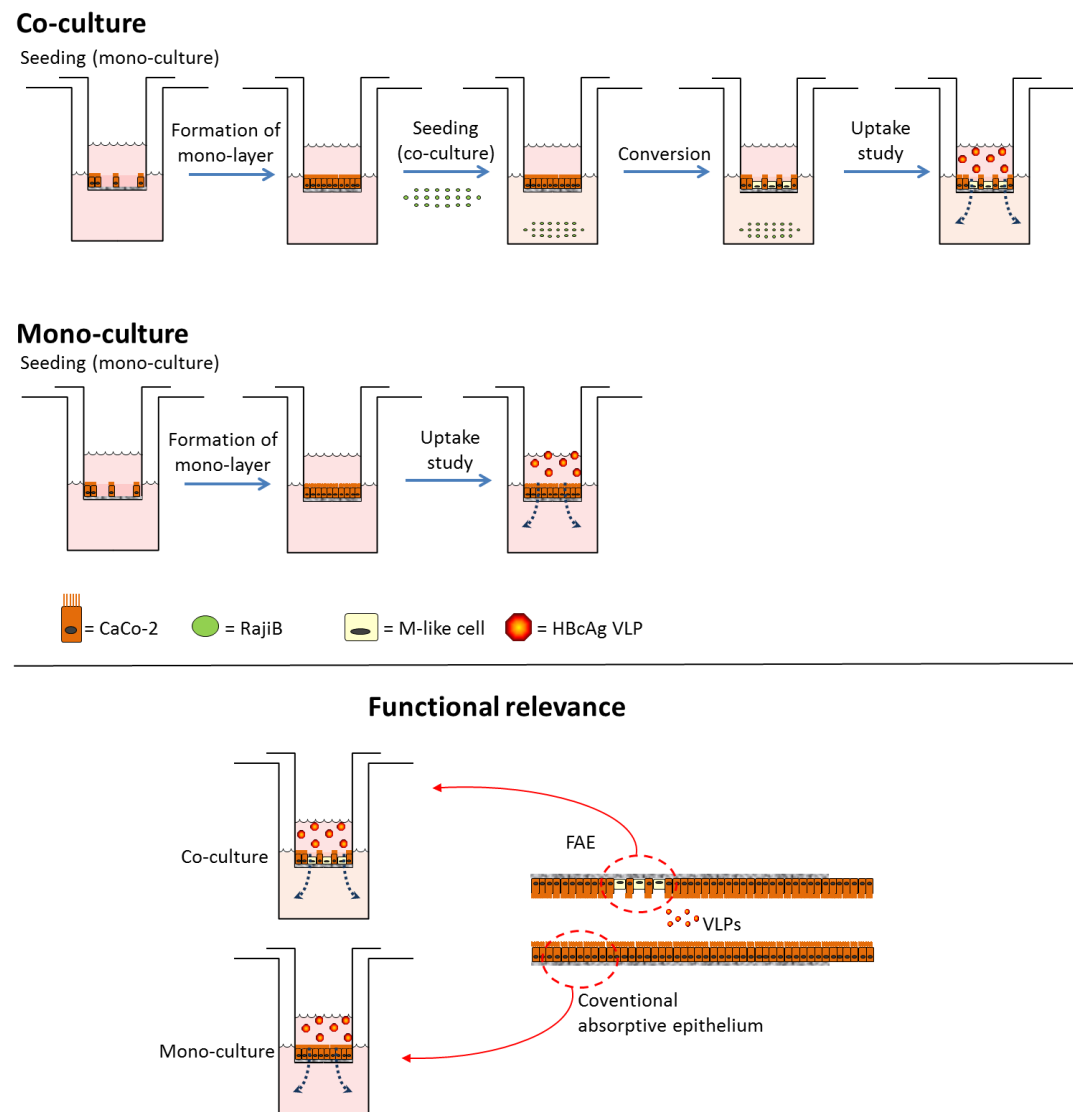


**Figure 6.1. Representation of the human FAE model.**

The top image illustrates how Caco-2 cell mono-layers were co-cultured with Raji B cells to induce the formation of M cells. In parallel, Caco-2 cell mono-cultures were used as a control. Transport studies were performed by evaluating the passage of HBcAg VLPs from the apical to the basolateral chamber. The bottom image shows the biological significance of this model: this fully functional small intestinal epithelium model enables the evaluation of both co-culture absorption and mono-culture absorption. The co-culture and the mono-culture mimic respectively the FAE and the conventional absorptive epithelium, respectively.

### 6.3.1.3 Quantification of Transport and $P_{app}$

The amount of HBcAg VLPs transported through the FAE mono-layer and through the undifferentiated epithelium mono-layer was quantified by indirect and sandwich ELISA. Results from the same experiments were expressed as amount of the donor solution for

each given loaded dose (Des Rieux et al., 2005) and as an apparent permeability ( $P_{app}$  in cm/s) (Slütter et al., 2009). Apparent permeability ( $P_{app}$ ) is calculated as follows:

$$P_{app} = \frac{\Delta Q}{\Delta t A C_0} \quad \text{Eq. (6.1)}$$

Where  $\Delta Q$  is the amount of HBcAg ( $\mu\text{g}$ ) present in the basal compartment as a function of time ( $t$ , in s),  $A$  is the area of the Transwell (in  $\text{cm}^2$ ),  $\Delta t$  is the time (in s) and  $C_0$  is the concentration of HBcAg (in  $\mu\text{g/mL}$ ) in the donor solution. The hypothesis that HBcAg transport was concentration-dependent was evaluated by a 2-tailed t-test for the two doses used. Statistical significance between results obtained with the FAE mono-layer and those obtained with the undifferentiated epithelium mono-layer at different doses was also assessed by a 2-tailed a t-test.

### 6.3.2 *In vivo* VLP Uptake Assay

#### 6.3.2.1 VLPs Preparation and Quantification

Four different formulations were prepared for this study and they include:

- HBcAg VLPs: plant expressed HBcAg was extracted from the leaves, purified through a sucrose gradient, dialysed against PBS and concentrated into a stock solution by ultrafiltration. The stock solution was then quantified by sandwich ELISA, diluted to 5 mg/mL in PBS and filtered through membrane filters.
- Heterotandem cores-GFP (CoHe7e-eGFP): plant expressed CoHe7e-eGFP was extracted from the leaves purified through a sucrose gradient and dialysed against PBS. Purified VLPs were then layered on the top of a second sucrose gradient in order to maximise the concentration of VLPs. CoHe7e-eGFP was then quantified by direct ELISA.
- VLP binding Green fluorescent protein (VLP-GFP): an innovative VLP, developed by Hadrien Peyret (JIC, unpublished data), was also employed for this study. This plant-expressed VLP makes use of the HBcAg amino-acidic sequence as a scaffold

to carry antibodies that are specific for GFP. The monomeric protein containing HBcAg sequence and the anti-GFP antibody is a 54 kDa protein which assembles into circa 30 nm diameter polymeric VLP. This particle was shown to strongly bind plant-expressed GFP (Hadrien Peyret lab notebook and personal communication). A stock of VLP-GFP, with the VLP already bound to the GFP, was kindly donated by Hadrien Peyret (JIC) and the sample was partially purified: upstream pre-incubation of the VLP with GFP, determined the formation of a particulate antigen-antibody interaction complex.

- Green fluorescent protein (GFP): GFP was also expressed in plant, using the *-HT* protein expression system (Sainsbury and Lomonossoff, 2008), combined with the pEAQ vector system (Sainsbury et al. 2009). GFP was extracted from plant as a clarified total protein crude extract and it was not further purified. This sample was also kindly donated by Hadrien Peyret (JIC).

The four formulations were analysed by Coomassie stained SDS-PAGE in order to evaluate the purity of the samples and to obtain a semi-quantitative estimation of VLP-GFP and GFP. The VLP suspensions were ultimately used for the transport studies.

### 6.3.2.2 Small Intestinal Loop Assay

11 to 12 weeks old c57BL/6 mice (Charles River, Margate, UK), maintained in an access-restricted room under conventional conditions were used for the study. The experiments were conducted under the guidelines of the Scientific Procedures Animal Act (1986) of the United Kingdom. Mice were starved overnight, anaesthetised by inhalation of isoflurane and kept under anaesthesia for the whole duration of the surgical procedure.

The manual handling of the animals as well as the surgical procedures were kindly carried out by Prof. Claudio Nicoletti and Miss Nadezhda Gicheva, in my presence.

Five animals were employed in this study:

- Mouse 1 was unchallenged (Control).
- Mouse 2 was challenged with HBcAg VLP for 15 minutes.

- Mouse 3 was challenged with HBcAg VLP for 40 minutes.
- Mouse 4 was challenged with VLP-GFP for 40 minutes.
- Mouse 5 was challenged with CoHe7e-eGFP and GFP for 40 minutes, whereby each formulation was injected into a different ligated loop.

Briefly, the abdomen of the mouse was opened by an incision along the midline, in order to expose the small intestine. Once the ileum was identified, small loops of a few centimeters in length were isolated by ligation with cotton surgical threads. Generally two or three Peyer's Patches (PPs) were contained within one loop. Different VLP formulations in PBS were injected into the loop via a 30 G needle. No more than circa 40 to 50  $\mu$ L of formulation per cm of loop was injected, as injection of higher volumes would have excessively distended the intestinal wall, diluting the mucus and possibly altering the epithelial barriers. Subsequent to the intra-luminal injection, the intestine was returned into the abdominal cavity. Care was taken in order to maintain a normal blood supply and the abdominal cavity was frequently moisturised with sterile PBS during the incubation time. At the end of the experiments (15 or 40 minutes), the mice were sacrificed by cervical dislocation. Immediately after, the tracts of intestine containing the loops were excised and removed from the body cavity. Sections of the gut of less than 0.5 cm in length, containing single PPs or non-lymphoid tissue, were cut. At this point, the tissues were handed to me for the final processing.

PP or non-lymphoid tissues were pinned out in Petri dishes coated with silicone elastomer. The luminal side was washed three times with a solution of dithiothreitol (DTT) 0.5 mM in PBS, in order to remove unbound protein and loosely adherent mucus. After a final rinse with PBS, the PP tissues were placed within two slices of pig liver (forming a "pig liver sandwich") and snap-frozen via an isopentane/dry ice bath. The pig liver sandwiches were created in order to maintain the delicate surfaces of the intestinal tissue protected from physical damage, during storage and handling (i.e. sectioning). Those samples were preserved at -80 °C until cryo-sectioning. The cryo-sections were used for fluorescent microscopy and IHC studies. Loops challenged with HBcAg formulation (mouse 2 and 3) were also destined for protein quantification. Two PPs per animal were washed with DTT and PBS and directly snap-frozen (without the formation of pig liver sandwich). Pieces of

non-lymphoid intestinal tissue from the same loops were also cut, washed with DTT and PBS and snap-frozen. Mouse 1, used as a control, was not challenged with any formulation. Following sacrifice, the intestinal tissue of the ileum was processed in a similar way to the other treated mice.

### 6.3.2.3 HBcAg Quantification in Intestinal Tissue

HBcAg was quantified in mouse 1, 2 and 3 following the loop study. Initially, frozen tissues were de-frosted. In the case of lymphoid tissues, excisions along the perimeter of the PPs were made, in order to isolate them from the remaining intestinal wall. Two PPs from the same mouse were pooled and weighed together. In parallel two tracts of non-lymphoid tissue were also weighed. An extraction buffer composed of 1% (v/v) Protease Inhibitor in CelLytic<sup>TM</sup> MT was freshly prepared. The tissues were homogenised using a FastPrep machine (MP Biomedicals) at a setting of 4.0 for 40 seconds. Approximately 20 µL of extraction buffer per mg of intestinal tissue were used. Each extracted sample was used for the quantification of tissue total protein and for HBcAg quantification. Total protein content was measured using a NanoDrop Spectrophotometer (Thermo Scientific), which automatically calculates the total protein concentration by measuring the UV absorbance at 280 nm. HBcAg concentration was measured using the sandwich ELISA assay described in Chapter 2. The presence of HBcAg VLPs in the PPs and the non-lymphoid tissues was calculated as weight of HBcAg in tissue per mg of total protein.

### 6.3.2.4 Fluorescent Microscopy and Immunohistochemistry

Frozen pig liver sandwiches were cryo-sectioned using a Leica CM1100 cryostat. Sections of 8 µm thickness were captured on microscopy slides. Slides were used for either fluorescence microscopy or immunohistochemistry.

For fluorescent microscopy, the slides were initially fixed in acetone at -20 °C for 8 minutes. Then they were washed three times with PBS and were covered with either 0.5 µg/mL 4', 6-diamidino-2-phenylindole (DAPI) or 1 µg/mL propidium iodide (PI) nuclear staining for subsequent analysis under a Zeiss Axioplan fluorescent microscope. Alternatively slides were not fixed and were directly stained with DAPI or PI. This was

attempted in order to eliminate the possible fluorescence quenching, due to the fixative-induced denaturation.

For immunohistochemistry studies, the sections were initially fixed and / or permabilised.

Several fixation approaches have been attempted:

- Acetone at -20 °C for 8 minutes.
- Methanol at -20 °C for 8 minutes.
- Paraformaldehyde (4%) at 4 °C for 10 minutes.
- Paraformaldehyde (4%) at 4 °C for 10 minutes, followed by methanol at -20 °C for 8 minutes.
- Paraformaldehyde (4%) at 4 °C for 10 minutes, followed by two washes with 0.1% saponin PBS.
- No fixation

Slides were then washed three times with PBS and blocked with 10% (v/v) FBS in PBS for 1 hour. After a further wash with PBS, the sections were incubated with rabbit anti-HBcAg antibody 5% FBS in PBS for 1 hour 30 minutes. Following three washes with PBS, the sections were incubated with donkey anti-rabbit secondary antibody 5% FBS (v/v) in PBS for a further 1 hour. After three washes with PBS, the sections were stained with DAPI and the fluorescence was analysed using the microscope. In some sections, the secondary antibody was co-incubated with anti CD11c antibody.

In the case of slides fixed with paraformaldehyde and washed with saponin, all washes and incubation steps were carried out using 0.1% saponin in PBS, rather than PBS which was used in all other cases.

At least two slides of the same tissue were imaged independently to confirm reproducibility.

#### **6.4 Results and Discussion**

A qualitative and quantitative investigation of the transport of plant-expressed HBcAg-derived VLPs in the complex intestinal mucosa is presented in the Paragraph. This

investigation has been tackled from two different sides. First, a FAE cell culture model provided an entirely human platform for an accurate simulation of the functional intestinal epithelium. Second, *in vivo* transport studies in mice allowed evaluation the transport under more physiological conditions.

#### **6.4.1 *In vitro* Human FAE Culture- Transport of HBcAg VLPs**

HBcAg, used in this study, was expressed in plant, extracted and purified according to the methods described in Chapter 2. Three different doses of HBcAg were prepared for the transport studies. The presence of HBcAg was quantified by sandwich ELISA.

The absorption of HBcAg VLPs in the GALT of the small intestine was evaluated by a human cell culture model, using Transwell plates (Gullberg et al., 2000). Since it was first published 13 years ago this entirely human FAE model has earned the reputation of an elegant experimental technique and it has been used widely to investigate empty nanobeads and loaded nanoparticles absorption (Des Rieux et al., 2007, 2005; Kadiyala et al., 2010; Slütter et al., 2009; Yoo et al., 2010).

This study introduces a novel application of the FAE model where it has been exploited to evaluate the intestinal absorption of a virus-like, particulate vaccine candidate. In this study, the co-culture model was used to simulate the FAE of the GALT, while the mono-culture, resembling the conventional absorptive epithelium, was kept as a control. The insert of the Transwell consists of two compartments separated by a filter, on which a layer of epithelial cells constitutes a physical barrier. The integrity of this physical barrier was monitored by TEER measurements, with the TEER values being above  $200 \Omega \text{ cm}^2$  for both co-cultures and mono-cultures before and after the experiments. Such TEER values are compatible with the integrity of mono-layers: it was in fact reported that TEER values of more than  $175 \Omega \text{ cm}^2$  represent cell mono-layers of uncompromised integrity (Gullberg, 2005; Gullberg et al., 2006). HBcAg transport through the mono-layer was measured by sandwich ELISA. Control wells where the co-culture and mono-culture were incubated with PBS did not show any unspecific immunoreactivity. Dose-dependency of the transport and permeability of the co-culture compared to the control mono-cultured were evaluated.

#### 6.4.1.1 Dose-dependent Transport

Firstly, the dose dependency of HBcAg transport was calculated. Three different doses of HBcAg (i.e. 200 µg, 50 µg and 10 µg) in 0.1 mL aliquots were added at the apical side of the inserts and the passage to the basolateral compartments was measured. The graph in Figure 6.2 illustrates the quantity of HBcAg measured in the basolateral compartment at the end of the experiment at the three different doses, in the FAE and in the control cell mono-layer. Within the co-culture model, the transport of HBcAg clearly increased with increasing loaded doses: doses of 200 µg demonstrated a 3.7 fold increase in HBcAg transported compared to 50 µg doses ( $P < 0.01$ ), while the latter demonstrated a 2.6 fold increase compared to 10 µg doses ( $P < 0.01$ ). Therefore, the transport proved to be dose-dependent in the FAE.

Absorption by the conventional epithelium is less relevant for vaccines and nanoparticles delivery; however, it was measured for control purposes. In the mono-culture, used as a control, doses of 200 µg resulted in a 15.9 fold increase in transport compared to 50 µg doses ( $P < 0.05$ ), while doses of 50 µg resulted in only a 1.1 fold transport increase compared to 10 µg doses ( $P > 0.05$ ). It could therefore be concluded that among the three doses used there was a significant difference between the first two highest doses, but not between the second and the third. This could be explained by the very low quantities of HBcAg transported through the conventional Caco-2 mono-layer. The HBcAg measured values were quite close to the lower detection limit of the ELISA assay. In other words, extremely low levels of absorption can be difficult to be accurately calculated. Probably for the same reason, the evaluation of dose-dependency in the conventional Caco-2 mono-layer was ignored in a similar research using nanobeads (Des Rieux et al., 2005).

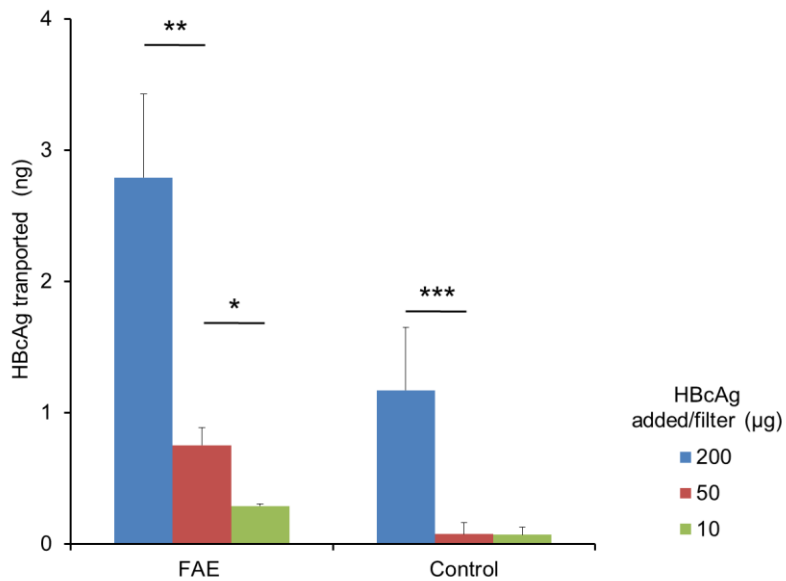


**Figure 6.2. HBcAg dose-dependent transport.**

Different doses (200 µg, 50 µg, 10 µg) of purified HBcAg in PBS were added to the insert above the cell monolayers and incubated for 3 hours. The transport of VLPs was significantly higher in the FAE incubated at higher doses. In the control mono-culture the transport was significantly higher when the loaded dose was 200 µg, compared to 50 µg, while there was no significant difference between loaded doses of 10 µg, compared to 50 µg. Statistical significance was calculated using a 2-tailed T-test. Significant differences values are indicated by \* =  $P < 0.001$ ; \*\* =  $P < 0.005$  and \*\*\*  $P < 0.05$ . Error bars indicate SD,  $n = 3$ .

#### 6.4.1.2 FAE Selective Transport

This model was most importantly used to assess whether HBcAg VLPs could be selectively transported by the FAE, rather than being transported via the conventional absorptive epithelium (control). For this purpose the data from the previous experiment were also expressed in terms of HBcAg permeability through the co-culture as compared to the control mono-culture. To enable  $P_{app}$  to be calculated, as shown in Eq. 6.1, the amount of antigen on the donor side was expressed as a concentration (2000, 500 and 100 µg/mL), rather than as an amount (200, 50 and 10 µg). The results are shown in Figure 6.3.

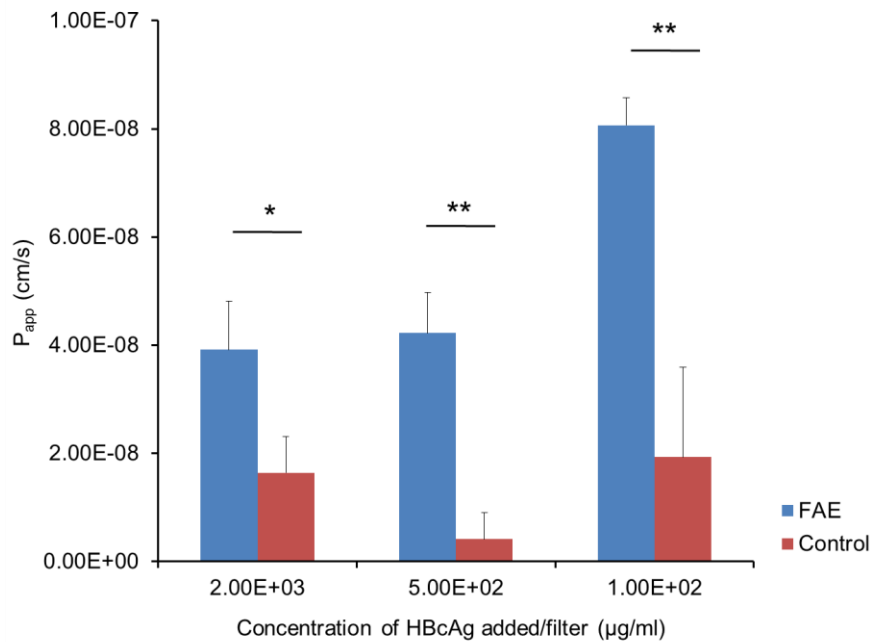


**Figure 6.3. HBcAg transport in co-culture and mono-culture.**

HBcAg transport is given as values of apparent permeability ( $P_{app}$ ) as a function of concentration of HBcAg added. The transport was assessed at three different loaded concentrations (2000, 500 and 100  $\mu\text{g/mL}$ ) of purified HBcAg VLP in PBS. Statistical significance was calculated using a 2-tailed T-test. Significant differences in  $P_{app}$  values between FAE and control are indicated by \* and \*\* where  $P$  is  $< 0.05$  and  $< 0.005$ , respectively. Error bars indicate SD,  $n = 3$ .

At the three concentrations the permeability and hence the transport was always significantly higher in the FAE than in the control (i.e. the conventional absorptive epithelium). The permeability in co-culture was 2.4 fold ( $P < 0.05$ ), 10.2 fold ( $p < 0.005$ ) and 4.2 fold ( $P < 0.005$ ) higher than that in mono-culture, at concentrations of 2000, 500 and 100  $\mu\text{g/mL}$ , respectively.

A similar investigation using the FAE model, but on antigen-loaded nanoparticles of larger size, gave comparable results in terms of ratio of particles transported in the FAE and in the control mono-layer, statistical significance and the order of magnitude of  $P_{app}$  (Slütter et al., 2009). Nevertheless, those experimental *in vitro* models have a certain degree of variability and therefore numerical data should be evaluated in terms of order of magnitude of transport, rather than as absolute values (Des Rieux et al., 2005). The order of magnitude of  $P_{app}$  obtained in this study and stated by others (Slütter et al., 2009) is extremely low compared to the typical permeability ( $P_{app}$ ) values obtained with small

molecules in *in vitro* Caco-2 cells mono-layers: drugs or peptides with *in vitro*  $P_{app}$  values less than  $10^{-7}$  cm/s have been correlated to *in vivo* oral absorption in humans of less than 1% (Artursson and Karlsson, 1991). In the case of macromolecules and particles of nano-dimensions, oral absorption of less than 1% is not surprising: it has been shown that absorption of PEG of only 2 kDa molecular weight is less than 2% when administered to mice via gavage (Donovan et al., 1990). For a size comparison it can be remembered that HBcAg VLP are made by the self-assembly of 180 or 240 units of 20 kDa-long proteins. The low bioavailability of conventional macromolecular therapeutics via the oral route is generally accepted and it is debatable whether oral therapeutic effect will be ever achieved, given this limitation (Florence, 2005). However in vaccine delivery, the dose-dependency is much less stringent than in therapeutic drug delivery (McConnell et al., 2008b) and paradoxically too high doses or too high absorption could induce tolerance (Garside et al., 1995; Mayer et al., 2001). Therefore, low intestinal absorption might not be as much of an issue with vaccines as with therapeutics. Nevertheless case by case considerations must be undertaken.

#### 6.4.2 HBcAg VLPs Intestinal Permeability *In vivo*

The intestinal uptake of HBcAg VLPs was further studied using the small intestinal loop model. This intestinal *in vivo in situ* model has been used to study the oral delivery of nanoparticles (Porta et al., 1992; Primard et al., 2010; Prosser et al., 1998). It is indeed an exceptionally useful tool to selectively analyse the small intestinal absorption: the inoculation of particles dispersion directly into the animal gut, compared to oral gavage, allows the study of oral absorption *in vivo*, circumventing the risk of excessive dilution and / or degradation of the compound in the upper GI. On the other hand, the invasive surgical procedure does not allow the animal to be kept alive for long after the surgery (Gamboa and Leong, 2013): it is therefore not possible, in most cases, to collect efficacy data or to measure antibodies production for vaccine candidates.

##### 6.4.2.1 Fluorescent VLPs and HBcAg Preparation

Concentrated HBcAg VLP was quantified by sandwich ELISA and diluted in PBS to a final concentration of 5 mg/mL. CoHe7e-eGFP was concentrated by two consecutive

sucrose gradients and quantified by direct ELISA. A final concentration of CoHe7e-eGFP of 80 µg/mL was measured using HBcAg as a standard.

Furthermore the four formulations used in this Chapter including HBcAg, CoHe7e-eGFP, VLP-GFP and GFP (Paragraph 6.4.2.1) had been analysed by Coomassie stained SDS-PAGE, as shown in Figure 6.4. HBcAg (lane 5) showed a degree of purity comparable to the commercially available recombinant HBcAg standards (lanes 2 and 6). CoHe7e-eGFP (lane 3) was slightly less pure. VLP-GFP (lane 1) and GFP (lane 4) were not pure; however, this experiment did not require highly purified formulations, because of the non-parenteral route of administration and the short incubation time. In the case of VLP-GFP, both the monomer forming the VLP and the bound GFP were distinguishable. By comparison with the known concentration of the standards, the concentration of VLP-GFP (lane 1) can be visually estimated as circa 0.5 to 1 mg/mL (lanes 2 and 6). Considering the complexity of these three-layered particles, i.e. VLP-GFP, it would have been difficult to develop a more precise quantification technique. Finally, GFP concentration can be estimated as circa 2 mg/mL.

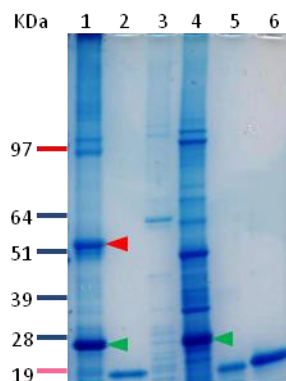


**Figure 6.4. Coomassie stained SDS-PAGE gel of the formulations administered.**  
HBcAg, CoHe7e-eGFP, VLP-GFP and GFP preparations were analysed. Lane 1 = VLP-GFP; 2 = 0.2 mg/mL yeast HBcAg standard; 3 = CoHe7e-eGFP, 4 = GFP; 5 = HBcAg (diluted 1/20) and 6 = 0.5 mg/mL yeast HBcAg standard. Green arrows indicate GFP and the red arrow denotes the HBcAg-based monomer containing the anti-GFP antibody.

#### 6.4.2.2 Localisation of Fluorescent VLPs in the Ileum

Ligated intestinal loops of mice 4 and 5 were inoculated with fluorescent VLPs as described in Paragraph 6.4.2.2: mouse 4 was inoculated with VLP-GFP, while mouse 5 was inoculated with CoHe7e-eGFP in one ligated loop and with GFP in the other.

CoHe7e-eGFP was used as a fluorescent-labelled version of the wild-type HBcAg. The loop inoculated with CoHe7e-eGFP did not show any more fluorescence than the background fluorescence shown in the control mouse. The 80 µg/mL dose inoculated into the gut was probably too low for the detection of this construct by fluorescent microscopy. However, given the tendency of the tandem VLPs proteins (i.e. CoHe7e-eGFP) to aggregate (personal communication with Dr Eva Thuenemann), it could be problematic to obtain considerably higher concentrations by means of ultrafiltration.

VLP-GFP is a complex structure, displaying antibodies on the HBcAg moiety that bind GFP. By comparing the transport of soluble GFP with that of the VLP-GFP particulate complex, it should have been possible to demonstrate whether the HBcAg-based scaffold could improve the oral absorption of GFP by the gut. In fact, if the encapsulation of a protein into nanoparticles can increase its absorption (Ensign et al., 2011; Kammona and Kiparissides, 2012), it is possible that a protein bound to a VLP frame by an antigen-antibody interaction could similarly increase the protein permeability into the gut. For this purpose, HBcAg-based VLP could function as an efficient oral carrier for proteins bound to its particulate structure. Unfortunately, intestinal tissues inoculated with GFP or VLP-GFP did not show any more fluorescence than the background fluorescence observed in the control mouse. Several fixation protocols (Paragraph 6.3.2.4) were attempted or alternatively the slides were analysed without any fixation, to assess whether the fixation methodology was the cause of this "negative" result. However even in the absence of fixation, the result was the same, suggesting that the low fluorescence was not due to the possible denaturation effect of the fixative on the GFP, which could result in partial or total fluorescence quenching. Figure 6.5 shows fluorescence microscopy images relative to an intestinal section of the control mouse and another intestinal section of the mouse inoculated with VLP-GFP.

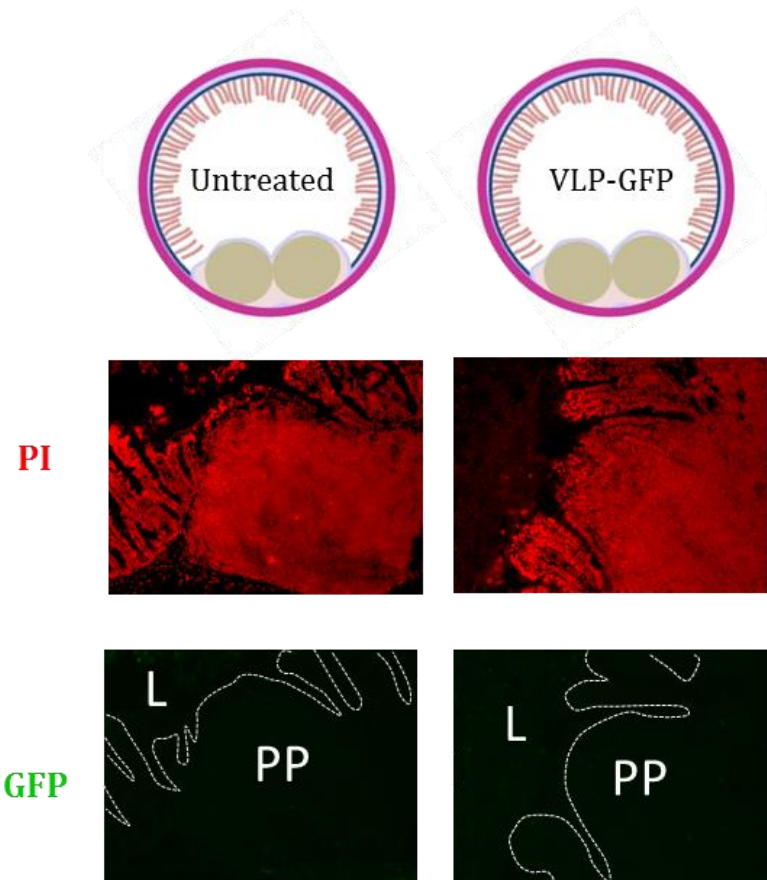


**Figure 6.5. Fluorescence microscopy.**

Microscopy images (10x), obtained for PPs areas of an untreated intestinal section, control, (left side) and of an *in vivo* ligated ileal loop inoculated with the VLP-GFP preparation and incubated 40 minutes (right side). PI (red) shows the tissue structure; GFP (green) shows the green fluorescence in the tissue. L = Lumen, PP = Peyer's patches. The white line outlines the interface between the tissue and the lumen. Images obtained without fixation.

The lack of detection of “soluble” GFP is not surprising, as other studies have shown that GFP-containing constructs without an appropriate adjuvant vehicle do not elicit detectable fluorescence in the ileum of mice, when given by oral gavage or inoculated in ligated intestinal loops (Kadaoui and Corthésy, 2007; Limaye et al., 2006). However, one would have expected that the binding of GFP to a VLP structure could have increased the intestinal penetration of GFP. It is unclear whether this enhanced intestinal penetration did not occur at all or whether (perhaps more likely) VLP-GFP particles were simply undetectable. The latter suggestion could be possibly related to a certain degree of instability of the VLP-GFP complex in the relatively harsh intestinal lumen environment that strongly diminished the fluorescence down to undetectable levels. This seems particularly probable considering that the GFP is bound to the VLP only through numerous

weak Van der Waals interactions. Furthermore, high green auto-fluorescence background was noticed in the mice guts and this is also documented by other immunofluorescent images of the gut found in the literature (Limaye et al., 2006). Therefore, the fluorescence background, probably intrinsic to the tissue, could mask the fluorescence of the GFP, if the latter signal was not strong enough. Finally it has been reported that GFP is highly degraded when incubated in simulated intestinal fluid (Richards et al., 2003); therefore, it is also possible to hypothesise that GFP was partially or totally digested during the incubation in the intestinal fluids of the mice gut.

Overall the dose inoculated into the mice loop was considerably high for both GFP and VLP-GFP and far higher than potentially therapeutic doses. However searching into literature, enormous doses up to almost 5 mg of fluorescent nano-beads have been inoculated into loops of just 1.5 cm, in order to study their permeability in mouse intestine by fluorescent microscopy (Primard et al., 2010). In this study circa 100-fold fewer particles were inoculated into the intestinal loops. Accordingly, a possible approach to obtain better results could be to increase the concentration of the formulation of at least one order of magnitude, provided that such high concentrations of protein are compatible with protein physical stability and do not lead to agglomeration or instability of the VLP complex.

#### **6.4.2.3 Immunological Localisation of HBcAg in the Ileum**

HBcAg VLPs can be expressed and purified in high-yield in plants much more efficiently than the more complex CoHe7e-eGFP (Chapter 2) and VLP-GFP constructs. However, HBcAg VLPs are not fluorescently labelled, and an alternative approach to fluorescent microscopy was used to assess their permeability in the gut. Immunohistochemistry (IHC) studies as well as tissue homogenisation, followed by VLP quantification were carried out (Paragraph 6.4.2.3 and 6.4.2.4), in order to understand the fate of HBcAg VLPs after short-term intraluminal intestinal incubation.

For the IHC studies, several fixation and permeabilisation combinations were employed on the tissue sections. The best compromise between epitopes retrieval and maintenance of

integrity of the tissue structure was achieved using acetone for the fixation-permeabilisation step.

Firstly the fate of HBcAg in the intestinal ileum was assessed by comparing the detection of anti-HBcAg antibody in an untreated ileal tissue (control) to that in an ileal tissue acquired from a loop, inoculated with a 5 mg/mL dose of HBcAg (40-50  $\mu$ L/cm of loop) for 15 and 40 minutes. HBcAg VLPs were detected by monitoring the fluorescent signals emitted from the Alexa 594 secondary antibody, bound to the anti-HBcAg primary antibody. DAPI cellular staining was used to outline the section structure. Figure 6.6 shows the microscopy image of untreated intestinal sections (control), for the villi (left side) and PPs (right side) areas. DAPI (blue) shows the tissue structure (top); Alexa 594 (red) shows the HBcAg immunoreactivity (middle) and DAPI + Alexa 594 (red + blue) show the merged images (bottom). The absence of red fluorescent signal confirmed the lack of unspecific binding or background fluorescence in both the PP and villi areas.

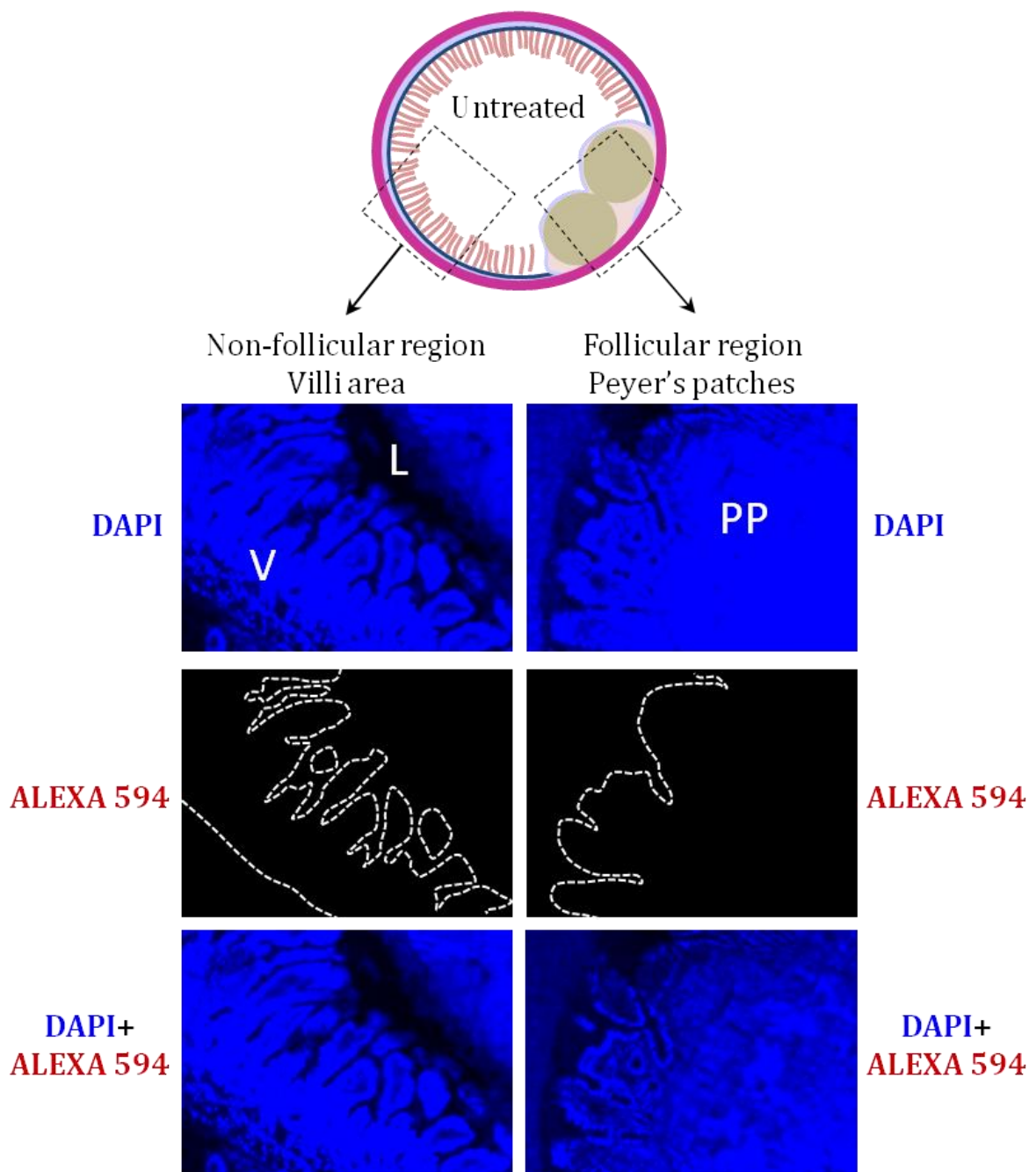


**Figure 6.6. IHC of intestinal sections (control).**

Microscopy images (10x), obtained for villi (left side) and PPs (right side) areas, of untreated (i.e. non-inoculated) intestinal sections (control). DAPI (blue) shows the tissue structure; Alexa 594 (red) shows the HBcAg immunoreactivity and DAPI + Alexa 594 (red + blue) show the merged images. L = Lumen, V = Villi; PP = Peyer's patches. The white line outlines the interface between the tissue (i.e. villi or PPs) and the lumen.

On the other hand Figure 6.7 shows intestinal cryosections, following an *in vivo* ligated ileal loop inoculated with 5 mg/mL HBcAg (40-50  $\mu$ L/cm of loop) and incubated for 15 minutes. Images were obtained for villi (left side) and PPs (right side) areas. In these

images, red fluorescence, corresponding to HBcAg immunoreactivity, was present in the mucus of the ileum in both follicular and non-follicular regions. In the follicular region, most of the red fluorescence was accumulated mainly at the interface between the epithelium of the PP and the lumen and only very few dots were detected inside the PP epithelium. At an incubation time of 15 minutes, it could be concluded that some HBcAg VLPs could penetrate the first intestinal barrier constituted by the mucus. However, the penetration through the second barrier, i.e. the epithelium, seemed minimal in both non-follicular and follicular (Peyer's patches) regions.

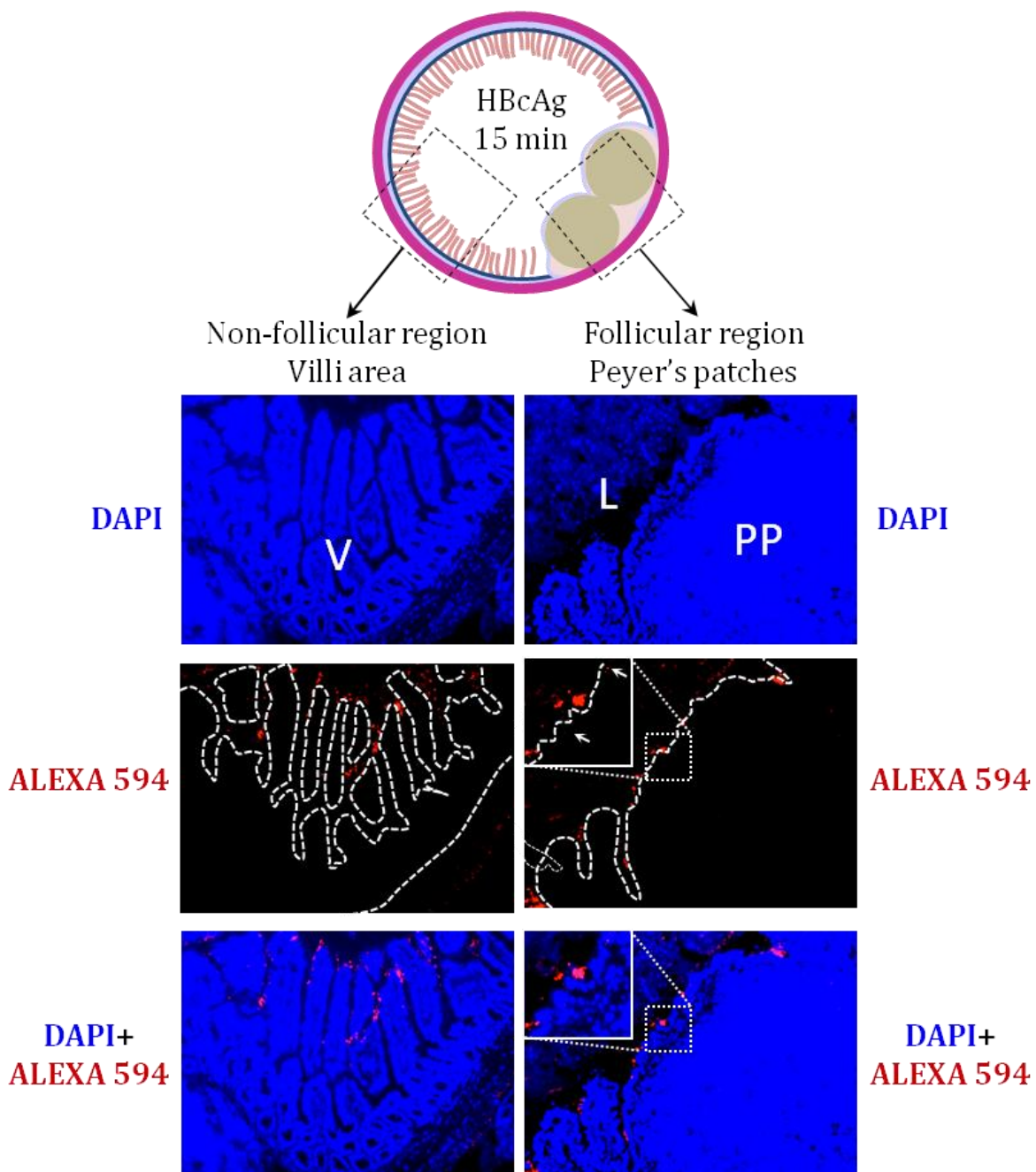


**Figure 6.7. IHC of intestinal sections after 15 minutes incubation with HBcAg.**  
 Microscopy images (10x), obtained for villi (left side) and PPs (right side) areas, of an *in vivo* ligated ileal loop inoculated with 5 mg/mL HBcAg and incubated for 15 minutes. DAPI (blue) shows the tissue structure and Alexa 594 (red) shows the HBcAg immunoreactivity. DAPI + Alexa 594 (red+blue) shows the merged images. L = Lumen, V = Villi; PP = Peyer's patches. The white line outlines the interface between the tissue (i.e. villi or PPs) and the lumen. Enlarged images of the PP epithelium illustrate HBcAg uptake inside the PP, as indicated by the white arrows.

The effect of increasing the incubation time of HBcAg in the ileal lumen is illustrated in Figure 6.8. The ileal sections, following 40 minutes incubation of HBcAg into the intestinal ligated loop, showed much stronger HBcAg immunoreactivity in the mucus than that observed after 15 minutes incubation, in both villus and PP areas. Furthermore, red fluorescence corresponding to HBcAg immunoreactivity was seen clearly in the PP below the epithelial interface with the lumen and a few dots were also present more internally in the follicular region. Limited red fluorescence could be also seen on a few villi. Overall, the images demonstrate that a longer incubation time favoured the penetration of HBcAg VLPs through the mucus barrier and supported a certain internalisation of VLPs particularly into the PP.

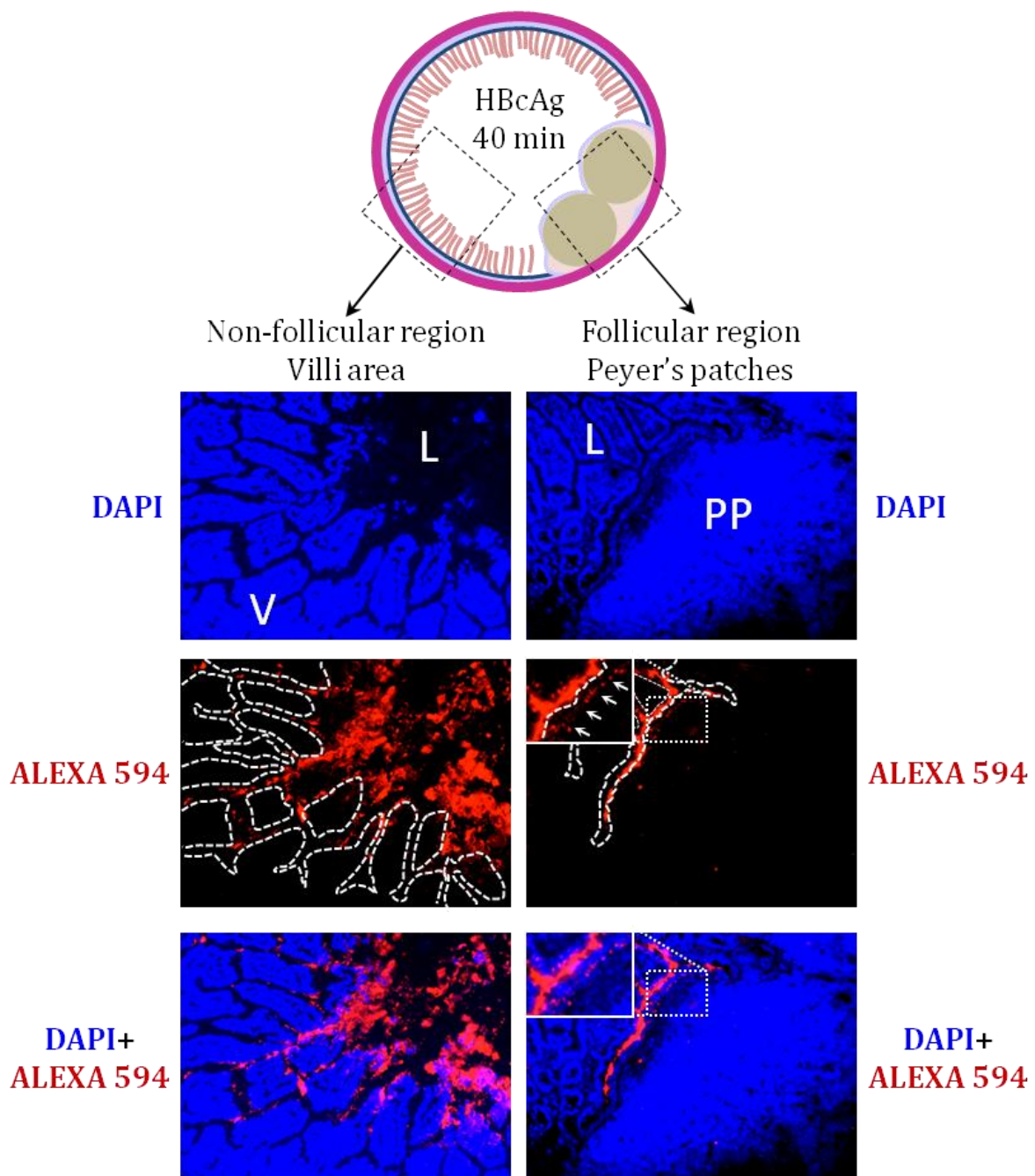


**Figure 6.8. IHC of intestinal sections after 40 minutes incubation with HBcAg.**

Microscopy images (10x), obtained for villi (left side) and PPs (right side) areas, of an *in vivo* ligated ileal loop inoculated with 5 mg/mL HBcAg and incubated for 40 minutes. DAPI (blue) shows the tissue structure; Alexa 594 (red) shows the HBcAg immunoreactivity and DAPI + Alexa 594 (red + blue) show the merged images. L = Lumen, V = Villi; PP = Peyer's patches. The white line outlines the interface between the tissue (villi or PP) with the lumen. Enlarged images of the PP epithelium illustrate HBcAg uptake inside the PP, as indicated by the white arrows.

A further IHC study was undertaken in order to better understand the absorption of HBcAg in the FAE covering the PP. In this experiment, HBcAg VLPs were visualised in some of the cryosections by the detection of the fluorescent signal emitted by the Alexa 488 secondary antibody (green fluorescence), bound to the anti-HBcAg primary antibody. At the same time, anti-CD11c antibody allowed the recognition of CD11c cells in the sub-epithelial domain (SED) of the PP (purple fluorescence). As discussed in Chapter 1, CD11c cells are a class of dendritic cells (DCs), within the PP, which strategically populate the area just underneath the epithelium (SED). Hence their function is that of promptly taking up antigens from M cells for presentation to immune cells and further processing (Kunisawa et al., 2012). Staining of these cells, together with DAPI cellular staining was important, because it enabled the localisation of the FAE within the PP: the DAPI stained (blue) region between the lumen and the SED (purple) denoted the FAE. Figure 6.9 illustrates the penetration of HBcAg VLPs from the lumen to the FAE. Green fluorescence, corresponding to the immunoreactivity of HBcAg, can be visualised at the external surface of the PP in the tissue in which HBcAg was incubated for 15 minutes. In the tissue incubated for 40 minutes, HBcAg some immunoreactivity was also seen inside the FAE. The untreated ileal tissue that was not incubated with HBcAg (control) showed a stronger green background than the one obtained previously using the red-fluorescent antibody. However, this green background of the control can be neglected when compared to the much more intense signal elicited by the HBcAg immunoreactivity. Overall, this result confirmed the previous finding: HBcAg initially penetrated the mucosal barrier covering the PPs and after longer exposure small amounts could also breach the FAE overlying the SED.

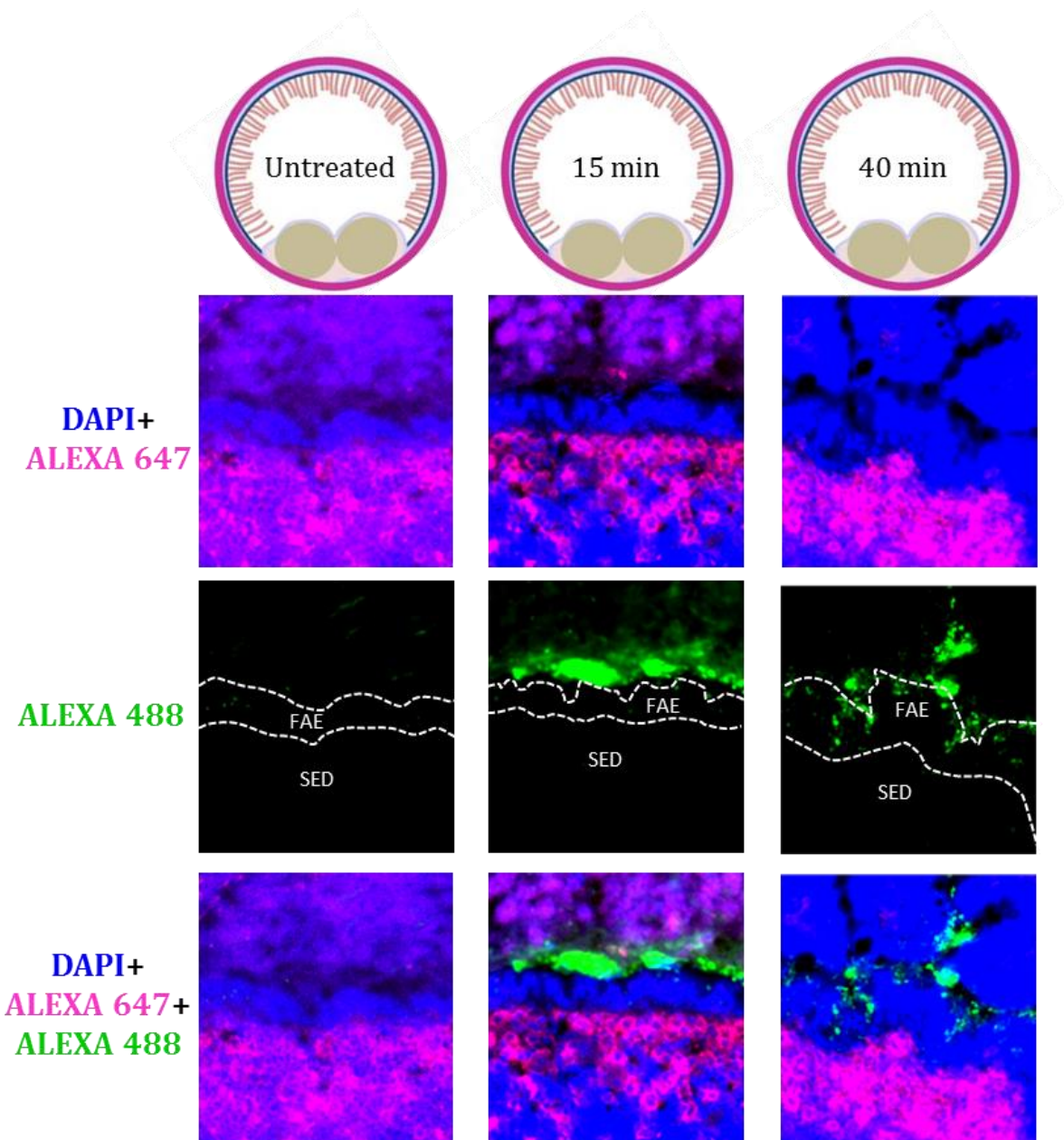


**Figure 6.9. IHC of the FAE after incubation with HBcAg.**

Microscopy images (10x), obtained for external PPs areas, of an untreated intestinal section, control, (left side) and of an in vivo ligated ileal loop inoculated with 5 mg/mL HBcAg and incubated for 15 (centre) and 40 minutes (right side).. DAPI (blue) + Alexa 647 (purple) show the tissue structure and CD11c immunoreactivity, respectively, and Alexa 488 (green) shows HBcAg immunoreactivity. DAPI + Alexa 647 + Alexa 488 show the merged blue pink and red fluorescence. FAE = Follicle associated epithelium; SED = Sub-epithelial domain.

#### 6.4.2.4 Immunological Quantification of HBcAg in the Ileum

As an alternative approach, ileal tissues recovered from the intestinal loop studies were used for protein quantification. Intestinal tissues were accurately cut into PPs and villi areas and extensively washed with 0.5 mM DTT solution in PBS. The tissues were then snap-frozen. A few days later, the following six different tissues were briefly thawed at room temperature and homogenised separately:

- PPs of untreated intestine (control)
- Villi area tissue of untreated intestine (control)
- PPs of ileum from loop pre-incubated with HBcAg for 15 minutes
- Villi area of ileum from loop pre-incubated with HBcAg for 15 minutes
- PPs of ileum from loop pre-incubated with HBcAg for 40 minutes
- Villi area of ileum from loop pre-incubated with HBcAg for 40 minutes

For each sample, two pieces of tissue collected from distal parts of the loop were pooled and processed together. This was done in order to obtain a sample concentrated enough to allow reliable protein detection. Then, HBcAg content was measured by sandwich ELISA and the total protein content was measured by Nanodrop. The results are reported as HBcAg/total protein content of the tissue. Figure 6.10 illustrates the data for the protein quantification. The HBcAg/total protein ratio was higher in the Peyer Patches (PPs) than in the villi areas. The ratio was 21.2% and 17.8% higher in the PPs incubated with HBcAg for 15 and 40 minutes, respectively. In the untreated intestine used as control no HBcAg was found.

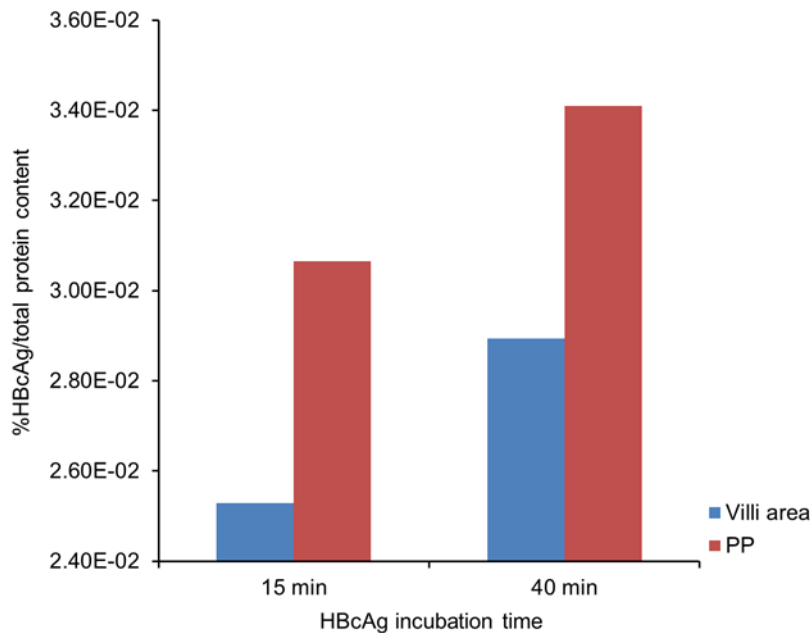


**Figure 6.10. HBcAg quantification in the intestinal tissue.**

HBcAg quantification in the villi and PP given as a ratio between HBcAg content and the total protein content of the tissue as a function of the incubation time. *In vivo* intestinal loops incubated with 5 mg/mL HBcAg for 15 and 40 minutes were used. Each value results from two tissues of the same loop pooled together.

The fact that a considerable amount of HBcAg was present in the villi area can possibly be explained by the inefficiency of the washing step with diluted DTT solutions (0.5 mM) to extensively remove the mucus and bound HBcAg. This is also confirmed by the microscopy studies clearly showing HBcAg immunoreactivity in the mucosal surfaces covering the intestinal epithelium. Furthermore, an interesting study reported that even aggressive luminal flushes with 10 mM DTT solution cannot efficiently remove the mucus (Sandberg et al., 1994). It is therefore possible that most of the VLPs measured were HBcAg embedded into the mucus and not internalised into the gut tissue. This could have created a high background concentration and it is possible to speculate that this background could have led to underestimation of the ratio between HBcAg measured in the PP and in the villi. Furthermore, physiologically the presence of mucus is relatively less in the PP than in the villi (Ensign et al., 2011), therefore, this trapping effect of HBcAg by the mucus could be less accentuated in the PP tissue. Finally, it is worth mentioning that in this experiment HBcAg could be detected by sandwich ELISA, which is specific for un-denatured VLPs. This implies that HBcAg was in an intact particulate state after being incubated for 15 and 40 minutes in the mouse intestinal lumen.

### 6.4.3 Contextualisation and Relevance of the Findings

The aim of this study was to evaluate whether HBcAg VLPs could be absorbed in the intestine, overcoming the two mucosal barriers constituted by mucus and the epithelial barrier. Interestingly, previous research on the penetration of mucus by macromolecules showed that some VLPs of viruses, which infect the mucosal surfaces, can diffuse rapidly through explanted human cervical mucus. In contrast, polystyrene nanoparticles (59 to 1000 nm), unmodified or functionalised with carboxylate, epoxy, or amino groups did not cross the mucus at all (Olmsted et al., 2001). This result was regarded as a “lesson from nature”; the intrinsic properties of microorganisms, which have evolutionally adapted to infect mucosal tissues, could explain this result and they include: (1) the small size, (2) the net neutral, yet hydrophilic surface (typical of many proteins) and (3) the lack of superficial hydrophobic area (Olmsted et al., 2001). These properties were thought to provide the VLPs with the perfect characteristics to penetrate low viscosity pores in the mucus. Nevertheless, not all VLPs could penetrate efficiently this cervical gel, probably due to the larger size and the presence of exposed hydrophobic patches, which were able to interact with the mucus (Cone, 2009; Lai et al., 2009). Based on this work, it is possible to hypothesise that HBcAg VLPs, bearing small size and being made of amphiphilic monomers, could also penetrate the intestinal mucus in the current study. In agreement, using the IHC approach in this work, HBcAg VLPs were found to be able to diffuse into the ileal mucus *in vivo*. The fact that HBcAg VLPs were found in direct contact with the intestinal epithelial surfaces even after 15 minutes of incubation clearly shows deep and fast penetration of the mucus. This result is particularly relevant as the loop was not “filled up” with non-physiological volumes of formulation and thus excessive dilution of the mucus barrier and consequent facilitated penetration was minimised.

However the second mucosal barrier, i.e. the epithelial layer, seemed to create a greater obstacle to particle penetration: in fact only small traces of HBcAg could be detected in the intestinal tissue, mainly in the FAE epithelium (Figure 6.7, 6.8 and 6.9). This result is in accordance with the quantitative *in vitro* experiment illustrated in Paragraph 6.5.1.2, which demonstrated that the loaded doses of HBcAg can cross the epithelial barrier at an order of magnitude of 0.001%. This ratio supports the *in vivo* results where a potent HBcAg signal was detected on the mucus at the luminal interface of the epithelial barrier, acting as a

highly concentrated reservoir of VLPs. However, only a minute amount of the particles could cross the epithelium, giving rise to limited patches of signal, particularly in the FAE of the PPs. As discussed in Paragraph 6.4.1, only small amounts of macromolecules can be absorbed orally; however, this might not be a problem in case of oral vaccines, whose efficacy is generally not strictly dose-dependent.

The fact that HBcAg VLPs could breach the gut epithelium covering the PP, even if in small quantities, could have significant implications in oral vaccine delivery. It has already been shown that Cowpea Mosaic Virus (CPMV), a virus infecting plants, can be internalised inside PPs *in vivo* (Gonzalez et al., 2009). This current work suggests that HBcAg, a VLP derived from human infectious pathogens, can also be internalised inside the PPs of the ileum, intriguingly being a non-enteric pathogen. Enteric pathogens, normally infective through the oral route, have developed complex and often elegant evolutionary mechanisms to invade the gut over thousands of years (Brayden et al., 2005). However, the epithelial absorption of HBcAg, which is not an enteric pathogen, is likely to be merely due to the physical particulate structure which could favour M cells-mediated transport (Florence et al., 2000). This can suggest that the non-enteric nature of HBcAg VLP can also count for the relatively low amount of transport. It can therefore be easily proposed that by decorating the VLP with adjuvant sequences to target M cells, higher absorption might be achieved (Azizi et al., 2010; Brayden et al., 2005). Recombinant biology techniques or chemically coupling could be used to modify the VLP for this purpose.

#### 6.4.4 Conclusions

The GALT is an organised apparatus which finely regulates foreign antigen sampling and immunogenic responses. The presence of such a functional immune machinery makes the gut a possible target for mucosal vaccine delivery.

In this Chapter the permeability of HBcAg VLP in the GALT was evaluated both *in vitro* and *in vivo*. As a first approach an entirely human cell culture model of functional FAE was grown on Transwells inserts in order to quantify the VLP permeability of this barrier: plant-expressed HBcAg, extracted and purified, was shown to cross the epithelial barrier of

the intestinal cell mono-layer in a concentration-dependent manner. More importantly it was shown that, at the three different doses used, the permeability through the FAE was always significantly higher than the permeability through the conventional absorptive epithelium, suggesting selective absorption of these VLP in the PPs. Nevertheless, the magnitude of all the permeability values obtained clearly showed very low absorption. These quantitative results were confirmed by *in vivo* experiments in mice: HBcAg inoculated into ligated intestinal loops and incubated for 15 and 40 minutes, was shown to be absorbed after 40 minutes in the FAE of the PPs. Moreover mucus constitutes a further physiological barrier to the intestinal absorption of large molecules; the ligated loop study showed that HBcAg VLPs deeply penetrate the mucus and accumulate at the interface between the mucus and the epithelial barrier. Quantitative studies on the HBcAg presence in the lymphoid and non-lymphoid tissue of the inoculated intestinal loops suggested again the selective presence of HBcAg in the PP. However, HBcAg entrapment in the mucus constitutes background interference in the quantification which renders precise absorption measurement *in vivo* elusive. Overall in this Chapter it was shown that HBcAg can penetrate the mucus and can be poorly, yet selectively absorbed by the FAE of the PPs. The results obtained are in line with the general trend of absorption of nanoparticles and they suggests that in the research towards the development of oral vaccines, the VLP approach could flank more “traditional” nanoparticulate methods.

## 7 Outlook and Future Work

The aim of this thesis was to investigate the potential use of a recombinant protein expressed in plants as an oral vaccine. The antigen chosen was Hepatitis B core antigen (HBcAg) virus-like particle (VLP) and the plant used as an expression host was *Nicotiana benthamiana*. More specifically, the main objectives of this research were to determine if and to what extent HBcAg VLP could withstand and overcome some of the gastro-intestinal (GI) barriers and to evaluate whether the compartmentalisation of the antigen in the plant material in which it is expressed could offer some aid to the oral delivery of HBcAg VLPs. The final objective was that of producing an oral formulation of HBcAg, exploiting its expression in plant.

It was previously reported that HBcAg is highly immunogenic when administered parenterally, but only poorly immunogenic when given orally (Huang et al., 2006; Milich et al., 1987b). In this context, a novel investigative approach was undertaken, where the instability in the GI fluid and the low gut permeability, both possibly responsible for the poor antigen immunogenicity, were analysed separately, in order to understand the cause of the poor oral response. For this purpose, scientific methods usually utilised in drug delivery studies of small molecules, and more recently nanoparticles, were employed. This represents a novelty in the field, as previously used candidate VLP vaccines, transiently expressed in plants, were directly administered to laboratory animals by gavage. The oral administration to animals offers the possibility of evaluating the immune response to the given antigen (Huang et al., 2006, 2005; Nuzzaci et al., 2010; Santi et al., 2008). However, the real “bottle-neck” of the delivery of antigens with poor oral immunogenicity cannot be identified, because such an approach, i.e. gastro-gavage, does not allow the independent analysis of the impact of each gastro-intestinal barrier to the given antigen. Hence, the research presented here suggests that drug delivery studies could fill a gap of knowledge in a research area traditionally confined at the interface between biotechnology and immunology.

In this scenario, the first technological hurdle to overcome was to establish a production, extraction and purification protocol, which could routinely produce considerable quantities

of purified or unpurified HBcAg VLPs from plants to be used in further drug delivery studies. Sainsbury and Lomonossoff (2008) showed that high-yield transient expression of HBcAg VLPs in plant could be achieved using the *-HT* system. The exploitation of this method for the production of HBcAg offered a unique opportunity to produce milligram quantities of this complex biopharmaceutical protein at bench scale. Chapter 2 described the development of a robust method for routine production, extraction and purification of HBcAg in plant. This method allowed the generation of several milligrams of purified HBcAg stock on a fortnight-base by a single operator. This constituted the bulk material used for the pharmaceutical research described in this study. Moreover in Chapter 2, characterisation and quantification techniques for HBcAg VLP were described. Virology (i.e. sucrose gradient and native agarose gel), immunology (immunodetection methods) and imaging (TEM) techniques were the ones chosen. Interestingly, the combination of the various techniques enabled a thorough characterisation of the complex chemical and three-dimensional structure of HBcAg. It was also shown, as a proof of concept, that HBcAg could be also expressed in edible plants such as lettuce.

In Chapter 3, it was demonstrated that HBcAg VLPs were highly physically and chemically unstable in simulated human gastric media. For this purpose different bio-relevant gastric conditions were used in order to account for the extremely high variation in acid and enzymatic composition observed in the human stomach *in vivo* (Efentakis and Dressman, 1990; Gomes et al., 2003). Moreover, it was shown that HBcAg is digested in simulated human intestinal fluid (SIF) and *ex-vivo* pig intestinal fluids, but surprisingly the main digested form of HBcAg maintained the particulate three-dimensional structure and the most antigenic epitopes. This Chapter offered an important prediction about the stability of HBcAg administered orally. Additionally, the fact that intestinal digestion did not lead to physical instability suggested that physical and chemical stability should be always analysed separately when evaluating the stability of such complex biopharmaceuticals in bio-relevant media. The methodology used in the Chapter could be also put forward as a potential approach to investigate the stability of other VLPs in bio-relevant media.

In Chapter 4, it was shown that leaves expressing HBcAg can be efficiently dried by oven- or freeze-drying and that the physical and chemical stability of HBcAg were significantly

---

maintained upon drying processes. Further studies suggested that HBcAg VLPs within the leaves were strongly digested by the simulated human GI fluids. Nevertheless, the unpurified plant material containing the antigen was exploited for the formulation of “green” tablets. Such tablets were then film-coated with a pH-dependent polymer. The resulting formulation showed effective *in vitro* HBcAg gastro-protection and enabled the antigen to be released in simulated intestinal fluid (SIF). Potentially, this formulation could enable the delivery of HBcAg undigested to the small intestine where absorption could take place.

Plant vaccine enthusiasts suggest that plant-bioencapsulation can provide additional protection of the labile antigen from GI degradation (Walmsley and Arntzen, 2000). This hypothesis did not prove correct in the current study. However, the plant tissue acted as a natural lyoprotectant, maintaining the VLP stability when the leaves were dried. Moreover, the homogeneity of HBcAg content within the tablets suggested that such an alternative formulation could overcome the poor homogeneity issues typical of low dose active oral formulations (i.e. a suggested dose of HBcAg could be in the range of tens of micrograms). It was previously speculated that plant-made vaccines, in particular if orally delivered, could produce an improvement in global health, by reducing the incidence of major infectious diseases, particularly in developing countries (Penney et al., 2011). The current study suggests that plant-expressed vaccines could be processed into an oral dosage form, potentially cheap and easy to produce. Moreover, application of gastro-protective coating could overcome one of the major GI barriers (i.e. the gastric instability of the antigen), hence enhancing the chances of efficacy of the oral dosage form.

In Chapter 5, the development of solid dosage forms of purified HBcAg VLPs potentially usable for oral delivery was described. The drying of the antigen from the liquid state, following extraction and purification from the leaf material, was an initial challenge: desiccation of granules containing HBcAg VLPs in the binder solutions resulted in low antigen stability. Instead, HBcAg VLPs could be effectively encapsulated within spray dried or spray freeze-dried microparticles of a pH-dependent polymer. However, such microparticles could not offer efficient gastro-protection. Finally, purified HBcAg was freeze-dried using different stabiliser excipients. Interestingly, excipients which freeze-dried as amorphous solids offered good HBcAg VLP stability, while excipients which

freeze-dried as crystalline solids led to greater antigen instability. However, thermal analysis studies revealed that freeze-dried amorphous excipients were metastable upon exposure to high relative humidity, while crystalline ones maintained their physical form. Freeze-dried solids which are metastable are not preferred dosage forms, particularly when, as in the case of this project, the final aim is that of further processing of the solid material into an oral dosage form which will be stored under ambient conditions (Costantino et al., 1998; Wang, 2000). In conclusion, amorphous excipients, which could offer higher in-process HBcAg VLP stability than crystalline ones upon freeze-drying, could not however be used for processing or storage at ambient conditions.

Even though a final dosage form which was effectively gastro-protective could not be produced, important considerations could be drawn. The screening of different drying methods suggested that HBcAg VLP can be dried efficiently by spray-, freeze- and spray freeze-drying, using amorphous excipients. However, desiccation and freeze-drying using stabilisers which dry as crystalline solids were not compatible with the antigen stability. Moreover, the lack of gastro-protection obtained with the microencapsulation, compared to the efficient gastro-protection obtained with the film-coated “green” tablets (in Chapter 4), suggests that the protection of highly gastro-labile biopharmaceuticals requires a certain coating thickness to enable effective gastro-resistance. Finally, the freeze-drying experiment re-proposed a very recurrent problem in protein formulations: excipients which freeze-dry as amorphous are excellent protein stabilisers. However, amorphous solids can absorb moisture, which could act as a plasticiser and reduce the glass transition temperature to a point where re-crystallisation occurs. This phenomenon can often jeopardise proteins’ stability upon storage (Costantino et al., 1998; Wang, 2000). A possible option to overcome this problem could be that of using lyoprotectant excipients that freeze-dry as amorphous solids, but have a high glass transition temperature. However, the moisture absorbed acts as a plasticiser on amorphous solids, lowering their glass transition temperatures. This phenomenon could be further reduced, if the amorphous solid is non-hygroscopic. For example, it has been shown that freeze-dried inulin has a higher glass transition temperature and much lower tendency to re-crystallise than trehalose (Hinrichs et al., 2001). Another alternative approach could be that of freeze-drying the stabiliser (i.e. trehalose) with excipients that have higher glass transition temperatures and with excipients which could absorb moisture after freeze-drying. For instance, it has been

reported that a low glass transition substance (simvastatin) could be spray dried together with PVP and Aerosil 200. Such excipients inhibited the tendency of spray dried simvastatin to re-crystallise upon storage. This was mainly due the increase of glass transition temperature, mediated by the PVP and to the selective absorption of the moisture onto the Aerosil, which functioned as a “buffer” for the spray dried system (Ambike et al., 2005). This knowledge could be also extrapolated to freeze-drying: for instance the re-crystallisation tendency of stabilisers, whose glass transition temperature is low or tends to be lowered by the moisture absorption, could be prevented by addition of PVP (for elevation of glass transition temperature) and Aerosil 200 (as adsorbent) in the solution to be freeze-dried. Moreover, other excipients with similar properties could be used.

In future work it could be suggested to freeze-dry HBcAg VLPs using inulin as a stabiliser, as the freeze-dried material could be further processed into a final dosage form (i.e. enteric coated capsules or tablets), if good in-process stabilisation could be achieved. Alternatively, a mixture of trehalose, PVP and Aerosil could be taken forward to further processing of the freeze-dried solid material into an oral formulation, if these excipients proved to be effective in stabilising HBcAg VLP upon freeze-drying and if the resulting solid exhibited low tendency to re-crystallise.

In Chapter 6 the intestinal permeability of HBcAg VLPs was evaluated. Selective absorption of the antigen through the Follicle-associated epithelium (FAE) could be assessed using an *in vitro* human cell culture model. Moreover, *in vivo* mouse intestinal loop studies confirmed that HBcAg VLPs could cross easily the mucus barrier and that small amounts of HBcAg VLPs could breach the intestinal epithelial barrier, in particular through the epithelium covering the Peyer’s patches (PPs). However, the results obtained both *in vitro* and *in vivo* suggested that HBcAg VLPs, as most macromolecules, were very poorly absorbed.

Nevertheless, immunogenic responses are not strictly dose-dependent (McConnell et al., 2008b): the influence of the extent of antigen absorption on the induction of tolerance or immunogenic response is extremely complicated and not fully understood yet. Therefore, it is not possible to predict whether such low absorption could mediate tolerance or immunity and this can be determined only experimentally. Unfortunately, when performing loop

studies it is advisable to sacrifice the animal soon after the invasive procedure. As a result, the animals are not kept alive long enough to measure the immunogenic response to the antigen. Thus, this study could have been alternatively performed administering HBcAg VLP by oral gavage if the immunogenic response is to be determined. However, the results in Chapter 3 discourage this approach, because the antigen is likely to be extensively degraded in the animal's stomach upon gavage. Hence, a gastro-protected formulation should have been used. This would have presented a major obstacle, as mice are too small for the administration of conventional tablets or even mini-tablets or mini-capsules. The use of Eudragit pH-responsive microparticles, containing HBcAg VLPs, would have been an elegant way to obviate this problem. This formulation was therefore developed, as described in Chapter 5. However, the limited gastro-protection of such formulation discouraged from taking it further to the animal studies. Moreover, it has been reported that the GI pH of Balb/c mice greatly differs from that of humans: the pH measured in the mouse fasted stomach and fasted intestine was circa 3 and 5, respectively (McConnell et al., 2008a). In humans, the pH in the stomach generally ranges from pH 1 to 2.5 in normal fasted state conditions, while it generally ranges from pH 6.3 to 7.5 in the intestine (Evans et al., 1988). It is therefore evident that pH-dependent polymers, whereby the delivery pattern is totally dependent on the environmental pH, should not be tested in mice if the intention is to relate the results to the human situation. For instance, formulations of Eudragit L 100 or S 100 with a threshold of dissolution of pH 6 and 7, respectively, are unlikely to dissolve in the gut of mice. For this purpose it could be advisable to use animal models, whose GI physiology can be better correlated to that of the humans GI [i.e. rats or even better, rabbits (McConnell et al., 2008a; Merchant et al., 2011)]. In this regard, a possible suggestion for future work could be that of preparing film-coated mini-capsules or mini-tablets containing HBcAg VLP and to gavage them to rabbits. HBcAg VLP could be either formulated as unpurified plant material ("green tablets") or could be extracted, purified and then formulated.

A final suggestion for future work can be proposed: it has been demonstrated that the administration of vaccines to the large intestine can elicit stronger local immunity at rectal and genital mucosal sites, compared to the oral administration to the small intestine (McConnell et al., 2008c; Zhu et al., 2008). Therefore, the delivery of vaccines to the colon could offer an effective way of protection against sexually transmitted infections, including

Hepatitis B. Hence it could be interesting to evaluate the absorption of HBcAg VLP in the large intestine: the particulate nature, the intrinsic strong immunogenicity and the relatively high stability of VLP combined with the low enzymatic environment and long residence time in the colon could offer an effective and novel approach for delivering vaccines. Studies of colonic delivery of vaccines have been mainly performed by intracolorectal administration; however colonic delivery of vaccines was recently achieved using oral pH-dependent formulations for targeted delivery to the colon (Zhu et al., 2012). Therefore oral formulations of HBcAg VLPs for targeted colonic delivery could be investigated.

The first objective of this thesis was to have a better understanding about the oral delivery of HBcAg VLPs: Huang et al. (2006) showed that HBcAg VLPs elicit only a poor immunogenic response when administered orally to mice. However, a question remained as to what could be the cause of the poor immunogenicity. In other words, it was not clear whether the poor immunogenicity was mainly due to the GI instability or to the lack of absorption. The results from this thesis suggest that an evident limitation to the oral delivery of this antigen is the very high gastric instability. As the stomach is the first physico-chemical barrier, such an upstream obstacle could have influenced the downstream delivery of the antigen, i.e. crossing the intestinal fluids, crossing the epithelium and eventually eliciting an immunogenic response. Nevertheless, the intestinal digestion itself, devoid from the upstream gastric instability, was shown to be compatible with the maintenance of HBcAg particulate structure and immunogenicity. Finally, it was shown that when the GI instability was overcome and the absorption was evaluated independently, small amounts of HBcAg could be absorbed by the FAE of the PPs. As PPs are thought to be a major site for the induction of immunogenic response in the gut (Neutra et al., 2001), this finding suggested that undigested HBcAg VLPs can be delivered to the gut immune machinery. However, from the current work it is not known whether such low levels of absorption could trigger tolerance or elicit strong immune responses. The findings of this research taken together suggest that HBcAg could be delivered orally, definitely within a gastro-protected formulation. However, co-administration of mucosal adjuvants that are able to improve the oral adsorption might be needed to induce strong immunogenic responses.

Another important question that was answered in this thesis was that regarding the claimed possibility of protecting labile antigens from the harsh GI environment, by delivering the antigen within the plant material in which it is expressed as a recombinant protein. In the case of HBcAg VLP and *Nicotiana benthamiana*, plant bio-encapsulation could not protect the labile antigen from the simulated GI media and hence could not substitute the use of polymer-based pH-dependent formulations. However, the expression in plant offered the novel possibility of preparing “green” tablets, which were subsequently film-coated. This approach exploited the fact that the antigen would be expected to be reasonably well distributed in the leaf material and hence would mitigate against homogeneity issues commonly observed in low dose formulations. These results also highlighted that high antigen stability can be maintained upon drying, simply by oven drying or freeze-drying the leaves.

Finally, the formulation studies on purified HBcAg VLPs offered a good insight into the options available for the development of stable HBcAg VLP solid dosage forms. The preparation techniques of choice should be either spray drying, spray freeze-drying or freeze-drying and the excipients chosen should preferentially dry as amorphous solids. However, it is advisable to choose excipients or combinations of excipients that could withstand processing at ambient conditions without the risk of excessive moisture absorption or re-crystallisation. Moreover, it can be suggested that when gastro-labile antigens, such as HBcAg, have to be included within a gastro-resistant formulation, the choice of the formulation should not fall on micron-sized dosage forms, such as microspheres, as, based on the current results, these are unlikely to offer the same level of protection as more conventional, monolithic gastro-resistant formulations, such as tablets.

The work described in this thesis constitutes a distinctive investigation at the interface between the drug delivery and plant biotechnology fields. The fact that such research could be successfully carried out, obtaining these interesting results, suggests that the two scientific fields could work alongside each other: pharmaceutical research could enable a better understanding of novel biotechnological discoveries and could elucidate their potential applications. More specifically, this research provided important information about the use of plant-expressed HBcAg VLP as an oral candidate vaccine, evaluating the delivery and formulation of the antigen and also exploiting its expression in plant.

---

Overall the current study suggest that HBcAg VLP expressed in plant could not be used as such, as an effective vaccine candidate for oral delivery, mainly due to the high intrinsic instability in the simulated gastric environment. Moreover the very low intestinal absorption might represent a futher limitation to the vaccine effectivity. It is therefore possible that the efficacy of this plant VLP vaccine approach could be enhanced by protecting the antigen within a gastro-resistant oral formulation (as described in Chapter 4) and by adding in the formulation an adjuvant which could improve the intestinal absorption. A similar approach of an HBV vaccine should be first tested in animal models and then it could be potentially brought to clinic.

## 8 References

Abdul-Fattah, A.M., Kalonia, D.S., Pikal, M.J., 2007. "The challenge of drying method selection for protein pharmaceuticals: product quality implications." *Journal of Pharmaceutical Sciences* 96(8): 1886–1916.

Aguilar, J.C., Lobaina, Y., Muzio, V., 2004. "Development of a nasal vaccine for chronic hepatitis B infection that uses the ability of hepatitis B core antigen to stimulate a strong Th1 response against hepatitis B surface antigen". *Immunology and Cell Biology* 82(5): 539–546.

Akers, M., 2002. "Excipient–drug interactions in parenteral formulations". *Journal of Pharmaceutical Sciences* 91(11): 2283–2300.

Alderborn, G., 2007. "Tablets and Compaction.", in: Aulton, M.E. (Ed.), *Aulton's Pharmaceutics: The Design and Manufacture of Medicines*. Elsevier Limited, pp. 397–438.

Alhnan, M.A., Cosi, D., Murdan, S., Basit, A.W, 2010. "Inhibiting the Gastric Burst Release of Drugs from Enteric Microparticles: The Influence of Drug Molecular Mass and Solubility". *Powder Diffraction* 99(11): 4576–4583.

Alhnan, M.A., Kidia, E., Basit, A.W, 2011. "Spray-drying enteric polymers from aqueous solutions: a novel, economic, and environmentally friendly approach to produce pH-responsive microparticles." *European Journal of Pharmaceutics and Biopharmaceutics* 79(2): 432–9.

Ambike, A.A., Mahadik, K.R., Paradkar, A., 2005. "Spray-dried amorphous solid dispersions of simvastatin, a low tg drug: in vitro and in vivo evaluations." *Pharmaceutical Research* 22(6): 990–8.

Amorij, J.-P., Huckriede, A, Wilschut, J., Frijlink, H.W., Hinrichs, W.L.J., 2008. "Development of stable influenza vaccine powder formulations: challenges and possibilities." *Pharmaceutical Research* 25(6): 1256–73.

Amorij, J.-P., Kersten, G.F.A., Saluja, V., Tonnis, W.F., Hinrichs, W.L.J., Slütter, B., Bal, S.M., Bouwstra, J.A., Huckriede, A., Jiskoot, W., 2012. "Towards tailored vaccine delivery: needs, challenges and perspectives." *Journal of Controlled Release* 161(2): 363–76.

Año, G., Esquisabel, A., Pastor, M., Talavera, A., Cedré, B., Fernández, S., Sifontes, S., Aranguren, Y., Falero, G., García, L., Solís, R.L., Pedraz, J.L., 2011. "A new oral vaccine candidate based on the microencapsulation by spray-drying of inactivated *Vibrio cholerae*." *Vaccine* 29(34): 5758–64.

Arques, J.L., Hautefort, I., Ivory, K., Bertelli, E., Regoli, M., Clare, S., Hinton, J.C.D., Nicoletti, C., 2009. "Salmonella induces flagellin- and MyD88-dependent migration of bacteria-capturing dendritic cells into the gut lumen." *Gastroenterology* 137(2): 579–87.

Artursson, P., 1990. "Epithelial transport of drugs in cell culture. I: A model for studying the passive diffusion of drugs over intestinal absorptive (Caco-2) cells." *Journal of Pharmaceutical Sciences* 79(6): 476–482.

Artursson, P., Karlsson, J., 1991. "Correlation between oral drug absorption in humans and apparent drug permeability coefficients in human intestinal epithelial (Caco-2) cells." *Biochemical and Biophysical Research Communications* 175(3): 880–885.

Astwood, J., Leach, J., Fuchs, R., 1996. "Stability of food allergens to digestion in vitro". *Nature Biotechnology* 14(10): 1269–1273.

Ausar, S.F., Foubert, T.R., Hudson, M.H., Vedvick, T.S., Middaugh, C.R., 2006. "Conformational stability and disassembly of Norwalk virus-like particles. Effect of pH and temperature." *The Journal of Biological Chemistry* 281(28): 19478–88.

Awaad, A., Nakamura, M., Ishimura, K., 2012. "Imaging of size-dependent uptake and identification of novel pathways in mouse Peyer's patches using fluorescent organosilica particles." *Nanomedicine : Nanotechnology, Biology, and Medicine*, 8 (5): 627–636.

Azizi, A., Kumar, A., Diaz-Mitoma, F., Mestecky, J., 2010. "Enhancing oral vaccine potency by targeting intestinal M cells." *PLoS Pathogens* 6(11): e1001147.

Balamuralidhara, V., Pramodkumar, T.M., Srujana, N., Venkatesh, M.P., Vishal G.N., Krishna, K.L., Gangadharappa, H.V., 2011. "pH Sensitive Drug Delivery Systems: A Review". *American Journal of Drug Discovery and Development* 1(1): 24–48.

Barta, A., Sommergruber, K., Thompson, D., Hartmuth, K., Matzke, M., Matzke, A.M., 1986. "The expression of a nopaline synthase — human growth hormone chimaeric gene in transformed tobacco and sunflower callus tissue". *Plant Molecular Biology* 6(5): 347–357.

Betancourt, A.A., Delgado, C.A.G., Estévez, Z.C., Martínez, J.C., Ríos, G.V., Aureoles-Roselló, S.R.M., Zaldívar, R.A., Guzmán, M.A., Baile, N.F., Reyes, P.A.D., Ruano, L.O., Fernández, A.C., Lobaina-Matos, Y., Fernández, A.D., Madrazo, A.I.J., Martínez, M.I.A., Baños, M.L., Alvarez, N.P., Baldo, M.D., Mestre, R.E.S., Pérez, M.V.P., Martínez, M.E.P., Escobar, D.A., Guanche, M.J.C., Cáceres, L.M., Betancourt, R.S., Rando, E.H., Nieto, G.E.G., González, V.L.M., Rubido, J.C.A., 2007. "Phase I clinical trial in healthy adults of a nasal vaccine candidate containing recombinant hepatitis B surface and core antigens." *International Journal of Infectious Diseases* 11(5): 394–401.

Bilati, U., Allémann, E., Doelker, E., 2005. "Strategic approaches for overcoming peptide and protein instability within biodegradable nano- and microparticles." *European Journal of Pharmaceutics and Biopharmaceutics* 59(3): 375–88.

Birnbaum, F., Nassal, M., 1990. "Hepatitis B virus nucleocapsid assembly: primary structure requirements in the core protein". *Journal of Virology* 64(7): 3319–3330.

Borde, A., Ekman, A., Holmgren, J., Larsson, A., 2012. "Effect of protein release rates from tablet formulations on the immune response after sublingual immunization." *European Journal of Pharmaceutical Sciences* 47(4): 695–700.

Borghesi, C., Taussig, M. J., Nicoletti, C., 1999. "Rapid appearance of M cells after microbial challenge is restricted at the periphery of the follicle-associated epithelium of Peyer's patch." *Laboratory Investigation* 79(11): 1393–1401.

Böttcher, B., Wynne, S.A., Crowther, R.A., 1997. “Determination of the fold of the core protein of hepatitis B virus by electron cryomicroscopy”. *Nature* 386(6620): 88–91.

Brayden, D.J., Jepson, M.A., Baird, A.W., 2005. “Keynote review: Intestinal Peyer’s patch M cells and oral vaccine targeting”. *Drug Discovery Today* 10(17): 1145–1157.

British Pharmacopeia, 2012. “London, TSO (The Stationery Officer) Ltd.”

Broos, K., Vanlandschoot, P., Maras, M., Robbens, J., Leroux-Roels, G., Guisez, Y., 2007. “Expression, purification and characterization of full-length RNA-free hepatitis B core particles”. *Protein Expression and Purification* 54(1): 30–37.

Buckton, G., Yonemochi, E., Hammond, J., Moffat, A., 1998. “The use of near infra-red spectroscopy to detect changes in the form of amorphous and crystalline lactose”. *International Journal of Pharmaceutics* 168(2): 231–241.

Buda, A., Sands, C., Jepson, M.A., 2005. “Use of fluorescence imaging to investigate the structure and function of intestinal M cells.” *Advanced Drug Delivery Reviews* 57(1): 123–34.

Burnet, F.M., 1976. “A Modification of Jerne’s Theory of Antibody Production using the Concept of Clonal Selection”. *CA: A Cancer Journal for Clinicians* 26(2): 119–121.

Cabanes-Macheteau, M., Fitchette-Lainé, A.C., Loutelier-Bourhis, C., Lange, C., Vine, N.D., Ma, J.K.-C., Lerouge, P., Faye, L., 1999. “N-Glycosylation of a mouse IgG expressed in transgenic tobacco plants.” *Glycobiology* 9(4): 365–72.

Cañizares, M.C., Liu, L., Perrin, Y., Tsakiris, E., Lomonossoff, G.P., 2006. “A bipartite system for the constitutive and inducible expression of high levels of foreign proteins in plants”. *Plant Biotechnology Journal* 4(2): 183–193.

Carpenter, J.F., Crowe, J.H., 1989. “An infrared spectroscopic study of the interactions of carbohydrates with dried proteins.” *Biochemistry* 28(9): 3916–22.

Center for Disease Control (CDC), 2011. “Ten Great Public Health Achievements—United States, 2001–2010”. *JAMA* 306(1): 36–38.

Center for Disease Control and Prevention (CDC), 2012. “Hepatitis B”, in: Epidemiology and Prevention of Vaccine-Preventable Diseases, “Pink Book”. pp. 115–138.

Chadwick, S., Kriegel, C., Amiji, M., 2010. “Nanotechnology solutions for mucosal immunization.” *Advanced Drug Delivery Reviews* 62(4-5): 394–407.

Challacombe, S.J., Rahman, D., Jeffery, H., Davis, S.S., O’Hagan, D.T., 1992. “Enhanced secretory IgA and systemic IgG antibody responses after oral immunization with biodegradable microparticles containing antigen.” *Immunology* 76(1): 164–8.

Chen, D., Kapre, S., Goel, A., Suresh, K., Beri, S., Hickling, J., Jensen, J., Lal, M., Preaud, J.M., Laforce, M., Kristensen, D., 2010. “Thermostable formulations of a hepatitis B vaccine and a meningitis A polysaccharide conjugate vaccine produced by a spray drying method.” *Vaccine* 28(31): 5093–9.

Clark, D.P., Pazdernik, N.J., 2011. “Immune technology”, in: *Biotechnology: Academic Cell Update Edition*. Academic Press, pp. 199–200.

Coghlan, A., 2005. “Breaking News: Potato-based vaccine success comes too late”. *NewScientist. Com News Service*.

Cone, R.A., 2009. “Barrier properties of mucus.” *Advanced Drug Delivery Reviews* 61(2): 75–85.

Conley, A.J., Zhu, H., Le, L.C., Jevnikar, A.M., Lee, B.H., Brandle, J.E., Menassa, R., 2011. “Recombinant protein production in a variety of Nicotiana hosts: a comparative analysis.” *Plant Biotechnology Journal* 9(4): 434–44.

Cornes, J.S., 1965. “Number, size, and distribution of Peyer’s patches in the human small intestine: Part I The development of Peyer's patches”. *Gut* 6(3): 225–229.

Corr, S.C., Gahan, C.C.G.M., Hill, C., 2008. “M-cells: origin, morphology and role in mucosal immunity and microbial pathogenesis.” *FEMS Immunology and Medical Microbiology* 52(1): 2–12.

Costantino, H.R., Carrasquillo, K.G., Cordero, R.A., Mumenthaler, M., Hsu, C.C., Griebenow, K., 1998. “Effect of excipients on the stability and structure of

lyophilized recombinant human growth hormone.” *Journal of Pharmaceutical Sciences* 87(11): 1412–20.

Cox, E., Verdonck, F., Vanrompay, D., Goddeeris, B., Oxa, E.C., Erdoncka, F.V., Anrompayb, D.V., Oddeerisa, B.G., 2006. “Adjuvants modulating mucosal immune responses or directing systemic responses towards the mucosa”. *Veterinary Research* 37(3): 511–539.

Craig, D.Q.M., Reading, M., 2007. “Principles of Differential Scanning Calorimetry”, in: *Thermal Analysis of Pharmaceuticals*. CRC Press, pp. 1–21.

Crowther, R.A., Kiselev, N.A., Böttcher, B., Berriman, J.A., Borisova, G.P., Ose, V., Pumpens, P, 1994. “Three-dimensional structure of hepatitis B virus core particles determined by electron cryomicroscopy”. *Cell* 77(6): 943–950.

Cutt, T., Fell, J.T., Rue, P.J., Spring, M.S., 1986. “Granulation and compaction of a model system. I. Granule properties”. *International Journal of Pharmaceutics* 33(1-3): 81–87.

D’Aoust, M.-A., Couture, M.M.-J., Charland, N., Trépanier, S., Landry, N., Ors, F., Vézina, L.-P., 2010. “The production of hemagglutinin-based virus-like particles in plants: a rapid, efficient and safe response to pandemic influenza.” *Plant Biotechnology Journal* 8(5): 607–19.

Daniell, H., Singh, N.D., Mason, H.S., Streatfield, S.J., 2009. “Plant-made vaccine antigens and biopharmaceuticals”. *Trends in Plant Science* 14(12): 669–679.

Des Rieux, A., Fievez, V., Garinot, M., Schneider, Y.-J., Préat, V., 2006. “Nanoparticles as potential oral delivery systems of proteins and vaccines: a mechanistic approach.” *Journal of Controlled Release* 116(1): 1–27.

Des Rieux, A., Fievez, V., Théate, I., Mast, J., Préat, V., Schneider, Y.-J., 2007. “An improved in vitro model of human intestinal follicle-associated epithelium to study nanoparticle transport by M cells.” *European Journal of Pharmaceutical Sciences* 30(5): 380–91.

Des Rieux, A., Ragnarsson, E.G.E., Gullberg, E., Préat, V., Schneider, Y.-J., Artursson, P., 2005. “Transport of nanoparticles across an in vitro model of the human intestinal follicle associated epithelium.” *European Journal of Pharmaceutical Sciences* 25(4-5): 455–65.

Dewettinck, K., Huyghebaert, A., 1998. “Top-Spray Fluidized Bed Coating: Effect of Process Variables on Coating Efficiency”. *Food Science and Technology* 31(6): 568–575.

Diakidou, A., Vertzoni, M., Abrahamsson, B., Dressman, J., Reppas, C., 2009. “Simulation of gastric lipolysis and prediction of felodipine release from a matrix tablet in the fed stomach.” *European Journal of Pharmaceutical Sciences* 37(2): 133–40.

Doan, T., Melvold, R., Viselli, S., Waltenbaugh, C., 2008a. “Innate Immune Function”, in: Harvey, R.A., Champe, P.C. (Eds.), *Immunology*. pp. 41–54.

Doan, T., Melvold, R., Viselli, S., Waltenbaugh, C., 2008b. “The Well Patient: How Innate and Adaptive Immune Responses Maintain Health”, in: Harvey, R.A., Champe, P.C. (Eds.), *Immunology*. pp. 183–187.

Dong, W., Bodmeier, R., 2006. “Encapsulation of lipophilic drugs within enteric microparticles by a novel coacervation method.” *International Journal of Pharmaceutics* 326(1-2): 128–38.

Donnelly, J.J., Friedman, A., Martinez, D., Montgomery, D.L., Shiver, J.W., Motzel, S.L., Ulmer, J.B., Liu, M.A., 1995. “Preclinical efficacy of a prototype DNA vaccine: enhanced protection against antigenic drift in influenza virus”. *Nature Medicine* 1(6): 583–587.

Donovan, M.D., Flynn, G.L., Amidon, G.L., 1990. “Absorption of polyethylene glycols 600 through 2000: the molecular weight dependence of gastrointestinal and nasal absorption.” *Pharmaceutical Research* 7(8): 863–868.

Efentakis, M., Dressman, J.B., 1990. “Gastric juice as a dissolution medium: surface tension and pH.” *European Journal of Drug Metabolism and Pharmacokinetics* 23(2): 97–102.

Ensign, L.M., Cone, R., Hanes, J., 2011. “Oral drug delivery with polymeric nanoparticles: The gastrointestinal mucus barriers.” *Advanced Drug Delivery Reviews* 64(6): 557–570.

Eudragit, 2011. “EUDRAGIT® Application Guidelines (12th edition).”

Evans, D.F., Pye, G., Bramley, R., Clark, A.G., Dyson, T.J., Hardcastle, J.D., 1988. “Measurement of gastrointestinal pH profiles in normal ambulant human subjects.” *Gut* 29(8): 1035–41.

Evonik Industries, 2013. “PlasACRYL™”. URL <http://eudragit.evonik.com/product/eudragit/en/products-services/eudragit-products/plasacrylt20/Pages/default.aspx>

Fakes, M.G., Dali, M. V., Haby, T.A., Morris, K.R., Varia, S.A., Serajuddin, A.T., 2000. “Moisture sorption behavior of selected bulking agents used in lyophilized products.” *PDA Journal of Pharmaceutical Science and Technology* 54(2): 144–149.

Ferrer, J., Scott, W.I., Weegman, B.B.P., Scott, W.E., Suszynski, T.M., Sutherland, D.E.R., Hering, B.J., Papas, K.K., 2008. “Pig pancreas anatomy: implications for pancreas procurement, preservation, and islet isolation.” *Transplantation* 86(11): 1503–10.

Fifis, T., Gamvrellis, A., Crimeen-Irwin, B., Pietersz, G.A., Li, J., Mottram, P.L., McKenzie, I.F.C., Plebanski, M., 2004. “Size-dependent immunogenicity: therapeutic and protective properties of nano-vaccines against tumors.” *Journal of Immunology* 173(5): 3148–54.

Fischer, R., Emans, N., 2000. “Molecular farming of pharmaceutical proteins.” *Transgenic Research* 9(4-5): 279–99.

Fischer, R., Stoger, E., Schillberg, S., Christou, P., Twyman, R.M., 2004. “Plant-based production of biopharmaceuticals.” *Current Opinion in Plant Biology* 7(2): 152–8.

Floreani, A., Baldo, V., Cristofolletti, M., Renzulli, G., Valeri, A., Zanetti, C., Trivello, R., 2004. “Long-term persistence of anti-HBs after vaccination against HBV: an 18 year experience in health care workers”. *Vaccine* 22(5-6): 608–611.

Florence, A.T., 2005. "Nanoparticle uptake by the oral route: Fulfilling its potential?" *Drug Discovery Today: Technologies* 2(1): 75–81.

Florence, A.T., Sakthivel, T., Toth, I., 2000. "Oral uptake and translocation of a polylysine dendrimer with a lipid surface." *Journal of Controlled Release* 65(1-2): 253–9.

Folttmann, H., Quadir, A., 2008. "Polyvinylpyrrolidone (PVP)—one of the most widely used excipients in pharmaceuticals: an overview". *Drug Delivery Technology* 8(6): 22–27.

Fotaki, N., Symillides, M., Reppas, C., 2005. "Canine versus in vitro data for predicting input profiles of L-sulpiride after oral administration." *European Journal of Pharmaceutical Sciences* 26(3-4): 324–33.

Fox, J.L., 2012. "First plant-made biologic approved". *Nature Biotechnology* 30(6): 472–472.

Franken, E., Teuschel, U., Hain, R., 1997. "Recombinant proteins from transgenic plants". *Current Opinion in Biotechnology* 8(4): 411–416.

Gallina, A., Bonelli, F., Zentilin, L., Rindi, G., Muttini, M., Milanesi, G., 1989. "A recombinant hepatitis B core antigen polypeptide with the protamine-like domain deleted self-assembles into capsid particles but fails to bind nucleic acids". *Journal of Virology* 63(11): 4645–4652.

Galwey, A.K., Craig, D.Q.M., 2007. "Thermogravimetric Analysis: Basic Principles.", in: Craig, D.Q.M., Reading, M. (Eds.), *Thermal analysis of pharmaceuticals*. Boca Raton, CRC Press, Taylor and Francis Group, pp. 139–191.

Gamboa, J.M., Leong, K.W., 2013. "In vitro and in vivo models for the study of oral delivery of nanoparticles". *Advanced Drug Delivery Reviews* 65(6): 800–810.

Garside, P., Steel, M., Worthey, E.A., Satoskar, A., Alexander, J., Bluethmann, H., Liew, F.Y., Mowat, A.M., M., 1995. "T helper 2 cells are subject to high dose oral tolerance and are not essential for its induction." *The Journal of Immunology* 154(11): 5649–5655.

Gehin, A., Gilbert, R., Stuart, D., Rowlands, D., 2007. "Hepatitis B core antigen fusion proteins". US Patent 7270821 B2.

Giudice, E.L., Campbell, J.D., 2006. "Needle-free vaccine delivery". Advanced Drug Delivery Reviews 58(1): 68–89.

Gleba, Y., Marillonnet, S., Klimyuk, V., 2004. "Engineering viral expression vectors for plants: the 'full virus' and the 'deconstructed virus' strategies." Current Opinion in Plant Biology 7(2): 182–8.

Gomes, R.A.D.S., Batista, R.P., De Almeida, A.C., Da Fonseca, D.N., Juliano, L., Hial, V., 2003. "A fluorimetric method for the determination of pepsin activity". Analytical Biochemistry 316(1): 11–14.

Gonzalez, M.J., Plummer, E.M., Rae, C.S., Manchester, M., 2009. "Interaction of cowpea mosaic virus (CPMV) nanoparticles with antigen presenting cells in vitro and in vivo". PloS One 4(11): e7981.

Gourley, T.S., Wherry, E.J., Masopust, D., Ahmed, R., 2004. "Generation and maintenance of immunological memory." Seminars in Immunology 16(5): 323–33.

Grgacic, E.V.L., Anderson, D.A., 2006. "Virus-like particles: passport to immune recognition." Methods 40(1): 60–5.

Gullberg, E., 2005. "Particle transcytosis across the human intestinal epithelium". PhD Thesis. Uppsalla university.

Gullberg, E., Keita, Å., Sa'ad, Y., 2006. "Identification of cell adhesion molecules in the human follicle-associated epithelium that improve nanoparticle uptake into the Peyer's patches". The Journal of Pharmacology and Experimental Therapeutics 319(2): 632–639.

Gullberg, E., Leonard, M., Karlsson, J., Hopkins, A.M., Brayden, D.J., Baird, A.W., Artursson, P., 2000. "Expression of specific markers and particle transport in a new human intestinal M-cell model." Biochemical and Biophysical Research Communications 279(3): 808–13.

Hannigan, B.M., Moore, C.B., Quinn, D.G., 2009a. “The lymphatic system”, in: Immunology. Scion Publishing Ltd, pp. 12–21.

Hannigan, B.M., Moore, C.B., Quinn, D.G., 2009b. “Lymphocytes development”, in: Immunology. Scion Publishing Ltd, pp. 44–64.

Haq, T.A., Mason, H.S., Clements, J.D., Arntzen, C.J., 1995. “Oral immunization with a recombinant bacterial antigen produced in transgenic plants.” *Science* 268(5211): 714–716.

Harlow, E., Lane, D., 1988. “Immunoassay”, in: Antibodies. Cold Spring Harbor Laboratory Press, pp. 190–191.

Hayden, C.A., Egelkrout, E.M., Moscoso, A.M., Enrique, C., Keener, T.K., Jimenez-Flores, R., Wong, J.C., Howard, J.A., 2012. “Production of highly concentrated, heat-stable hepatitis B surface antigen in maize.” *Plant Biotechnology Journal* 10(8): 979–84.

Heel, K.A., 1997. “Review: Peyer’s patches”. *Journal of Gastroenterology and Hepatology* 12: 122–136.

Hefferon, K.L., 2010. “The mucosal immune response to plant-derived vaccines.” *Pharmaceutical Research* 27(10): 2040–2.

Heljo, V.P., Nordberg, A., Tenho, M., Virtanen, T., Jouppila, K., Salonen, J., Maunu, S.L., Juppo, A.M., 2012. “The effect of water plasticization on the molecular mobility and crystallization tendency of amorphous disaccharides.” *Pharmaceutical Research* 29(10): 2684–97.

Herbst-Kralovetz, M., Mason, H.S., Chen, Q., 2010. “Norwalk virus-like particles as vaccines”. *Expert Review of Vaccines* 9(3): 299–307.

Herrington, B.L., 1934. “Some Physico-Chemical Properties of Lactose”. *Journal of Dairy Science* 17(7): 501–518.

Hidalgo, I.J., Raub, T.J., Borchardt, R.T., 1989. "Characterization of the human colon carcinoma cell line (Caco-2) as a model system for intestinal epithelial permeability." *Gastroenterology* 96(3): 736–749.

Hilgers, A.R., Conradi, R.A., Burton, P.S., 1990. "Caco-2 cell monolayers as a model for drug transport across the intestinal mucosa". *Pharmaceutical Research* 7(9): 902–910.

Hinrichs, W.L., Prinsen, M.G., Frijlink, H.W., 2001. "Inulin glasses for the stabilization of therapeutic proteins." *International Journal of Pharmaceutics* 215(1-2): 163–74.

Holmgren, J., Cerkinsky, C., 2005. "Mucosal immunity and vaccines." *Nature Medicine* 11(4 Suppl): S45–53.

Huang, D.B., Wu, J.J., Tyring, S.K., 2004. "A review of licensed viral vaccines , some of their safety concerns , and the advances in the development of investigational viral vaccines". *Journal of Infection* 49(3): 179–209.

Huang, Z., Elkin, G., Maloney, B.J., Beuhner, N., Arntzen, C.J., Thanavala, Y., Mason, H.S., 2005. "Virus-like particle expression and assembly in plants: hepatitis B and Norwalk viruses". *Vaccine* 23(15): 1851–1858.

Huang, Z., LePore, K., Elkin, G., Thanavala, Y., Mason, H.S., 2008. "High-yield rapid production of hepatitis B surface antigen in plant leaf by a viral expression system". *Plant Biotechnology Journal* 6(2): 202–209.

Huang, Z., Santi, L., LePore, K., Kilbourne, J., Arntzen, C.J., Mason, H.S., 2006. "Rapid, high-level production of hepatitis B core antigen in plant leaf and its immunogenicity in mice". *Vaccine* 24(14): 2506–2513.

Hunter, N.E., Frampton, C.S., Craig, D.Q.M., Belton, P.S., 2010. "The use of dynamic vapour sorption methods for the characterisation of water uptake in amorphous trehalose." *Carbohydrate Research* 345(13): 1938–44.

Hussain, N., Jaitley, V., Florence, A.T., 2001. "Recent advances in the understanding of uptake of microparticulates across the gastrointestinal lymphatics." *Advanced Drug Delivery Reviews* 50(1-2): 107–42.

Huyghebaert, N., Vermeire, A., Neirynck, S., Remaut, E., 2005a. "Development of an enteric-coated formulation containing freeze-dried, viable recombinant *Lactococcus lactis* for the ileal mucosal delivery of human interleukin-10." *European Journal of Pharmaceutics and Biopharmaceutics* 60(3): 349–59.

Huyghebaert, N., Vermeire, A., Neirynck, S., Steidler, L., Remaut, E., Remon, J.P., 2005b. "Evaluation of extrusion/spheronisation, layering and compaction for the preparation of an oral, multi-particulate formulation of viable, hIL-10 producing *Lactococcus lactis*." *European Journal of Pharmaceutics and Biopharmaceutics* 59(1): 9–15.

Iglesias, H.A., Chirife, J., Buera, M.P., 1997. "Adsorption isotherm of amorphous trehalose". *Journal of the Science of Food and Agriculture* 75(2): 183–186.

Iwarson, S., Tabor, E., Thomas, H.C., Snoy, P., Gerety, R.J., 1985. "Protection against hepatitis B virus infection by immunization with hepatitis B core antigen." *Gastroenterology* 88(3): 763–767.

Jackson, A.D., McLaughlin, J., 2009. "Digestion and absorption". *Surgery (Oxford)* 27(6): 231–236.

Jani, P., Halbert, G.W., Langridge, J., Florence, A.T., 1990. "Nanoparticle Uptake by the Rat Gastrointestinal Mucosa: Quantitation and Particle Size Dependency". *Journal of Pharmacy and Pharmacology* 42(12): 821–826.

Jean-Jean, O., Salhi, S., Carlier, D., 1989. "Biosynthesis of hepatitis B virus e antigen: directed mutagenesis of the putative aspartyl protease site". *Journal of Virology* 63(12): 5497–5500.

Jennings, G.T., Bachmann, M.F., 2008. "The coming of age of virus-like particle vaccines". *Biological Chemistry* 389(5): 521–536.

Jiang, X., Wang, M., Graham, D.Y., Estes, M.K., 1992. "Expression, self-assembly, and antigenicity of the Norwalk virus capsid protein." *Journal of Virology* 66(11): 6527–32.

Jung, T., Kamm, W., Breitenbach, A., Kaiserling, E., Xiao, J.X., Kissel, T., 2000. “Biodegradable nanoparticles for oral delivery of peptides: is there a role for polymers to affect mucosal uptake?” *European Journal of Pharmaceutics and Biopharmaceutics* 50(1): 147–60.

Kadaoui, K., Corthésy, B., 2007. “Secretory IgA mediates bacterial translocation to dendritic cells in mouse Peyer’s patches with restriction to mucosal compartment”. *The Journal of Immunology* 179: 7751–7757.

Kadiyala, I., Loo, Y., Roy, K., Rice, J., Leong, K.W., 2010. “Transport of chitosan–DNA nanoparticles in human intestinal M-cell model versus normal intestinal enterocytes”. *European Journal of Pharmaceutical Sciences* 39(1–3): 103–109.

Kalantzi, L., Goumas, K., Kalioras, V., Abrahamsson, B., Dressman, J.B., Reppas, C., 2006. “Characterization of the human upper gastrointestinal contents under conditions simulating bioavailability/bioequivalence studies.” *Pharmaceutical Research* 23(1): 165–76.

Kaminskyj, S.G.W., Dahms, T.E.S., 2008. “High spatial resolution surface imaging and analysis of fungal cells using SEM and AFM.” *Micron* 39(4): 349–61.

Kammona, O., Kiparissides, C., 2012. “Recent Advances in Nanocarrier-based Mucosal Delivery of Biomolecules”. *Journal of Controlled Release* 161(3): 781–794.

Kapusta, J., Modelska, A., Figlerowicz, M., Pniewski, T, Letellier, M., Lisowa, O., Yusibov, V, Koprowski, H., Plucienniczak, A., Legocki, A.B., 1999. “A plant-derived edible vaccine against hepatitis B virus”. *FASEB Journal* 13(13): 1796–1799.

Kararli, T., 1995. “Comparison of the gastrointestinal anatomy, physiology, and biochemistry of humans and commonly used laboratory animals”. *Biopharmaceutics & Drug Disposition* 16(5): 351–380.

Kendall, R.A., Alhnan, M.A., Nilkumhang, S., Murdan, S., Basit, A.W., 2009. “Fabrication and in vivo evaluation of highly pH-responsive acrylic microparticles for targeted gastrointestinal delivery.” *European Journal of Pharmaceutical Sciences* 37(3-4): 284–90.

Kernéis, S., Kerne, S., Bogdanova, A., Kraehenbuhl, J.P., Pringault, E., 1997. "Conversion by Peyer's Patch Lymphocytes of Human Enterocytes into M Cells that Transport Bacteria". *Science* 277(5328): 949–952.

Khan F.H., 2009. "Immune response to infectious agents", in: *The Elements of Immunology*. Pearson Education India, p. 339.

Kim, A.I., Akers, M.J., Nail, S.L., 1998. "The physical state of mannitol after freeze-drying: effects of mannitol concentration, freezing rate, and a noncrystallizing cosolute." *Journal of Pharmaceutical Sciences* 87(8): 931–5.

Kong, Q., Richter, L.J., Yang, Yu Fang, Arntzen, C.J., Mason, H.S., Thanavala, Y., 2001. "Oral immunization with hepatitis B surface antigen expressed in transgenic plants". *Proceedings of the National Academy of Sciences of the United States of America* 98(20): 11539–11544.

Kraehenbuhl, J.P., Neutra, M.R., 2000. "Epithelial M cells: differentiation and function." *Annual Review of Cell and Developmental Biology* 16: 301–32.

Kunisawa, J., Kurashima, Y., Kiyono, H., 2012. "Gut-associated lymphoid tissues for the development of oral vaccines." *Advanced Drug Delivery Reviews* 64(6): 523–30.

Kunisawa, J., Nuchi, T., Kiyono, H., 2008. "Immunological commonalities and distinctions between airway and digestive immunity." *Trends in Immunology* 29(11): 505–13.

Kushnir, N., Streatfield, S.J., Yusibov, V., 2012. "Virus-like particles as a highly efficient vaccine platform: diversity of targets and production systems and advances in clinical development." *Vaccine* 31(1): 58–83.

Kwon, K.-C., Verma, D., Singh, N.D., Herzog, R., Daniell, H., 2013. "Oral delivery of human biopharmaceuticals, autoantigens and vaccine antigens bioencapsulated in plant cells". *Advanced Drug Delivery Reviews* 65(6):782-99.

Lai, S.K., Wang, Y.-Y., Hanes, J., 2009. "Mucus-penetrating nanoparticles for drug and gene delivery to mucosal tissues." *Advanced Drug Delivery Reviews* 61(2): 158–71.

Lang, R., Winter, G., Vogt, L., Zurcher, A., Dorigo, B., Schimmele, B., 2009. "Rational design of a stable, freeze-dried virus-like particle-based vaccine formulation." *Drug Development and Industrial Pharmacy* 35(1): 83–97.

Lavanchy, D., 2004. "Hepatitis B virus epidemiology, disease burden, treatment, and current and emerging prevention and control measures". *Journal of Viral Hepatitis* 11(2): 97–107.

Le Ferrec, E., Chesne, C., Artusson, P., Brayden, D., Fabre, G., Gires, P., Guillou, F., Rousset, M., Rubas, W., Scarino, M.-L., 2001. "In vitro models of the intestinal barrier". *Alternatives to Laboratory Animals* 29(6): 649–668.

Lebre, F., Borchard, G., Lima, M. De, Borges, O., 2011. "Progress towards a needle-free hepatitis B vaccine". *Pharmaceutical Research* (28): 986–1012.

Lee, H.J., 2002. "Protein drug oral delivery: the recent progress." *Archives of Pharmacal Research* 25(5): 572–84.

Lee, K.W., Tan, W.S., 2008. "Recombinant hepatitis B virus core particles: association, dissociation and encapsidation of green fluorescent protein." *Journal of Virological Methods* 151(2): 172–80.

Lee, R.W.H., Pool, A.N., Ziauddin, A., Lo, R., 2003. "Edible vaccine development: stability of Mannheimia haemolytica A1 leukotoxin 50 during post-harvest processing and storage of field-grown transgenic white clover". *Molecular Breeding* 11(4): 259–266.

Li, X., Zhang, Y., Yan, R., Jia, W., Yuan, M., Deng, X., Huang, Z., 2000. "Influence of process parameters on the protein stability encapsulated in poly-DL-lactide-poly(ethylene glycol) microspheres." *Journal of Controlled Release* 68(1): 41–52.

Lico, C., Santi, L., Twyman, R.M., Pezzotti, M., Avesani, L., 2012. "The use of plants for the production of therapeutic human peptides." *Plant Cell Reports* 31(3): 439–51.

Liljeqvist, S., Ståhl, S., 1999. "Production of recombinant subunit vaccines: protein immunogens, live delivery systems and nucleic acid vaccines." *Journal of Biotechnology* 73(1): 1–33.

Limaye, A., Koya, V., Samsam, M., Daniell, H., 2006. "Receptor-mediated oral delivery of a bioencapsulated green fluorescent protein expressed in transgenic chloroplasts into the mouse circulatory system." *FASEB Journal* 20(7): 959–61.

Ling, H.-Y., Edwards, A.M., Gantier, M.P., Deboer, K.D., Neale, A.D., Hamill, J.D., Walmsley, A.M., 2012. "An interspecific *Nicotiana* hybrid as a useful and cost-effective platform for production of animal vaccines." *PloS One* 7(4): e35688.

Listiohadi, Y., Hourigan, J., 2009. "Thermal analysis of amorphous lactose and  $\alpha$ -lactose monohydrate". *Dairy Science and Technology* 89: 43–67.

Liu, S., He, J., Shih, C., Li, K., Dai, A., Hong Zhou, Z., Zhang, J., 2010. "Structural comparisons of hepatitis B core antigen particles with different C-terminal lengths". *Virus Research* 149(2): 241–244.

Lobaina, Y., García, D., Abreu, N., Muzio, V., Aguilar, J.C., 2003. "Mucosal immunogenicity of the hepatitis B core antigen". *Biochemical and Biophysical Research Communications* 300(3): 745–750.

Lobaina, Y., Palenzuela, D., Pichardo, D., Muzio, V., Guillén, G., Aguilar, J.C., 2005. "Immunological characterization of two hepatitis B core antigen variants and their immunoenhancing effect on co-delivered hepatitis B surface antigen." *Molecular Immunology* 42(3): 289–94.

Ludwig, C., Wagner, R., 2007. "Virus-like particles--universal molecular toolboxes". *Current Opinion in Biotechnology* 18(6): 537–545.

Lycke, N., 2012. "Recent progress in mucosal vaccine development: potential and limitations." *Nature Reviews. Immunology* 12(8): 592–605.

Ma, J.K.-C., Drake, P.M.W., Christou, P., 2003. "The production of recombinant pharmaceutical proteins in plants." *Nature Reviews. Genetics* 4(10): 794–805.

Ma, J.K.-C., Hiatt, A., Hein, M., Vine, N.D., Wang, F., Stabila, P., Van Dolleweerd, C., Mostov, K., Lehner, T., 1995. "Generation and assembly of secretory antibodies in plants". *Science* 268(5211): 716–719.

Mahato, R.I., Narang, A.S., Thoma, L., Miller, D.D., 2003. "Emerging trends in oral delivery of peptide and protein drugs." *Critical Reviews in Therapeutic Drug Carrier Systems* 20(2-3): 153–214.

Makidon, P., Bielinska, A., Nigavekar, S., 2008. "Pre-clinical evaluation of a novel nanoemulsion-based hepatitis B mucosal vaccine". *PLoS One* 3(8): e2954.

Man, A.L., Lodi, F., Bertelli, E., Regoli, M., Pin, C., Mulholland, F., Satoskar, A.R., Taussig, M.J., Nicoletti, C., 2008. "Macrophage migration inhibitory factor plays a role in the regulation of microfold (M) cell-mediated transport in the gut." *Journal of Immunology* 181(8): 5673–80.

Martín, J., Odoom, K., Tuite, G., Dunn, G., Hopewell, N., Cooper, G., Fitzharris, C., Hall, W.W., Minor, P.D., Martí, J., Butler, K., 2004. "Long-Term Excretion of Vaccine-Derived Poliovirus by a Healthy Child Long-Term Excretion of Vaccine-Derived Poliovirus by a Healthy Child". *Journal of Virology* 78(24): 13839–13847.

Mason, H.S., Haq, T.A., Clements, J.D., Arntzen, C.J., 1998. "Edible vaccine protects mice against *Escherichia coli* heat-labile enterotoxin (LT): potatoes expressing a synthetic LT-B gene". *Vaccine* 16(13): 1336–1343.

Mason, H.S., Lam, D.M., Arntzen, C.J., 1992. "Expression of hepatitis B surface antigen in transgenic plants". *Proceedings of the National Academy of Sciences of the United States of America* 89(24): 11745–11749.

Mason, H.S., Warzeka, H., Mor, T., Arntzen, C.J., 2002. "Edible plant vaccines: applications for prophylactic and therapeutic molecular medicine". *Trends in Molecular Medicine* 8(7): 324–329.

Mayer, L., Sperber, K., Chan, L., Child, J., Toy, L., 2001. "Oral tolerance to protein antigens." *Allergy* 56 (suppl 67): 12–5.

McConnell, E.L., Basit, A.W., Murdan, S., 2008a. "Measurements of rat and mouse gastrointestinal pH, fluid and lymphoid tissue, and implications for in-vivo experiments." *The Journal of Pharmacy and Pharmacology* 60(1): 63–70.

McConnell, E.L., Fadda, H.M., Basit, A.W., 2008b. "Gut instincts: explorations in intestinal physiology and drug delivery." *International Journal of Pharmaceutics* 364(2): 213–26.

McConnell, E.L., Liu, F., Basit, A.W., Murdan, S., 2008c. "Colonic antigen administration induces significantly higher humoral levels of colonic and vaginal IgA, and serum IgG compared to oral administration." *Vaccine* 26(5): 639–46.

McGarvey, O.S., Kett, V.L., Craig, D.Q.M., 2003. "An Investigation into the Crystallization of  $\alpha,\alpha$ -Trehalose from the Amorphous State". *The Journal of Physical Chemistry B* 107(27): 6614–6620.

McGhee, J., Mestecky, J., Dertzbaugh, M., 1992. "The mucosal immune system: from fundamental concepts to vaccine development". *Vaccine* 10(2): 75–88.

Mechtcheriakova, I.A., Eldarov, M.A., Nicholson, L., Shanks, M., Skryabin, K.G., Lomonossoff, G.P., 2006. "The use of viral vectors to produce hepatitis B virus core particles in plants". *Journal of Virological Methods* 131(1): 10–15.

Menassa, R., Du, C., Yin, Z.Q., Ma, S., Poussier, P., Brandle, J., Jevnikar, A.M., 2007. "Therapeutic effectiveness of orally administered transgenic low-alkaloid tobacco expressing human interleukin-10 in a mouse model of colitis." *Plant Biotechnology Journal* 5(1): 50–9.

Merchant, H.A., McConnell, E.L., Liu, F., Ramaswamy, C., Kulkarni, R.P., Basit, A.W., Murdan, S., 2011. "Assessment of gastrointestinal pH, fluid and lymphoid tissue in the guinea pig, rabbit and pig, and implications for their use in drug development." *European Journal of Pharmaceutical Sciences* 42(1-2): 3–10.

Metzger, K., Bringas, R., 1998. "Proline-138 is essential for the assembly of hepatitis B virus core protein." *The Journal of General Virology* 79: 587–90.

Meunier, V., Bourrie, M., Berger, Y., Fabre, G., 1995. "The human intestinal epithelial cell line Caco-2; pharmacological and pharmacokinetic applications". *Cell Biology and Toxicology* 11(3-4): 187–194.

Meynell, H.M., Thomas, N.W., James, P. S., Holland, J., Taussig, M.J., Nicoletti, C., 1999. "Up-regulation of microsphere transport across the follicle-associated epithelium of Peyer's patch by exposure to *Streptococcus pneumoniae* R36a". *The FASEB Journal* 13(6): 611–619.

Milich, D.R., Chen, M., Schödel, F., Peterson, D.L., Jones, J.E., Hughes, J.L., 1997. "Role of B cells in antigen presentation of the hepatitis B core." *Proceedings of the National Academy of Sciences of the United States of America* 94(26): 14648–53.

Milich, D.R., McLachlan, A., Moriarty, A., Thornton, G.B., 1987a. "Immune response to hepatitis B virus core antigen (HBcAg): localization of T cell recognition sites within HBcAg/HBeAg." *Journal of Immunology* 139(4): 1223–31.

Milich, D.R., McLachlan, A., Thornton, G.B., Hughes, J.L., 1987b. "Antibody production to the nucleocapsid and envelope of the hepatitis B virus primed by a single synthetic T cell site." *Nature* 329(6139): 547–549.

Moser, M., Leo, O., 2010. "Key concepts in immunology." *Vaccine* 28(suppl 3): C2–13.

Mowat, A.M., 2003. "Anatomical basis of tolerance and immunity to intestinal antigens." *Nature Reviews. Immunology* 3(4): 331–41.

Murray, K., Bruce, S.A., Hinnen, A., Wingfield, P., Van Erd, P.M., De Reus, A., Schellekens, H., 1984. "Hepatitis B virus antigens made in microbial cells immunise against viral infection." *The EMBO Journal* 3(3): 645–50.

Nassal, M., Skamel, C., Vogel, M., Kratz, P.A., Stehle, T., Wallich, R., Simon, M.M., 2008. "Development of hepatitis B virus capsids into a whole-chain protein antigen display platform: new particulate Lyme disease vaccines." *International Journal of Medical Microbiology* 298(1-2): 135–42.

Nath, N., Hickman, K., Nowlan, S., Shah, D., Phillips, J., Babler, S., 1992. "Stability of the recombinant hepatitis B core antigen". *Journal of Clinical Microbiology* 30(6): 1617–1619.

Neutra, M.R., Kozlowski, P.A., 2006. "Mucosal vaccines: the promise and the challenge." *Nature Reviews. Immunology* 6(2): 148–58.

Neutra, M.R., Mantis, N.J., Kraehenbuhl, J.P., 2001. "Collaboration of epithelial cells with organized mucosal lymphoid tissues." *Nature Immunology* 2(11): 1004–9.

Newman, M., Suk, F.-M., Cajimat, M., Chua, P.K., Shih, C., 2003. "Stability and Morphology Comparisons of Self-Assembled Virus-Like Particles from Wild-Type and Mutant Human Hepatitis B Virus Capsid Proteins". *Journal of Virology* 77(24): 12950–12960.

Nicoletti, C., 2000. "Unsolved mysteries of intestinal M cells." *Gut* 47(5): 735–9.

Nicoletti, C., Regoli, M., Bertelli, E., 2009. "Dendritic cells in the gut: to sample and to exclude?" *Mucosal Immunology* 2(5): 462.

Niikura, M., Takamura, S., Kim, G., Kawai, S., Saijo, M., Morikawa, S., Kurane, I., Li, T.-C., Takeda, N., Yasutomi, Y., 2002. "Chimeric recombinant hepatitis E virus-like particles as an oral vaccine vehicle presenting foreign epitopes." *Virology* 293(2): 273–80.

Niwa, T., Shimabara, H., Kondo, M., Danjo, K., 2009. "Design of porous microparticles with single-micron size by novel spray freeze-drying technique using four-fluid nozzle". *International Journal of Pharmaceutics* 382(1-2): 88–97.

Noad, R., Roy, P., 2003. "Virus-like particles as immunogens". *Trends in Microbiology* 11(9): 438–444.

Nuzzaci, M., Vitti, A., Condelli, V., Lanorte, M.T., Tortorella, C., Boscia, D., Piazzolla, P., Piazzolla, G., 2010. "In vitro stability of Cucumber mosaic virus nanoparticles carrying a Hepatitis C virus-derived epitope under simulated gastrointestinal

conditions and in vivo efficacy of an edible vaccine.” *Journal of Virological Methods* 165(2): 211–5.

O’Hagan, D.T., McGee, J.P., Holmgren, J., Mowat, A.M., Donachie, A.M., Mills, K.H., Gaisford, W., Rahman, D., Challacombe, S.J., 1993. “Biodegradable microparticles for oral immunization.” *Vaccine* 11(2): 149–54.

O’Neill, M.J., Bourre, L., Melgar, S., O’Driscoll, C.M., 2011. “Intestinal delivery of non-viral gene therapeutics: physiological barriers and preclinical models.” *Drug Discovery Today* 16(5-6): 203–18.

Olmsted, S.S., Padgett, J.L., Yudin, A.I., Whaley, K.J., Moench, T.R., Cone, R.A., 2001. “Diffusion of macromolecules and virus-like particles in human cervical mucus.” *Biophysical Journal* 81(4): 1930–7.

Omar, A.M., Roos, Y.H., 2007a. “Water sorption and time-dependent crystallization behaviour of freeze-dried lactose–salt mixtures”. *LWT - Food Science and Technology* 40(3): 520–528.

Omar, A.M., Roos, Y.H., 2007b. “Glass transition and crystallization behaviour of freeze-dried lactose–salt mixtures”. *LWT - Food Science and Technology* 40(3): 536–543.

Owen, R., Jones, L., 1974. “Epithelial cell specialization within human Peyer’s patches: an ultrastructural study of intestinal lymphoid follicles”. *Gastroenterology* 66(2): 189–203.

Pappo, J., Mahlman, T., 1993. “Follicle epithelial M cells are a source of interleukin-1 in Peyer’s patches”. *Immunology* 78(3): 505–507.

Park, K., Kwon, I.C., 2011. “Oral protein delivery: Current status and future prospect”. *Reactive and Functional Polymers* 71(3): 280–287.

Parmentier, J., Becker, M.M.M., Heintz, U., Fricker, G., 2011. “Stability of liposomes containing bio-enhancers and tetraether lipids in simulated gastro-intestinal fluids.” *International Journal of Pharmaceutics* 405(1-2): 210–7.

Pasek, M., Goto, T., Gilbert, W., Zink, B., Schaller, H., MacKay, P., Leadbetter, G., Murray, K., 1979. "Hepatitis B virus genes and their expression in *E. coli*". *Nature* 282(5739): 575–579.

Pastor, M., Esquível, A., Talavera, A., Año, G., Fernández, S., Cedré, B., Infante, J.F., Callicó, A., Pedraz, J.L., 2013. "An approach to a cold chain free oral cholera vaccine: in vitro and in vivo characterization of *Vibrio cholerae* gastro-resistant microparticles." *International Journal of Pharmaceutics* 448: 247–258.

Paul, M., Ma, J.K.-C., 2010. "Plant-made immunogens and effective delivery strategies." *Expert Review of Vaccines* 9(8): 821–33.

Pelosi, A., Piedrafita, D., De Guzman, G., Shepherd, R., Hamill, J.D., Meeusen, E., Walmsley, A.M., 2012. "The Effect of Plant Tissue and Vaccine Formulation on the Oral Immunogenicity of a Model Plant-Made Antigen in Sheep". *PloS One* 7(12): e52907.

Pelosi, A., Shepherd, R., De Guzman, G., Hamill, J., Meeusen, E., Sanson, G., Walmsley, A.M., 2011a. "The Release and Induced Immune Responses of a Plant-made and Delivered Antigen in the Mouse Gut." *Current Drug Delivery* 8(6): 612–21.

Pelosi, A., Shepherd, R., Walmsley, A.M., 2011b. "Delivery of plant-made vaccines and therapeutics." *Biotechnology Advances* 30(2): 440–448.

Penney, C.A., Thomas, D.R., Deen, S.S., Walmsley, A.M., 2011. "Plant-made vaccines in support of the Millennium Development Goals." *Plant Cell Reports* 30(5): 789–98.

Perlovich, G., Hansen, L.K., Bauer-Brandl, A., 2001. "The polymorphism of glycine. Thermochemical and structural aspects". *Journal of Thermal Analysis and Calorimetry* 66: 699–715.

Plummer, E.M., Manchester, M., 2011. "Viral nanoparticles and virus-like particles: platforms for contemporary vaccine design". *Wiley Interdisciplinary Reviews. Nanomedicine and Nanobiotechnology* 3: 174–196.

Pniewski, T., Kapusta, J., Bociąg, P., Kostrzak, A., Fedorowicz-Strońska, O., Czyż, M., Gdula, M., Krajewski, P., Wolko, B., Płucienniczak, A., 2012. "Plant expression, lyophilisation and storage of HBV medium and large surface antigens for a prototype oral vaccine formulation." *Plant Cell Reports* 31(3): 585–95.

Pniewski, T., Kapusta, J., Bociąg, P., Wojciechowicz, J., Kostrzak, A., Gdula, M., Fedorowicz-Strońska, O., Wójcik, P., Otta, H., Samardakiewicz, S., Wolko, B., Płucienniczak, A., 2011. "Low-dose oral immunization with lyophilized tissue of herbicide-resistant lettuce expressing hepatitis B surface antigen for prototype plant-derived vaccine tablet formulation." *Journal of Applied Genetics* 52(2): 1–12.

Poland, G.A., Jacobson, R.M., 2001. "Understanding those who do not understand: a brief review of the anti-vaccine movement." *Vaccine* 19(17-19): 2440–5.

Porta, C., James, P S, Phillipst, A.D., Savidget, T.C., Smith, M.W., Phillips, A.D., Savidge, T.C., Cremaschi, D., 1992. "Confocal analysis of fluorescent bead uptake by mouse Peyer's patch follicle-associated M cells". *Experimental Physiology* 77(6): 929–932.

Primard, C., Rochereau, N., Luciani, E., Genin, C., Delair, T., Paul, S., Verrier, B., 2010. "Traffic of poly(lactic acid) nanoparticulate vaccine vehicle from intestinal mucus to sub-epithelial immune competent cells." *Biomaterials* 31(23): 6060–8.

Pron, B., Boumaila, C., Jaubert, F., Sarnacki, S., Monnet, J.P., Berche, P., Gaillard, J.L., 1998. "Comprehensive study of the intestinal stage of listeriosis in a rat ligated ileal loop system." *Infection and Immunity* 66(2): 747–55.

Prosser, E., Meehan, E., Malley, D.O., Clarke, N., Ramtoola, Z., Brayden, D., McClean, S., O'Malley, D., 1998. "Binding and uptake of biodegradable poly-dl-lactide micro- and nanoparticles in intestinal epithelia". *European Journal of Pharmaceutical Sciences* 6(2): 153–163.

Pumpens, P., Grens, E., 1999. "Hepatitis B core particles as a universal display model: a structure-function basis for development". *FEBS Letters* 442(1): 1–6.

Purcell, A.W., McCluskey, J., Rossjohn, J., 2007. "More than one reason to rethink the use of peptides in vaccine design." *Nature Reviews. Drug Discovery* 6(5): 404–14.

Pyne, A., Chatterjee, K., Suryanarayanan, R., 2003. "Solute crystallization in mannitol-glycine systems-implications on protein stabilization in freeze-dried formulations." *Journal of Pharmaceutical Sciences* 92(11): 2272–83.

Rae, C.S., Khor, I.W., Wang, Q., Destito, G., Gonzalez, M.J., Singh, P., Thomas, D.M., Estrada, M.N., Powell, E., Finn, M.G., Manchester, M., 2005. "Systemic trafficking of plant virus nanoparticles in mice via the oral route." *Virology* 343(2): 224–35.

Rescigno, M., Urbano, M., Valzasina, B., Francolini, M., Rotta, G., Bonasio, R., Granucci, F., Kraehenbuhl, J.P., Ricciardi-Castagnoli, P., 2001. "Dendritic cells express tight junction proteins and penetrate gut epithelial monolayers to sample bacteria." *Nature Immunology* 2(4): 361–7.

Reuter, F., Bade, S., Hirst, T.R., Frey, A., 2009. "Bystander protein protects potential vaccine-targeting ligands against intestinal proteolysis." *Journal of Controlled Release* 137(2): 98–103.

Richards, H.A., Han, C.-T., Hopkins, R.G., Failla, M.L., Ward, W.W., Stewart, C.N., 2003. "Safety assessment of recombinant green fluorescent protein orally administered to weaned rats." *The Journal of Nutrition* 133(6): 1909–12.

Rogers, T.L., Hu, J., Yu, Z., Johnston, K.P., Williams, R.O., 2002. "A novel particle engineering technology: spray-freezing into liquid." *International Journal of Pharmaceutics* 242(1-2): 93–100.

Roos, Y.H., 2009. "Solid and Liquid States of Lactose", in: McSweeney, P., Fox, P.F. (Eds.), *Advanced Dairy Chemistry*. Springer New York, pp. 17–34.

Rybicki, E.P., 2009. "Plant-produced vaccines: promise and reality." *Drug Discovery Today* 14(1-2): 16–24.

Rybicki, E.P., 2010. "Plant-made vaccines for humans and animals." *Plant Biotechnology Journal* 8(5): 620–37.

Sainsbury, F., Cañizares, M.C., Lomonosoff, G.P., 2010. "Cowpea Mosaic Virus: The Plant Virus-Based Biotechnology Workhorse". *Phytopathology* 48: 437–455.

Sainsbury, F., Lomonosoff, G.P., 2008. "Extremely High-Level and Rapid Transient Protein Production in Plants without the Use of Viral Replication". *Plant Physiology* 148(3): 1212–1218.

Sainsbury, F., Thuenemann, E.C., Lomonosoff, G.P., 2009. "pEAQ: versatile expression vectors for easy and quick transient expression of heterologous proteins in plants". *Plant Biotechnology Journal* 7(7): 682–693.

Sambrook, J., Russel, D.W., 2001a. "Molecular Cloning", Third Edit. Cold Spring Harbor Laboratory Press, A8.40.

Sambrook, J., Russel, D.W., 2001b. "Molecular Cloning", Third Edit. Cold Spring Harbor Laboratory Press, A9.25, A9.28.

Sandberg, J.W., Lau, C., Jacomino, M., Finegold, M., Henning, S.J., 1994. "Improving access to intestinal stem cells as a step toward intestinal gene transfer." *Human Gene Therapy* 5(3): 323–9.

Sansonetti, P.J., Phalipon, A., 1999. "M cells as ports of entry for enteroinvasive pathogens: mechanisms of interaction, consequences for the disease process." *Seminars in Immunology* 11(3): 193–203.

Santi, L., Batchelor, L., Huang, Z., Hjelm, B., Kilbourne, J., Arntzen, C.J., Chen, Q., Mason, H.S., 2008. "An efficient plant viral expression system generating orally immunogenic Norwalk virus-like particles." *Vaccine* 26(15): 1846–54.

Saroja, C., Lakshmi, P., Bhaskaran, S., 2011. "Recent trends in vaccine delivery systems: A review." *International Journal of Pharmaceutical Investigation* 1(2): 64–74.

Seifer, M., Standring, D.N., 1994. "A protease-sensitive hinge linking the two domains of the hepatitis B virus core protein is exposed on the viral capsid surface". *Journal of Virology* 68(9): 5548–5555.

Seitz, S., Urban, S., Antoni, C., Böttcher, B., 2007. "Cryo-electron microscopy of hepatitis B virions reveals variability in envelope capsid interactions." *The EMBO Journal* 26(18): 4160–7.

Shenoy, D., Robinson, J., 2009. "Sugar glassified virus-like particles (VLPs). WO Patent 2009108689 A1."

Silin, D.S., Lyubomska, O. V., Jirathitikal, V., Bourinbaiar, A.S., 2007. "Oral vaccination: where we are?" *Expert Opinion on Drug Delivery* 4(4): 323–40.

Simonsen, L., Kane, A., Lloyd, J., 1999. "In Focus-Unsafe injections in the developing world and transmission of bloodborne pathogens: A review". *Bulletin of the World Health Organization* 77(10): 789–800.

Singh, M.N., Hemant, K.S., Ram, M., Shivakumar, H.G., 2010. "Microencapsulation: A promising technique for controlled drug delivery." *Research in Pharmaceutical Sciences* 5(2): 65–77.

Sitaula, R., Bhowmick, S., 2006. "Moisture sorption characteristics and thermophysical properties of trehalose-PBS mixtures." *Cryobiology* 52(3): 369–85.

Slütter, B., Plapied, L., Fievez, Virgine, Sande, M.A., Des Rieux, A., Schneider, Y.-J., Van Riet, E., Jiskoot, W., Préat, V., 2009. "Mechanistic study of the adjuvant effect of biodegradable nanoparticles in mucosal vaccination." *Journal of Controlled Release* 138(2): 113–21.

Sood, A., Panchagnula, R., 2001. "Peroral route: an opportunity for protein and peptide drug delivery." *Chemical Reviews* 101(11): 3275–303.

Spök, A., Twyman, R.M., Fischer, R., Ma, J.K.-C., Sparrow, P.A.C., 2008. "Evolution of a regulatory framework for pharmaceuticals derived from genetically modified plants." *Trends in Biotechnology* 26(9): 506–17.

Strobel, S., Mowat, A.M., 1998. "Immune responses to dietary antigens: oral tolerance." *Immunology Today* 19(4): 173–81.

Stuart, L.M., Ezekowitz, R.A.B., 2005. "Phagocytosis: elegant complexity." *Immunity* 22(5): 539–50.

Summers, M., Aulton, M.E., 2007. “Granulation”, in: Aulton, M.E. (Ed.), Aulton’s Pharmaceutics: The Design and Manufacture of Medicines. Elsevier Limited, pp. 365–378.

Tacket, C.O., Mason, H.S., 1999. “A review of oral vaccination with transgenic vegetables.” *Microbes and Infection / Institut Pasteur* 1(10): 777–83.

Tacket, C.O., Mason, H.S., Losonsky, G., Clements, J.D., Levine, M.M., Arntzen, C.J., 1998. “Immunogenicity in humans of a recombinant bacterial antigen delivered in a transgenic potato.” *Nature Medicine* 4(5): 607–609.

Tacket, C.O., Mason, H.S., Losonsky, G., Estes, M.K., Levine, M.M., Arntzen, C.J., 2000. “Human Immune Responses to a Novel Norwalk Virus Vaccine Delivered in Transgenic Potatoes”. *Journal of Infectious Diseases* 182(1): 302–305.

Takamura, S., Niikura, M., Li, T.-C., Takeda, N., Kusagawa, S., Takebe, Y., Miyamura, T., Yasutomi, Y., 2004. “DNA vaccine-encapsulated virus-like particles derived from an orally transmissible virus stimulate mucosal and systemic immune responses by oral administration.” *Gene Therapy* 11(7): 628–35.

Thanavala, Y., Lugade, A., 2010. “Oral transgenic plant-based vaccine for hepatitis B”. *Immunologic Research* 46(1): 4–11.

Thanavala, Y., Mahoney, M., Pal, S., Scott, A., Richter, L.J., Natarajan, N., Goodwin, P., Arntzen, C.J., Mason, H.S., 2005. “Immunogenicity in humans of an edible vaccine for hepatitis B”. *Proceedings of the National Academy of Sciences of the United States of America* 102(9): 3378–3382.

Thanavala, Y., Yang, Y.F., 1995. “Immunogenicity of transgenic plant-derived hepatitis B surface antigen”. *Proceedings of the National Academy of Sciences of the United States of America* 92(8): 3358–3361.

Thuenemann, E.C., 2010. “Virus-like particle production using Cowpea Mosaic Virus-based Vectors”. PhD Thesis. John Innes Centre.

Thuenemann, E.C., Meyers, A.E., Verwey, J., Rybicki, E.P., Lomonossoff, G.P., 2013. “A method for rapid production of heteromultimeric protein complexes in plants: assembly of protective bluetongue virus-like particles.” *Plant Biotechnology Journal* In press: 1–8.

Tiwari, S., Verma, P.C., Singh, P.K., Tuli, R., 2009. “Plants as bioreactors for the production of vaccine antigens”. *Biotechnology Advances* 27(4): 449–467.

Tiwari, S., Vyas, S.P., 2011. “Novel approaches to oral immunization for hepatitis B.” *Current Infectious Disease Reports* 13(1): 4–12.

Ulmer, J.B., Valley, U., Rappuoli, R., 2006. “Vaccine manufacturing: challenges and solutions.” *Nature Biotechnology* 24(11): 1377–83.

Vanlandschoot, P., Cao, T., Leroux-Roels, G., 2003. “The nucleocapsid of the hepatitis B virus: a remarkable immunogenic structure”. *Antiviral Research* 60(2): 67–74.

Vehring, R., 2008. “Pharmaceutical particle engineering via spray drying.” *Pharmaceutical Research* 25(5): 999–1022.

Velasquez, L.S., Shira, S., Berta, A.N., Kilbourne, J., Medi, B.M., Tizard, I., Ni, Y., Arntzen, C.J., Herbst-Kralovetz, M.M., 2011. “Intranasal delivery of Norwalk virus-like particles formulated in an in situ gelling, dry powder vaccine.” *Vaccine* 29(32): 5221–31.

Vertzoni, M., Dressman, J., Butler, J., Hempenstall, J., Reppas, C., 2005. “Simulation of fasting gastric conditions and its importance for the in vivo dissolution of lipophilic compounds.” *European Journal of Pharmaceutics and Biopharmaceutics* 60(3): 413–7.

Vicente, T., Roldão, A., Peixoto, C., Carrondo, M.J.T., Alves, P.M., 2011. “Large-scale production and purification of VLP-based vaccines”. *Journal of Invertebrate Pathology* 107: S42–S48.

Walmsley, A.M., Arntzen, C.J., 2000. “Plants for delivery of edible vaccines”. *Current Opinion in Biotechnology* 11(2): 126–129.

Wan, L.S.C., Heng, P.W.S., Muhuri, G., 1992. "Incorporation and distribution of a low dose drug in granules". *International Journal of Pharmaceutics* 88(1-3): 159–163.

Wang, L., Coppel, R., 2008. "Oral vaccine delivery: can it protect against non-mucosal pathogens?" *Expert Review of Vaccines* 7(6):729-738.

Wang, Q., Fotaki, N., Mao, Y., 2009. "Biorelevant dissolution: Methodology and application in drug development". *Dissolution Technologies* 16(3): 6–12.

Wang, W., 2000. "Lyophilization and development of solid protein pharmaceuticals." *International Journal of Pharmaceutics* 203(1-2): 1–60.

Watts, P.J., Smith, A., 2011. "Re-formulating drugs and vaccines for intranasal delivery: maximum benefits for minimum risks?" *Drug Discovery Today* 16(1-2): 4–7.

Wei, Y., Neuveut, C., Tiollais, P., Buendia, M.M., 2010. "Molecular biology of the hepatitis B virus and role of the X gene." *Pathologiebiologie* 58(4): 267–72.

Weiner, H.L., Da Cunha, A.P., Quintana, F., Wu, H., 2011. "Oral tolerance." *Immunological Reviews* 241(1): 241–59.

Weir, E., Hatch, K., 2004. "Preventing cold chain failure: vaccine storage and handling." *Canadian Medical Association Journal* 171(9): 1050.

Whitacre, D., Lee, B., Milich, D.R., 2009. "Use of hepadnavirus core proteins as vaccine platforms". *Expert Review of Vaccines* 8(11): 1565–1573.

Whitcomb, D.C., Lowe, M.E., 2007. "Human pancreatic digestive enzymes." *Digestive Diseases and Sciences* 52(1): 1–17.

WHO, 2013. "Live-attenuated vaccines.". URL [http://www.who.int/vaccine\\_research/diseases/tb/vaccine\\_development/live\\_attenuated/en/](http://www.who.int/vaccine_research/diseases/tb/vaccine_development/live_attenuated/en/)

Wiedermann, G., Ambrosch, F., Kollaritsch, H., Hofmann, H., Kunz, C., D'Hondt, E., Delem, A., André, F.E., Safary, A., Stéphenne, J., 1990. "Safety and immunogenicity of an inactivated hepatitis A candidate vaccine in healthy adult volunteers." *Vaccine* 8(6): 581–4.

Wilku, J.S., McNeil, S.E., Anderson, D.E., Perrie, Y., 2013. "Characterization and optimization of bilosomes for oral vaccine delivery". *Journal of Drug Targeting* 21(3): 291–299.

Wingfield, P.T., Stahl, S.J., Williams, R.W., Steven, A.C., 1995. "Hepatitis core antigen produced in *Escherichia coli*: subunit composition, conformational analysis, and in vitro capsid assembly." *Biochemistry* 34(15): 4919–32.

Wynne, S.A., Crowther, R.A., Leslie, A.G.W., 1999. "The Crystal Structure of the Human Hepatitis B Virus Capsid". *Molecular Cell* 3(6): 771–780.

Xu, J., Dolan, M.C., Medrano, G., Cramer, C.L., Weathers, P.J., 2012. "Green factory: Plants as bioproduction platforms for recombinant proteins". *Biotechnology Advances* 30(5): 1171–1184.

Yang, X., Lu, J., Wang, X.-J., Ching, C.-B., 2008. "Effect of sodium chloride on the nucleation and polymorphic transformation of glycine". *Journal of Crystal Growth* 310(3): 604–611.

Yee, S., 1997. "In vitro permeability across Caco-2 cells (colonic) can predict in vivo (small intestinal) absorption in man--fact or myth." *Pharmaceutical Research* 14(6): 763–6.

Yoo, M.-K., Kang, S.-K., Choi, J.-H., Park, I.-K., Na, H.-S., Lee, H.-C., Kim, E.-B., Lee, N.-K., Nah, J.-W., Choi, Y.-J., Cho, C.-S., 2010. "Targeted delivery of chitosan nanoparticles to Peyer's patch using M cell-homing peptide selected by phage display technique." *Biomaterials* 31(30): 7738–47.

Zepp, F., 2010. "Principles of vaccine design-Lessons from nature." *Vaccine* 28 (suppl 3): C14–24.

Zhang, X., Buehner, N.A., Hutson, A.M., Estes, M.K., Mason, H.S., 2006. "Tomato is a highly effective vehicle for expression and oral immunization with Norwalk virus capsid protein." *Plant Biotechnology Journal* 4(4): 419–32.

Zheng, J., Schödel, F., Peterson, D.L., 1992. "The structure of hepadnaviral core antigens. Identification of free thiols and determination of the disulfide bonding pattern." *The Journal of Biological Chemistry* 267(13): 9422–9.

Zhu, Q., Talton, J., Zhang, G., Cunningham, T., Wang, Z., Waters, R.C., Kirk, J., Eppler, B., Klinman, D.M., Sui, Y., Gagnon, S., Belyakov, I.M., Mumper, R.J., Berzofsky, J. a, 2012. "Large intestine-targeted, nanoparticle-releasing oral vaccine to control genitorectal viral infection." *Nature Medicine* 18(8): 1291–1297.

Zhu, Q., Thomson, C.W., Rosenthal, K.L., McDermott, M.R., Collins, S.M., Gauldie, J., 2008. "Immunization with adenovirus at the large intestinal mucosa as an effective vaccination strategy against sexually transmitted viral infection." *Mucosal Immunology* 1(1): 78–88.